UNIVERSITY OF NAPLES FEDERICO II

DEPARTMENT OF STRUCTURES FOR ENGINEERING AND ARCHITECTURE

PH.D. PROGRAMME IN

STRUCTURAL, GEOTECHNICAL AND SEISMIC ENGINEERING

XXXII CYCLE

COORDINATOR PROF. ENG. LUCIANO ROSATI

ROBERTA VENTINI

PH.D. THESIS

MECHANICAL BEHAVIOUR OF ROCKFILL WITH DIFFERENT DEGREES OF SATURATION

TUTORS

PROF. ENG. CLAUDIO MANCUSO
PROF. ENG. ALESSANDRO FLORA
PROF. ENG. STEFANIA LIRER

2020

To my beloved family

ACKNOWLEDGEMENTS

This dissertation is the product of the generosity and assistance of many mentors, colleagues, friends and family members. I have drawn on the knowledge and kindness of so many over these three years, and I am indebted to all of them.

I would express immense gratitude to Prof. Claudio Mancuso who has been a constant source of ideas and support. I am very grateful to him for his kind academic guidance, constructive comments, kindness, high spirits and many inspirational conversations. His guidance has given me the chance to deep love for research.

Many thanks to Prof. Alessandro Flora who valuable contributed to my research, helping me to deepen my knowledge and supporting me even when I was doubtful and enabling me to open my mind.

I would like to thank Prof. Stefania Lirer for always encouraging me. I am indebted to her for the many forms of academic support and particularly for constructive discussions and moments of personal exchange.

I am deeply grateful to Calcestruzzi Capuano s.a.s. and to Prof. Giovanni Dente for the supply of the Coreno and Redisole rockfill respectively and for the kindness and unlimited availability.

It has been my privilege to work with the technicians of the geotechnical engineering laboratory of the Department of Civil, Architectural and Environmental Engineering (DICEA) of the University of Napoli Federico II, Antonio Cammarota and Alfredo Ponzo. I am grateful to both for giving me the opportunity to watch

and learn from their knowledge and experience. I would like to address a special thanks to Antonio for being the amazing friend and mentor he is and for believing in me.
I would like to thank also all my colleagues, precious companions in this journey, for the (hopefully reciprocated) support they have given me during all this time. A particular thought goes to Domenico, Filomena and Stefania for making me feel like home in a work environment. I would also like to thank Francesca and Gianluca for sharing this adventure with me from the very first moment.
Special thanks go to my colleague and sweet friend Annachiara who has shared with me fun, difficulties and daily chats that eased the burden of study when the accomplishment of the task looked very far away.
I have no words to thank Valeria, a colleague but above all a great friend and confidant. I owe to her the most beautiful, fun and special moments of these last three years.
My heartfelt thanks go to my parents, my brother and his family for their love, patience and support every day during my studies. I dedicate all my successes to them.

Table of Contents

LIST OF FIGURES

LIST OF TABLES

ABSTRACT

Coarse-grained soils are used in many civil engineering structures, such as land reclaiming, rockfills embankments and dams. In order to ensure an appropriate performance of these structures in working conditions, it is required to understand the main factors affecting the mechanical behaviour of granular materials.

Looking for answers to these problems, the thesis, of a distinctly experimental nature, is aimed at the analysis of the main state variables influencing the stress-strain response of coarse-grained soils.

After an in-depth examination of the scientific literature, the thesis describes the equipment and experimental procedures used, with emphasis on a "large" triaxial cell for specimens of an unconventional size (diameter equal to 200 mm and height of 410 mm). This prototype is capable to investigate on the behaviour of saturated and partially saturated granular materials, as well as their mechanical response on transition from unsaturated to the saturated state. The contribution of unsaturated soil mechanics is required for a proper understanding of the basic mechanisms of soil deformation that occur in a wide variety of engineering situations. In fact, the environmentally induced change in water content is generally the triggering mechanism of soil deformations in many situations involving unsaturated soils. This is a well-known phenomenon which has received a continuous interest ever since the widespread

use of rockfill in dams for which rapid “collapse” settlements have been associated with water impoundment.

The extensive experimental program presented starts from the description of the procedures used for the preparation of compacted specimens of two gravels with different mineralogy. The aim is to highlight how the characteristics of individual particles and the packing conditions affect the mechanical behaviour. For both materials, the results of mechanical tests obtained using grain size distributions different by uniformity coefficient and maximum particle size are presented and critically discussed. For each of the materials resulting from the different mineralogy and the grain size distribution, the influence of several stress and hydro-volumetric state variables on their mechanical response is analysed. This analysis leads to the following two main topics: i) the change of the grain size distribution due to particle breakage, and ii) the relationship between the stress-strain response and particle breakage. Concerning this second topic, a micromechanical analysis has been performed to justify the observed changes of the grain-size distribution due to variations in the stress paths followed during the tests.

Some of the tests performed are aimed at assessing the effect of the degree of saturation and the transition from partial to total saturation on the stress-strain behaviour of the tested rockfills.

Once the factors affecting rockfill behaviour have been identified, a model able to predict the influence of the relevant factors on the performance of rockfill materials has been introduced, with specific

insights into some aspects such as the effects of particle breakage and degree of saturation on their behaviour.

Keywords: *rockfill, degree of saturation, particle breakage, large triaxial tests, large oedometric tests*

CHAPTER 1

INTRODUCTION

1.1 Purposes

Rockfill materials are coarse-grained soils consisting of grains with dimensions varying from centimetres to metres and different shapes, depending on the geological origin of the parent rock and the type of transport to which they were subjected.

The behaviour of the single grains and of the soil skeleton of these materials largely depends on their geological origin, shape, size, structure, compaction, strength, stress and relative humidity.

In geotechnical engineering, rockfill materials become more and more recognized for their economy and adaptability to widely varying site conditions. So, the use of rockfill in different engineering structures such as dams, harbours, roads and railways steadily increased during the last century. The engineering design of these structures requires a deep understanding of rockfill behaviour in order to ensure safety and lifetime stability.

In the past, the primary source of information about rockfill behaviour was the observation of real rockfill structures. The deformations of the structure during the construction and operational stages, and incidents caused by hydraulic fracture, internal erosion, long term effects and other combined cases gave rise to intense experimentation in situ and in the laboratory.

Against the background of studies conducted in the past, the scope of this investigation is to characterize the behaviour of rockfill materials collected from two different sites, to determine the characteristics of their particles and to analyse the effects of some factors such as degree of saturation and particle breakage on the response of the tested materials.

Starting from the observation of deformations exhibited by structures in granular materials, Terzaghi (1960) has suggested that a possible cause for these high strains could be the rock particles breakage in the contact points, with a consequent rearrangement of the granular structure towards a more stable configuration. The experimental program conducted by Marsal (1973) confirmed that the cause of the deformations that occurred in granular materials is the contacts breakage and the splitting of highly stressed particles. From these studies it emerged that the particle breakage has a basic role in the rockfill behaviour.

The grain size greatly affects the number of contact points between the particles and, consequently, the distribution of the internal stress state. Larger particles determine a small number of contact points and so bear more of the load, on average, than the smaller ones. This is the main reason of the particle breakage in coarse-grained soils, together with the fact that larger grains show greater fragility due to imperfections. It is widely recognized that for the same mineralogical origin with a homogeneous distribution of flaws, a larger particle will have more defects than a smaller one. Then for

the same tensile stress it will have a higher probability of breakage. Grain fragmentation leads to smaller and more resistant particles.
Marsal (1973) has suggested that granular materials should have a well graded grain size distribution in order to increase the number of contact points between the particles and reduce contact stresses.
The mechanical characterization of the coarse-grained materials give rise to well-known experimental problems, mainly linked to the considerable dimension of single grains. Anyway, despite the limitations imposed by size, laboratory research works allowed gaining much of the understanding, at least in a qualitative way, about the physical and chemical phenomena involved in rockfill mechanics (Oldecop and Alonso, 2013). Pioneering experimental work in large-scale testing of a wide range of different materials was developed in the sixties and early seventies by Marsal (1967, 1973), Fumagalli (1969) and Marachi et al. (1969, 1972).
The experimental researches developed in the 1970s provided a good overall understanding of the rockfill mechanical behaviour. Tests were conducted with the purpose of obtaining insight into the main factors affecting their shear strength and compressibility. It was realized, for instance, that it is not possible to define a single normal compression line. Pestana e Whittle (1995) suggest a model that provides for the convergence to very high stresses of all the curves towards a single final condition (Limit Compression Curve, LCC) governed by the particle breakage and dependent on their mineral composition.

Marsal (1973) carried out an extended testing program on large specimens using different materials. Upon flooding of the specimens subjected to one-dimensional compression, he observed volumetric collapse deformations and, comparing the grain size distributions obtained before and after each test, showed that some particle crushing occurred. To quantify particle breakage, Marsal defined a breakage factor (B_g).

Nobari and Duncan (1972) carried out one-dimensional and triaxial compression tests on crushed argillite to investigate the factors that influence the collapse of rockfill upon flooding. They found that the initial water content was the most important factor determining the amount of collapse upon flooding: the larger the initial water content, the smaller was the collapse deformation. Sowers et al. (1965) showed that flooding rockfill specimens subjected to one-dimensional compression lead to a sudden settlement (volumetric collapse) attributed also to the breakage of particles due to rock weakening induced by water.

Oldecop and Alonso (2001) attributed the particle breakage upon flooding to the increase in the crack propagation velocity in the grains looking at water as a corrosive agent. It has been shown that water has an important influence on the breakage mechanism and therefore on the mechanical behaviour of granular materials with large particles.

Particle breakage and degree of saturation have been identified as a fundamental factor to explain the experimental observations. The first was identified as the reason behind the qualitative differences

observed between the behaviour of sand (at low and moderate stress level) and rockfill.

The general objective of this work, which follows an experimental approach, is to study the stress-strain behaviour of rockfill in oedometric and triaxial conditions. The main aspects on which it focuses concern the determination of the influence of several factors on the compressibility and strength of the granular materials studied, such as particle size, initial relative density, degree of saturation and stress path. Of importance is the influence of grain breakage on the mechanical response of the materials supplied and its dependence on the water content. To carry out the study, a non-secondary effort has been devoted to set-up of some improvements and upgrades of existing equipment.

1.2 Thesis outline

The present work is organized in 7 chapters.

In the **Chapter 1** a discussion of the background from the existing studies on granular materials is given, defining the main objectives of the thesis.

Chapter 2 presents the state of knowledge on the hydro-mechanical behaviour of granular materials, including a discussion on the influence of particle breakage on the compressibility and shear strength of rockfill materials.

The experimentation developed requires special equipment that effectively reproduces load and environmental conditions to which the materials are subjected. A detailed description of the equipment

and experimental techniques used in this research is presented in C**hapter 3**.

Granular materials have different behaviour depending on the particle size, shape, density, strength and degree of saturation. **Chapter 4** presents some of the basic properties of the two materials used and the results of crushing tests on dry and saturated grains of different dimensions. Finally, the details of the selected grain size distributions and of the specimen preparation technique used are reported.

The experimental programme is described in detail in **Chapter 5**. The total stress paths and total suction paths followed in the triaxial tests are then described in order to evaluate the effects on the mechanical behaviour. The deviatoric phases with controlled rate of straining were brought to an axial strain greater than or equal to 20%, when possible, to verify the existence of the critical state condition. Chapter 5 studies triaxial and oedometric behaviour of the two materials tested using different grain size distributions and densities. The results of the isotropic compression tests and those of the oedometric tests in different saturation conditions are also presented.

Chapter 6 discusses the results obtained, with the aim of deducing the most important features of the mechanical behaviour of granular materials and the effects of several factors on which it depends. Finally, in C**hapter 7** a unified hydro-mechanical framework is proposed and discussed.

1.3 References

Fumagalli E. (1969). *Tests on cohesionless materials for rockfill dams*. Journal of the Soil Mechanics and Foundations Division, ASCE, 95(1), 313-332.

Marachi N. D., Chan C. K., Seed H. B. (1972). *Evaluation of properties of rockfill materials*. Journal of Soil Mechanics & Foundations Div, 98(1), 95-114.

Marachi N. D., Chan C. K., Seed H. B., Duncan J. M. (1969). *Strength and deformation characteristics of rockfill materials.* Department of Civil Engineering, Report No. TE-69-5. University of California.

Marsal R. J. (1967). *Large scale testing of rockfill materials*. Journal of the Soil Mechanics and Foundation Division, ASCE, 93(2), 27-43.

Marsal R. J. (1973). *Mechanical properties of rockfill*. Embankment Dam Engineering, Casagrande Volume, Wiley, New York, 109–200.

Nobari E. S., Duncan J. M. (1972). *Effect of reservoir filling on stresses and movements in earth and rockfill dams.* Department of Civil Engineering, Report No. TE-72-1. University of California.

Oldecop L. A., Alonso E. E. (2001). *A model for rockfill compressibility*. Géotechnique, 51, 127-139.

Oldecop L. A., Alonso E. E. (2013). *Rockfill mechanics*. Advances in Unsaturated Soils – Caicedo et al. (eds), Taylor & Francis Group, London, ISBN 978-0-415-62095-6.

Pestana J. M., Whittle A. J. (1995). *Compression model for cohesionless soils*. Géotechnique, 45(4), 611-631.

Sowers G. F., Williams R. C., Wallace T. S. (1965). *Compressibility of broken rock and settlement of rockfills*. Proc. of 6th ICSMFE. Montreal, 2, 561-565.

Terzaghi K. (1960). *Discussion on salt springs and lower bear river dams*. Transactions of ASCE, 125(2), 139-148.

CHAPTER 2

HYDRO-MECHANICAL BEHAVIOUR OF GRANULAR SOILS

2.1 Introduction

Granular materials are rock fragments produced by erosive actions. Their size and shape depend on the quality of the parent rock from which they originated, the level of resistance to atmospheric agents and the wear and tear they suffered during transport. Rockfill material consists of gravel, cobbles and boulders obtained either from the natural riverbed or by blasting a rock quarry. Riverbed rockfill materials consist of rounded/sub-rounded particles instead blasted quarried rockfill material consists of angular/subangular particles.

Rockfill materials are commonly used in the construction of many civil structures such as roads, railway embankments and earth and rockfill dams. The availability of coarse gravelly deposits and rock quarries makes strong interest in these structures. In fact, locally available materials make rockfill structures economical as well. Furthermore, the interest in rockfill materials is justified by their inherent flexibility, adaptability to various structures and conditions and capacity to absorb strong seismic shakings.

Therefore, understanding and characterization of the behaviour of these materials are of considerable importance for analysis and safe design of the rockfill structures. Because of its widespread use,

numerous experimental studies are available that describe rockfill behaviour under different loading conditions. In this chapter the main aspects of the behaviour investigated in literature are briefly discussed.

2.2 Influence of particle breakage

2.2.1 Experimental observations

Grain crushing is one of the micro-mechanisms that govern the stress–strain behaviour of a granular material and also its permeability by altering the grain size distribution (Marketos and Bolton, 2007). The mechanical behaviour of granular materials subjected to external loadings shows significant changes with increasing particle size. The variation in properties is largely attributed to particle breakage (Marsal, 1963; Marachi et al., 1969; Nobari and Duncan, 1972; Biarez and Hicher, 1997; McDowell and Bolton, 1998; among others). Therefore, the original engineering properties with which a structure was designed will change during its engineering life.

In fact, the monitoring of real rockfill structures has allowed the observation of a phenomenon of slow accumulation of deformations. Terzaghi (1960) suggested that the reason for these high strains could lie in the particle breakage at the contacts, under high stresses and in the consequent rearrangement of the granular structure in a more stable configuration. The grain sizes resulting from the quarry operations are very uniform, which means that the

number of contacts between the particles is small. When the contact points between the particles decrease, the contact forces increase and stresses that are generated may be greater than the strength of the rock causing particle breakage. This generates further strains and redistribution of forces.

In a plate with a unitary surface in contact with a mass of granular material, the number of contacts with the plate increases as the diameter of the particles decreases. Marsal (1963) used this concept to estimate the magnitude of average contact forces. The evaluation was carried out on a sand (with a diameter of 0.2 mm) and a breakwater (with a diameter of 20 cm) with uniformly sized particles, subject to a hydrostatic stress of 98 kPa. A greater breakage of the grains in the breakwater than in the sand clearly emerged.

Subsequent studies highlighted that grain crushing is influenced by several factors such as soil particle strength, angularity, gradation, porosity, moisture content, induced stress level and anisotropy (Lee and Farhoomand, 1967; Hardin, 1985; Hagerty et al., 1993; Lade et al., 1996; McDowell and Bolton, 1998; Takei et al., 2001; Coop et al., 2004; Tarantino and Hyde, 2005; Valdes and Caban, 2006; Erzin and Yilmaz, 2008; Melboucil et al., 2008; Wood and Maeda, 2008).

One of the most important factors influencing the crushing of a mass of granular materials is the crushing resistance of the grains. Variation of tensile strength with particles diameter has been observed experimentally by Marsal (1973), Barton and Kjaernsli

(1981), Lee (1992), Nakata et al. (2001), among others. If we consider grains with the same mineralogic origin and a homogeneous distribution of flaws, a bigger particle will have more defects than a smaller one. Then for the same tensile stress a bigger particle will have a higher probability of breakage.

In tests on granular materials, the application of loads greater than the tensile strength of the single particle causes a change in the grain size distribution curve. An experimental example is given by the results of triaxial tests proposed by Lee and Farhoomand (1967). Coarse granitic sand particles with an average diameter of 2.8 mm experienced breakage at pressures equal to 2 MPa, while calcareous shells began crushing at 0.05-0.2 MPa. As shown in Figure 2.1, from the comparison between the grain size distributions before and after the test on a granitic gravel, the particles breakage is more significant for bigger grains. According to Lee and Farhoomand (1967) results, by increasing the stress ratio ($K_c = \sigma_1/\sigma_3$) the particles crushing increase also showing a dependency on the magnitude of deviatoric stress.

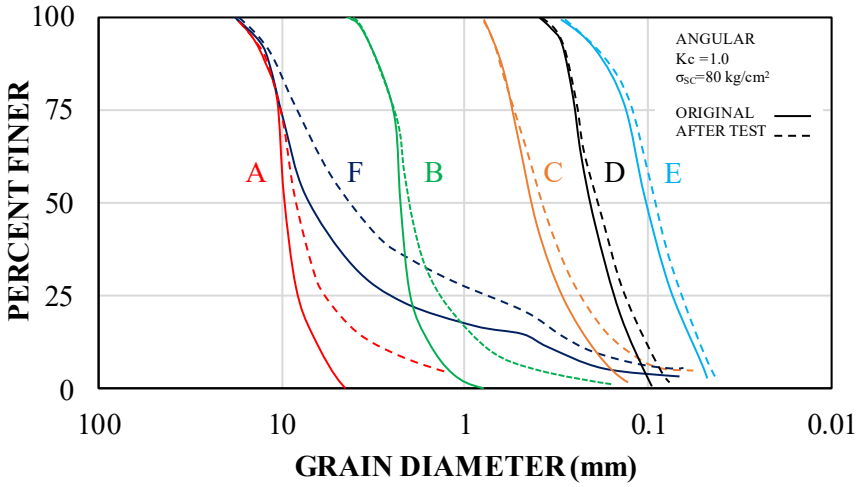

Figure 2.1 Changes in grain size distributions after triaxial tests, After Lee and Farhoomand (1967)

Furthermore, it can be observed that there is a level of stress from which the particle breakage begins to be more significant. The stress level in a soil sample is transmitted to the particles and, obviously, with higher stress level, contact forces between particles are higher. As a result, there is a higher probability of particles breakage. This aspect was observed in the experimental study of drained and undrained triaxial compression and extension tests at high pressures presented by Lade et al. (1996). In those tests confining pressures from 0.5 to 70 MPa on dense Cambria sand were applied. After testing, a sieve analysis was performed on the dried soil to evaluate the grain-size distribution. The results from triaxial tests showed that high confining pressures cause large amounts of particle crushing. However, it was highlighted that triaxial compression tests exhibited higher amounts of particle

crushing than triaxial extension tests. Lade et al. (1996) also showed that if uniform sand is crushed, the grain size distribution resulting from large compressive loads gradually approaches that of a well graded soils as the load increases.

Tarantino and Hyde (2005) observed the effect of crushing on shear strength properties by using simple direct shear tests on carbonate sand. The shear tests were carried out on monogranular and fractal grains at vertical stresses ranging from 0.2 to 1.4 MPa and horizontal displacements from 0.5 to 8 mm. In order to compare particle breakage with different particle sizes, specimens were prepared with a sample height of about $20 \cdot D_{50}$. Grain size distributions were measured before and after shearing. These authors found that the apparent critical state friction angle contain both frictional and clastic components and concluded that the apparent critical state angle of friction increases as the rate of particle crushing (normalized with respect to the normal force) increases.

According to the literature, other factors that influence the amount of particle breakage in a soil are the initial void ratio and particle shape. Particle breakage increases with increasing initial void ratio because higher void ratios generally determine a smaller number of particle contacts in a coarse-grained soil (Lade et al., 1996; McDowell and Bolton, 1998; Nakata et al., 2001).

As widely recognized in the literature (Lee and Farhoomand, 1967; Hardin, 1985; Lade et al., 1996), particle breakage increases if the particle angularity increases. Angular particles break more easily

because stresses can concentrate along their sharp edges. Stresses can also concentrate at angular contact points, causing their crushing.

Furthermore, a stiffer specimen would suffer more particle damage by sustaining larger stresses during constant volume-undrained shear (Nakata et al., 2005).

The particle breakage is also influenced by the variation in the degree of saturation of the material. Several authors (Sowers et al., 1965; Nobari and Duncan, 1972; Oldecop and Alonso, 2001) showed that flooding rockfill specimens subjected to one-dimensional compression lead to a sudden settlement (volumetric collapse) attributed also to the breakage of particles due to rock weakening induced by wetting.

Nobari and Duncan (1972) carried out a systematic investigation of the factors that influence the collapse of rockfill upon flooding. Their work included one-dimensional and triaxial compression tests on crushed argillite. They found that the initial water content is the most important factor determining the amount of collapse upon flooding: the larger is the initial water content, the smaller is the collapse deformation. Sieve analysis carried out before and after flooding the samples showed that during collapse some particle crushing occurs. This observation suggests that the reduction of rock strength due to wetting may be the mechanism that determines the volumetric collapse behaviour. Nobari and Duncan (1972), showed that one of the major factors contributing to the development of differential movements during reservoir filling is

the compression due to wetting which occurs in a wide variety of different types of soils. They observed that the introduction of water into a collection of susceptible particles, such as when raising the reservoir behind a rockfill dam for the first time, also causes particle breakage; this results in settlements in the dam.

Wetting performed during triaxial testing on large diameter specimens (e.g. Terzaghi, 1960) also identified the partial collapse during the combined effect of mean and deviatoric stress and the reduction of strength of flooded samples if compared with the “dry” ones.

Particle breakage has a significant effect on the mechanical behaviour of rockfill. In a triaxial test on gravel specimen prone to crushing, the dilatancy of the material decreases considerably. If the confining pressure increases, there is a point where the dilatancy can disappear.

Dilatancy depends strongly on the particle angularity and roughness (Santamarina and Cho, 2004). These authors hypothesize that angularity will add difficulty to particle rotation, roughness will hinder slippage, and both will enhance dilatancy and anisotropy. In the case where the elongated particles are oriented horizontally with their larger size the dilatancy will be reduced since the sliding tends to occur above the smaller particle size. In the case in which the greater size corresponds to the vertical one, the dilatancy is increased. When there is a combination of confinement pressure and intergranular forces, such that at some point the particle resistance is exceeded and a particle failure happens, a rearrangement occurs.

The breakage and rearrangement of the particles reduce the dilation component.

On the other hand, in an oedometric test the particle breakage increases the compressibility of the material. In various laboratory oedometer tests on granular materials performed at typical rockfill dam vertical stress levels (usually lower than 3 MPa), according to McDowell and Bolton (1998) and as elaborated by Oldecop and Alonso (2001), there is a point from which the compressibility of the material changes. In the vertical stress-strain curve there is a point where the slope of the curve changes slightly, this change in tendency has been attributed to the beginning of the particle breakage.

2.2.2 A conceptual model for rockfill prone to crushing

Breakage is the result of crack propagation inside particles. Considering the classical theory of fracture mechanics and according to subcritical crack propagation phenomenon, Oldecop and Alonso (2001) elaborated a conceptual model for rockfill volumetric deformation (Figure 2.2). In this model the crack propagation velocity depends on the stress intensity factor of the crack, K. The K factor is a function of the crack length, the applied load, the geometry and the size of the body containing the crack and the loading mode (tensile, shear normal to crack tip or shear parallel to crack tip). The value of K that marks the onset of crack

propagation for a given material is called fracture toughness, K_C, and can be obtained for each load mode.

According to Oldecop and Alonso (2001), in a steady situation the rockfill does not deform. However, when a load increment is applied to rockfill, cracks with stress intensities higher than a critical value (fracture toughness K_C) propagate immediately, particles break and, at the volume element level, an instantaneous increment of strain is observed (associated with sudden compression). Instead, cracks with stress intensities smaller than K_C but greater than the limit value (stress corrosion limit, K_0) propagate with time until failure and cause the time-dependent component of deformation. Under constant load, the number of cracks with stress intensities greater than K_0 but smaller than K_C will decrease with time, implying a reduction of strain rate with time.

On the other hand, the theory of stress corrosion establishes that the atomic links at the tip of a crack are more vulnerable to a corrosive agent that those located far away from the tip. As part of their research Oldecop and Alonso (2001) suggest that water has a corrosive effect and as consequence produces the softening of the material. This softening will develop cracks for lower values of K_C.

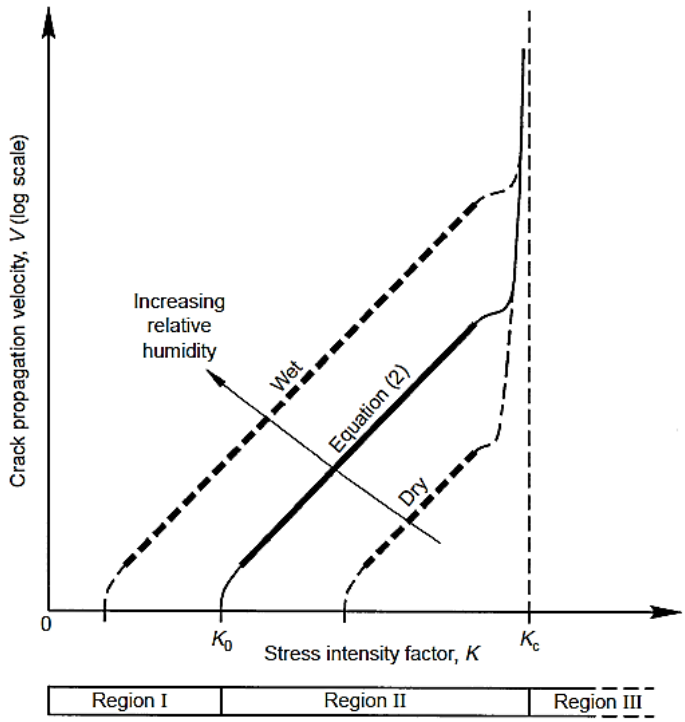

Figure 2.2 Schematic subcritical crack growth curves and conceptual model of rockfill volumetric deformation, Oldecop and Alonso (2001)

The authors used a theoretical thermodynamic formulation to introduce a direct relationship between crack propagation velocity, stress intensity factor, and relative humidity (RH) of the air in connection with crack tips. The thermodynamic balance at the environment implies that the liquid and gaseous phases held the same chemical potential, and then they produce the same corrosion effect and the same speed of propagation of cracks. It means that whether the corrosive agent (water) is in a liquid or gas state it will produce the same corrosion. The only parameter controlling the

speed of propagation of cracks is the relative humidity (RH). The use of RH in the thermodynamic formulation is a convenient way to measure the chemical potential of the corrosive agent, that is water, which governs the rate of the corrosion reaction under constant K (Wiederhorn et al., 1982). In fact, if RH increases at a given time, cracks with stress intensities greater than K_0 but smaller than K_C will increase their propagation velocity, causing a sudden increase in the strain rate. The increase in the RH causes a decrease in K_0 and therefore more cracks will have stress intensities greater than K_0, causing an additional amount of strain. This explains the volumetric collapse observed in rockfill structures, so an increment of rockfill strain not related to an increment in load (Oldecop e Alonso, 2001).

2.2.3 Measures of grain breakage

The amount of particle crushing that occurs in a granular material influence most of the engineering properties such as stress-strain behaviour, volume change and variation in permeability. It is important to quantify the amount of particle breakage and its effect on engineering properties. The problem is to choose a measure that adequately integrates the breakage occurring in the various size fractions of the material.

Particles do not share equally in the bearing of the applied load but some of them carry more load than others. The particles with highly loaded contacts are usually aligned in chains (Cundall and Strack, 1979). Crushing starts when these highly loaded particles fail and break into smaller pieces that move into the voids of the original

material. These load chains change in intensity and direction as the crushing develops in the particle assemblage. On crushing, fines are produced and the grain size distribution curve becomes less steep. Consequently, with continued crushing, the soil becomes less permeable and more resistant to crushing (Al Hattamleh et al.). The grain size distribution is a suitable measure to assess the extent of crushing (Hardin, 1985; Lade et al., 1996; Tarantino and Hyde, 2005; Einav, 2007).

For this reason, several authors proposed different particle breakage factors by using a single number or measure. The most widely used particle breakage indices are the ones (Figure 2.3) developed by Marsal (1967), Lee and Farhoomand (1967), and Hardin (1985).

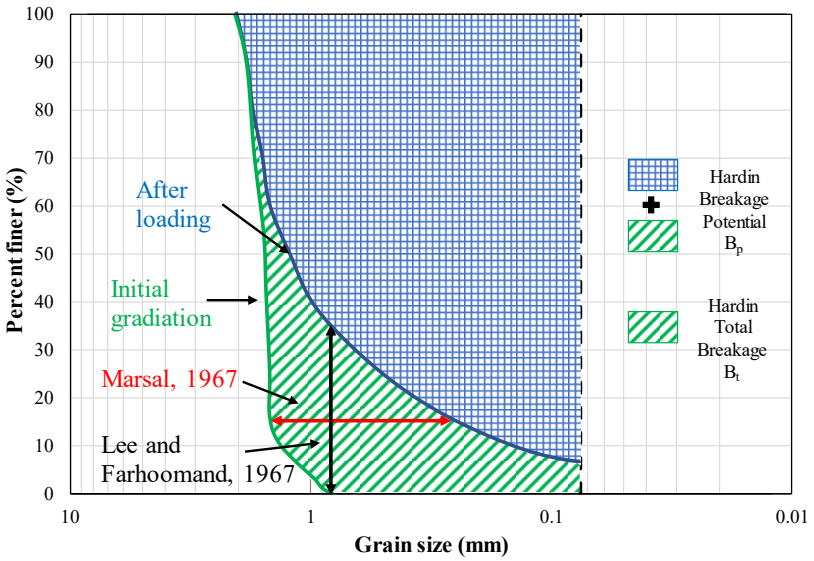

Figure 2.3 Definitions of Particle Breakage Factors Proposed by Marsal (1967), Lee and Farhoomand (1967) and Hardin (1985); After Lade et al. (1996)

Marsal (1967), with reference to triaxial and one-dimensional strain testing of rockfill materials, observed that the most important factor affecting both shear strength and compressibility is the particle breakage undergone by a granular body when subjected to changes in its state of stresses, both during the uniform compression stage and during deviator load application. He subsequently developed a breakage index, B_g, to quantify this breakage. Marsal's breakage index is calculated from the changes in individual particle sizes between the initial and final grain-size distributions. The difference in the percentage retained is computed for each sieve size. This difference will be either positive or negative. Due to the particle breakage, the percentage of the particles retained in large size sieves will decrease and the percentage of particles retained in small size sieves will increase (Aghaei-Araei et al., 2010). Marsal's breakage factor, B_g, is the sum of the differences having the same sign. The lower limit of Marsal's index is zero percent instead the theoretical upper limit is 100%.

Lee and Farhoomand (1967) based on studies on earth dam filter materials have proposed a breakage index. They performed a series of isotropic and proportional loading tests on sands to study particle breakage. According to the authors, the breakage factor expressing the change in a single particle diameter, namely that corresponding to 15% finer on the grain-size distribution curves before and after testing. These grain sizes were chosen because gravel filter drainage requirements were commonly based on this particle size. Their measure of particle breakage was expressed as the ratio

$D_{15(initial)}$/ $D_{15(final)}$. Since particle size is plotted on a log scale, this ratio is determined by the horizontal distance between particle size distribution curves at 15% finer. The lower limit of this ratio is unit and there is no upper limit.

Hardin (1985) based his measure of particle breakage on changes in the entire particle-size distribution. He defined new measure to account for particle breakage, called breakage potential (B_p), total breakage (B_t) and relative breakage (B_r). The breakage potential B_p is equal to the area between a uniform curve corresponding to a grain size equal to 0.074 mm (corresponding to silt size) and the part of the initial gradation curve for which D > 0.074 mm (Figure 2.3).

Hardin (1985) limited the lower grain size to the No. 200 U.S. sieve size because there is limited amount of crushing below this size. It is also more difficult to obtain particle size distributions below this particle size using a standard sieve analysis (Lade et al., 1996).

The total breakage B_t is defined as the area between the original grain size distribution curve and the final grain-size distribution curve, as shown in Figure 2.3. At the end, the relative breakage B_r is the ratio of total breakage divided by the potential breakage (B_t/B_p). The relative breakage has a lower limit of zero and a theoretical upper limit of unit and seems to be approximately independent of particle size distribution.

These particle breakage factors satisfy the need for measurements of particle breakage so the amount of particle crushing can be quantified and reasonable comparisons can be made.

2.3 Oedometric and triaxial tests on rockfill at different degree of saturation

It is widely recognized in the literature that the water content influences the behaviour of rockfill, both in isotropic and deviatoric conditions. Several in situ tests have shown that wetting may induce large settlements in rockfill structures. This is a well-known phenomenon which has received a continuous interest ever since the widespread use of rockfill in dams. In these structures the water impoundment has been associated with a rapid collapse settlements but strong rainfalls may also contribute to significant volumetric deformations during the early life of dams. However, collapse phenomena of coarse-grained soils have been observed also in laboratory tests (Sowers et al., 1965; Nobari and Duncan, 1972; Marsal, 1973; Oldecop and Alonso, 2001) as shown in the following sections.

2.3.1 Oedometric tests

The mechanical behaviour of rockfill in oedometric conditions was investigated by several authors (Fumagalli, 1969; Nobari and Duncan, 1972; Marsal, 1973; Oldecop and Alonso, 2001).

Oldecop and Alonso (2001) presented the results of oedometric tests on a quartzitic slate rockfill in which the pore air relative humidity was controlled. An oedometer test program, including five tests, was carried out in a Rowe-type cell, 300 mm sample diameter and an approximate sample height of 200 mm. The experimental programme included three classic oedometer tests with specimen

flooding at some confining stress (tests 1, 2 and 3) and two oedometer tests with relative humidity control (tests 4 and 5) as shown in Figure 2.4. It can be seen that the amount of collapse strain observed on flooding in test 3 is very close to the strain difference between the normal compression lines (NCL) corresponding to the dry state and the saturated state. The subsequent loading after collapse leads to a stress-strain curve that follows the NCL for the saturated material obtained in tests 1 and 2. Test 4 has the same stress path of test 3 but wetting was induced by increasing the relative humidity of the pore air by steps up to 100%. Despite the specimen in the test 4 was never flooded (contrary to what happened in test 3), the amount of collapse was almost the same observed in test 3. So, the main conclusion of this experimental programme is that bringing the relative humidity to 100% within the rockfill voids leads to a collapse strain equal to that observed in flooded specimens.

Any situation leading to a change in water content of the rock particles can cause collapse deformations and also increase the material compliance against further loading. This conclusion is consistent with the rain-induced settlements observed in rockfill dams and embankments. On the basis of these results, Oldecop and Alonso (2001) proposed an elastoplastic constitutive model for rockfill compression. It considers a threshold confining stress that marks the transition between the particle rearrangement and clastic yielding.

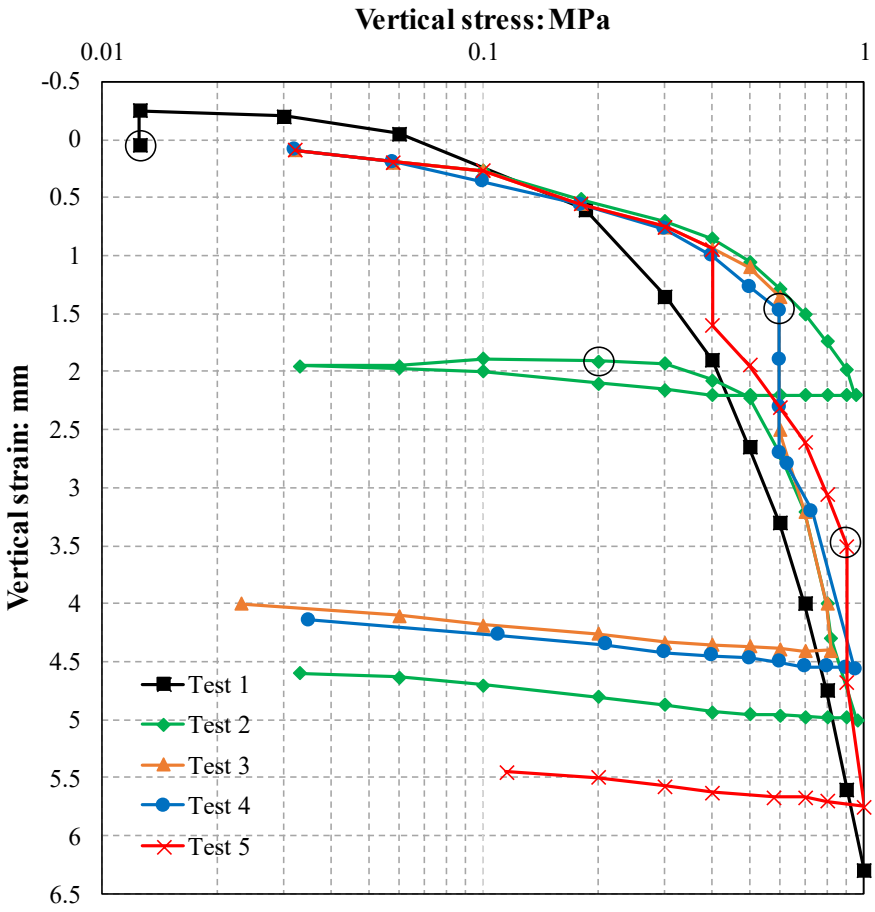
Vertical stress: MPa
0.01
0.1
1
Vertical strain: mm
-0.5
0
0.5
1
1.5
2
2.5
3
3.5
4
4.5
5
5.5
6
6.5
Test 1
Test 2
Test 3
Test 4
Test 5

a)

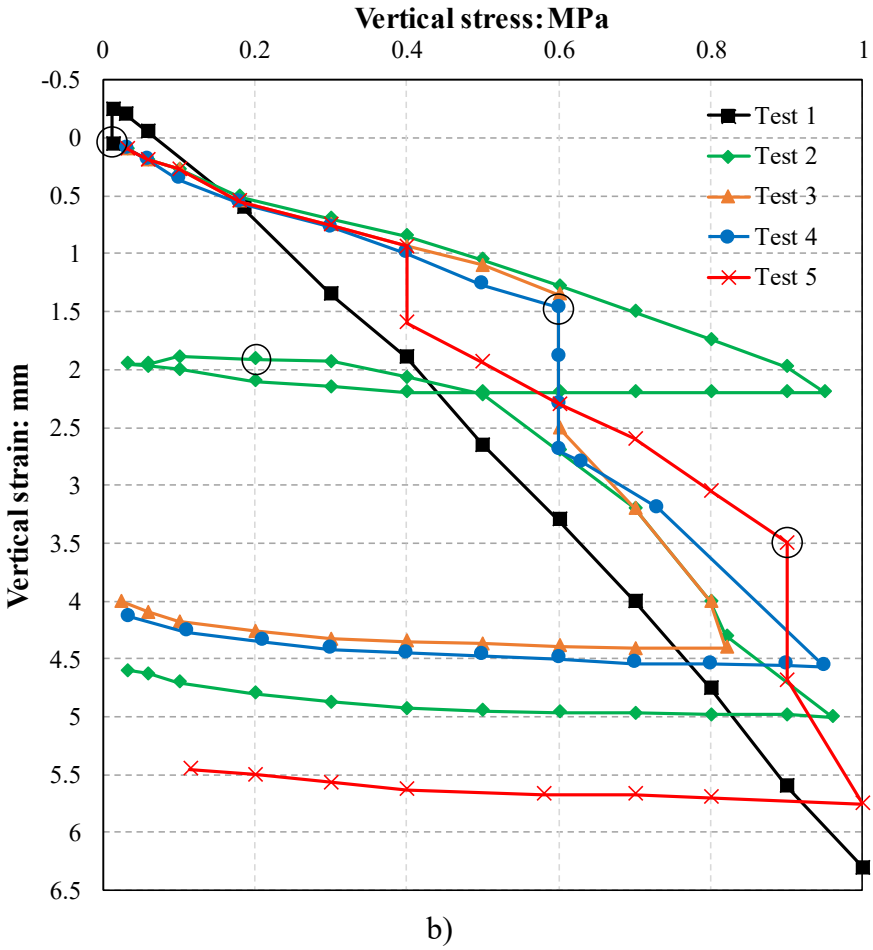

Figure 2.4 Results of one-dimensional compression test on rockfill: a) vertical stress in logarithmic scale; b) (overleaf) vertical stress in natural scale. Broken lines indicate the saturated condition of rock pores (either by specimen flooding or by RH increase). Open circles indicate specimen flooding (after Oldecop and Alonso, 2001)

Figure 2.5 shows a collection of flooding collapse strain measurements, for different rockfill materials tested in oedometric

devices, under various vertical stresses, in the range of engineering interest (Oldecop and Alonso, 2013).

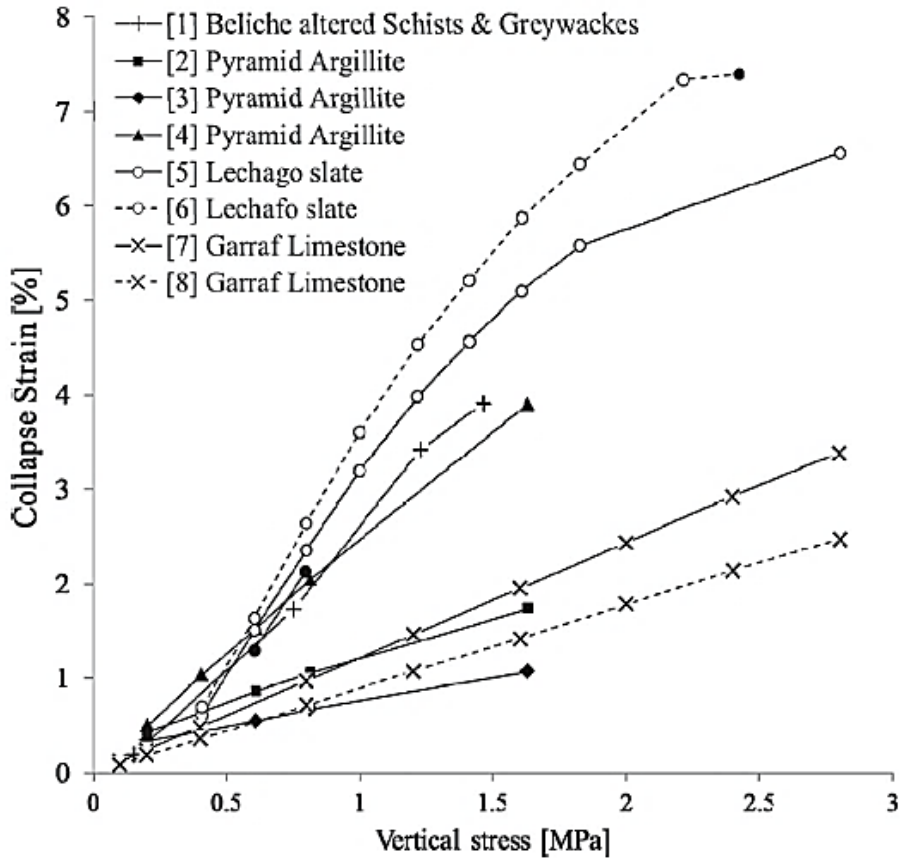

Figure 2.5 Collapse strains following flooding of rockfill specimens tested in oedometer (Oldecop and Alonso, 2013)

Filled symbols correspond to values really measured while open symbols to collapse amounts derived by difference between compression curves of dry and flooded specimens. It is evident that collapse strain increases with stress almost linearly for most rockfill materials and that it does not tend to vanish under high stresses, as

observed in sands (Alonso et al., 1990). However, linearity is lost for specimens of weak rock undergoing high strain levels. By comparing the features of the different materials included in Figure 2.5, the authors concluded that the collapse deformations increase for: 1) weaker rock particles, 2) larger particle size 3) grain size uniformity, 4) lower relative density, 5) lower initial moisture. All these observations are consistent with the hypothesis relating collapse with particle breakage (Oldecop and Alonso, 2013).

2.3.2 Triaxial tests

The study of the influence of water in the mechanical behaviour of rockfill material was performed in triaxial apparatus by Chávez (2004) and Ortega (2008). They used the same grain size distribution but two different rockfill materials: Lechago slate rockfill and Garraf Limestone respectively.

The authors performed an experimental programme in the triaxial cell designed to test specimens of 250 mm diameter. Tests (consolidated/drained) carried out on a rockfill with a maximum particle size of 40 mm showed how the shear strength and the dilatancy of rockfill under shear are incremented when the relative humidity (in equilibrium with the material) decreases. The results are shown in Figure 2.6. The mentioned effects are more pronounced in the Lechago slate rockfill than in the tougher Garraf Limestone. According to the authors the particle breakage was enhanced by the humidity of the rockfill, and it is responsible for the loss of strength and dilatancy diminution.

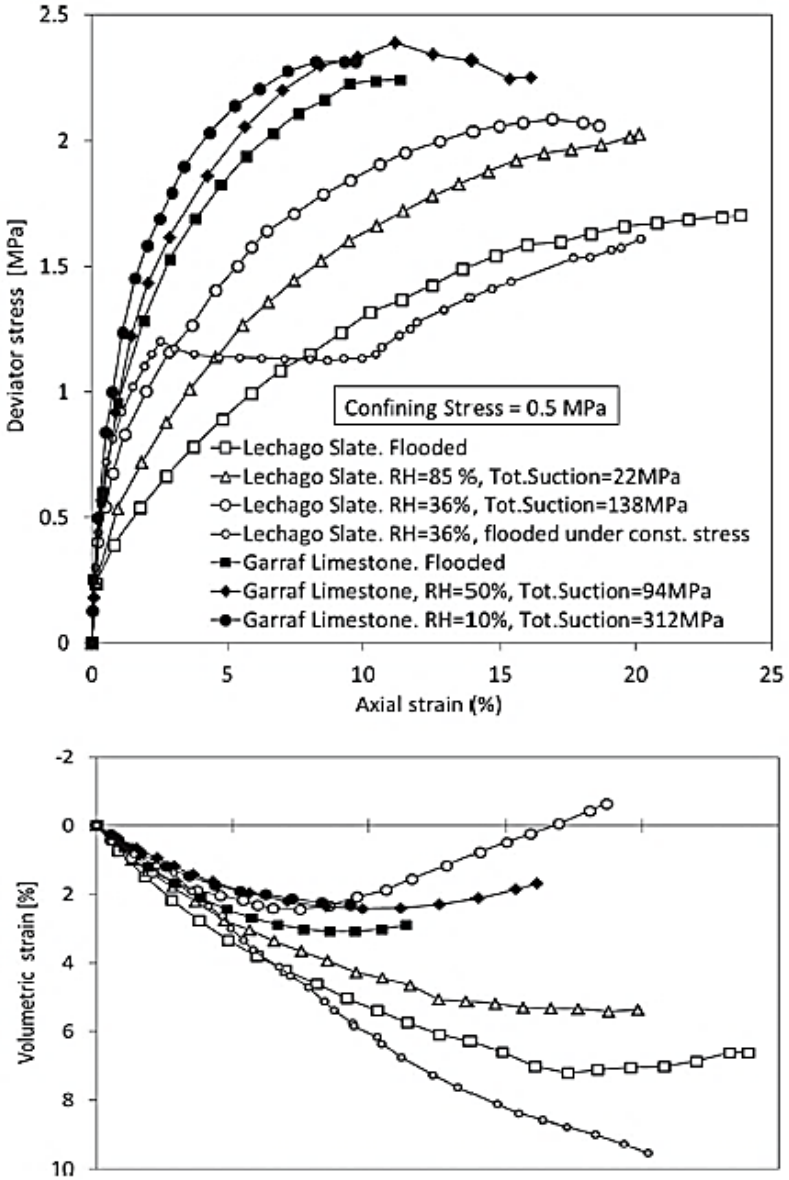

Figure 2.6 Triaxial tests of rockfill with RH control. Data of Lechago slate obtained by Chávez (2004) and from Garraf Limestone obtained by Ortega (2008) and reported by Oldecop and Alonso (2013)

In the experimental programme reported by Chávez (2004) there is a test in which a gradual wetting path under constant stress was performed by means of a relative humidity (RH) control system. RH was increased up to 100% and the sample was finally flooded. The effect of wetting was a gradual increase of axial and volumetric strain (both in compression). In this test the strains due to wetting are greater than those exhibited by the saturated specimen subjected to the same stress state. The author justifies this phenomenon as a result of both humidification induced collapse and time-dependent deformation since the test took a significantly longer time than the others in the same figure.

Alonso et al. (2016) reported the results of suction-controlled triaxial tests performed on compacted samples of two well-graded granular materials in the range of coarse sand–medium gravel particle sizes: a quartzitic slate and a hard limestone (Figure 2.7 and Figure 2.8). Specimens exhibit a ductile behaviour under all the stress and suctions tested. For a given vertical strain, the mobilized deviatoric stress is systematically smaller for tests conducted at RH = 100%. Strong positive dilatancy is recorded during the initial applications of deviatoric stresses; this is a consequence of particle breakage and grain contact crushing. Dilatancy rates decrease continuously as the deviatoric strains accumulate. It was evident the profound effect of RH on dilatancy. Low RH values (high suction) enhance dilatancy (volumetric expansion) and reduce volumetric contraction. This is explained by the reduced rate of crack propagation in particles in the presence of high suctions.

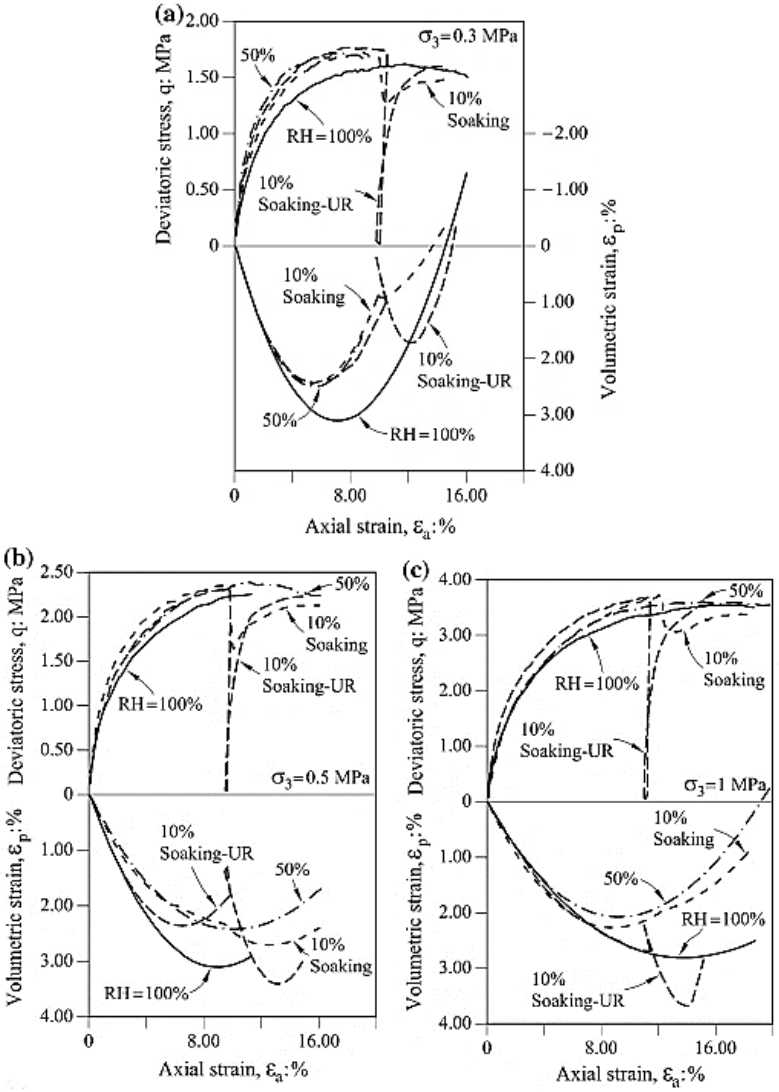

Figure 2.7 Suction-controlled triaxial tests on W samples of Garraf limestone under a) σ_3 = 0.3 MPa; b) σ_3 = 0.5 MPa; c) σ_3 = 1 MPa (Alonso et al., 2016)

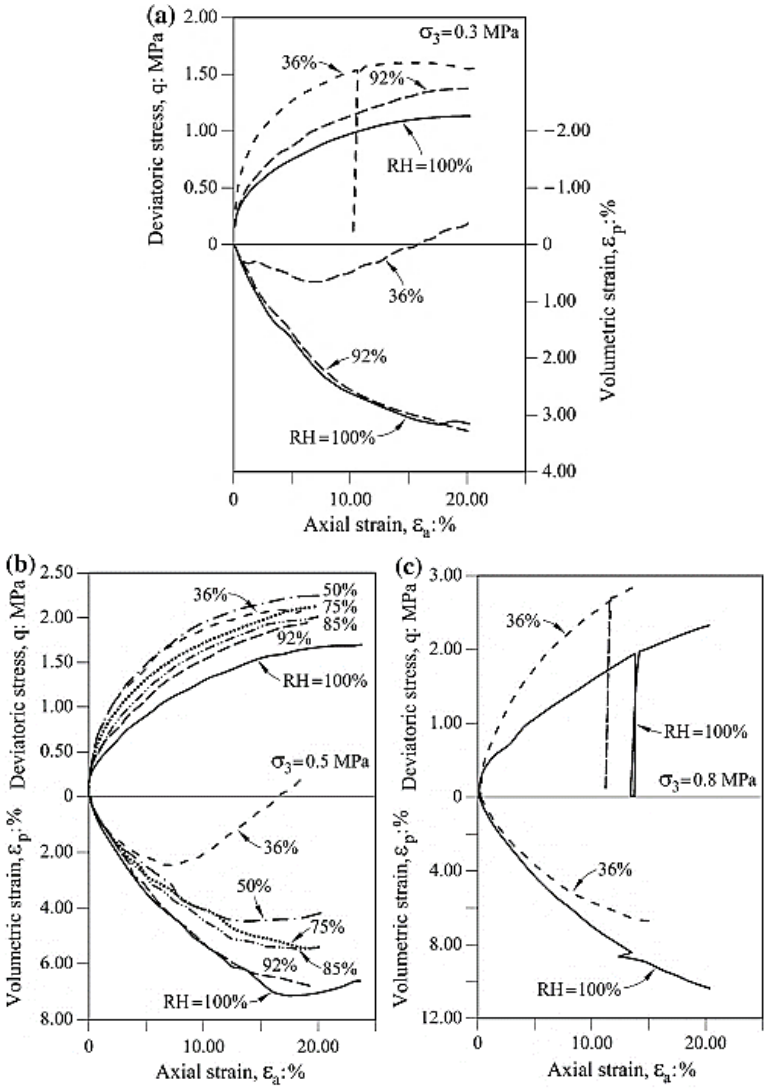

Figure 2.8 Suction-controlled triaxial tests on Pancrudo slate under a) σ_3 = 0.3 MPa; b) σ_3 = 0.5 MPa; c) σ_3 = 0.8 MPa (Alonso et al., 2016)

As recognized in the literature, water effects are associated with particle breakage because the velocity of crack propagation is

significantly affected by relative humidity or total suction. The slate gravel is expected to be more sensitive to water effects, if compared with the limestone gravel (Alonso et al., 2016).

2.4 Dilatancy and strength

The shear resistance of granular materials is the result of interparticle friction and dilation. Taylor (1948) considered shearing resistance to be a question of energy consumption such that external work is dissipated by internal friction and volumetric changes. Rowe (1962) developed Taylor's original work equation into a stress-dilatancy relationship in which the components of shearing resistance due to inter-particle friction and volumetric changes are described mathematically by the critical state friction angle (φ'_{cv}) and dilatancy angle (ψ), respectively, resulting in Equation 2.1:

$$\varphi' = \varphi'_{cv} + \psi \tag{2.1}$$

with φ' mobilized friction angle. The mobilized friction angle represents the frictional resistance which may be mobilized in a soil element at a specific level of deformation.

Equation 2.1 may also be expressed in terms of the stress components acting on the plane of shearing using the following relation:

$$\left(\frac{\tau}{\sigma'}\right) = \tan(\varphi') = \tan\left(\varphi'_{cv} + \psi\right) \tag{2.2}$$

with τ = shear stress and σ' = normal effective stress.

For axisymmetric conditions, such as those of triaxial testing, φ' may be deduced from the Mohr's circle of stress through Equation 2.3:

$$\sin(\varphi') = \frac{\frac{\sigma'_1}{\sigma'_3} - 1}{\frac{\sigma'_1}{\sigma'_3} + 1} \quad (2.3)$$

where $\sigma'_1/\sigma'_3 = N$ = flow number, stress obliquity, or effective principal stress ratio.

According to Rowe (1962), depending on the confining pressure and density, the mobilized friction angle at the onset of dilation, φ' varies in the range:

$$\varphi'_\mu \leq \varphi' \leq \varphi'_{cv} \quad (2.4)$$

with φ'_μ the interparticle friction angle associated with resistance to interparticle sliding. The mobilized friction angle φ' depends on the particle packing arrangements and the number of sliding contacts.

A stress-dilatancy relationship for plane strain based on minimum energy assumptions (Rowe, 1962; De Josselin de Jong, 1976) can be described as:

$$N = M \cdot N_c \quad (2.5)$$

with M the dilatancy number and N_c the flow number at critical state that can be expressed as follow:

$$M = \frac{1+sin\psi}{1-sin\psi} = tan^2(45° + \frac{\psi}{2}) \quad (2.6)$$

$$N_c = \frac{1+sin\varphi_c}{1-sin\varphi_c} = tan^2(45° + \frac{\varphi'_{cv}}{2}) \quad (2.7)$$

The value of ψ is observed to approach a maximum at the minimum dilatancy rate in typical granular soils (Schofield and Wroth, 1968) and can be deduced for axisymmetric conditions from the Mohr's circle of strain as:

$$\sin(\psi) = \frac{\frac{d\varepsilon_1}{2d\varepsilon_3}+1}{\frac{d\varepsilon_1}{2d\varepsilon_3}-1} \quad (2.8)$$

Taylor (1948) and Rowe (1962) recognized that the mobilized friction angle must take into account the sliding resistance at contacts as well as dilation owing to particle rearrangement and overriding each other. However, in the presence of particle crushing, Taylor's work equation is invalidated as energy consumption due to particle breakage leads to additional work being dissipated within the soil element (Tarantino and Hyde, 2005). In soil that may exhibit significant changes in particle size and/or shape during loading, a third component associated with energy dissipation due to particle breakage is required for an accurate analysis of the mechanical response.

In the stress-dilatancy equation based on energy principles presented by Rowe (1962), the friction and dilation angle were assumed to be constant. However, the dilatancy changes during deformation due to factors such as stress level, void ratio and particle crushing. Bolton (1986) by means of laboratory tests on different sands, observed the overestimation of the dilation angle proposed by Rowe (1962) and suggested the following relation between the peak (φ'_p) and the critical state (φ'_{cv}) angles:

$$\varphi'_p = \varphi'_{cv} + 0.8\,\psi \quad (2.9)$$

Bolton (1986) further proposed that the relationship between φ'_{cv} and the mobilized friction angle at peak conditions, φ'_p, can be expressed using the relative dilatancy index, I_R:

$$\varphi'_p - \varphi'_{cv} = A_\psi I_R \quad (2.10)$$

where A_ψ is equal to 3 and 5, for axisymmetric and plane-strain conditions, respectively. For each set of boundary conditions, I_R can be expressed as:

$$I_R = -\frac{10}{3}\left(\frac{d\varepsilon_v}{d\varepsilon_1}\right)_{max} \tag{2.11}$$

with ε_v the volumetric strain. The relative dilatancy index may be related to the relative density (D_R) and the peak mean effective stress (p'_p) as follow:

$$I_R = \frac{D_R}{100}\left[Q - ln\left(\frac{100p'_p}{p_A}\right)\right] - R \tag{2.12}$$

with p_A the reference stress and Q, R intrinsic parameters of the material. Therefore, Bolton (1986) accounted for the combined effects of the state variables (D_R and p'_p) and particle breakage through the relative dilatancy index, I_R.

2.5 Critical state condition for granular soils

The critical state condition is a limit condition for which the deformations can develop indefinitely without volume or effective stress changes. The acceptance of a critical state line allows for an evaluation of the qualitative response expected in any triaxial compression test on a soil with a consolidation history.

The critical state concept has been developed based on the experimental and analytical research undertaken from 1950 to 1970 (Roscoe et al., 1958; Roscoe and Schofield, 1963; Roscoe and Burland, 1968). It was successfully applied to clay during shearing under drained or undrained condition (Roscoe et al., 1958). Over the last few decades, many additional experimental tests have been

performed on several types of soils (e.g. sand, rock). They generally confirm the validity of the critical state mechanics (e.g. Been and Jefferies, 1985; Wood, 1990; Klotz and Coop, 2002).

The application of the general concept of critical states to sands was less successful and is still debated because of the difficulty in determining the critical state line (CSL) in the laboratory (Wroth and Bassett, 1965; Vesic and Clough, 1968; Been et al., 1991; Coop and Atkinson, 1993). The measurement problems were apparently resolved by Castro (1969) who used undrained, stress-controlled triaxial tests on very loose sands to obtain a steady state line. Generally, critical state is associated with drained test and steady state with undrained test. Been et al. (1991) reported a series of laboratory tests carried out on sand in which the steady state line and the critical state line are coincident. This observation seems to be supported by other studies (e.g. Verdugo and Ishihara, 1996; Jefferies and Been, 2006). The critical state line reported by Been et al. (1991) is a curved line and it can be approximated as bilinear line. The critical and steady states are shown to be independent of stress path, sample preparation method and initial density. Hence, results suggested that the critical state friction angle in sands may be a function of the critical state void ratio.

With reference to the unique critical state, Wroth and Bassett (1965) and Been and Jefferies (1985) proposed to use a state parameter to characterise the state of a sand. Been and Jefferies (1985) proposed the state parameter Ψ as a semiempirical normalizing parameter for sand behaviour. The state parameter Ψ defines the void ratio (e) and

mean stress level (p') of a sand relative to a reference state (the steady state) as shown in Figure 2.9 (Been and Jefferies, 1985).

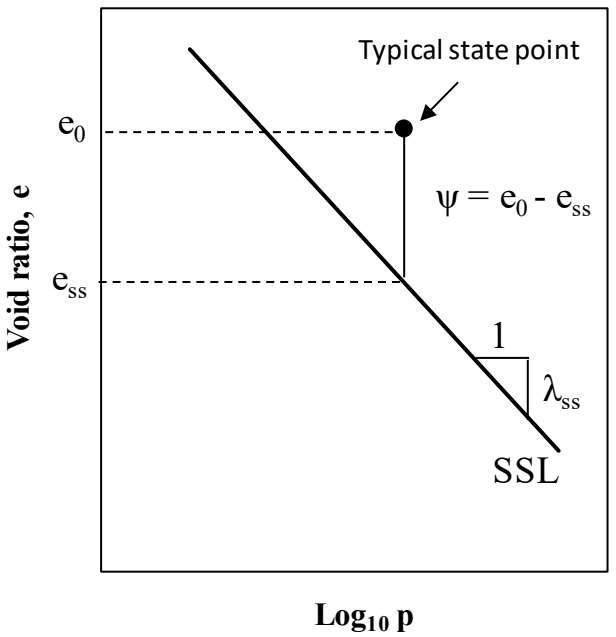

Figure 2.9 Definition of state parameter (after Been & Jefferies, 1985)

This concept requires knowledge of the critical/steady state line, which provides a reference state from which the state parameter and the most important sand behaviours are derived.

However, many experimental investigations have been carried out on sands to find the effect of different parameters influencing the critical state/steady state. Critical state has enabled to interpret the response of monotonically and cyclically loaded gravels with an elasto-platic model by Modoni et al. (2011).

It has been concluded by various researchers that the critical state is mainly influenced by effective confining pressure (Konrad J., 1990; Been et al., 1991; Vaid et al., 1990) but, at present, the influence of particle breakage on the gradient and location of the CSL in the e-log(p) space has not been fully clarified. The problem is which roles particle breakage and current gradation play in determining the location of the CSL in e-log(p) space in rockfill material. In fact, at high stress levels particles undergo breakage that results in a continuous change of soil gradation and this becomes important in the critical state framework.

The CSL for individual soils over a large range of pressures have been described by a three parts mathematical formulation, as shown in Figure 2.10 (Ghafghazi et al., 2014). This is consistent with the three zones of behaviour identified by Vesić and Clough (1968): very low stress where dilatancy controls behaviour and breakage is negligible; elevated stress where breakage becomes more pronounced and suppresses dilatancy effects; and very high stress where the effects of initial density vanish, very little void space remains within the material, and soil behaves like an elastic material.

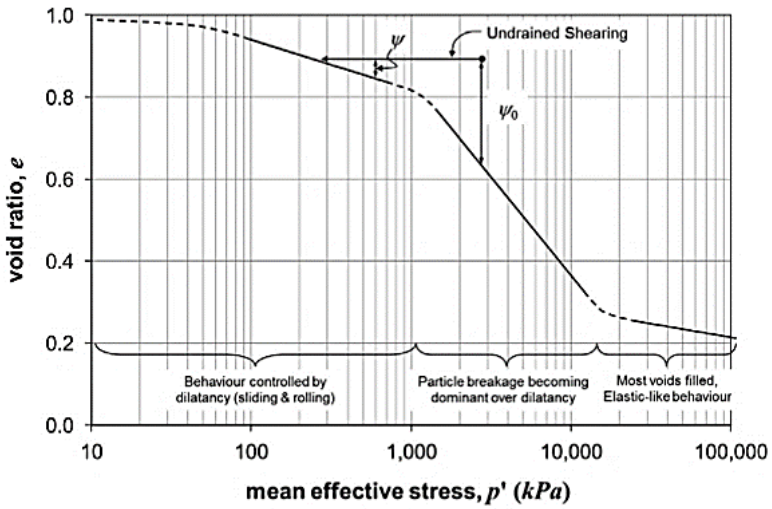

Figure 2.10 Full stress range CSL in e–log p' space and a schematic undrained triaxial test (Ghafghazi et al., 2014)

Been et al. (1991) showed that the critical state line for Erksak sand has a break in the line occurring at a stress level of about 1 MPa and that this break is probably due to a change in shearing mechanism at this stress level, to one in which breaking or crushing of sand grains becomes significant. Other experimental investigations on sands revealed a unique CSL in the e-log(p) space, which steepened at a higher pressure with the onset of great particle crushing (Been and Jefferies, 1985; Verdugo and Ishihara, 1996). The particle breakage causes grading changes producing a different material with different basic constitutive properties such as critical states volumetric conditions. So, it is accepted that grading evolution influence the mechanical response of granular materials (Wood and Maeda,

2008). Obviously, this phenomenon is more evident in rockfill prone to crushing.

In order to highlight the effect of the particle breakage on the critical state, Wood and Maeda (2008) suggested to determine a gradation index I_G which was defined as the ratio of the area under the current gradation to the area under the final gradation, useful for quantifying the gradation of sand. Consequently, any given soil will have a grading which can be characterised by a value of I_G such that $0<I_G<1$. As expected, the results of DEM analyses reported by the authors showed that the current grading influences the critical state conditions. Projections of the three-dimensional critical state surface (for the crushable soil) onto three coordinate planes are shown in Figure 2.11.

In the conventional compression plane of specific volume vs mean stress (Figure 2.11a) the critical state lines fall as crushing increases (I_G goes from 0 to 1). The dashed line indicates a condition beyond which, if the mean stress increases, crushing would inevitably occur and the operational critical state line would drop.

Contours of constant mean stress in the plane of specific volume and grading state index I_G are shown in Figure 2.11b. The contours are longest at the lowest stress level; the dashed line indicates the limiting combinations of specific volume and grading state index. Finally, Figure 2.11c shows contours of specific volume in the plane of mean stress and grading state index. For any value of I_G there is a limit to the mean stress that can be sustained indicated by the dashed line.

This result is important because it shows that the final CSL is not unique, due to variations in particle breakage with the historic maximum stress.

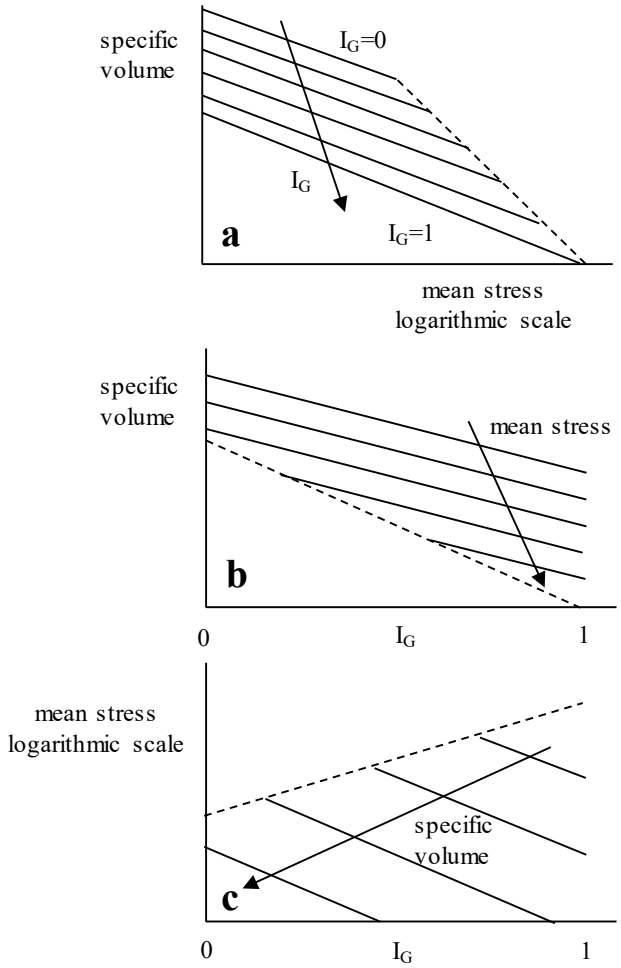

Figure 2.11 Projections of critical state surface for material with change of grading resulting from particle crushing: a) specific volume and mean stress; b) specific volume and grading state parameter; c) mean stress and grading state parameter (After Wood and Maeda, 2008)

Lade et al. (1998) investigated the effect of adding fine particles to a sand and showed that, while the fine particles are merely filling the voids in the coarse material, reference densities for the material rise because the space is filled more efficiently. Once breakage has permitted grains to repack at lower volume, by small fragments fitting large voids, it becomes impossible for granular assemblies to regain the high voids ratios of the initial material.

Cheng et al. (2005) showed that no unique line of final critical voids ratios could be found but they varied with stress-path and stress-history. Soils with different grain size distributions, due to crushing, have different critical voids ratios.

Therefore, the effect of particle breakage was to move the CSL (with no change of gradient) continually downwards. This implies that the constitutive models that include a CSL as a basic feature controlling strength and dilatancy as a function of state parameter (Been and Jefferies, 1985), will be particularly influenced by the possibility of a dynamically changing critical state line and they must therefore be able to incorporate this effect.

2.6 Final remarks

Particle breakage is a factor that significantly affects the volumetric and deviatoric behaviour of granular materials. In general, the greater is the particle breakage, the greater is compressibility and the smaller is dilatancy.

The break is determined by the level of stress, the geological origin of the material, the particle shape and the mechanism of application

of the load (it was observed that in the deviatoric stress paths there is more breakage than the isotropic ones).

It emerges that the shear strength of a dry material is greater than that of a saturated one, but the compressibility of a saturated material is greater than that of a dry material. If the dry material is wet, a volumetric collapse (further deformation) occurs, causing the particle breakage in the material softened by the corrosive action of the water. It is widely accepted that the particle breakage resulting from compression at constant RH up-to a given value of the vertical stress (σ^*_v) and then followed by collapse and that of originally saturated samples compressed at σ^*_v are very similar.

The differences in hydraulic and mechanical behaviour, between fine granular materials (sand) and coarse (gravel, rockfill), are produced by the particle breakage. The sands have less particle breakage than rockfill materials for the same applied stress. It is necessary to apply high stresses so that the breakage of particles in the sand occurs. As a result, sands subjected to heavy stresses behave similarly to rockfill at low stresses.

The crushing of particles influences basic constitutive properties of the soil, such as critical state line (CSL) and dilatancy. A critical state framework where particle breakage shifts down the critical state locus in void ratio versus mean effective stress space without changing its slope was discussed. Particle breakage suppresses dilatancy and increases the mobilized friction angle (Coop et al., 2004; Tarantino and Hyde, 2005). Dilatancy is also suppressed with increasing mean effective stress as reported by Bolton (1986).

Bolton (1986) presented a stress-dilatancy equation which, unlike the one proposed by Rowe (1962), accounts for the effect of state variables and particle breakage.

2.7 References

Aghaei Araei A., Soroush A., Rayhani M.H.T. (2010). *Large-scale triaxial testing and numerical modeling of rounded and angular rock_ll materials*. Scientia Iranica, Transaction A: Civil Engineering, 169-83.

Al Hattamleh O., AlShalabi F., Al Qablan H., Al-Rousan T. (2010). *Effect of grain crushing and bedding plane inclination on Aqaba sand behaviour.* Bulletin of Engineering Geology and the Environment, 69(1), 41-49.

Alonso E. E., Gens A., Josa A. (1990). *A constitutive model for partially saturated soils*. Géotechnique, 40(3), 405-30.

Alonso E. E., Romero E. E., Ortega E. (2016). *Yielding of rockfill in relative humidity-controlled triaxial experiments*. Acta Geotechnica, 11, 455-477.

Barton, N., B. Kjaernsli (1981). *Shear strength of rockfill*. Journal of the Geotechnical Engineering Division. ASCE 107(GT7), 873-891.

Been K., Jefferies M. G. (1985). *A state parameter for sands*. Géotechnique, 35(2), 99-112.

Been K., Jefferies M. G., Hachey J. E. (1991). *The critical state of sands*. Géotechnique, 41(3), 365-381.

Biarez J., Hicher P. Y. (1997). *Influence de la granulométrie et de son évolution par ruptures de grains sur le comportement mécanique de matériaux granulaires*. Revue Française de Génie Civil, 1(4), 607-631.

Bolton M. D. (1986). *The strength and dilatancy of sands.* Géotechnique, 36(1), 65-78.

Castro G. (1969). *Liquefaction of Sand*. Ph.D. Thesis, Division of Engineering and Applied Physics, Harvard University, Cambridge.

Chávez C. (2004). *Estudio del Comportamiento Triaxial de Materiales Granulares de Tamaño Medio con Énfasis en la Influenciade la Succión*. PhD Thesis, Universitat Politècnica de Catalunya, Spain.

Cheng Y. P., Bolton M. D., Nakata Y. (2005). *Grain crushing and critical states observed in DEM simulations*. Powders and Grains – Garcia-Rojo, Hermann and McNamara (eds), Taylor & Francis Group, London, ISBN 0 415 38348 X, 1393-1397.

Coop M. R., Atkinson J. H. (1993). *The mechanics of cemented carbonate sands*. Géotechnique, 43(1), 53-67.

Coop M. R., Sorensen K. K., Bodas-Freitas T., Georgoutos G. (2004). *Particle Breakage during Shearing of a Carbonate Sand*. Géotechnique, 54(3), 157-163.

Cundall P. A., Strack O. D. L. (1979). *A discrete numerical model for granular assemblies*. Géotechnique, 29(1), 47–65.

De Josselin de Jong G. (1976). *Rowe's Stress-Dilatancy Relation Based on Friction*. Géotechnique, 26(3), 527-534.

Einav I. (2007). *Breakage mechanics—part I: theory.* Journal of the Mechanics and Physics of Solids, 55(6), 1274-1297.

Erzin Y., Yilmaz I. (2008). *Case study of crushing resistance of Anatolian sands at lower and higher density*. Bulletin of Engineering Geology and the Environment, 67(1), 71-77.

Ghafghazi M., Shuttle D. A., DeJong J. T. (2014). *Particle breakage and the critical state of sand*. Soils and Foundation, 54(3), 451-461.

Hagerty M. M., Hite D. R., Ulrich C. R., Hagerty D. J. (1993). *One-Dimensional-High Pressure Compression of Granular Media*. ASCE Journal of Geotechnical Engineering, 119(1), 1-18.

Hardin B. O. (1985). *Crushing of soil particles*. ASCE Journal of Geotechnical Engineering, 111(10), 1177–1192.

Jefferies M., Been K. (2006). *Soil liquefaction: A critical state approach*. CRC Press.

Klotz E. U., Coop M. R. (2002). *On the identification of critical state lines for sands*. Geotechnical Testing Journal, 25(3), 289-302.

Konrad J. (1990). *Minimum undrained strength of two sands*. Journal of Geotechnical Engineering, ASCE, 116(6), 932-947.

Lade P. V., Liggio C. D., Yamamuro J. A. (1998). *Effects of non-plastic fines on minimum and maximum void ratios of sand*. Geotechnical Testing Journal, 21(4), 336-347.

Lade P. V., Yamamuro J. A., Bopp P. A. (1996). *Significance of particle crushing in granular materials*. ASCE Journal of Geotechnical Engineering, 122(4), 309–316.

LaRochelle P., Leroueil S., Trak B., Blais-Leroux L., Tavenas F. (1988). *Observational approach to membrane and area corrections in triaxial tests*. Adv Triaxial Test Soil Rock STP 977, 715–731.

Lee D. M. (1992). *The angles of friction of granular fills*. Ph.D. dissertation, University of Cambridge.

Lee K. L., Farhoomand I. (1967). *Compressibility and crushing of granular soil in anisotropic triaxial compression*. Canadian Geotechnical Journal 4(1), 68–86.

Marachi N. D., Chan C. K., Seed H. B., Duncan J. M. (1969). *Strength and deformation characteristics of rockfill materials.*

Department of Civil Engineering, Report No. TE-69-5. University of California.

Marketos G., Bolton M. D. (2007). *Quantifying the extent of crushing in granular materials: a probability-based predictive method*. J. Mech. Phys Solids 55(10), 2142–2156.

Marsal R. J. (1963). *Contact Forces in Soil and Rockfill Materials*. Proc. 2nd Pon-Am CSMFE, Brazil.

Marsal R. J. (1967). *Large scale testing of rockfill materials*. Journal of the Soil Mechanics and Foundation Division, ASCE, 93(2), 27-43.

Marsal R. J. (1973). *Mechanical properties of rockfill*. Embankment Dam Engineering, Casagrande Volume, Wiley, New York, 109–200.

McDowell G. R., Bolton M. D. (1998). *On the micromechanics of crushable aggregates*. Géotechnique, 48(5), 667-679.

Modoni G., Koseki J., Anh Dan L. Q. (2011). *Cyclic stress–strain response of compacted gravel.* Géotechnique, 61(6), 473-485.

Nakata Y., Bolton M. D., Cheng Y. P. (2005). *Relating particle characteristics to macro behavior of DEM crushable material*. In Powders and grains. Taylor & Francis Group, London, 1387-1391.

Nakata Y., Kato Y., Hyodo M., Hyde A. F. L., Murata H. (2001). *One-dimensional compression behaviour of uniformly graded sand related to single particle crushing strength.* Soils and foundations, 41(2), 39-51.

Nobari E. S., Duncan J. M. (1972). *Effect of reservoir filling on stresses and movements in earth and rockfill dams.* Department of Civil Engineering, Report No. TE-72-1. University of California.

Oldecop L. A., Alonso E. E. (2001). *A model for rockfill compressibility*. Géotechnique, 51, 127-139.

Oldecop L. A., Alonso E. E. (2013). *Rockfill mechanics*. Advances in Unsaturated Soils – Caicedo et al. (eds), Taylor & Francis Group, London, ISBN 978-0-415-62095-6.

Ortega E. (2008). *Comportamiento de materiales granulares gruesos. Efecto de la succión*. PhD Thesis, Universitat Politècnica de Catalunya, Spain.

Roscoe K. H., Burland J. B. (1968). *On the generalized stress-strain behaviour of wet clay.* In: Heymann G., Leckie FA, editors. Engineering Plasticity, Cambridge, UK: Cambridge University Press, 535-609.

Roscoe K. H., Schofield A. N. (1963). *Mechanical behaviour of an idealized 'wet' clay.* In: Proceeding of the 3rd European Conference Soil Mechanics and Foundation Engineering. Wiesbaden, 47-54.

Roscoe K. H., Schofield M. A., Wroth C. P. (1958). *On the yielding of soils*. Géotechnique, 8(1), 22-53.

Rowe P. W. (1962). *The stress-dilatancy relation for static equilibrium of an assembly of particles in contact*. Proceedings of the Royal Society of London, 269, 500-527.

Schofield A. N., Wroth C. P. (1968). *Critical State Soil Mechanics.* McGraw-Hill Book Company: New York.

Sowers G. F., Williams R. C., Wallace T. S. (1965). *Compressibility of broken rock and settlement of rockfills*, Proc. of 6th ICSMFE. Montreal, 2, 561-565.

Takei M., Kusakabe O., Hayashi T. (2001). *Time dependent behavior of crushable materials in one-dimensional compression tests*. Soils Foundation, 41(1), 97-121.

Tarantino A., Hyde A. F. L. (2005). *An experimental investigation of work dissipation in crushable materials*. Géotechnique, 55(8), 575-584.

Taylor D. W. (1948). *Fundamentals of soil mechanics*. John Wiley & Sons Inc., New York.

Terzaghi K. (1960). *Discussion on salt springs and lower bear river dams*. Transactions of ASCE, 125(2), 139-148.

Vaid Y. P., Chung E. K. F., Keurbis R. H. (1990). *Stress path and steady state*. Canadian Geotechnical Journal, 27(1), 1-7.

Valdes J. R., Caban B. (2006). *Monitoring the hydraulic conductivity of crushing sands.* Geotechnical Testing Journal, 29(4), 322-329.

Verdugo R., Ishihara K. (1996). *The steady state of sandy soils. Soils and Foundations*, 36(2), 81-91.

Vesic A. S., Clough G. W. (1968). *Behavior of granular materials under high stresses*. Journal of the Soil Mechanics and Foundations Division, 94(3), 661-688.

Wiederhorn S. M., Freiman S. W., Fuller E. R., Simmons C. J. (1982). *Effects of water and other dielectrics on crack growth*. J. Mater. Sci. 17, 3460-3478.

Wood D. M. (1990). *Soil behaviour and critical state soil mechanics.* Cambridge, UK: Cambridge University Press.

Wood D. M., Maeda K. (2008). *Changing grading of soil: effect on critical states.* Acta Geotechnica, 3(1), 3-14.

Wroth C. P., Bassett R. A. (1965). *A stress-strain relationship for the shearing behaviour of a sand.* Géotechnique, 15(1), 32-56.

CHAPTER 3

EXPERIMENTAL EQUIPMENT AND TECHNIQUES

3.1 Introduction

The use of rockfill in civil engineering works such as earth and rockfill dams, road and railway embankments, increased along the last century especially for sustainability reasons. In order to obtain a more solid scientific basis for the design of these structures, it was necessary to carry out more exhaustive studies on rockfill. Pioneering research efforts forming the basis for understanding rockfill behaviour were made by Marsal (1967), Fumagalli (1969), Marachi et al. (1969) and Nobari and Duncan (1972). In the sixties and early seventies considerable investments were made for the construction of large size oedometer and triaxial equipment, with the aim of testing materials with dimensions similar to those used on a one-to-one scale.

However, despite the huge effort of operating large testing devices, rockfills with grain size of the order of tens of centimetres or even meters are impossible to test by laboratory equipment. These considerations gave rise to an intense experimental activity aimed at studying the scale effect on the mechanical properties of granular materials. In fact, despite the referred limitations imposed by size, laboratory research works allowed gaining much of the understanding, at least in a qualitative way, about the physical and chemical phenomena involved in rockfill mechanics. Moreover,

laboratory tests can be used reliably if the equipment is of adequate size compared to the grain size. With reference to the triaxial tests, according to ASTM recommendations D4767 (2002), the maximum diameter (d_{max}) of the particles under study must be less than a fixed value, equal to 1/6 of the diameter of the equipment (D). As regards the oedometer ring, the height (h) and the radius (r) must be chosen to have values of both the ratios $2 \cdot r/d_{max}$ and h/d_{max}, large enough to ensure that the specimen is larger than the soil REV (Representative Element Volume). Some data from the literature (e.g. Penman, 1971; Marsal, 1973) on gravels or rockfills indicate that such ratios should be not less than 5 or 6.

The limit value that the D/d_{max} ratio can assume in the triaxial and oedometric tests on rockfill involves a change in the grain size distribution of the original material that can be very different from the tested one. The changes in the grain size distribution of the original material that result in a reduction in the maximum grain size, influence particle breakage: the larger the particle is the more it breaks (Marsal, 1963).

In order to study the mechanical behaviour of rockfill under a set of conditions expected to occur during their life (grain crushing, changing in degree of saturation), at the Laboratory of Geotechnical Engineering of the University of Naples Federico II, an experimental research was started using a large triaxial cell (D = 20 cm, H = 41 cm), a large soft oedometer (D = 49 cm, H = 25 cm) and a small oedometer (D = 15 cm, H = 5.5 cm).

3.2 Large triaxial cell

3.2.1 General description of the equipment

The High-Pressure Stress Path (HPSP) cell is a large triaxial device based on the Bishop and Wesley (1975) hydraulic control of stress path (Figure 3.1).

Figure 3.1 Large triaxial apparatus

The triaxial apparatus shown in Figure 3.1 allows to test saturated and unsaturated specimens with a diameter of 200 mm and a height of 410 mm. The cell has been designed to operate at a maximum cell pressure of 2 MPa. The triaxial cell scheme is reported in Figure 3.2.

The apparatus is equipped with an inner submergible load cell directly placed on the top of the specimen. The load cell used is the CCt Transducers type BP01 with a load capacity of 200 kN and a maximum overload of 150%. It is designed to operate in water with an accuracy better than 0.1% and is not affected by changes in cell pressure.

The axial compression load is applied by means of a hydraulic piston placed at the bottom of the equipment while the top of the specimen contrasts with the fixed load cell. The piston has a maximum stroke of 200 mm and a diameter of 60 mm.

The loading control system consists of three independent pressure circuits: one for the cell pressure, one for the back pressure and one (containing hydraulic oil) to adjust the pressure in the loading ram. For the measurement of pore pressure and cell pressure Druck PDCR810 transducers with a full scale of 15 bar and 35 bar and an accuracy of 0.1% are used. Moreover, the measurement of the differential pressure is carried out by a Druck transducer STX2100 with a 60 mbar full scale and an accuracy of 0.1%.

Separate lines of drainage are connected to the lower and upper bases of the specimen with independent lines for pore pressures and volumetric strains measurements. Taps on the mentioned lines allow the hydraulic disconnection of the drainage circuits, ensuring a high versatility in execution of different tests.

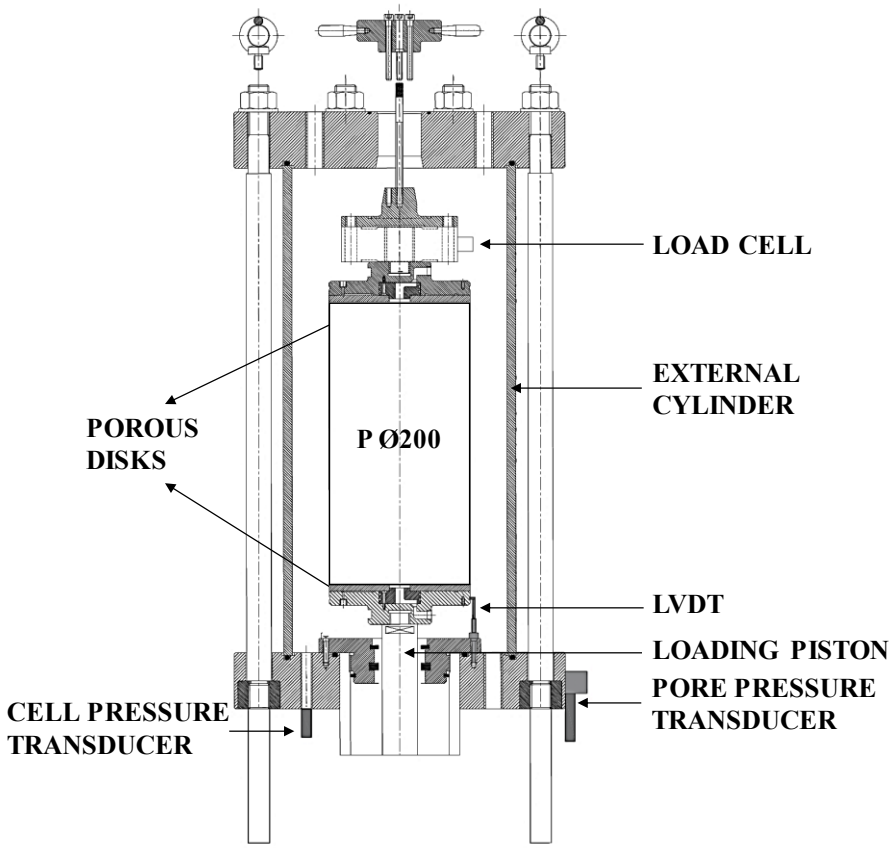

Figure 3.2 Triaxial cell scheme

The HPSP apparatus includes an external control unit containing the electrical supply of transducers, the digital acquisition systems of the signals from the mentioned transducers and the electro-valves for the control in feedback of the water and cell pressures. The cell is finally equipped with a hydraulic power pack able to pressurise a RAM actuator up to the maximum pressure and a personal

computer that runs a software for the feedback management of the tests.

Compared to a conventional triaxial cell, the HPSP differs mainly in the fact that the axial load is applied by means of a piston which pushes the soil specimen against a fixed internal load cell. Axial displacements are measured internally using a submerged LVDT transducer (±120 mm stroke, 0.3% accuracy) that is fixed to the loading piston allowing the measurement of the axial strain of the specimen.

The HPSP is able to perform both controlled rate of loading (CRL) and controlled rate of straining (CRS) tests with automatic feedback control. In the case of CRL tests, the feedback signal is provided by the load cell; in the case of CRS tests the control is on the displacement and the feedback signal is provided by the LVDT for the axial displacement.

The current state of the specimen is elaborated by the control system that regulates the pressures and is detected by a series of transducers, such as:

- the load cell for measuring axial load on the specimen;
- two pressure transducers (CELL and PORE) transmitting the feedback signal for cell and pore pressure control;
- a differential pressure transducer (DPT) to measure the volume changes of the specimen by the volume of water exchanged along the drainage line (tests on water saturated specimen) or by the volume of water exchanged by the cell (tests on unsaturated specimens);

- the LVDT for measurement of axial strains;
- an LVDT for measurement of the displacements of the pressure multiplier (external Volume Gauge).

It is therefore possible to perform a wide variety of tests by means of independent controls of cell, axial load and pore pressures.
The whole system is located in a temperature-controlled room where the maximum temperature variation is ±1.5 °C.

3.2.2 Auxiliary equipment

The large triaxial apparatus was equipped with two new systems: the magnetic shape/volume detection system and a relative humidity control system. The first one called Magnetic Shape Detector (MSD) was introduced for the measurement of local axial and radial strains, as well as for global volumetric strains. The second system is used to impose partially saturated conditions in the specimen: the control of the relative humidity, and therefore of the total suction, is achieved by water vapor transfer using a forced convection system and is carried out by means of saline solutions placed inside an external vessel.

3.2.2.1 Magnetic Shape Detector system

In the HPSP cell, the measurement of volumetric strains in saturated conditions is performed in a classical way, i.e. by means of burettes collecting the water exchanged by the samples or by the cell and measuring the change of the water level in the measuring burette by

a differential pressure transducer (DPT). Accurate measurement of volume changes in partially saturated specimens, including changes in water and air volumes in the pores, results in greater difficulties than in saturated specimens.

Several techniques, described in the literature, can be used to measure the volumetric strains of a specimen in saturated and partially saturated conditions, starting from the direct measurement of axial and radial displacements, both global and local measurements, depending on the position of the transducers. These techniques can be further divided into contact and non-contact methods. Among the non-contact methods an innovative technique was developed by Romero et al. (1997) and more recently by Messerklinger et al. (2004), who used a laser system to measure respectively radial strains and volume changes during triaxial test.

Moreover, the contact method is a commonly used method in which local displacement sensors are directly attached onto the specimen to measure axial/radial strains during the test. Generally, radial displacements are measured at one to three discrete points and assumptions are made on the shape of the specimens to assess the volumetric strain. This method is generally applicable only for rigid specimens with small deformations and requires the use of specially designed sensors such as miniature LVDTs, LDT and Hall effect transducers. A Hall effect sensor is a transducer that varies its output voltage in response to a magnetic field. They were used by Clayton et al. (1986) for measuring the local radial and axial strains in triaxial tests.

In the HPSP cell, it was decided to combine the traditional system of global measurement with an innovative magnetic shape/volume detection system called Magnetic Shape Detector (MSD) built using Hall effect sensors. This system was designed for the measurement of local axial and radial strains as well as for the measurement of global volume strains in saturated and partially saturated conditions. The use of both global and local measurements allows detecting experimental problems such as membrane penetration on isotropic compression and shearing, as well as membrane sliding on shearing at low confining stresses.

The MSD system consists of six N40 cylindrical magnets in neodymium, iron and boron alloy (NdFeB) with a diameter of 10 mm and a height of 40 mm (Figure 3.3b), and as many triples of Hall sensors. Immediately before the closure of the cell, the magnets are glued in the positions shown in Figure 3.3a on the latex membrane which wraps the specimen (Figure 3.4).

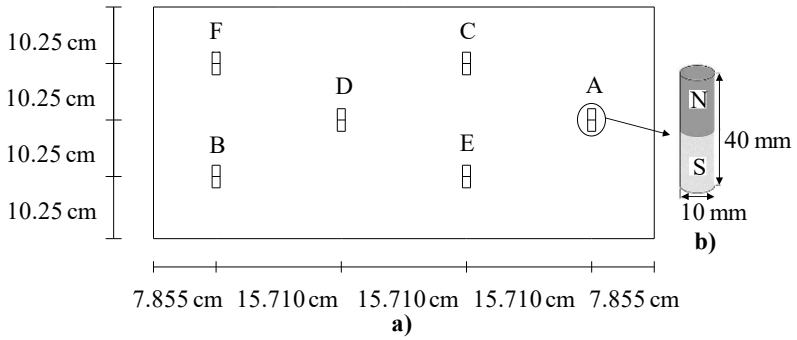

Figure 3.3 Magnetic shape detector system: a) positioning scheme of the magnets on the external surface of the sample; b) zoom of the magnet

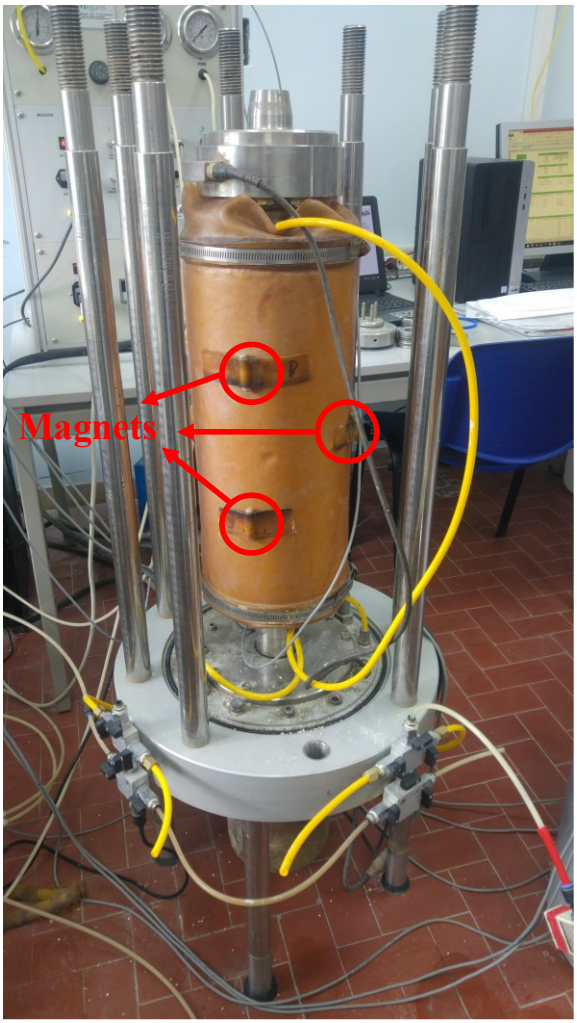

Figure 3.4 Sample at the beginning of the test with magnets placed on the latex membrane

The sensors are locked in fixed positions on the inner part of the external aluminium cylinder of the triaxial cell, so that, at the beginning of the test, sensors' centres of gravity are aligned with the magnets' ones (Figure 3.5).

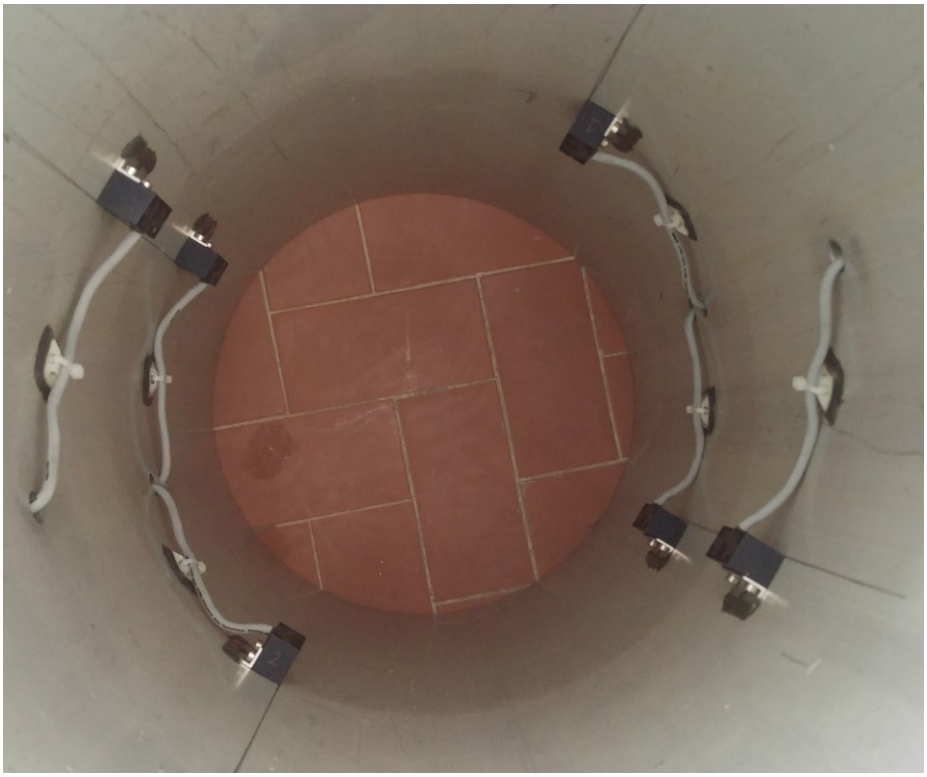

Figure 3.5 Magnetic shape detector system: sensors on the internal surface of the external aluminium cylinder of the triaxial cell

The sensors and the magnets mounted inside the triaxial cell are used to scan the specimen's surface during the tests. In fact, the sensors used are able to detect axial and radial displacements and rotations of the magnets placed in positions B, C, E, F (see Figure 3.3a) while the remaining magnets A and D are able to detect only axial and radial displacements. The proposed system allows linear measurement through a vertical displacement of 10 mm (0/-10 mm) for magnets C and F, of 20 mm (15/-5 mm) for magnets A and D and of 30 mm (±15 mm) for magnets B and E. Moreover, the MSD

system allows linear measurement through a radial displacement of 11 mm for magnets A and D and of 5 mm for the others. Finally, the maximum rotation measured by the system is equal to 8° approximately.

A data processing software allows the display of the magnets' movements during the test time thanks to the calculation of the changes in the magnetic field induced by the permanent cylindrical magnet. Based on the measured displacements a software is also able to return the variation of the side profile of the specimen by means of an interpolation method. In particular, the software mediates the position of the magnets placed at the same initial height and, given the lack of information related to the rotation of the magnets in the central positions A and D, assumes vertical tangents at the centre and at the lower base of the specimen. The vertical zero position of the profile is set at the base of the upper fixed porous stone, to exclude bedding errors due to the initial compliance of the axial loading system. This fixed point marks the zero value of the vertical axis measuring the position of any target along the lateral surface of the specimen, and is directed towards the lower base, while the axis measuring the horizontal displacements is directed towards the outside of the specimen. Having noted the positions of the bases and the lateral profile, the current volume of the specimen is easily measured by an integral calculation.

It has been demonstrated in literature (Foletto et al., 2013) that the region of linear response of a magnet is only around its centre thus explaining why only a short path can be measured with a single

sensor. The increased linearity error depends on the type of sensor and on the strength of the magnetic field. In order to create an accurate system, the linearity errors have been reduced by using more than two sensors, a magnet with large dimensions and a post-processing compensation such as linearization to correct residual error.

3.2.2.2 Suction application system

3.2.2.2.1 General aspects

In rockfill particle breakage depends on the stress level, the grain size distribution, the strength and shape of the individual grains, the relative density and the relative humidity (RH) in the rockfill voids.
Relative humidity is the ratio of the quantity of water vapor present in a mass of air to the maximum quantity that the same air can contain in the same conditions of temperature and pressure. Therefore, relative humidity is an alternative measure of water vapor concentration.
The vapor equilibrium technique that is based on the relative humidity control (vapor transfer) allows controlling suction in soils. In fact, if the liquid, or the water contained in the pores of the rock, reaches equilibrium with the vapor phase, the psychrometric law allows an easy determination of the total suction starting from relative humidity (Coussy, 1995):

$$RH = exp\left[-\frac{\nu\,(s+\pi)}{RT}\right] \tag{3.1}$$

where ν is the molar volume of water, R is the gas constant, T the absolute temperature, s the matric suction, π the osmotic suction due to the presence of solute in the water contained in the pores. The sum $\psi = s + \pi$ is the total suction. Matrix suction and total suction are equal if pores contain pure water.

When using the vapor equilibrium technique, the granular material is placed in a closed environment with a saline solution contained in a vessel that regulates the relative humidity. Equation 3.1 implies that control of the total suction, in any specimen placed in a closed system, can be achieved by controlling the relative humidity of the surrounding environment, provided that a thermodynamic equilibrium condition is reached. In this procedure the transport of water takes place exclusively through the gaseous phase, by the processes of advection and molecular diffusion.

3.2.2.2.2 Suction control system in HPSP cell

The HPSP cell has been upgraded to apply the vapor equilibrium technique already successfully implemented by Oldecop and Alonso (2001) in oedometric tests as shown in Figure 3.6.

The relative humidity control in the HPSP apparatus is obtained by introducing a saline solution into a closed circuit inside the test system, as shown in Figure 3.7. The solution is placed in an external vessel in order to avoid the direct contact with the specimen, allowing connection with only the gas phase of the system.

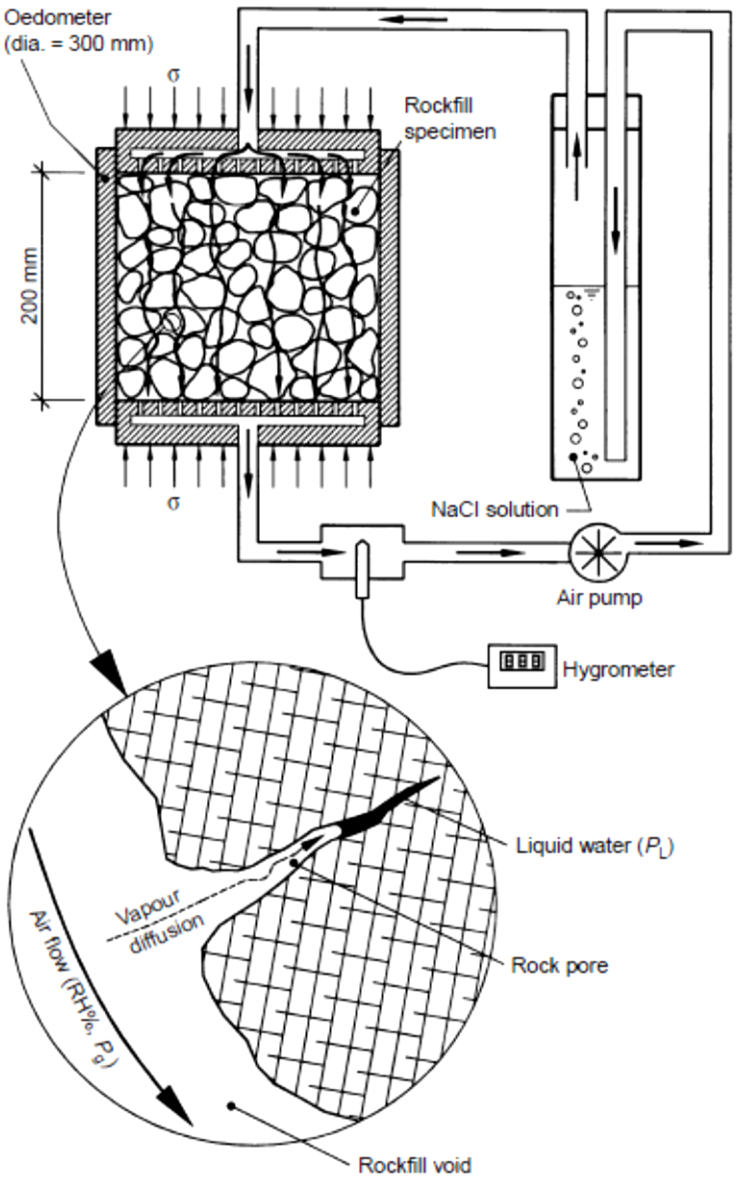

Figure 3.6 Rockfill oedometer test set-up with a relative humidity control system (Oldecop & Alonso, 2001)

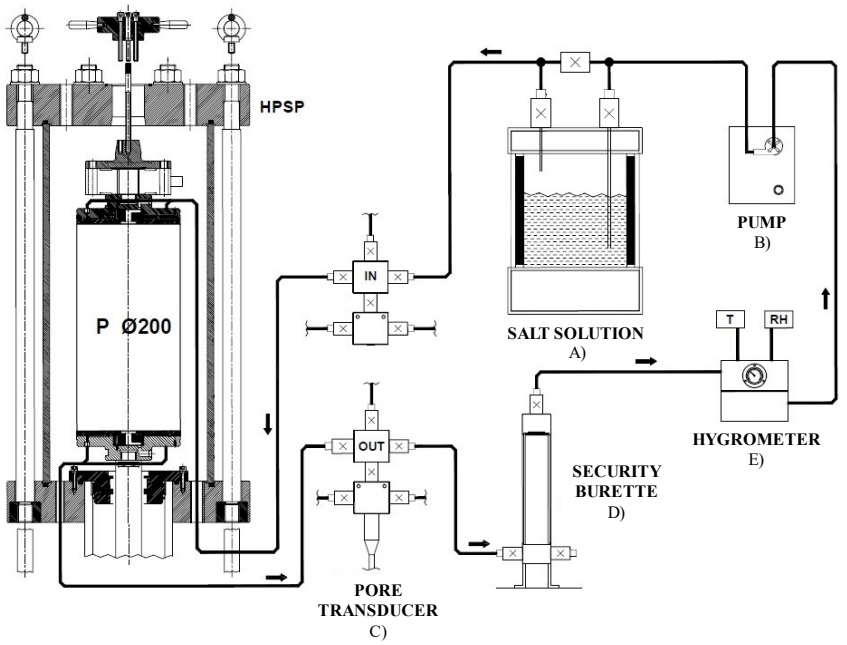

Figure 3.7 Relative humidity control system with the HPSP cell

The transport of water, from the saline solution to the specimen, takes place in the form of water vapor. When water vapor transport is carried out exclusively by molecular diffusion, thermodynamic equilibrium requires very long times, incompatible with experimentation. To make more efficient the water vapor transfer, a forced convection system was used driven by an air pump (B in Figure 3.7). In this way, water vapor is transported by advection, a more efficient transport mechanism than molecular diffusion. The water vapor leaving the vessel (A) is circulated through the specimen from the upper to the lower base, where it is collected by a hygrometer (E) installed in the air flow line exiting the specimen. This instrument allows temperature measurement and continuous

recording of relative humidity over time. In order to prevent the entry of water into the pneumatic circuit, a safety burette (D) is placed along the air flow line immediately before the hygrometer.

As mentioned before, a hygrometer inserted in the air flow coming out of the specimen allowed the progress of the test to be monitored. The hygrometer used is shown in Figure 3.8a. It is a HM1500LF humidity transducer designed for applications where a reliable and accurate measurement is needed. This instrument is specified for measurements within 10 to 95% RH with an accuracy of +/-5% RH. The hygrometer's temperature range begins at -30 °C and ends at +70 °C.

Therefore, in order to measure the relative humidity and the temperature directly inside the specimen, three iButton sensors (Figure 3.8b) have been used. The iButton temperature/humidity logger (DS1923) is a rugged, self-sufficient system that measures temperature and humidity and records the result in a protected memory section. The recording is done at a user-defined rate. A mission to collect data can be programmed to begin immediately, after a user-defined delay, or after a temperature alarm. The DS1923's temperature range begins at -20 °C and ends at +85 °C. In addition to temperature, the DS1923 can log humidity data in an 8-bit or 16-bit format. The DS1923's humidity range begins at 0% and ends at 100%. Humidity values are represented with a resolution of 0.64% RH in the 8-bit mode and 0.04% RH in the 16-bit mode.

The iButton temperature/humidity logger allows to verify if the thermodynamic equilibrium condition is reached. The three sensors supplied are positioned in three different sections of the specimen in order to identify any inhomogeneities in T and RH.

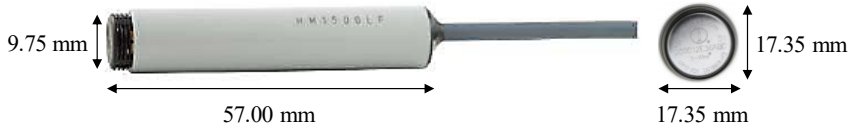

a) b)

Figure 3.8 Relative humidity measurement instruments: a) hygrometer HM1500LF; b) i-Button

Rockfill can be considered as having two sets of voids: voids formed by the inter-particle spaces and the pores due to the natural porosity of the rock. At the start of the system the water vapor driven by the pump flows inside the voids creating a gradient of RH between the inter-particle voids and the pores of the rock. This condition activates a process of vapor transport in the pores by molecular diffusion. When vapor transport ends, RH is equal in all points of the gas phase of the system indicating the achievement of the thermodynamic equilibrium condition. At equilibrium, relative humidity and total suction are correlated by equation 3.1.

The system is able to simulate both a wetting path using a solution that imposes a relative humidity greater than the RH into the specimen, and a drying path. According to the equation 3.1, the increase in the relative humidity of the specimen involves the

reduction of suction and therefore an increase in the amount of liquid water contained in the pores of the rock.

Since the relative humidity depends on the ambient temperature, an air conditioning system was installed in the laboratory to keep the temperature almost constant, so that the relative humidity was dependent only on the salt solution used. The temperature was set at 21 °C. In the records obtained during the tests, an average of 20.4 °C was obtained with a variation of ± 2 °C. Temperature control was considered adequate given the size of the laboratory room where the equipment is placed.

3.2.3 Sensors calibrations

Since the HPSP is a prototype, it was necessary to make a first phase of calibration of the measuring instruments, such as LVDT, pressure transducers and load cell.

As mentioned before, the axial displacements of the specimen are measured inside the triaxial cell by a submergible LVDT of the Lucas Schaevitz type 3000HCD with a linear stroke of ± 120 mm and accuracy better than 0.3%. The calibration of this device was carried out by comparing the measurements in millimetres read on a micrometre (accuracy = ± 0.001 mm) previously calibrated with the bit values recorded by the HPSP system. The results of the calibration showed that the relationship between the readings in bit and those in mm which can be considered linear (Figure 3.9).

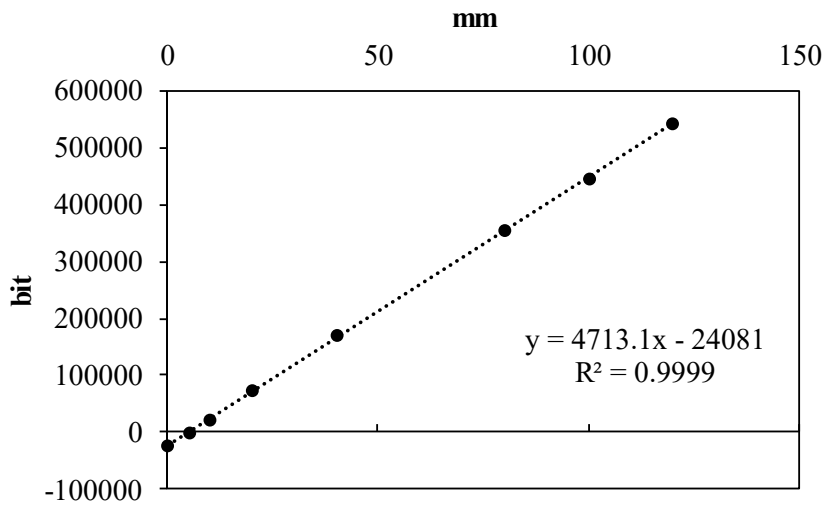

Figure 3.9 Results of the LVDT calibration

The cell has two pressure transducers needed to measure the cell pressure and the pore pressure respectively. Both were separately connected to a pressure source and a standard pressure gauge. Pressure was applied in predetermined increments over the full range of the pressure transducer. The pressure transducer output was compared at each increment to the HPSP bit readings. The bit-kPa relationship is linear as shown in Figure 3.10.

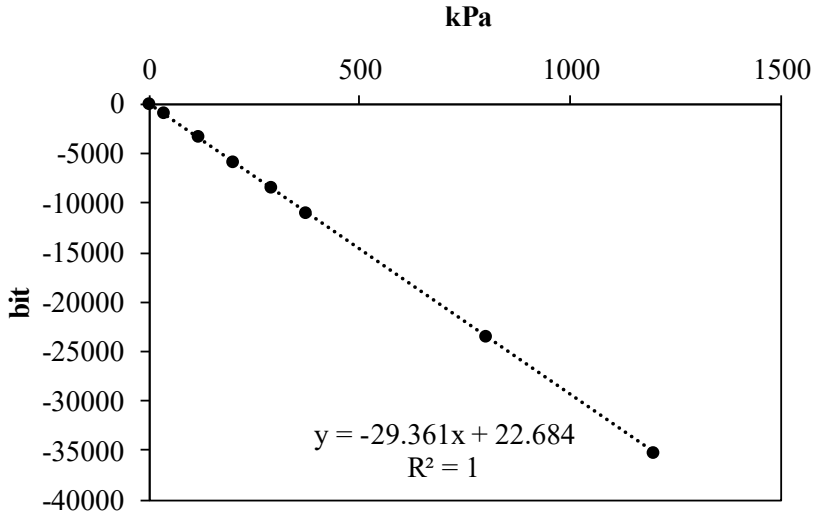

a)

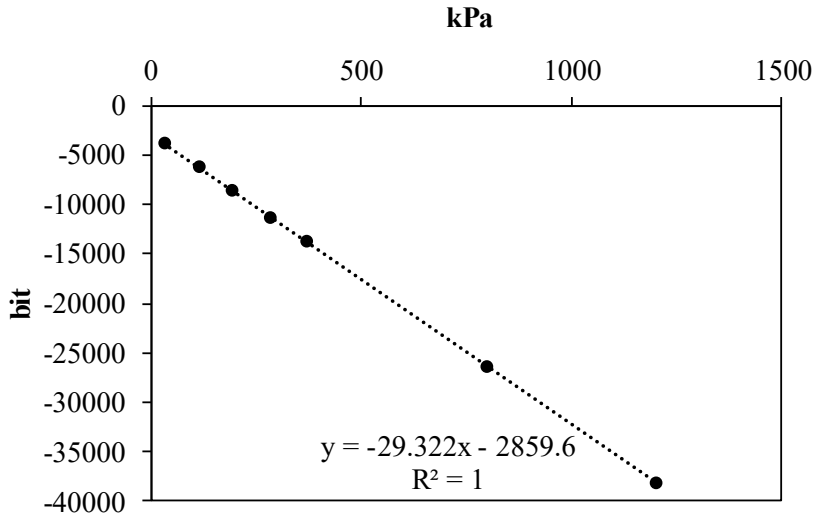

b)

Figure 3.10 Results of the pressure transducers calibrations: a) Pore pressure transducer; b) Cell pressure transducer

The load cell has been calibrated by connecting it to another load cell that has been previously calibrated and is traceable to standards. The commonly used test procedure includes a load-unload loop. The relationship between the load measured by the sample cell and the HPSP bit readings can be considered linear with good approximation as shown in Figure 3.11.

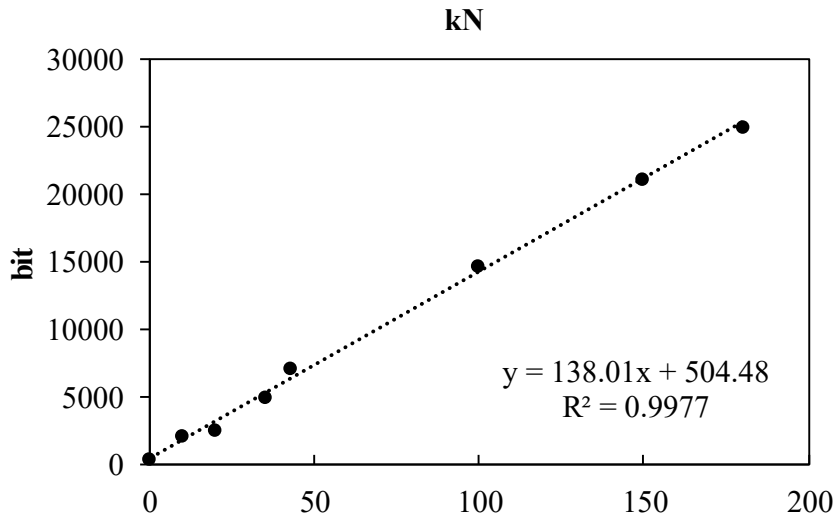

Figure 3.11 Results of the load cell calibration

Finally, in order to verify the accuracy of the MSD system, careful calibrations have been done to take into account non-linearity of the magnet's response. Calibrations were carried out with a device consisting of a beam on which the magnet is placed, whose displacements are measured by means of two micrometres, respectively in a horizontal and vertical direction (Figure 3.12). Both have a resolution of 0.001 mm. Starting from the "zero" condition, i.e. alignment of sensors and magnets' centres of gravity

and fixing the position of the magnet in one direction, a displacement in the other direction was imposed with the micrometre. Displacements z along the vertical direction and displacements r along the horizontal one were recorded.

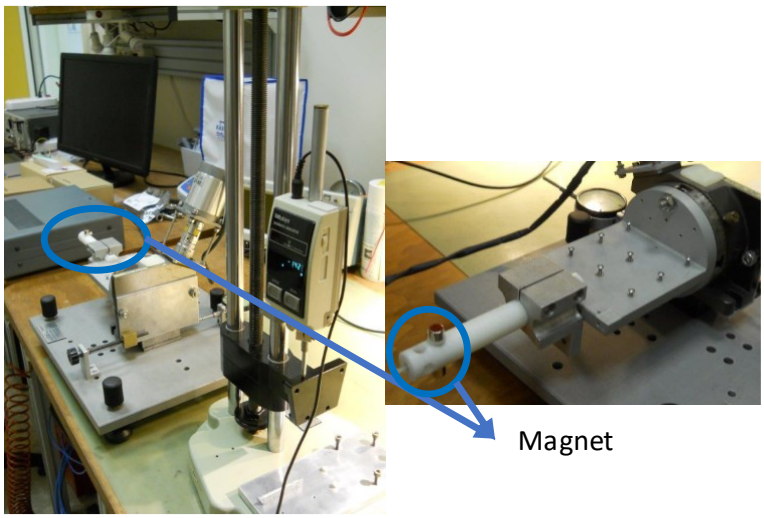

Figure 3.12 Device used to calibrate the MSD system

Results are shown in Figure 3.13. The diagrams show a good response of almost all the sensors.

However, on average the system records an accuracy of 0.2% in the vertical direction and 0.3% in the radial one. It can be thus argued that the MSD system is more accurate than traditional systems, also because it allows to collect more data than those provide by traditional systems.

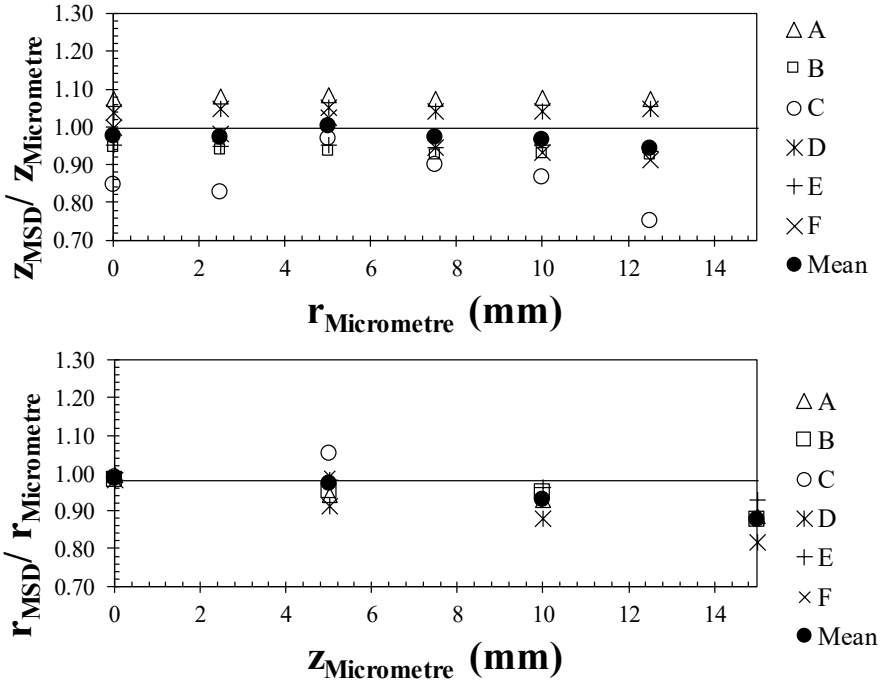

Figure 3.13 Calibration tests results on MSD system

3.3 Oedometer cell

3.3.1 Large soft oedometer

The large oedometer ring adopted in this work is a steel ($E_R = 2.1 \cdot 10^5$ MPa) cylinder with thickness t = 5 mm. The cylinder is placed on a base supported by a metal structure as shown in Figure 3.14. The apparatus allows to perform tests on cylindrical specimens with height H = 25 cm and diameter D = 49 cm, confined at the top and the bottom by two grooved still plates.

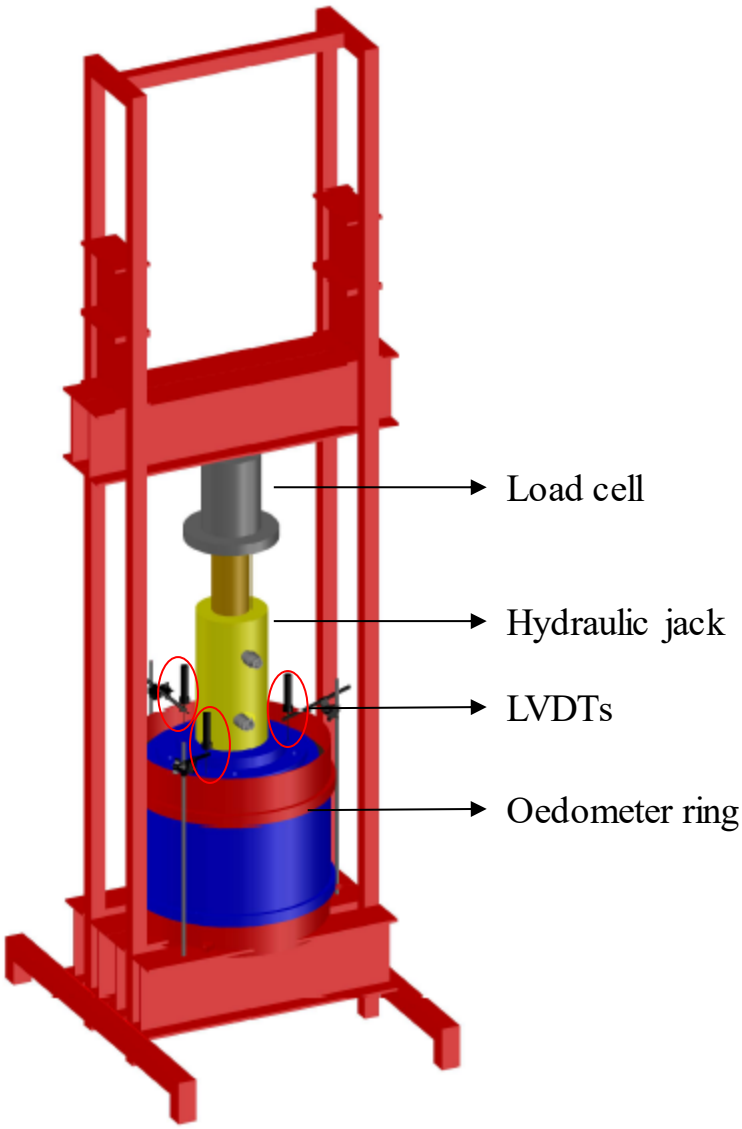

Figure 3.14 Large oedometer: 3D view

The vertical load is applied by a hydraulic jack (Figure 3.16a) and measured with a load cell (Figure 3.16b) on the top of the specimen. The load cell has been calibrated by using a high-quality reference

load cell already calibrated and is traceable to standards. Figure 3.15 shows the results of the calibration.

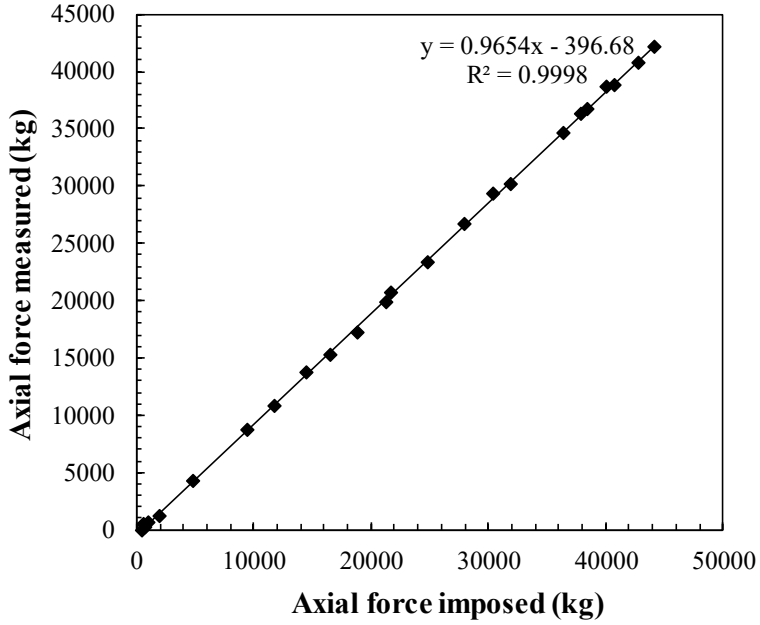

Figure 3.15 Results of the load cell calibration

The loading-unloading phases were carried out by means of a hydraulic pump (Figure 3.16c). The maximum applied stress at the top of the specimens is σ'_v = 2.5 MPa. The vertical displacement of the specimens is measured with three LVDTs (±120 mm stroke, 0.3% accuracy) placed on the loading cap (Figure 3.16d).

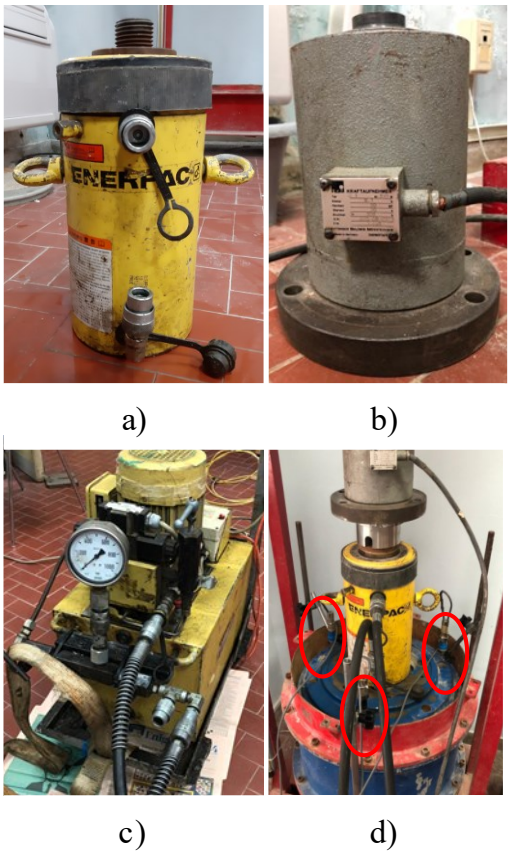

Figure 3.16 Elements of the oedometer apparatus: a) hydraulic jack; b) load cell; c) hydraulic pump; d) LVDTs

3.3.2 Small oedometer

In order to study the compressibility of rockfill with a different grain size distribution and a lower d_{max}, it was possible to use a small oedometer.

The loading scheme of the cell is the classical one of oedometers, in which a vertical load is applied to the sample under lateral

confinement. Therefore, the oedometer cell is held laterally by non-deformable walls and vertically between two porous stones that let the water freely circulate through its pores. Known vertical stresses are applied to the top face of the sample, using free weights and a lever arm. The maximum vertical stress is 2.5 MPa. Axial strain is measured using a certified LVDT (±5 mm stroke, 0.3% accuracy) registering top platen displacements. It has been calibrated by applying known displacements using steel blocks of known thickness and recording the corresponding Volt readings. Figure 3.17 shows the results of the calibration.

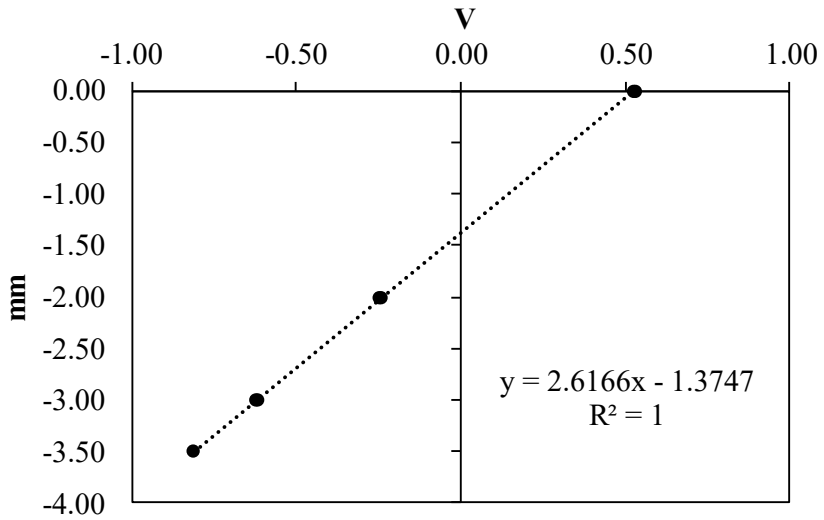

Figure 3.17 Results of the LVDT calibration

The geometrical dimensions of the oedometer have been chosen to limit the influence of side boundaries. An internal diameter of 15 cm has therefore adopted. Consequently, to ensure proper one-

dimensional conditions, hosted samples shall have heights equal to 5 cm (Figure 3.18).

a) b)

Figure 3.18 a) Small oedometer; b) external view of the oedometer and loading system

The oedometer used allows performing tests both on saturated specimens and on partially saturated specimens. It allows the relative humidity control using the system shown in the Figure 3.6. Finally, to induce the collapse of the specimen by flooding, the steam supply is removed and the oedometer cell is connected to a water source, passing from a completely dry to a saturated condition.

3.4 Final remarks

The equipment used was designed and instrumented to correctly reproduce stress paths and environmental conditions to which rockfill are generally subjected.

A triaxial cell was used to monitor global volume changes of the material on compression and shearing. In addition, the cell uses a novel technique to measure local axial and radial deformations. The triaxial equipment used allows the reproduction of paths with controlled rate of loading (CRL) and controlled rate of straining (CRS).

The two oedometer equipment described allows the study of the compressibility of granular material with different d_{max}.

Moreover, the partial saturation is achieved by imposing a total suction that is correlated with the relative humidity by the psychrometric law. Relative humidity control was achieved by water vapor transfer using a forced convection system, which is driven by an air pump transporting the air humidity to the sample, and it is controlled by saturated salt solutions placed in a vessel.

The triaxial and oedometer apparatus described have been used to study the mechanical behaviour exhibited by a coarse material at different initial states and for different stress/strain paths.

3.5 References

ASTM Standard D4767-04 (2002). *Consolidation Undrained Triaxial Compression Test for Cohesive Soil*. Annual Book of ASTM Standards, ASTM International, West Conshohocken, PA.

Bishop A.W., Wesley L.D. (1975). *A hydraulic triaxial apparatus for controlled stress path testing*. Géotechnique, 25(4), 657-670.

Camacho J.M., Sosa V. (2013). *Alternative method to calculate the magnetic field of permanent magnets with azimuthal symmetry*. Revista Mexicana de Fisica, 59, 8-17.

Clayton C. R. I., Khatrush S. A. (1986). *A new device for measuring local axial strains on triaxial specimens*. Géotechnique, 36(4), 593-597.

Coussy O. (1995). *Mechanics of porous continua*. John Wiley & Sons Ltd., Chichester.

Foletto A., Friedrich A., Gupta S. (2013). *Analysis of a Hall-Effect system with two linear sensor ICs for 30 mm displacement*. Allegro MicroSystems, LLC.

Fumagalli E. (1969). *Tests on cohesionless materials for rockfill dams*. Journal of the Soil Mechanics and Foundations Division, ASCE, 95(1), 313-332.

Marachi N. D., Chan C. K., Seed H. B., Duncan J. M. (1969). *Strength and deformation characteristics of rockfill materials.* Department of Civil Engineering, Report No. TE-69-5. University of California.

Marsal R. J. (1963). *Contact Forces in Soil and Rockfill Materials*. Proc. 2nd Pon-Am CSMFE, Brazil.

Marsal R. J. (1967). *Large scale testing of rockfill materials*. Journal of the Soil Mechanics and Foundation Division, ASCE, 93(2), 27-43.

Marsal R. J. (1973). *Mechanical properties of rockfill*. Embankment Dam Engineering, Casagrande Volume, Wiley, New York, 109-200.

Marsal R.J., Resendiz D.R. (1975). *Presas de Tierra y Enrocamiento. Mexico*. Ed Limusa, 237-239.

Messerklinger S., Bleiker E., Zweidler A., Springman S.M. (2004). *Displacement measurement with laser scanning in triaxial*

testing apparatuses. 16th European Young Geothecnical Engineers' Conference, 1-10, Vienna, Austria.

Nobari E. S., Duncan J. M. (1972). *Effect of reservoir filling on stresses and movements in earth and rockfill dams.* Department of Civil Engineering, Report No. TE-72-1. University of California.

Oldecop L. A., Alonso E. E. (2001). *A model for rockfill compressibility*. Géotechnique, 51, 127-139.

Oldecop L. A., Alonso E. E. (2004). *Testing rockfill under relative humidity control*. Geotechnical Testing Journal, 27(3), 269-278.

Penman A. D. M. (1971). *Rockfill*. Building Research Station (Great Britain). Current Paper 15/71.

Romero E., Facio J. A., Lloret A., Gens A., Alonso E. E. (1997). *A new suction and temperature controlled triaxial apparatus*. 4th ICSMFE Hamburg, 1, 185-188.

CHAPTER 4

MATERIALS AND LABORATORY TEST PROCEDURES

4.1 Introduction

A critical aspect of rockfill structure design is the need for a precise prediction of expected deformations. For this reason, rockfill behaviour was investigated in the past by authors involved in the design of rockfill structures (Fumagalli, 1969; Marachi, 1969; Marsal, 1973). The experimental programme performed in the 1970s provided a good basic understanding of rockfill behaviour. Tests were conducted with the purpose of obtaining two fundamental characteristics: strength and compressibility.

In recent years, several authors have implemented experimental programs to deepen the study of rockfill mechanics (e.g. Ortega, 2008; Frossard et al., 2012; Oldecop and Alonso, 2013). These testing programs involved large cells and the development of elastoplastic constitutive equations. The authors showed that the mechanical response of rockfill materials is influenced by factors such as mineral composition, particle size and shape, individual particle strength, void content and surface texture of the particles. Therefore, in this work two different grained soils were considered in order to highlight the effects of these factors on the behaviour of rockfill materials that is of considerable importance for analysis and safe design of the rockfill structures.

This chapter classifies the two materials tested, indicates the procedure used to evaluate the individual particle strength and the details of the experimental programme. Some criteria aimed at reducing the particle size so that specimens at lab scale can be prepared and tested are discussed. The procedure used to prepare the specimen are also presented.

4.2 Soil characterization

Two different coarse-grained soils were used in the laboratory tests. The first one is a limestone rock (Figure 4.1) that comes from a quarry in Coreno Ausonio (Italy), supplied by the company Calcestruzzi Capuano. It is first extracted by blasting and then crushed to the desired size. The material is a strong limestone with low-porosity typically employed in railway ballast, road and railway embankments. It has a specific gravity G_s = 2.76. Particle may be described as irregular prisms with sharp edges. The grains exhibit a high superficial roughness, regular sizes and no dominant dimensions. Particle breakage on loading is less likely to occur using this aggregate.

a)

b)

Figure 4.1 a) Quarry in Coreno Ausonio (Italy); b) Coreno rockfill

The second material tested is a heterogeneous rock obtained from Fiumarella River (Italy) and used to build the Redisole Dam (Figure 4.2), a rockfill upstream faced dam having a height of 40.4 m and mainly used for irrigation purposes. The mineralogical composition of this rock includes quartz, muscovite, calcite and dolomite. The tested soil, highly fractured, has a specific gravity G_s = 2.68. Moreover, particle shape is elongated and planar. This shape is expected to favour particle splitting on loading. This material was obtained in situ, further crushed in the laboratory and sieved.

a)

b)

Figure 4.2 a) Redisole dam on Fiumarella River (Italy); b) Redisole rockfill

A comparison between these two widely different gravelly materials helps to understand the role of rock matrix properties and particle strength on macroscopic behaviour.

4.3 Selection of the grain size distributions

As mentioned above, rockfill materials contain particles of large size: thus, testing of such soils in the laboratory requires large equipment. Bishop and Henkel (1962) recommend limiting the tests to soils with the maximum grain size, d_{max}, not greater than 1/10 of the diameter of the specimen D; instead, according to Penmann (1971) and Marsal (1973), the ratio $R = D/d_{max}$ should be not less than 5 or 6 in the tests performed on coarse-grained soils.

However, there are technological limitations that do not allow for the construction of equipment of formidable dimensions. Therefore, the limit values that the ratio R can assume generally involve a change in the grain size distribution and in the uniformity coefficient U_c of the original material. This change can influence its mechanical behaviour. For example, uniform materials at the densest state, will be less dense than materials composed of different particle size because smaller particles can fill the interstitial spaces. Furthermore, the grain size distribution also plays a role on the deformability: the denser rockfill material is, the stiffer it behaves.

Zeller and Wullimann (1957) showed how the shear strength is affected when, due to limitations of the testing equipment, part of the coarse component has to be removed from a given grain size distribution. Sudhindra et al. (1991) observed an increase in the angle of shearing resistance of alluvial materials with an increase in the grain size. On the other hand, for the materials produced by rock blasting, Marachi et al. (1972) showed a decrease in the angle of the shearing resistance with an increase in d_{max}. So overall, different rockfill materials could show opposite trends with respect to variation of the friction angle with the particle size. This is related to the fact that as the average particle size increases, lower-initial void ratio, which provides greater interlocking, is achieved for the same compactive effort (Lambe and Whitman, 1969).

The change of the grain size distribution also affects particle breakage. The use of lower d_{max} influences the distribution of forces

between the particles, by transmitting forces to smaller particles that have a lower breakage probability. Moreover, when the particle size decrease, lower degree of particle breakage also occurs because of the lower force per contact (Lambe and Whitman, 1969). The effect of the increase in interlocking is to increase the shearing resistance, while the effect of particle breakage is to decrease it. Furthermore, removing particles with $d>d_{max}$ from the original material could mean eliminating grains of a lithological nature different from that of the remaining part, or more fractured and therefore more prone to breaking. This aspect should not be overlooked (Flora, 1995). It is also known that an increase of the particle size results in an increase in volumetric strain at the same confining pressure (Marsal, 1967; Fumagalli, 1969; Marachi et al., 1972).

The sizes of the rockfill materials for testing are commonly reduced using four modelling techniques: the scalping technique (Zeller and Wullimann, 1957), parallel gradation technique (Lowe, 1964), generation of quadratic size distribution curve (Fumagalli, 1969) and method of replacing oversize materials by equal weight/cross sectional area/volume of the material (Frost, 1973). Among all the above-mentioned modelling techniques, the parallel gradation and scalping techniques are more frequently used.

By the scalping technique, the material with a diameter greater than the maximum needed to guarantee the ratio R is removed. In this way the uniformity coefficient U_c is reduced. In this case the rejected material must not exceed 50% or 60% by weight of the original grain size distribution. On the other hand, the parallel

gradation technique does not involve the change of U_c. To ensure that the specimen continues to be representative of the overall material, the material rejected must not exceed 40% or 50% by weight of the initial grain size distribution.

The original grain size distribution curve of the material coming from the Redisole dam, delivered at the Geotechnical Engineering Laboratory of the University of Naples Federico II, is shown in Figure 4.3. The diameter of the grains varies between 15 and 80 mm. In the context of a processing under contract, it was necessary to study the mechanical behaviour of the material in oedometric and triaxial conditions. To this end, given the dimensions of the equipment available, it was necessary to modify the original grain size distribution curve. In fact, in order to respect the minimum value of R suggested in the literature (Penmann, 1971) and having to use a triaxial cell with diameter D = 200 mm, d_{max} has been set equal to 40 mm. Figure 4.3 shows the curves obtained by applying the parallel gradation and scalping techniques. For design purposes the selected curve is the one obtained by means of the parallel gradation technique (black curve in Figure 4.3). This curve will be referred to as Parallel in the following.

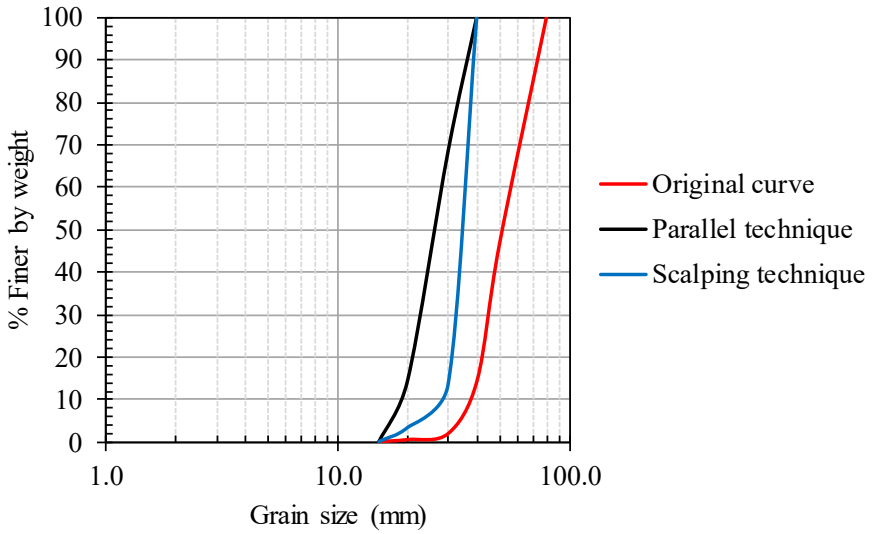

Figure 4.3 Parallel gradation and scalping techniques applied to the grain size distribution of the soil coming from Redisole dam

To study the effectiveness of parallel gradation and scalping techniques and the effect of d_{max} on the mechanical behaviour of rockfill materials, different grain size distributions have been considered. In addition to the Parallel curve with d_{max} = 40 mm and d_{min} = 15 mm, other three grain size distributions tested are (Figure 4.4):

1. Fine: it is a uniform slightly sandy gravel with d_{max} = 5 mm and d_{min} = 0.85 mm;
2. Medium: it is a well-graded gravelly soil with the same d_{min} of the Fine curve and the same d_{max} of the Coarse curve. It has a much greater uniformity coefficient than the others three grain size distributions;

3. Coarse: it is a uniform gravel with d_{max} = 30 mm and d_{min} = 5 mm.

The Coarse curve was obtained by applying the parallel technique to the Parallel grading curve and imposing d_{max} = 30 mm. Through the comparison between the Coarse grading curve and the Parallel one, considerations on the choice of R are possible.

The Fine grading curve was derived using the parallel gradation modelling technique applied on the Coarse grading curve. However, it could also be obtained by the scalping technique applied on the Medium grading curve by imposing d_{max} = 5 mm.

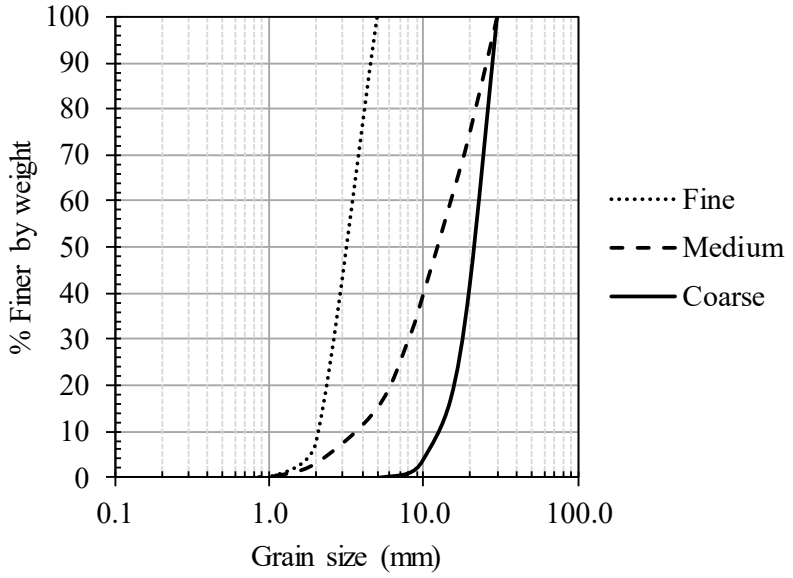

Figure 4.4 Grain size distributions of the tested soils

Values of the maximum and minimum diameter and uniformity coefficient for the modelled grain size distributions are presented in Table 4.1.

Table 4.1 Properties of the grain size distributions of the tested soils

Grain size distribution	**d_{min} (mm)**	**d_{max} (mm)**	**U_c**
Fine	0.85	5	1.85
Medium	0.85	30	3.95
Coarse	5.00	30	1.85
Parallel	15	40	1.85

The specimens of Coreno rockfill were prepared with the Fine, Medium and Coarse grain size distributions instead the specimens of Redisole rockfill were prepared with Fine, Coarse and Parallel grain size distributions. Figures 4.5 and 4.6 shows the three grain size distributions adopted for Coreno and Redisole rockfill respectively.

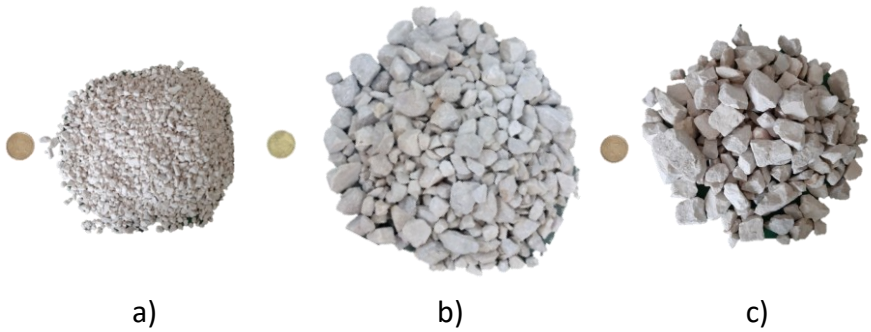

Figure 4.5 Grain size distributions of Coreno rockfill: a) Fine; b) Medium; c) Coarse

Figure 4.6 Grain size distributions of Redisole rockfill: a) Fine; b) Coarse; c) Parallel

4.3.1 Compaction tests

In order to prepare the specimens to be used in the triaxial and oedometric tests, it was necessary to determine the maximum and minimum void ratio indexes of the grain size distributions adopted for the two materials used. These indexes were determined through laboratory tests performed with a vertically vibrating table according to the ASTM D453 and ASTM D4254 standards.

The method consists in filling the mould of standard dimensions (H = 23 cm, D = 27.9 cm) with oven-dried soil previously mixed to provide a uniform distribution of particle sizes. Recording the mass of the soil P_s filling the mould and the unit weight of solids γ_s, the volume of solids V_s was derived as $V_s = P_s / \gamma_s$.

Knowing the volume of the mould, the maximum index void ratio e_{max} was determined as:

$$e_{max} = \frac{V_p}{V_s} = \frac{V_{mould} - V_s}{V_s} \quad (4.1)$$

Subsequently a surcharge base plate (14 kPa) was applied to the surface of the soil and the system was subjected to a vibration at constant frequency for 9 minutes.

After the vibration phase of the table was over, before emptying the mould and sifting the material with an electromagnetic sieve, the lowering of the top surface of the sample with respect to the upper edge of the mould was measured by means of a centesimal gauge as an average of three measurements taken at 120°. In this way it was possible to obtain a new total volume V' to be used in the calculation of the minimum index void ratio e_{min}:

$$e_{min} = \frac{V_p}{V_s} = \frac{V' - V_s}{V_s} \tag{4.2}$$

The entire procedure was repeated three times and then assumed the maximum and minimum index void ratio equal to the average of the three measurements. The results obtained for the two materials are shown in Table 4.2:

Table 4.2 Index void ratios of Coreno and Redisole rockfill

Soil	**Grain size distribution**	**e_{min}**	**e_{max}**
Coreno	Coarse	0.606	0.904
	Medium	0.418	0.688
	Fine	0.610	0.826
Redisole	Coarse	0.659	0.862
	Fine	0.738	1.004
	Parallel	0.634	1.053

4.4 Grain crushing tests

4.4.1 Test procedure

It is well known that particle fracture plays an important role in rockfill behaviour. In fact, the tensile strength of grains influences the mechanical response of an aggregate. In the past many efforts have been made to relate the micromechanics of grain fracture to the macroscopic deformation of crushable aggregate. However, it is not easy to define grain fracture to obtain a consistent definition of particle strength.

It is widely recognized in the literature that the failure of a spherical particle under compression is a tensile failure. Therefore, the tensile strength of rock grains can be indirectly measured by diametrical compression between flat platens (Jaeger, 1967). For this reason, the single particle crushing strength was determined in this work using the procedure suggested by Billiam (1967) and Marsal (1973) with a test set-up shown in Figure 4.7. Unconfined crushing tests were carried out on groups of three grains by placing them between two rigid and smooth steel plates, and then moving the lower plate at a constant rate of displacement. The upper plate and the load cell were fixed. The load measuring capacity was 20 kN with a resolution of 0.01 N. A displacement rate of 0.01 mm/min was imposed. During the tests, the applied forces P were measured by load cell while the displacements were calculated starting from the recorded times on the basis of the displacement rate.

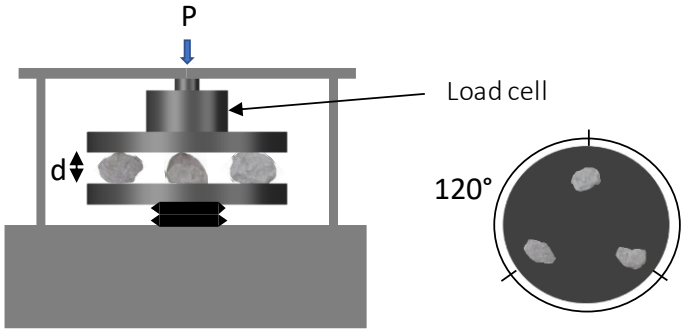

Figure 4.7 Particle tensile strength test set-up for dry grains

The three grains were chosen of similar size and placed on the plate so as to have a minimum number of contacts with the upper plate. This was possible thanks to the fact that all the materials used had grains with sharp edges, and it was therefore possible to find some that had almost continuous contact on the lower base and in a few points on the upper base. It is likely that the break occurs at these points.

Before starting the test, the average distance d between the two plates was determined by averaging three measurements at 120° using a centesimal gauge. This distance was assumed as the characteristic diameter of the grains. Sheets of black carbon copy paper were used to determine the total number of contacts between the particles and the plates, both at the beginning and at the end of the test. The average N of these two values, was used as a representative value of the number of contacts between particles and plates. This type of measurement is surely affected by some error, but its use is essential for the calculation of the individual

particle strength. Furthermore, the experimental results showed a low dispersion.

Finally, a non-secondary problem is represented by the choice of a value of the applied force P to be taken as a breaking value, P_f. Figure 4.8 shows a typical plot of platen load P as a function of the platen displacement obtained from these tests. It can be seen that there are some initial peaks in the load-displacement curve, which correspond to the fracturing of asperities, and the rounding of the particle as small corners break off. However, this cannot be described as failure of the particle: the asperity under the platen which has just broken off would have fractured irrespective of the size of the parent particle. Therefore, the particle crushing takes place progressively and in theory could continue until they are pulverized. If the test did not stop, the load would continue to grow steadily after all the peaks exhibited.

In order to determine the tensile strength of grains it was decided to use the solution proposed by Lee (1992). He compressed individual grains of Leighton Buzzard sand, oolitic limestone and carboniferous limestone, in such a manner shown in Figure 4.7. For a grain of diameter d under a diametral force P, a characteristic tensile stress induced within it may be defined as:

$$p = \frac{P}{d^2} \tag{4.3}$$

Lee calculated the tensile strength of grains as:

$$p_f = \frac{P_f}{Nd^2} \tag{4.4}$$

where the subscript f denotes failure. The failure condition is that for which a fragment weighing more than 25% of the original grain is detached from a grain.

It can be clearly seen in Figure 4.8 that each small peak is followed by a large peak and that the catastrophic failure (the particle split) is identified by a dramatic drops of P_f. Particle fracture is interpreted as particle 'splitting'.

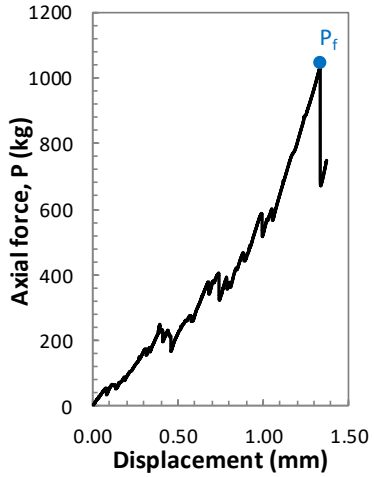

Figure 4.8 Typical load-displacement plot

Lee (1992) found that for particles of a given size and mineralogy, the tensile strength is not a constant but has a standard deviation about some mean value. Furthermore, he found the average tensile strength to be a function of particle size d:

$$p_f = \chi \cdot d^{\omega-2} \tag{4.5}$$

where χ and ω are constants dependent on the material.

The tests have been performed both on dry and saturated grains. In this second case the grains were previously placed in a closed vessel filled with pressurised water (Figure 4.9) and left several days under backpressure for saturation.

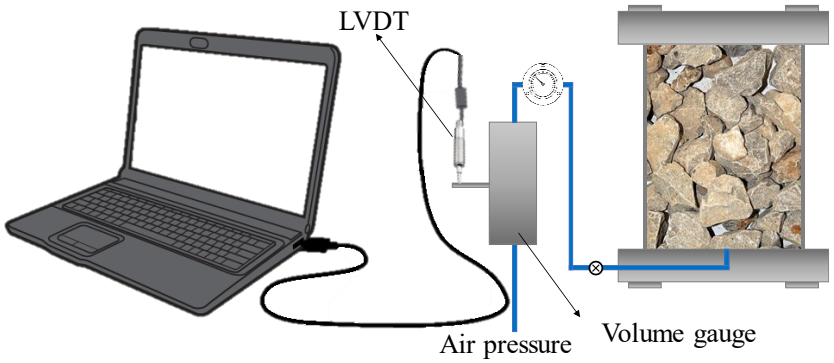

Figure 4.9 System used to saturate grains

In particular, the water pressure in the vessel was kept constant at 70 kPa. This pressure was chosen because it corresponds to the backpressure applied in the triaxial tests. Through an external volume gauge connected to the vessel, the volumes of water absorbed by the grains were estimated. The grains were kept in the vessel until the absorbed volume–time curve approached its horizontal asymptote. The curves obtained for the two materials considered are shown in Figure 4.10.

This procedure aims to completely saturate the pores of the grain. The grains saturated as described were subjected to crushing tests using the system shown in Figure 4.11. The only difference of this scheme compared to that shown in Figure 4.7 is that the saturated grains are kept in water during the crushing test.

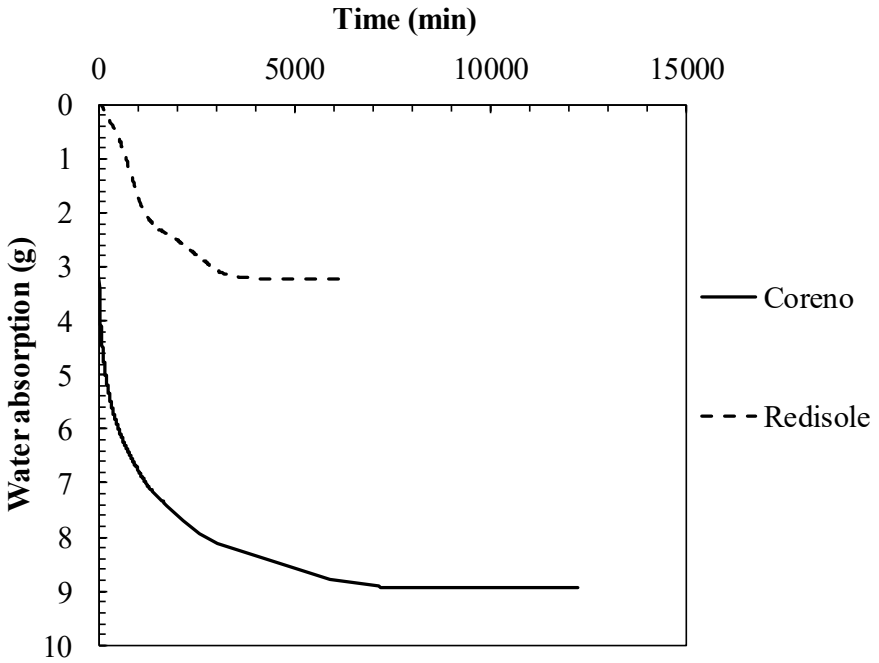

Figure 4.10 Absorption curve

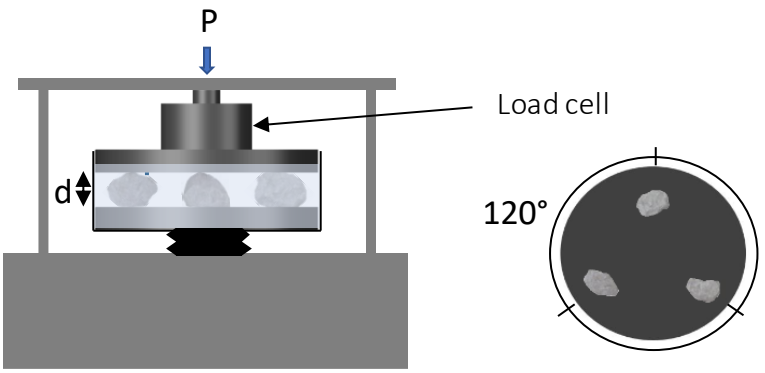

Figure 4.11 Particle tensile strength test set-up for saturated grains

4.4.2 Experimental results

Two series of tests were carried out, respectively on dry and saturated grains. Each series includes 10 tests on Coreno rockfill and 10 tests on Redisole rockfill. The results are shown in Figure 4.12.

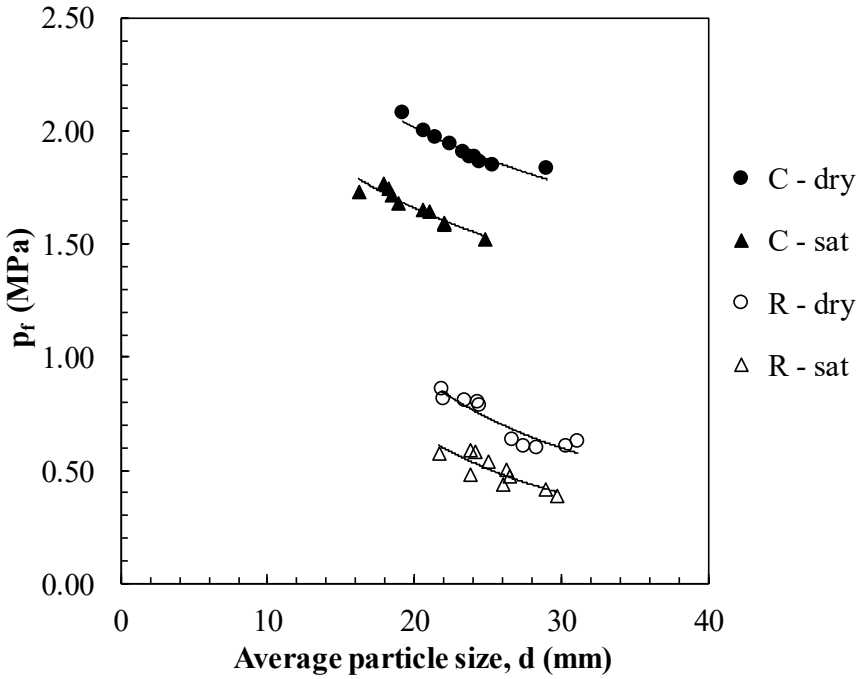

Figure 4.12 Results of grain crushing tests on Coreno and Redisole particles

Obviously the granulometric fraction investigated is the one of greater dimensions since it is most affected by the breakage.

According to literature, p_f decreases as the diameter increases for both materials, both for dry and saturated grains. The obtained regressions are shown in the Table 4.3.

Table 4.3 Obtained regressions from grain crushing tests

Soil	**S_r**	**Regression**
Coreno	0	$p_f = 5.304 \cdot d^{-0.323}$
	1	$p_f = 4.832 \cdot d^{-0.357}$
Redisole	0	$p_f = 25.623 \cdot d^{-1.104}$
	1	$p_f = 34.361 \cdot d^{-1.310}$

In order to use p_f as a parameter to normalize the experimental results, and therefore to verify its influence on the global mechanical behaviour, for the two materials the only value of p_f was assumed to be that obtained considering the diameter d_{50} of the adopted grain size distribution curve (Table 4.4).

Table 4.4 Diameter d_{50} of the grain size distributions adopted

Grain size distribution	**d_{50} (mm)**
Coarse	21.40
Medium	12.50
Fine	3.38
Parallel	26.60

The p_f values used in the research for the four grain size distributions of the two tested materials are shown in Table 4.5.

Table 4.5 Tensile strength of grains for the grain size distributions of the two soils tested

		p_f (MPa)			
Soil	**S_r**	**Coarse**	**Medium**	**Fine**	**Parallel**
Coreno	0	1.97	2.35	3.58	1.84
	1	1.62	1.96	3.13	1.50
Redisole	0	0.87	1.58	6.68	0.68
	1	0.62	1.26	6.97	0.47

The data highlight that (a) Redisole grains have a lower tensile strength than Coreno ones and (b) saturated grains have a lower strength than dry ones.

4.5 Specimen preparation

The rockfill specimens to be used in the tests were prepared in the laboratory. The quantity of various sizes of rockfill materials required to achieve the gradation of the modelled rockfill material for preparing the specimen at the specified density was determined by dry weight. The individual fractions were mixed thoroughly after drying the material in a stove at 105 °C. In this way, five layers with the selected grain size distribution and initial void ratio were prepared.

Regarding the triaxial tests, samples, 200 mm in diameter and 410 mm in height, were directly compacted in the triaxial cell base, with a 3 mm thick latex membrane placed into a split mould. A tamping method was applied to 5 layers. The number of blows applied per layer with the help of a Marshall Hammer depends on the desired

initial relative density. This piston had a diameter of 200 mm to avoid the particle breakage during compaction. The grain size distribution was determined after compaction (see Figure 4.13) to have an initial reference and therefore to be able to calculate the particle breakage produced only by the mechanical effect of the tests. It is evident that the particle breakage due to the compaction is not relevant for any grain size distribution. The mould was removed after compaction and the membrane provided a small confinement to maintain the sample geometry. Then the measuring and control devices were mounted, and the cell and auxiliary devices were assembled for testing.

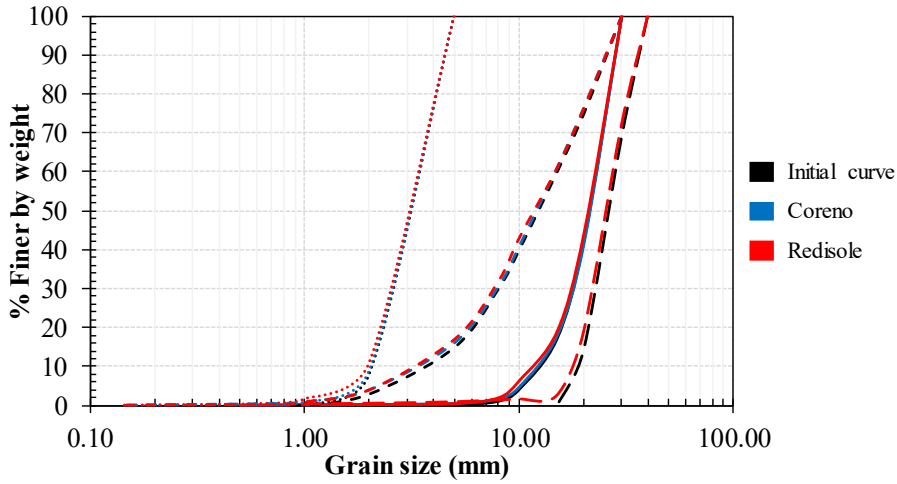

Figure 4.13 Comparison between grain size distributions before and after compaction for the two tested soils.

Regarding the large oedometric tests, the materials were compacted in five layers having thickness of 5 cm. Each layer of the fill was compacted in the oedometer ring using a vibrating table with a

frequency of 60 Hz. The procedure was evolved after several trials to get the required relative density. After compaction, the oedometer ring with the specimen were installed in the oedometer apparatus. The assembly was finished by clamping the top cap and setting up the LVDTs. Readings of vertical displacement and axial loads were taken at periodic intervals (5 s).

The material to be used in the small oedometer apparatus was divided into five equal parts for compacting into five layers inside the oedometer ring. Each layer of the fill having thickness of 1 cm was compacted using a Marshall Hammer with a diameter d =15 cm. Once the specimen is compacted, the oedometer was installed on the apparatus that allows the application of the load. If necessary, the sample was saturated by allowing water to pass through the base of the oedometer cell and using a top drainage system for removing air voids.

4.6 Final remarks

The materials used in this research are coarse-grained soils commonly used for the construction of dams, road and railway embankments. One rockfill comes from the Redisole dam on Fiumarella river (CS) while the other from a quarry located in Coreno (FR). The two rockfills have different geological origins and therefore different porosity and resistance but the same grain size distributions and initial relative densities were used in the laboratory tests.

In order to evaluate the effectiveness of the parallel gradation and scalping techniques used to adapt the grain size distribution curve to the large equipment supplied, four different grain size distributions have been adopted. These are correlated to each other because they were obtained precisely through the parallel gradation and scalping techniques.

Therefore, to evaluate the influence of the grain tensile strength on the mechanical behaviour exhibited in triaxial and oedometric tests, crushing tests were carried out both on grains with environmental humidity and on saturated grains. Finally, the details of the procedures used to prepare the specimen are reported in this chapter.

4.7 References

Billiam J. (1967). *Some aspects of the behaviour of granular material at high pressures*. Proc. of Roscoe Memorial Symposium on Stress-Strain Behaviour of Soils, Cambridge University, 69-80.

Bishop A.W., Henkel D.J. (1962). *The measurement of soil properties in the triaxial test*. Edward Arnold, London.

Flora A. (1995). *Caratterizzazione geotecnica e modellazione dei materiali a grana grossa*. PhD Thesis. University of Napoli Federico II.

Frossard E., Hu W., Dano C., Hicher, P.-Y. (2012). *Rockfill shear strength evaluation: a rational method based on size effects*. Géotechnique, 62(5), 415-427.

Frost R. J. (1973). *Some testing experiences and characteristics of boulder-gravel fills in earth dams*. STP 523:207, ASTM, Philadelphia.

Fumagalli E. (1969). *Tests on cohesionless materials for rockfill dams*. Journal of the Soil Mechanics and Foundations Division, ASCE, 95(1), 313-332.

Jaeger J. C. (1967). *Failure of rocks under tensile conditions*. Int. J. Rock. Min. Sci., 4, 219-227.

Lambe T. W., Whitman R. V. (1969). *Soil mechanics*, Wiley, New York.

Lee D. M. (1992). *The angles of friction of granular fills*. Ph.D. dissertation, University of Cambridge.

Lowe J. (1964). *Shear strength of coarse embankment dam materials*. Proc., 8th Int. Congress on Large Dams, ICOLD, Edinburgh, Scotland, 3, 745-761.

Marachi N. D., Chan C. K., Seed H. B. (1972). *Evaluation of properties of rockfill materials*. Journal of Soil Mechanics & Foundations Div, 98(1), 95-114.

Marachi N. D., Chan C. K., Seed H. B., Duncan J. M. (1969). *Strength and deformation characteristics of rockfill materials.* Department of Civil Engineering, Report No. TE-69-5. University of California.

Marsal R. J. (1973). *Mechanical properties of rockfill*. Embankment Dam Engineering, Casagrande Volume, Wiley, New York, 109-200.

McDowell G. R., Bolton M. D. (1998). *On the micromechanics of crushable aggregates*. Géotechnique, 48(5), 667-679.

Nobari E. S., Duncan J. M. (1972). *Effect of reservoir filling on stresses and movements in earth and rockfill dams.*

Department of Civil Engineering, Report No. TE-72-1. University of California.

Oldecop L. A., Alonso E. E. (2013). *Rockfill mechanics*. Advances in Unsaturated Soils – Caicedo et al. (eds), Taylor & Francis Group, London, ISBN 978-0-415-62095-6.

Ortega E. (2008). *Comportamiento de materiales granulares gruesos. Efecto de la succión*. Tesis Doctoral. Universitat Politècnica de Catalunya, Barcelona, España.

Penman A. D. M. (1971). *Rockfill*. Building Research Station (Great Britain). Current Paper 15/71.

Rzadkowski B., Zurek J. (1970). Influence de l'eau sur la déformabilité des roches broyées et sur le tassement des barrages en enrochement. Trans. 10th Conf. on Large Dams, Montreal, 1, 857-867.

Sowers G. F., Williams R. C., Wallace T. S. (1965). *Compressibility of broken rock and settlement of rockfills*. Proceedings of 6th ICSMFE. Montreal, 2, 561-565.

Sudhindra C., Venkatachalam K., Soni M. L., Sivakumar N., Sharma P. (1991). *Large size triaxial shear tests on rockfill materials for design parameters*. Proc., 56th Research and Development Session, CBIP, Hyderabad, 29-34.

Zeller J., Wullimann R. (1957). *The shear strength of the shell materials for the Go-Schenenalp Dam Switzerland*. Proc., 4th Int. Conf. on Soil Mechanics and Foundation Engineering, Butterworth's, London, 2, 399-404.

CHAPTER 5

EXPERIMENTAL RESULTS

5.1 Experimental programme

As previously specified, a series of triaxial and oedometric tests have been carried out on two different coarse-grained materials in order to examine the influence of some factors on their mechanical behaviour. This section describes in detail the stress and suction paths followed in the tests and discusses the experimental results.

5.1.1 Stress paths performed in a large triaxial cell

Consolidated drained triaxial tests were performed on the rockfill materials obtained from the limestone rock from the Coreno Ausonio (FR) quarry and a heterogeneous rock from the Redisole Dam in San Giovanni in Fiore (CS). Details of the tests are given in Table 5.1 and Table 5.2 for Coreno and Redisole rockfill materials respectively. In these tables, the consolidation and drainage conditions will not be specified because all the tests have been isotropically consolidated and sheared in drained conditions. In all the tests, membrane correction has been applied to the current stress and volume measurements as reported in Appendix A.1.

The test ID, with which the tests will be referred to below, is composed of some letters and numbers: the first letter refers to the material (C for Coreno and R for Redisole) and the second one to

the grain size distribution adopted (Fine, Medium, Coarse or Parallel, see Figures 4.3 and 4.4) while the number represents the confining stress σ'_c (or σ_c for unsaturated specimen) in bar. Finally, in Table 5.1, it can be observed that in some tests the deviatoric phase was performed with constant confining stress, while in others with constant mean effective stress. In this case, the last letter of the test ID is P. Instead, in all the drained triaxial tests on Redisole rockfill reported in Table 5.2, the deviatoric phase was carried out with constant confining stress.

When the deviatoric phase was performed in CRS (controlled rate of straining) conditions, a rate of 20.50 mm/h was adopted.

Furthermore, three triaxial tests were performed on Coreno rockfill (CF7-4, CF7-4P, CM7-4) during which the saturated specimens ($S_{r,i}$=1) were isotropically consolidated up to p'=700 kPa and then unloaded to p'=400 kPa. Subsequently, the deviatoric phase in CRS conditions was performed in order to analyse the effect of previous loading history on the shear stress-strain behaviour.

In Table 5.1 and Table 5.2 are also reported tests on unsaturated specimens ($S_{r,i}$=0). The CF2U and CC2U tests were performed on specimens prepared with ambient humidity material and then directly consolidated. These specimens were kept dry throughout the tests to study the effect of the degree of saturation on the strength and deformation behaviour of rockfill.

The CC2U-S and RP1U-S tests have been carried out on ambient humidity consolidated specimens. At the end of the consolidation phase, a CRL (controlled rate of loading) shear stage was started

(rate: 50 kPa/h) up to a specific value of the deviatoric stress (q = 500 kPa and 250 kPa respectively). At the end of this stress path, the specimen was saturated and loaded to failure in CRS conditions.

Finally, during two triaxial tests on saturated specimens (CC2-cyc; RP2-cyc) cyclic deviatoric phases were carried out. At the end of the consolidation phase, a CRL shear stage was carried out (rate: 100 kPa/h) by varying the values of the deviatoric stress q according to the following scheme: 5-100; 100-5; 5-300; 300-200; 200-600; 600-500 kPa. At the end of this stress path the specimen was loaded to failure in CRS conditions (rate: 20.50 mm/h).

On testing, a dry relative density of 70% was adopted for Coreno rockfill. For the material used in the construction of the Redisole dam, a relative density of 100% was adopted for specimens prepared with the Parallel grain size distribution. These values of relative density have been chosen for multiple reasons: they are a relevant in-situ values and provide a stable structure that won't easily collapse upon saturation. To evaluate the effects of the initial compaction state and the grain size distribution on the mechanical behaviour of the material, an initial relative density of 50% and 70% was used for specimens prepared with the Coarse curve for RC0.5 test and RC1 test respectively.

The range of confining pressures was chosen keeping in mind the typical stress levels in dams, the limits of the equipment and the main pressure supply lines in the laboratory.

Table 5.1 Details of consolidated drained triaxial tests on Coreno rockfill

Test ID	**Grain size distribution**	**D_r**	**$S_{r,i}$**	**σ_c, σ'_c**	**Deviatoric phase**	
					p, p'	**σ_c, σ'_c**
		-	**-**	**kPa**	**kPa**	**kPa**
CF0.5	Fine	0.7	1.0	50	variable	constant
CF2				200		
CF4				400		
CF2P				200	constant	variable
CF6P				600		
CF7P				700		
CF7-4P				↑700 ↓400		
CF7-4				↑700 ↓400	variable	constant
CF2U			0.0	200		
CM0.5	Medium	0.7	1.0	50	variable	constant
CM2				200		
CM4				400		
CM4P				400	constant	variable
CM7-4				↑700 ↓400	variable	constant
CC0.5	Coarse	0.7	1.0	50	variable	constant
CC2				200		
CC4				400		
CC2-cyc				200		var.-const.
CC2U-S			0.0	200		constant
CC2U				200		

Table 5.2 Details of consolidated drained triaxial tests on Redisole rockfill

Test ID	Grain size distribution	D_r -	$S_{r,i}$ -	σ_c, σ'_c kPa	Deviatoric phase	
					p, p' kPa	σ_c, σ'_c kPa
RC0.5	Coarse	0.5	1.0	50	variable	constant
RC1		0.7		100		
RP0.5	Parallel	1.0		50		
RP1				100		
RP2				200		
RP4				400		
RP2-cyc				200		
RP1U-S			0.0	100		

The stress paths performed in the large triaxial cell HPSP are shown in Figure 5.1 and Figure 5.2 for Coreno and Redisole rockfill materials respectively.

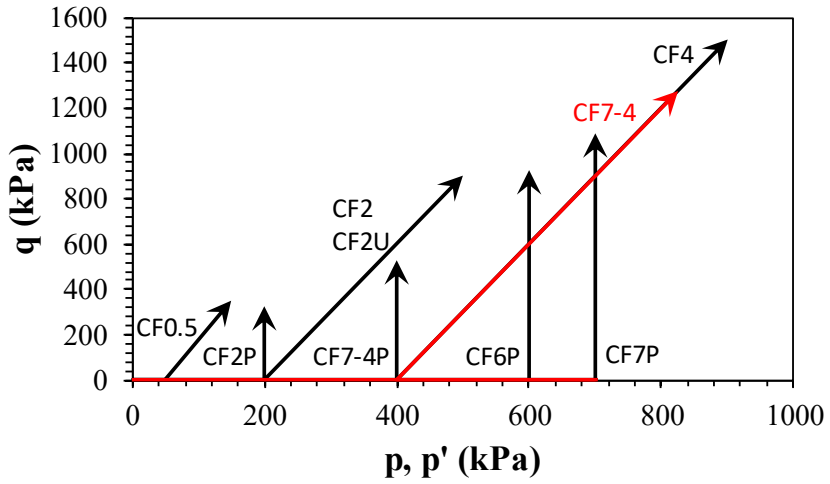
1600
1400
1200
1000
800
600
400
200
0
q (kPa)
0
200
400
600
800
1000
p, p' (kPa)
CF4
CF7-4
CF2
CF2U
CF0.5
CF2P
CF7-4P
CF6P
CF7P

a)

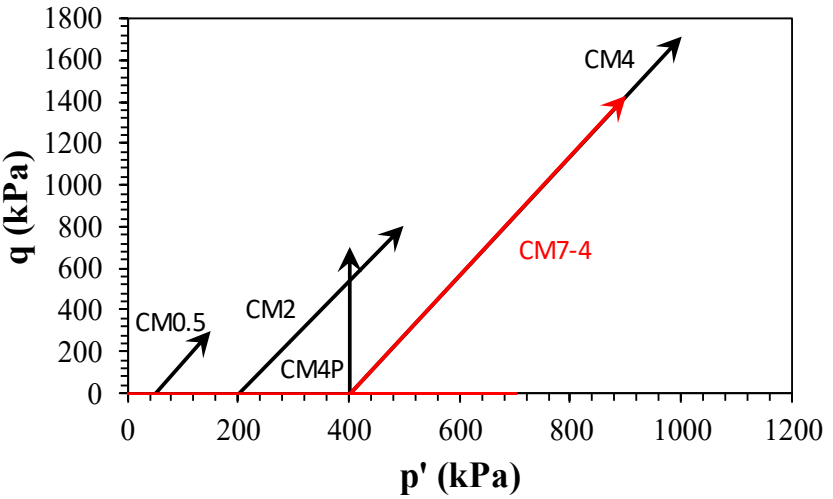
1800
1600
1400
1200
1000
800
600
400
200
0
q (kPa)
0
200
400
600
800
1000
1200
p' (kPa)
CM4
CM7-4
CM0.5
CM2
CM4P

b)

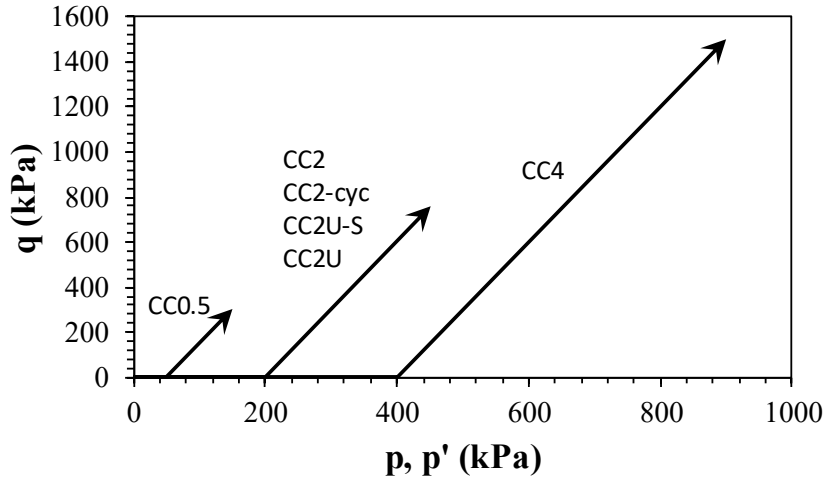

c)

Figure 5.1 Stress paths scheme for tests on Coreno rockfill: a) Fine; b) Medium; c) Coarse grain size distribution

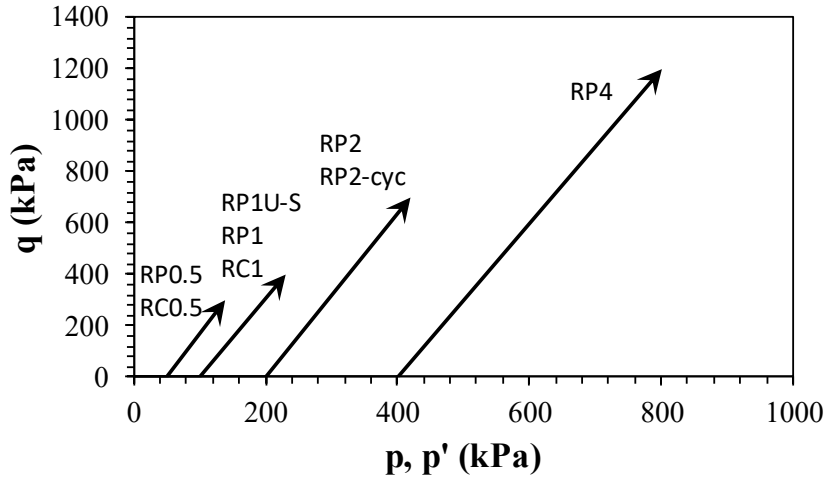

Figure 5.2 Stress paths scheme for tests on Redisole rockfill

The experimental programme includes isotropic compression tests (IC) on Coreno rockfill (Table 5.3) for each grain size distribution (Fine, Medium and Coarse). Two types of test labels are indicated: the first refers to the grain size distribution (F, M or C), and the second to the unsaturated (U) or saturated (S) conditions of the specimen. All the times the IC tests consisted of a CRL loading stage up to a mean stress p (or mean effective stress p' for saturated specimen) of 700 kPa followed by an unloading stage to p (or p') = 100 kPa. The adopted loading rate is always 50 kPa/h. In Table 5.3 some tests are indicated with three letters. The first one refers to the grain size distribution, the other two, i.e. US, indicate the fact that the triaxial test have been performed on unsaturated (U) specimens loaded up to a mean stress p of 700 kPa, then saturated (S) and finally unloaded to p'=100 kPa (rate of loading and unloading of 50 kPa/h). During this test, the specimen was saturated keeping constant the confining stress. At the end of the wetting, the same time have been waited before unloading in all tests of this type. In this way the strains recorded at constant confining stress in different tests are comparable.

In these isotropic compression tests, the volumetric strains of the unsaturated specimen were determined by measuring the volumes of water exchanged by the cell with a burettes system as detected by a differential pressure transducer (DPT). This measure was subsequently corrected by eliminating the volumes of water exchanged by the cell due to the strains of the external aluminium cylinder of the triaxial device and the plexiglass of the burettes

(Figure 5.3). The $\Delta V:\sigma_c$ correlation was determined by measuring the volumes of water exchanged by the system without the specimen (ΔV), as the cell pressure increases.

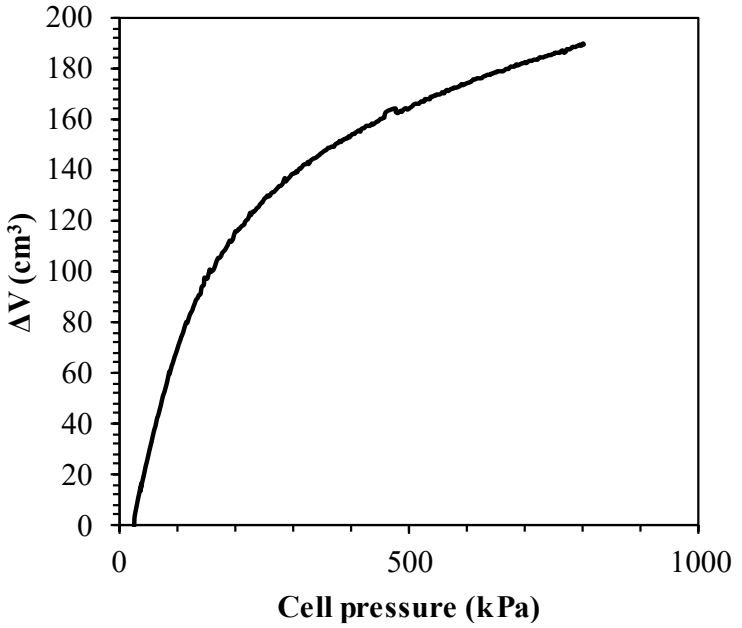

Figure 5.3 Cell pressure versus volumes of water exchanged by the cell due to the strains of the external aluminium cylinder of the triaxial device and the plexiglass of the burettes

The abbreviation RH reported in Table 5.3 indicates that the test was performed with relative humidity control system reported in Figure 3.7. The relative humidity has been controlled with a solution of Sodium chloride, NaCl. The target RH expected is 75%. The tests with relative humidity control have two stages.

The first stage consists in the application of the relative humidity of 75% to the pore air by a forced convection air flow at 75% relative

humidity. In this stage, the thermodynamic equilibrium, i.e. the relative humidity equalization in all points of the specimen, is verified by measuring the variation of relative humidity of the air outflowing from the specimen over time. Once the RH versus time measurements tend to its threshold, the first stage is stopped.

In the second stage the isotropic stress increases (or decreases) with a confining pressure rate of 50 kPa/h.

The unsaturated specimen has been prepared using material dried in a stove for 24 hours and subsequently left to ambient relative humidity for 2 days. The isotropic compression tests have been performed in drained conditions, keeping the specimen in contact with the external environment. The drains remain open even in tests with saturated specimens. In the tests with RH control, the open drains are not kept in contact with the external environment but with the closed relative humidity control circuit, kept in operation in order to preserve the RH value constant.

For testing, a dry density corresponding to 0% or 70% of relative density was adopted.

The subscripts i and f in Table 5.3 refer to initial and final conditions respectively.

Table 5.3 Isotropic compression tests on Coreno rockfill

Test ID	Grain size distribution	D_r -	$S_{r,i}$ -	$S_{r,f}$ -
IC-FU	Fine	0.7	0	0
IC-FUS			0	1
IC-F-RH			0	-
IC-FS			1	1
IC0-FU		0.0	0	0
IC0-F-RH			0	-
IC0-FS			1	1
IC-MU	Medium	0.7	0	0
IC-MUS			0	1
IC-M-RH			0	-
IC-MS			1	1
IC-CU	Coarse		0	0
IC-CUS			0	1
IC-C-RH			0	-
IC-CS			1	1

5.1.2 Oedometric tests on samples with variable degree of saturation

The experimental programme in the large oedometer (LO) ring involved three series of tests for each material considered (C or R) by using two different grain size distributions (Coarse or Parallel).
The I-series (letter S) have been performed under fully saturated conditions: once compacted, specimens were saturated and then compressed.

In the II-series (letter U) specimens compacted in an identical manner were maintained at ambient relative humidity during all the oedometric tests.

Finally, in the III-series (letter US) dry specimens were saturated at a constant vertical load of 10 bar for Coreno rockfill and 5, 10 or 20 bar for Redisole rockfill. A summary of the test programme is reported in Table 5.4. The subscripts i and f in Table 5.4 refer to initial and final conditions respectively.

Table 5.4 Details of large oedometric tests

Test ID	**Soil**	**Grain size distribution**	**D_r** -	**$S_{r,i}$** -	**$S_{r,f}$** -
LO-CCU	Coreno	Coarse	0.7	0	0
LO-CCU-S10				0	1
LO-CCS				1	1
LO-RCU	Redisole			0	0
LO-RCU-S5				0	1
LO-RCU-S10				0	1
LO-RCU-S20				0	1
LO-RCS				1	1
LO-RCU loose			0.5	0	0
LO-RPU		Parallel	1.0	0	0

It can be observed in Table 5.4 that the same type of oedometric test on an unsaturated specimen prepared with Redisole rockfill materials was repeated with three different initial relative density (i.e. three different initial void ratio). Two of these tests, LO-RCU and LO-RCU-loose, refer to specimens prepared using the same grading curve. Instead, the last one (LO-RPU test) was carried out

on a specimen prepared with the Parallel grain size distribution and therefore with a higher d_{max}. The aim of these three tests is to highlight the effects of the initial void ratio and the particle size on rockfill compressibility and particle breakage.

In order to study the effects of d_{max} and the degree of saturation S_r on the mechanical behaviour of coarse-grained material and the effectiveness of the parallel gradation techniques, several oedometric tests have been carried out by using the small oedometer apparatus (SO). Also in this case the experimental programme involved three series of tests for each material (C or R): the first on a saturated specimen (S), the second on an unsaturated specimen (U) and the third on a dry specimen saturated (US) after the application of a vertical load σ_v equal to 8 or 25 bar for Coreno rockfill and 8 bar for Redisole rockfill. All the specimens were prepared with the Fine grain size distribution and an initial relative density D_r =0.70.

Details on the test programme are reported in Table 5.5. Also in the small oedometer, a test with the relative humidity control was carried out. The desired value of RH was imposed with a solution of Sodium chloride, NaCl.

Table 5.5 Details of small oedometric tests

Test ID	Soil	D_r -	$S_{r,i}$ -	$S_{r,f}$ -
SO-CU	Coreno	0.7	0	0
SO-CU-S8			0	1
SO-CU-S25			0	1
SO-C-RH			0	-
SO-CS			1	1
SO-RU	Redisole		0	0
SO-RU-S8			0	1
SO-RS			1	1

5.2 Triaxial tests

The extensive application of rockfill materials in geotechnical structures, especially during recent decades, makes the precise recognition of different aspects of the behaviour of these materials ineluctable. This work contributes to the argument presenting an experimental program including dry-saturated large-scale triaxial tests performed in order to investigate the effects of degree of saturation, initial relative density and gradation curve on the stress-strain behaviour of a rockfill material.

5.2.1 Monotonic tests

In laboratory investigations, rockfill specimens were usually sheared with a constant cell pressure. There are few reported researches on the behaviour of rockfill along other stress paths,

despite of the wide acceptance that the stress-strain behaviour of soil is, in general, dependent on the loading path (Lambe et al., 1979). The stress path-dependent behaviour has been investigated extensively for fine grain soils (e.g. Bishop and Wesley, 1975; Lade and Duncan, 1975). For example, Lade and Duncan (1975) demonstrated in triaxial tests on sand that the strains induced by changing the stresses from one stress state to another depended not only on the end points, but also on the stress path. Instead there is uncertainty about the behaviour of rockfill along stress paths different from that carried out with a constant cell pressure.

To highlight some aspects of the mechanical behaviour of rockfill along more general stress paths large triaxial tests have been carried out on specimens with different initial grain size distributions, prepared with two rockfill materials (i.e. Coreno and Redisole).

The stress-strain-volume change behaviour of the modelled limestone rockfill of **Coreno** is shown from Figure 5.4 to Figure 5.11.

The results of deviatoric tests performed following different stress paths on specimens prepared with the Fine grading curve and consolidated at different stresses are shown in Figure 5.4. It is evident that the stress-strain and volumetric behaviour of the limestone are significantly influenced by the loading directions as well as the confining stresses. For example, the comparison between CF2 and CF2P tests results obtained at the same confining pressure, highlights that the different stress path followed during the deviatoric phase has a substantial effect both on the stress-strain

behaviour and on the volumetric response. In the CF2P test carried out at constant mean effective stress dilatancy is pronounced since the beginning of the stress path, while in the test CF2 (sheared at constant cell pressure) the specimen initially shows volumetric contraction.

However, dilatancy is gradually inhibited by elevated confining stress in both constant p' or constant σ'_c tests. In this second type of test, at confining pressure of 400 kPa, contraction seems to become dominant while in the tests carried out at constant p' dilatancy is always dominant. This highlights that the loading path has a significant effect on the dilatancy.

Obviously, the peak deviator stress increases with increasing applied confining pressure for both constant p' and σ'_c paths and the highest values are recorded in the constant σ'_c tests.

The angle between the loading direction and the p'- axial is $\alpha = 90°$ for tests with constant p' and $\alpha = 71.6°$ for tests with constant σ'_c. At low α the deformation was dominated by volumetric contraction and the specimen only reached its peak deviator stress at large axial strains, whereas at high α dilatancy was pronounced and the specimen mobilized its full strength at small axial strains. Furthermore, both axial and volumetric strains measured at the peak deviator stresses decrease gradually with increasing α. Xu et al. (2012) also observed similar behaviour for limestone rockfill.

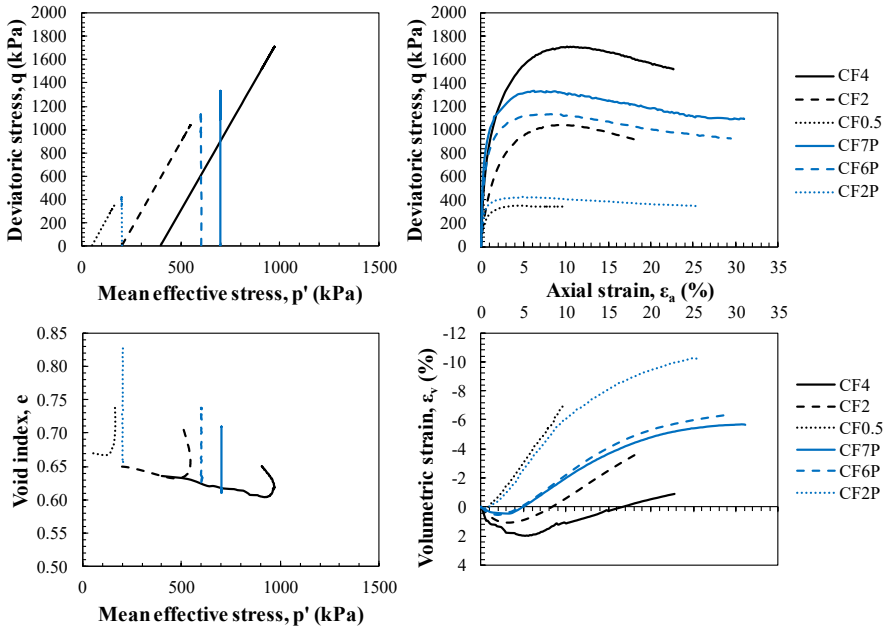

Figure 5.4 Stress-strain-volume change relationship for Coreno specimens prepared with Fine curve

The results of stress paths testing on three specimens prepared with Fine grading curve and sheared from the same isotropic effective stress state p'_0 = 400 kPa are shown in Figure 5.5. While in the isotropic stages of both CF7-4 and CF7-4P tests, the specimens were loaded up to 700 kPa and then unloaded up to p'_0, the CF4 specimen was directly loaded to p'_0. On shearing both the specimen CF4 and CF7-4 were loaded at constant mean effective stress while the deviatoric phase of the CF7-4P test was performed at constant p'.

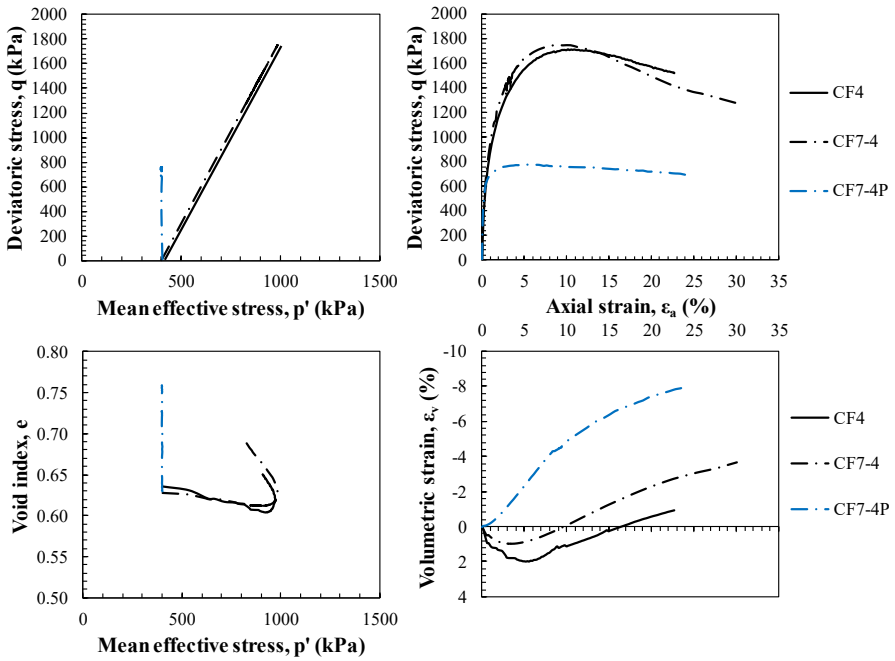

Figure 5.5 Stress-strain-volume change relationship for Coreno specimens prepared with Fine curve: effect of the stress path

From the comparison between CF4 and CF7-4 it can be observed that the previous loading history does not seem to have any significant effect on the peak deviator stress. However, the difference in the ultimate conditions of the test is quite marked, highlighting an effect of the loading history on the residual value of the deviator stress. In the axial-volumetric strain plane the two specimens CF4 and CF7-4 show a similar tendency but are not very closed. It seems that the different loading history influences the dilatancy shown by the specimen.

From the comparison between CF7-4 and CF7-4P once again appears evident that, as seen in Figure 5.4, the peak of the

deviatoric stress is recorded in the test in which α is lower. Moreover, also in Figure 5.5 it is possible to observe a marked dilatancy in the test characterised by greater α. The results seem to imply that greater dilatancy and stiffer initial response could be shown by the material if the distance along a loading path becomes shorter between the initial stress state and the failure envelope.

Results of triaxial tests have been plotted in Figure 5.6 for two S_r values: a dry state, $S_r = 0$ (CF2U test), and a saturated state, $S_r = 1$ (CF2 test). Specimens were loaded with constant confining pressure σ_c or $\sigma'_c = 200$ kPa to study the effect of moisture condition on the strength and deformation behaviour of limestone rockfill.

The presence of water does not determine a considerable variation of the deviatoric stress with respect to the dry condition, in fact the differences between $S_r = 0$ and $S_r = 1$ fall within the range of experimental variability. However, for a given axial strain, the volumetric strain is systematically smaller for tests conducted at $S_r = 0$.

Higher positive dilatancy (contractancy) is recorded during the initial applications of deviatoric stresses in saturated conditions; this is a consequence of particle breakage and grain contact crushing. Then, a second stage of negative dilatancy (expansion) is recorded, at essentially decreasing shearing strength in both tests. Dilatancy rate (in the negative range) increases when S_r decreases (dryer material).

Critical-state conditions were not reached in the tests and the variation of the void ratios seems to be independent of the degree of saturation.

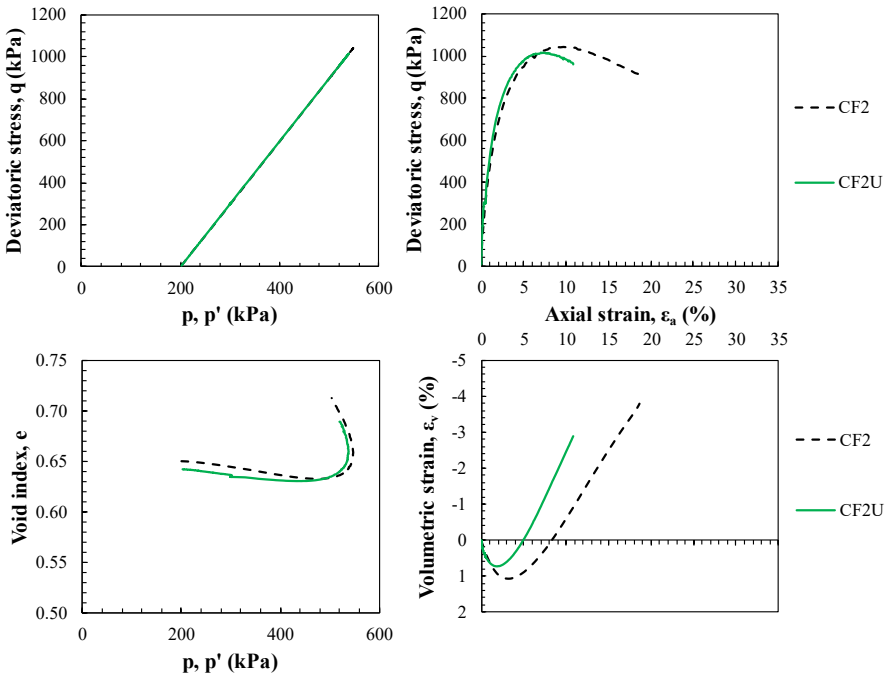

Figure 5.6 Stress-strain-volume change relationship for Coreno specimens prepared with Fine curve: effect of the initial degree of saturation

Limestone rockfill specimens prepared with the Medium grain size distribution were fully saturated before consolidation to the specified isotropic effective stress and then sheared to failure in constant σ'_c drained conditions. The results at three different confining stresses are presented in Figure 5.7. As expected, at low confining stress, dilatancy is pronounced despite of initial

volumetric contraction and gradually decreased as confining pressures increases. The same trend was seen in the tests with the Fine grading curve (Figure 5.4). Higher confining pressure induces more particle breakage, resulting in more contractive deformation behaviour as observed by Indraratna et al. (1993).

Obviously in these tests, as seen with the Fine grading curve (Figure 5.4), higher confining pressures correspond to higher deviatoric stresses for the same axial deformation.

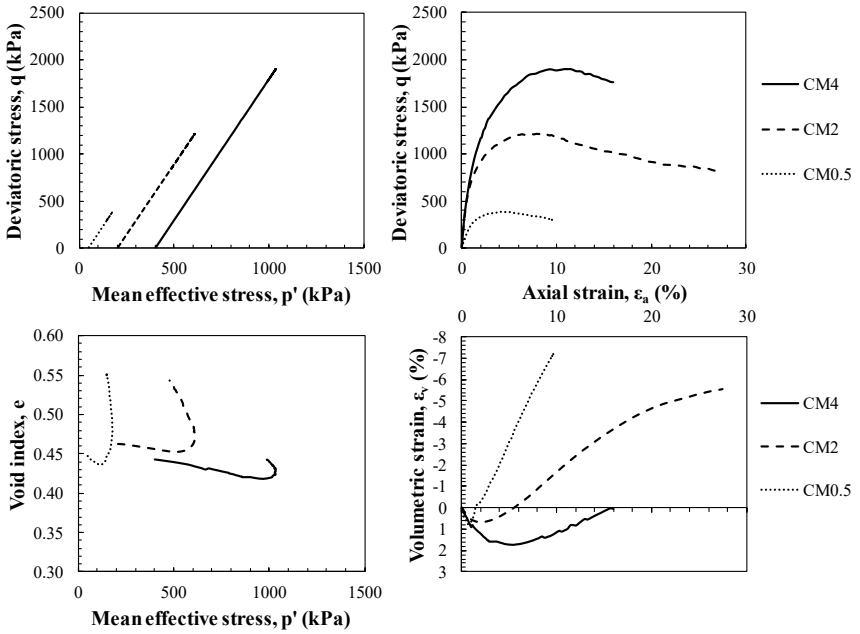

Figure 5.7 Stress-strain-volume change relationship for Coreno specimens prepared with Medium curve

Two additional tests with the Medium grading curve were performed to investigate the loading history and stress path effects. Specimen CM7-4 was first saturated, then isotropically consolidated

up to 700 kPa, isotropically unloaded to 400 kPa, and finally sheared at a constant σ'_c. The effect of the previous loading history can be highlighted comparing the CM7-4 and CM4 tests. Furthermore, the CM4P refers to a specimen sheared at a constant p'.

Figure 5.8 shows that CM4 and CM7-4 specimens exhibit a similar stress-strain behaviour independently of the previous loading history as already seen for the Fine grading curve (Figure 5.5).

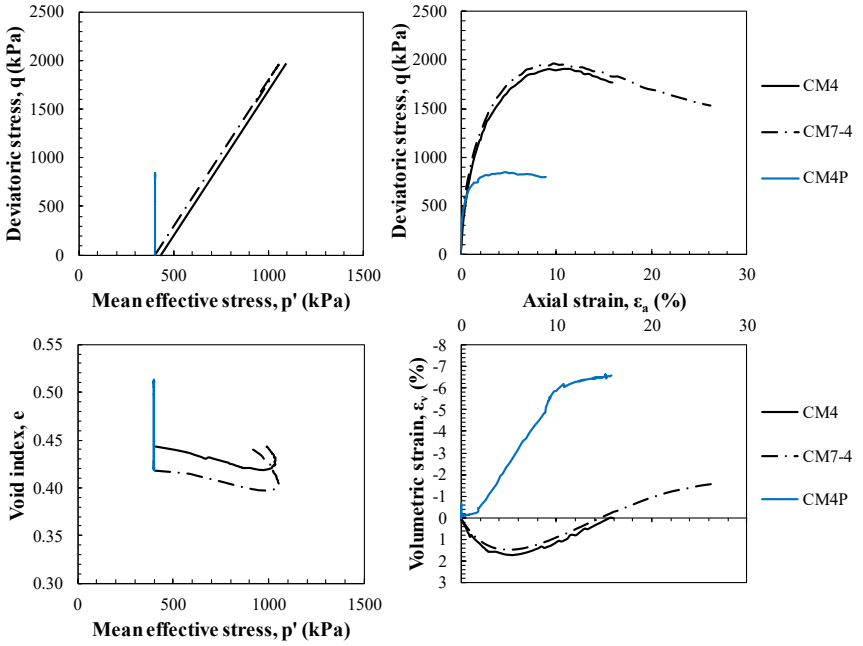

Figure 5.8 Stress-strain-volume change relationship for Coreno specimens prepared with Medium curve: effect of the stress path

As well known the different loading direction followed in the CM4 and CM4P tests greatly influences the mechanical response of the material. These results confirm what seen with the Fine grading

curve: as α increases, dilatancy becomes dominant from low levels of axial strain and the peak deviator stress decreases.

Conventional triaxial tests at three different confining stresses were carried out on specimens prepared with the Coarse grading curve (Figure 5.9): the same conclusions already highlighted for the tests on Fine and Medium grading curves also apply to the Coarse grained rockfill.

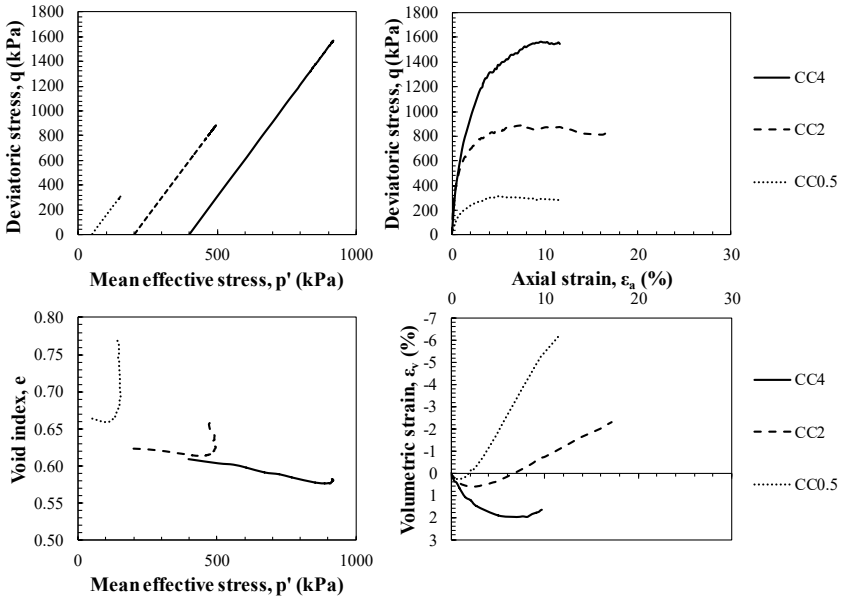

Figure 5.9 Stress-strain-volume change relationship for Coreno specimens prepared with Coarse curve

The experimental programme also consisted of three large scale strain-controlled triaxial tests aimed at studying the effect of the degree of saturation on the mechanical behaviour of the Coarse grained material. In particular, CC2 and CC2U specimens were kept in saturated and dry conditions respectively for the whole duration

of the test. The dry-saturated test CC2U-S, instead, refers to a specimen first compressed (in dry condition) up to a specified shear stress q of 500 kPa, then gradually submerged (from bottom to the top) under a very low water hydraulic gradient and finally sheared in CRS drained conditions.

The above mentioned three tests were carried out at the same confining pressure equal to 200 kPa.

As shown in Figure 5.10, in the CC2U-S test saturation causes a small increase of the axial strain at a constant deviatoric stress. This aspect has been considered by several authors (e.g. Naylor et al., 1986; Pourjafar et al., 2011).

According to the saturation-induced sudden settlements reported in the literature for oedometer and triaxial tests on rockfill materials (Alonso and Oldecop, 2000; Chávez, 2004), Figure 5.10 shows a sudden volumetric collapse at constant axial strain on water saturation.

The degree of saturation seems to influence the peak deviator stress but not its residual value. In fact, the end points of the curves are very close together. It is interesting to note that the residual strength of the dry specimen is comparable with the peak strength of the saturated specimen.

In Figure 5.10 the sudden increase of volumetric strain due to saturation is followed by dilatancy. A general trend of volume increase (negative values of volumetric strain) is observed on deviatoric loading due to relatively high dry density of the specimens. Considering the saturated specimen, the dilatancy effect

is attenuated at high levels of axial strain, differently from what happened in the other two tests.

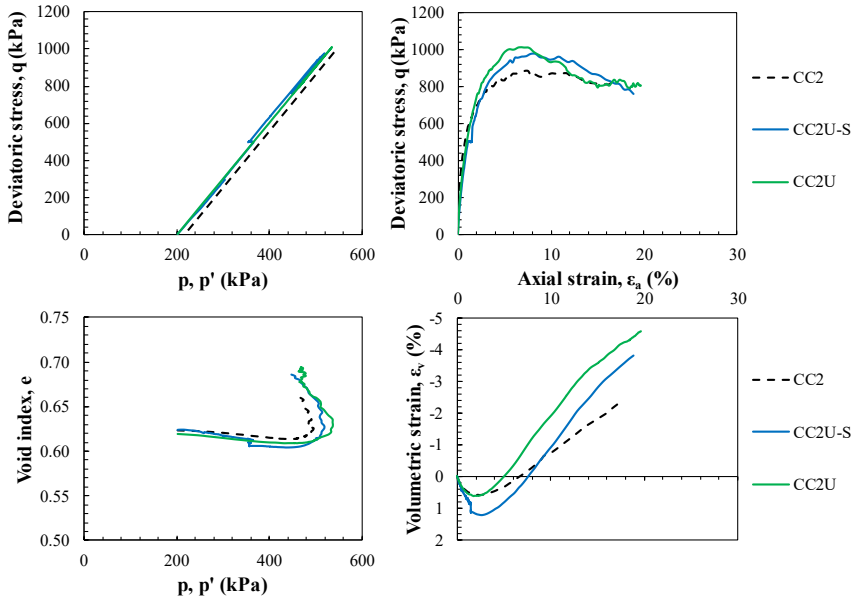

Figure 5.10 Stress-strain-volume change relationship for Coreno specimens prepared with Coarse curve: effect of degree of saturation

The behaviour of a Coarse specimen along an unconventional stress path was studied in the CC2-cyc test. The first part of the deviatoric phase was performed by varying the values of the deviatoric stress q according to the following stress history: 5-100; 100-5; 5-300; 300-200; 200-600; 600-500 kPa. Then the specimen was shared in CRS conditions (20.50 mm/h).

The effect of previous loading history can be obtained comparing the test on specimens CC2 and CC2-cyc, both of which were sheared at the confining stress σ'_c = 200 kPa (Figure 5.11). It can be

seen that these two specimens exhibit remarkably similar stress–strain behaviour despite the different loading path followed. It is noted that the peak strengths for both specimens are approximately identical while the difference in volumetric behaviour is significant. This is probably due to the onset of different particle breakage mechanism.

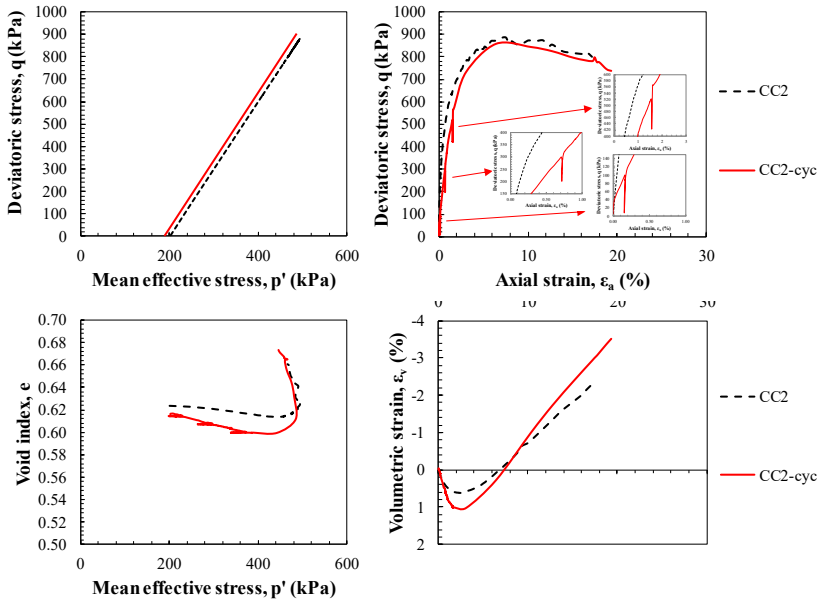

Figure 5.11 Stress-strain-volume change relationship for Coreno specimens prepared with Coarse curve: effect of the stress path

Rockfill material from **Redisole** dam have been also tested by triaxial tests. For testing, a dry density corresponding to 100% of relative density was adopted (Table 5.2). Results of tests carried out at a constant cell pressure are presented in Figure 5.12.

The results show that the stress–strain and volumetric behaviour of rockfill are significantly influenced by the confining stresses. As

obvious for the limestone rockfill, the peak deviator stresses exhibited by Redisole specimens increase as confining stress increases. On the contrary, the dilatancy is attenuated or zeroed by the increasing σ'_c. As expected, the confining stress has a major effect on the observed stress–strain and volumetric behaviour.

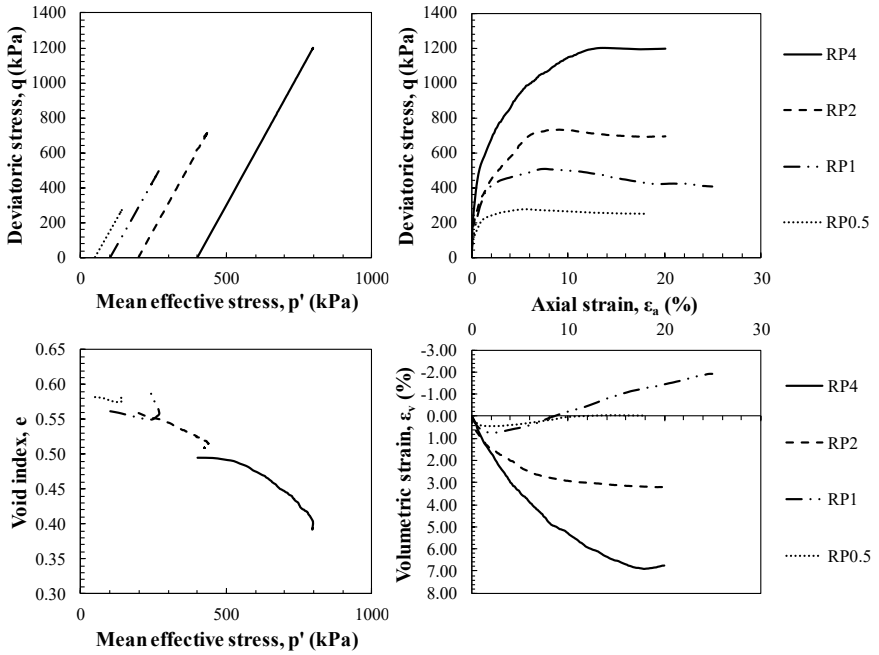

Figure 5.12 Stress-strain-volume change relationship for Redisole specimens prepared with Parallel curve

The same non-conventional stress path studied in the CC2-cyc test (Figure 5.11) was performed in the RP2-cyc test. As observed for the limestone tests, the different loading history followed in the RP2 and RP2-cyc tests, seems to have no significant effect on the deviatoric stress (Figure 5.13). In contrast, the volumetric strains along the loading paths followed in the RP2-cyc test are notably

greater than those at the same σ'_c derived from the conventional triaxial test, clearly highlighting the effect of the previous loading history. For specimen RP2-cyc, the loading-unloading procedure might cause significant changes to the rockfill particle arrangement through particle slippage, rotation and breakage, probably resulting in a higher degree of interlocking between particles. As a result, larger volumetric strain arises on shearing.

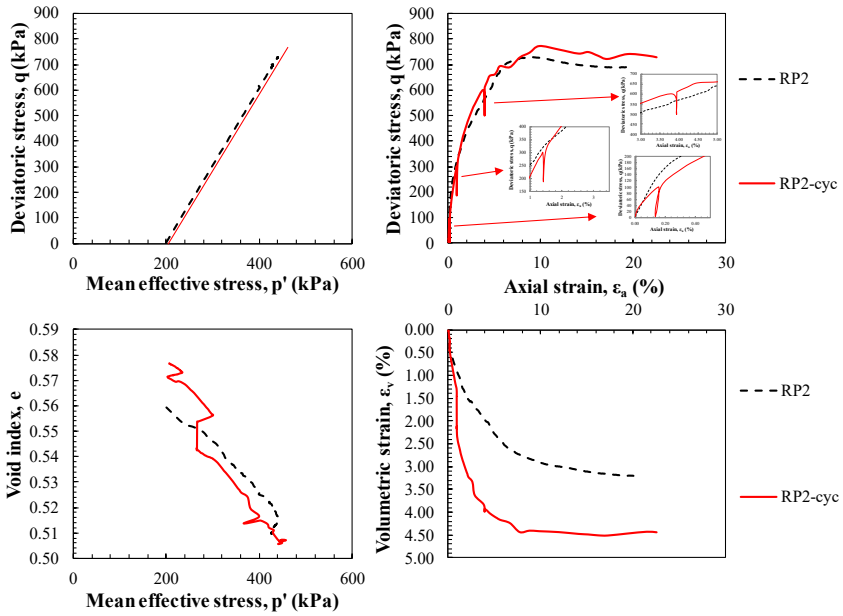

Figure 5.13 Stress-strain-volume change relationship for Redisole specimens prepared with Parallel curve: effect of the stress path

It has been well recognized that large wetting collapse settlement could be induced when dry rockfill is submerged under one-dimensional compression (Oldecop and Alonso, 2001). The effect of degree of saturation on the mechanical behaviour of Redisole rockfill is studied by comparing the test results of RP1 and RP1U-S

specimens, which were loaded in saturated and dry-saturated conditions, respectively, at the same σ'_c or σ_c = 100 kPa (Figure 5.14). In the dry-saturated tests (RP1U-S test), the specimens were first compressed (in dry condition) up to a specified shear stress level (q = 250 kPa), then gradually submerged from bottom to the top under very low water gradient and finally sheared in CRS conditions.

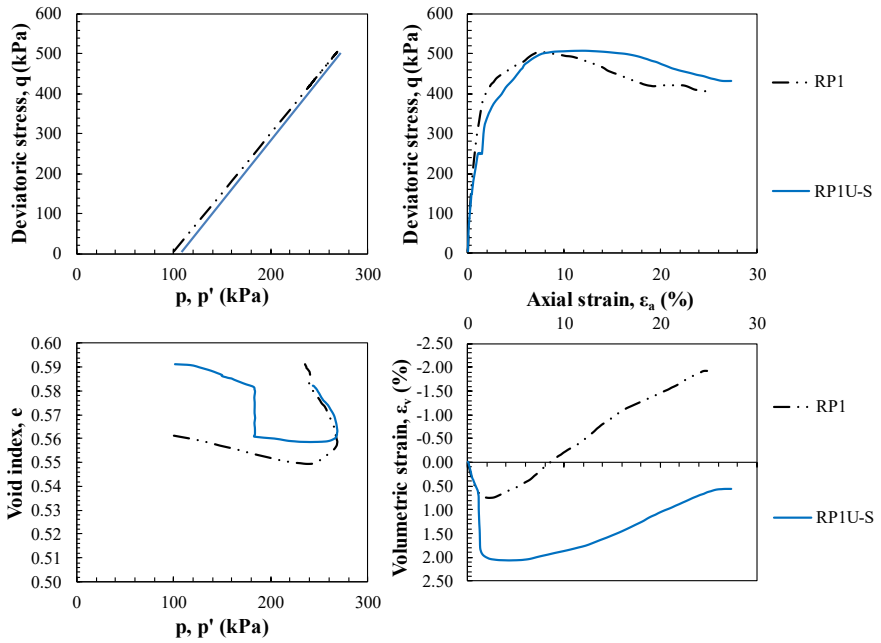

Figure 5.14 Stress-strain-volume change relationship for Redisole specimens prepared with Parallel curve: effect of the degree of saturation

The two specimens reached a similar peak deviator stress at approximately the same level of axial strain. The wetting causes a volumetric collapse of about 1.5% affecting the volumetric strain recorded by the RP1U-S specimen with respect to that of the

saturated specimen. In the oedometric tests performed by Oldecop (2000), after having wet or flooded the volumetric deformations obtained were similar to those of the saturated test. On the contrary, initially the volumetric deformations in the RP1U-S overlap those of the saturated specimen and then overcome them after wetting.

Finally, large triaxial tests were carried out to study the influence of grain size distribution on the mechanical behaviour of Redisole rockfill by using Parallel and Coarse curves (Figure 5.15). The values of the peak deviatoric stress for the Parallel material are higher than those for the Coarse rockfill material, thus increase with the particle size.

In all the tests the material showed compressive volumetric strain during initial loading and dilatancy on further loading. The cell pressure adopted in the tests are not very high so, as expected, the dilatancy is very pronounced.

The initial relative density of RC0.5 specimen at the beginning of the shear stage was smaller (D_r = 0.5) than that of RC1 (D_r = 0.7) and of other specimens (D_r = 1.0). The significant difference observed in the stress–strain behaviour shown in Figure 5.15 is probably also related to the difference in initial relative density. Furthermore, very different peak strengths also indicate that the difference in the density at the beginning of the shear stage has an effect on the mechanical strength.

It is interesting to note that the volume change behaviour of the two rockfill materials are not significantly different in the stress range considered.

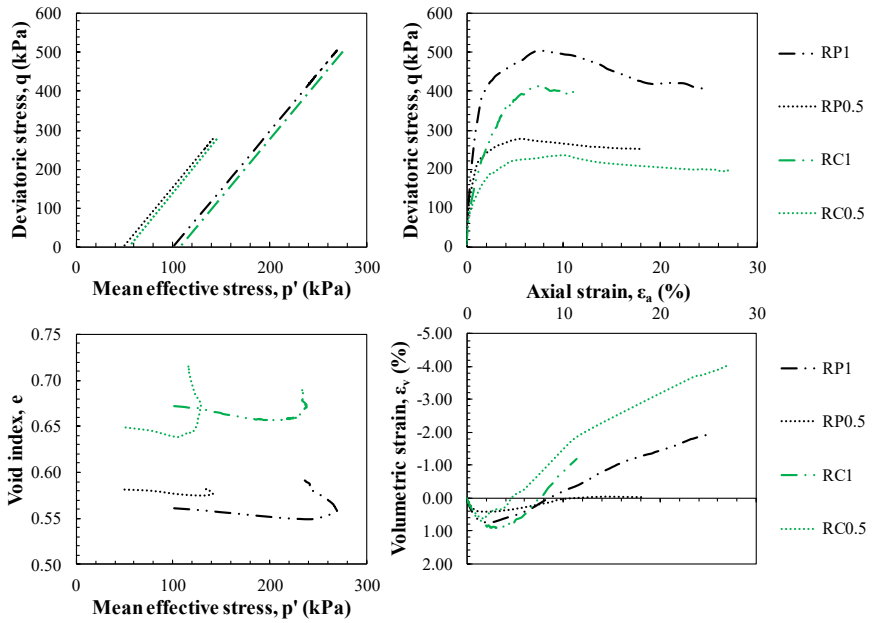

Figure 5.15 Stress-strain-volume change relationship for Redisole specimens prepared with Parallel and Coarse grading curves

5.2.2 Isotropic compression tests

In order to investigate the mechanical behaviour of rockfill, fundamental for land management and protection, isotropic triaxial tests were carried out on gravel specimens coming from **Coreno** pit (Ventini et al., 2019b). The results obtained on dense specimens (D_r=0.70) prepared with the grain size distributions Fine, Medium and Coarse are shown in Figure 5.16, Figure 5.17 and Figure 5.18 respectively.

It is interesting to note that at low stresses F and M specimens (Figure 5.16 and Figure 5.17 respectively), prepared with different initial degree of saturation, show similar compressibility. On the

contrary dry and saturated specimens prepared with the Coarse curve exhibit different compressibility since the beginning of the IC tests.

In all the cases as the stress level increases the saturated specimen exhibits greater volumetric strains than the dry specimen. On wetting the initially dry specimen (i.e. IC-FUS, IC-MUS and IC-CUS) undergoes volumetric collapse achieving volumetric strains ε_v greater than the saturated test (i.e. IC-FS, IC-MS and IC-CS). These results are of particular interest, since the modelling of the collapse of dams within the reservoir filling is commonly done by taking into account triaxial test in saturated and dry condition as reference (Nobari and Duncan 1972; Veiga Pinto 1983; Naylor et al. 1989; Soriano and Sánchez 1996).

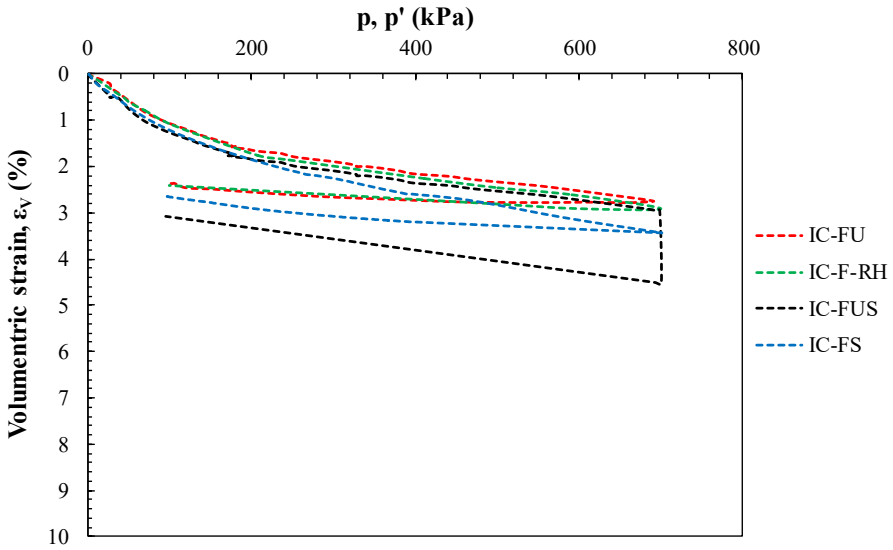

Figure 5.16 Results from isotropic compression tests performed on specimens prepared with the Fine grain size distribution

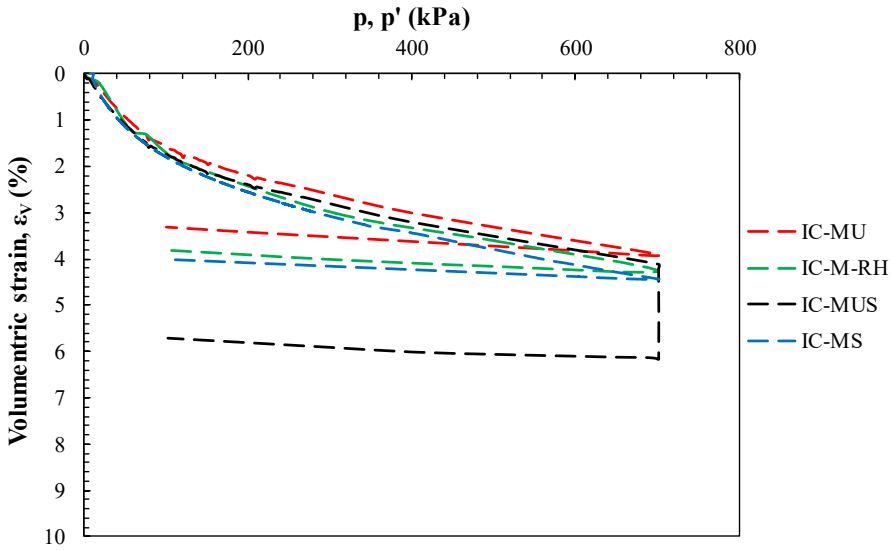

Figure 5.17 Results from isotropic compression tests performed on specimens prepared with the Medium grain size distribution

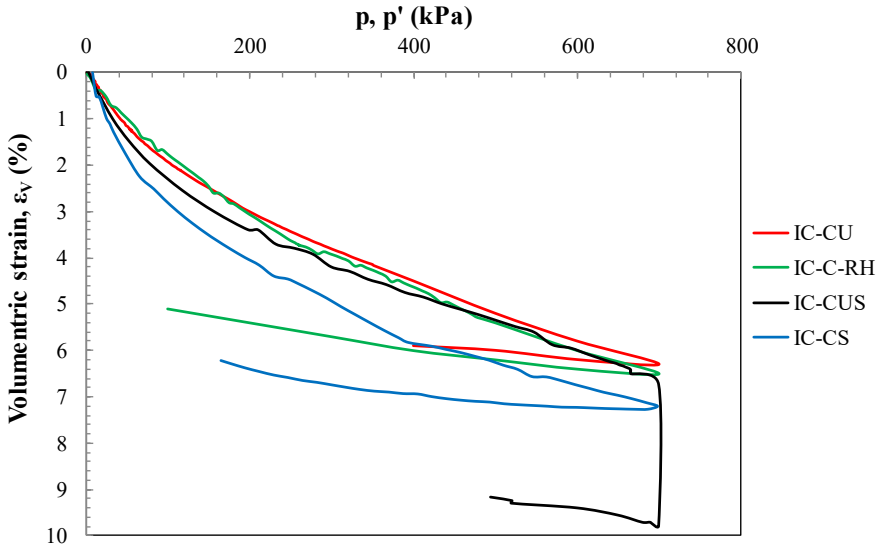

Figure 5.18 Results from isotropic compression tests performed on specimens prepared with the Coarse grain size distribution

In tests IC-MUS and IC-CUS the volumetric strain increases more significantly with the flooding under constant stress than the IC-FUS test as clearly shown in Figure 5.19.

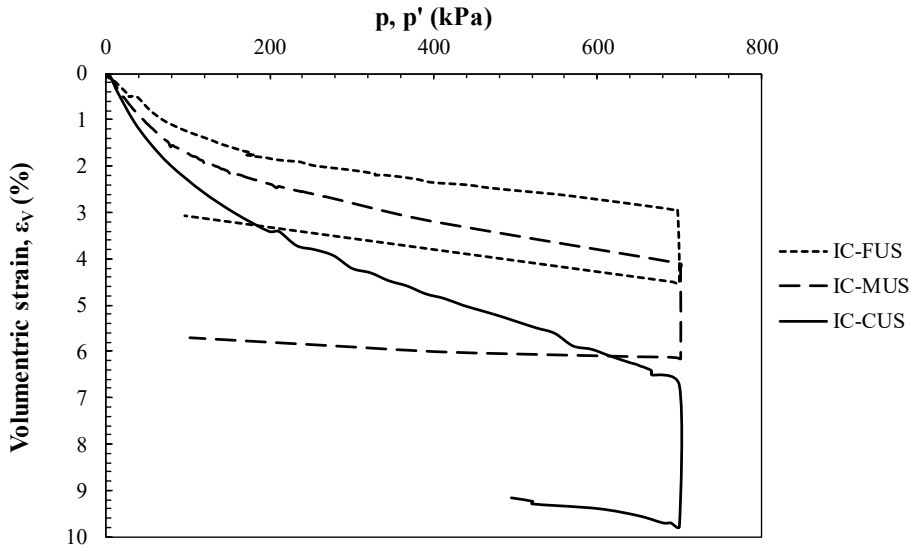

Figure 5.19 Comparison between tests with the wetting phase

It is noteworthy that the mentioned collapse effect shown by the three soils seems to be independent of the time effect as the duration of the phase of wetting in Figure 5.19 is the same in all tests.

A possible explanation of this different volumetric collapse is that rockfill deformation upon wetting is caused by the breakage of individual soil particles. The observed behaviour is well known in engineering practice for structures such as rockfill embankments and dams in which wetting leads to settlements. So, the volumetric strains observed in the tests should be related to soil fabric changes caused by the rearrangement of the fragments resulting from a

breakage process. In the particular case of the Coreno soil, however, the breakage process seems to not consist in breakage of single grains but in smoothing and breaking of the edges of individual soil particles. Indeed, it is well known that the bonds at the tip of a grain are more vulnerable to the attack of a corrosive agent, such as water. The corrosion reaction generated by water produces a weaker material (Oldecop and Alonso, 2001). This aspect is evident from the grain size distribution curves before and after testing of the material (Figure 5.20). This figure shows that there has been no significant change in the original grain size distributions but the formation of fine content not present in the original specimen. This implies that, under these test conditions, the weakening of the grains caused by water gave rise the breaking of asperities and not the splitting of the grains.

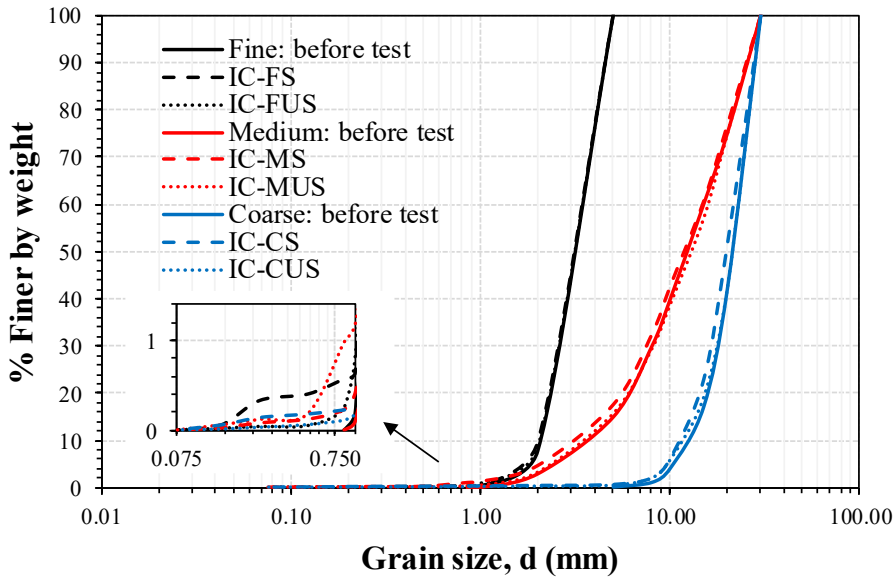

Figure 5.20 Grain size distributions of specimens tested

In order to understand the reasons of the different amount of volumetric collapse, somehow related to the characteristics of the individual grains, a simplified micromechanical analysis according to Flora et al. (2007) was carried out. This analysis allowed to estimate in an approximate way the total number of vertical contacts N on a face of a generic horizontal plane of the specimen, defined as:

$$N = N_{p,t} \cdot N_{c,p} \tag{5.1}$$

where $N_{p,t}$ is the total number of particles calculated using the following relation:

$$N_{p,t} = \frac{1}{\gamma_s \cdot \beta} \sum \frac{P_i}{d_{m,i}^3} \tag{5.2}$$

In Equation (5.2) γ_s is the unit weight of solids, β is a coefficient of proportionality between the volume of the single particle and its equivalent diameter, was assumed equal to 0.3, P_i is the weight of the i-th granulometric fraction which constitutes the specimen, with a medium diameter $d_{m,i}$. The term $N_{c,p}$ in Equation (5.1) represents the number of contacts in the vertical direction on one of the two sides of the considered plane and it is a function of the specimen porosity (n). In particular:

$$N_{c,p} = \frac{1}{2 \cdot n} \tag{5.3}$$

The average contact force F_i in the vertical direction acting on the single particle is therefore determined with the following relation:

$$F_{i,v} = \frac{\pi \cdot D^2 \cdot \sigma_v}{4 \cdot N} \tag{5.4}$$

In which D is the diameter of the specimen and σ_v is the current vertical stress. The total number of vertical contacts N calculated by Eq. (5.1) is about equal to $1.4 \cdot 10^6$ for the grain size distribution F, $5.7 \cdot 10^5$ for M and $1.1 \cdot 10^4$ for the soil C. So, as expected, the curve F that has a lower d_{max} has a greater number of intergranular contacts. For this reason, the average contact force in the vertical direction is significantly smaller in the IC-FS and IC-FUS tests, as shown in the Figure 5.21 and Figure 5.22.

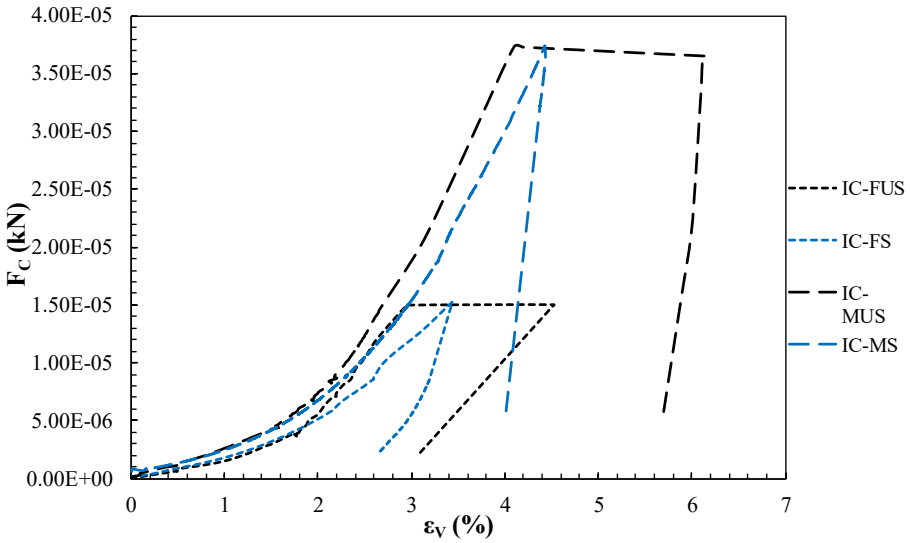

Figure 5.21 Average contact force in the vertical direction vs volumetric strain for Fine and Medium soils

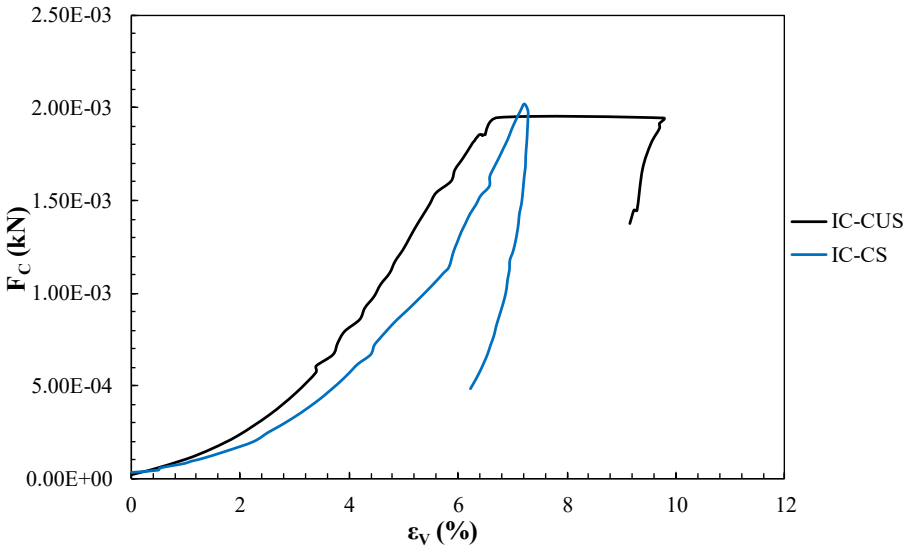

Figure 5.22 Average contact force in the vertical direction vs volumetric strain for Coarse soil

Notice that the curves related to the results of tests IC-CUS and IC-CS are shown in a separate figure (Figure 5.22) because the maximum value of the average contact force in the vertical direction is about 2 orders of magnitude greater than that of Fine and Medium grading curves.

The results of the simplified micromechanical analysis performed are confirmed by the comparison of the Breakage factor, B_g (Marsal 1967) reported in Table 5.6. The breaking of the edges and the consequent rearrangement of the grains in a more stable configuration mostly affects the specimens with d_{max} equal to 30 mm (i.e. Medium and Coarse curves), which show a volumetric collapse substantially greater than the soil Fine.

Furthermore, under the same test conditions the curve C shows a greater breakage of the grains. The values of B_g are also systematically greater in tests on initially saturated specimens, confirming the fact that the presence of water weakens the material: it is expected this effect depends on the contact time between soil grains and water.

Table 5.6 Breakage factors (Marsal 1967) of isotropic compression tests on dense specimens

Test	**B_g (%)**
IC-FUS	0.88
IC-FS	2.36
IC-MUS	3.28
IC-MS	3.78
IC-CUS	4.06
IC-CS	4.81

The comparison between the volumetric response of saturated specimen and dry specimen saturated after loading phase shows that flooding rockfill specimens subjected to a constant confinement stress lead to a sudden settlement (collapse) attributed also to the breakage of particle edges due to rock weakening induced by wetting. This fact must be taken into account during reservoir filling analysis of dams or embankments exposed to rainfall conditions.

Figure 5.23 and Figure 5.24 also present results obtained on IC in relative humidity controlled conditions (RH=75%). The volume change evolution in tests with relative humidity control are very similar to that obtained on dried specimens, independently of the

grain size distribution adopted. In general, the tests results show that the relative humidity does not have a remarkable effect on the Coreno material behaviour.

Contrary to the previous test results, Figure 5.23 shows that the volumetric strains are significantly increased with relative humidity in the tests on specimens prepared with an initial relative density D_r=0%. Obviously, the loose specimens exhibit volumetric deformations greater than the dense and more rigid ones.

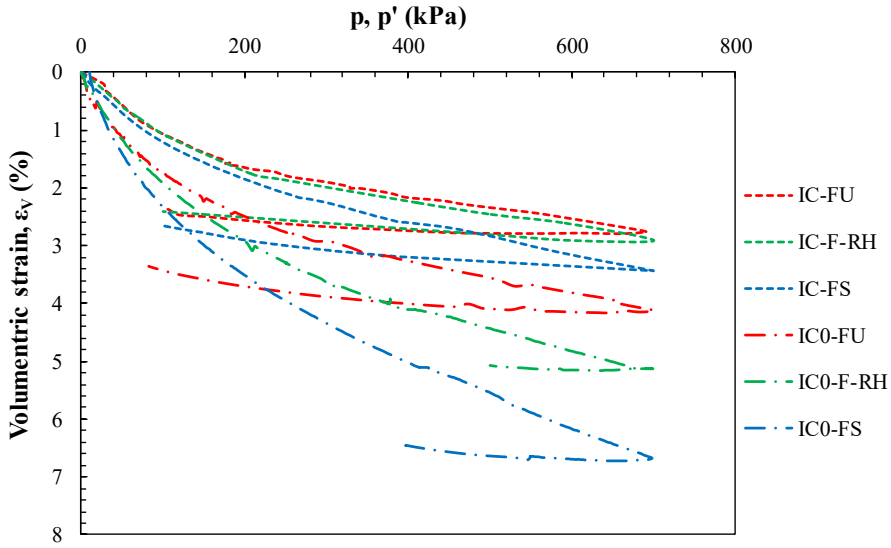

Figure 5.23 Comparison between the volumetric strains exhibited by the specimens prepared with different initial relative density

Figure 5.24 shows the same strain data from Figure 5.23 in terms of the evolution of the specimen void index. A significant change in void index is observed on loading the "RH" loose specimen. In particular, the curve of the loose specimen humidified at 75% lies between that of the dry and the saturated specimens.

In the case of loose specimens, the greater the relative humidity, the smaller the void index obtained at the end of the loading phase.

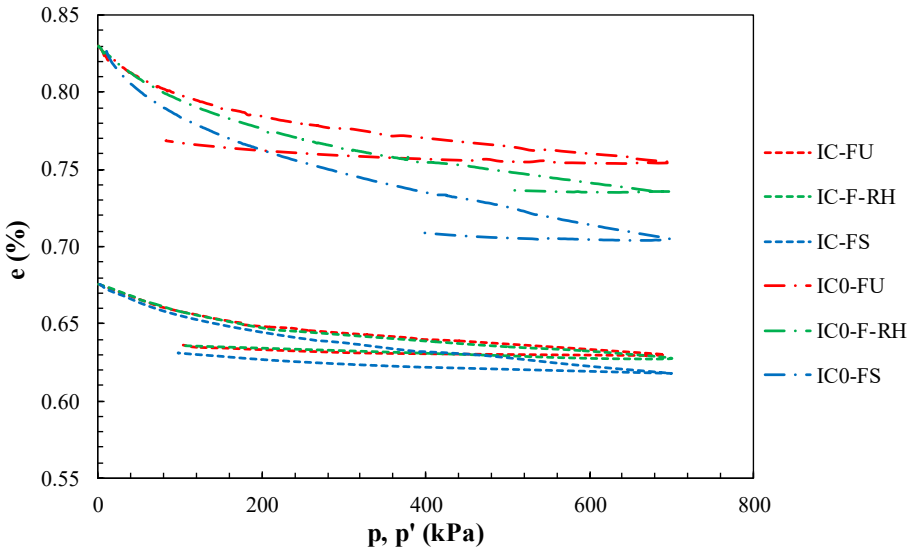

Figure 5.24 Comparison between the void index trend exhibited by the specimens prepared with different initial relative density

The evolution of the relative humidity during the IC0-F-RH test is plotted in Figure 5.25. Three curves are reported. The two identical ones were obtained from data collected by the iButtons (see paragraph 3.2.2.2.2) placed inside the specimen in two different sections (H_1=14 cm and H_2=28 cm) while the last one refers to an iButton placed in the room where the apparatus is located. This trend is representative of all those recorded in the tests with relative humidity control.

Given the almost perfect overlap between the two curves detected by the iButtons placed in the specimen, it seems that the vapor transfer and equalization technique were quite satisfactory allowing

to control the water content in the sample around the expected value.

Given the temperature dependence on the vapor pressure at saturation, the relative humidity also varied from the expected value (i.e. 75%) as a consequence of small changes in temperature (Figure 5.26).

It is important to highlight that confining pressure application does not seem to affect the equilibrated relative humidity of the specimen.

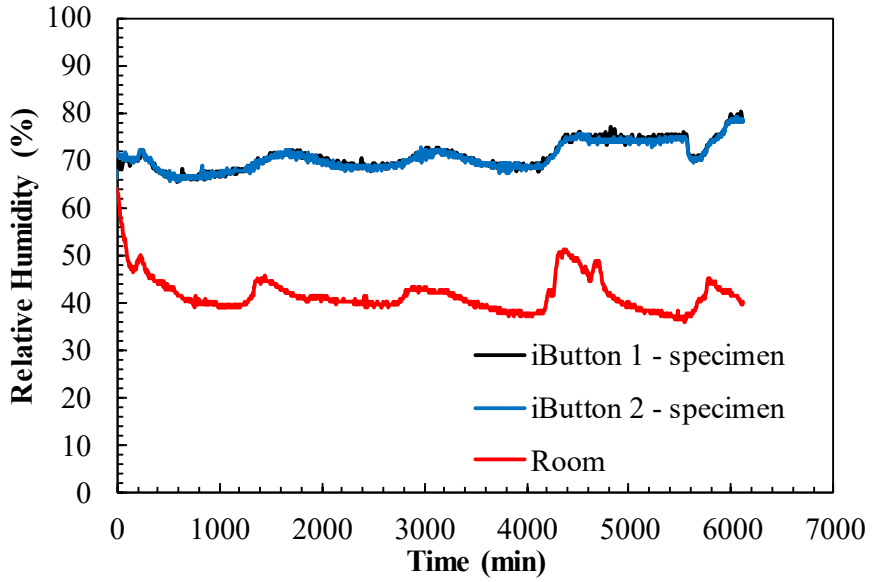

Figure 5.25 Measurements of the relative humidity (RH) during the IC0-F-RH test

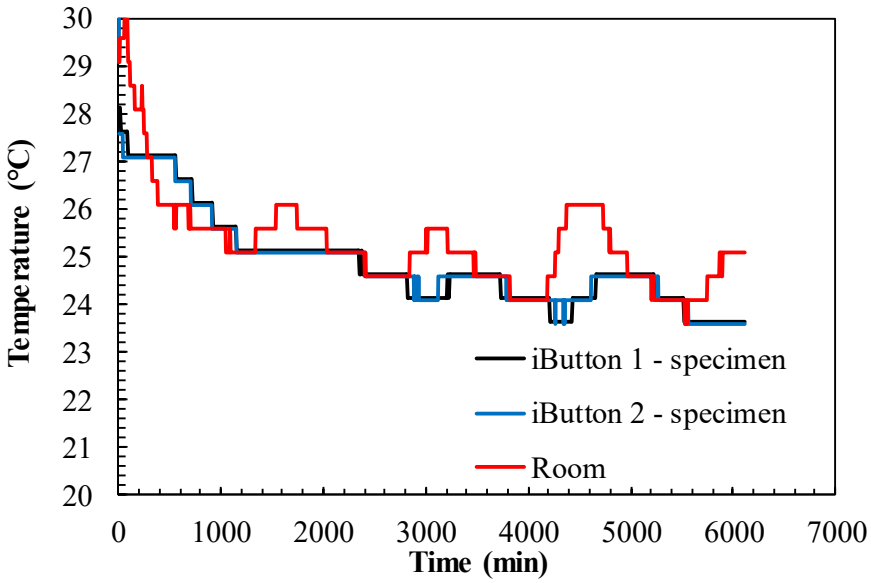

Figure 5.26 Measurements of the temperature during the IC0-F-RH test

Differences between results on loose and dense specimens, presented in Figure 5.23 and Figure 5.24, are related to the fact that, due to the larger rockfill voids in loose specimen, a relatively large air flow can be passed through the specimen, making water transfer more efficient.

By changing the RH, passing from the dry specimen to the RH = 75% up to the saturated one, the ability of liquid water (which is in direct contact with the crack tips) to produce the stress corrosion reaction is changed. In particular, as demonstrate from the B_g values reported in Table 5.7, the breakage of the grains is quantitatively greater in the saturated specimen and affects less the dry specimen.

Table 5.7 Breakage factors (Marsal 1967) of isotropic compression tests on loose specimens

Test	B_g (%)
IC0-FU	0.87
IC0-F-RH	1.03
IC0-FS	1.69

5.2.3 Local strain vs Global strain

The triaxial cell HPSP uses a novel technique to measure local axial and radial strains, i.e. the Magnetic Shape Detector (MSD) system. Baldi et al. (1988) and Dendani et al. (1998) showed the importance of using local instrumentation mainly to minimize loading system compliance, to avoid bedding errors during triaxial compression, and to reduce membrane penetration effects. To quantify and detect possible errors on testing, the new cell was equipped with local and global instrumentation, specifically designed to monitor axial, radial, and volumetric deformations with an adequate resolution.

The use of both global and local measurements allows detecting experimental problems such as membrane penetration on isotropic compression and shearing, as well as membrane sliding on shearing at low confining stresses.

Selected test results are presented to show the capability of the new measurement system MSD during isotropic CRL compression. These test results are representative of the trend observed in some

triaxial tests and are useful to highlight limits and potential of the proposed magnetic system.

With reference to the IC-FS test in which the specimen was saturated and then isotropically compressed up to the maximum value of the mean effective stress p' of 700 kPa, a comparison between the values of the relative axial displacements (Δz) of each magnet and the base displacements measured by the LVDT, all normalized with respect to its initial position is shown in Figure 5.27. The axial relative displacements measured by the local magnetic system are lower than the ones obtained by the external LVDT transducer, as expected. It is known that internal systems offer greater measurement accuracy than external ones.

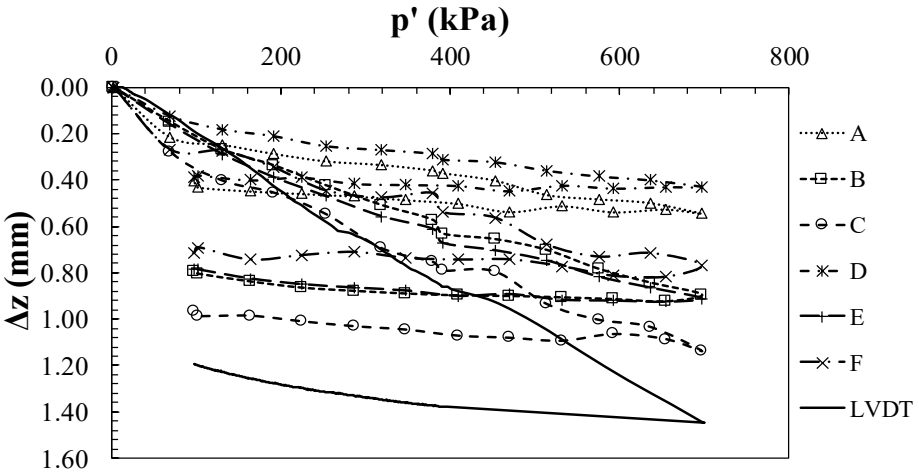

Figure 5.27 Relative axial displacements Δz versus mean effective stress p' measured by the magnets (MSD) and LVDT transducer (Ventini et al., 2019a)

Figure 5.28 shows the elaboration of the mentioned Δz in terms of axial strains averaged from the values recorded by all magnets (A, B, C, E and F). The two curves plotted in Figure 5.28, show a good agreement between the two measuring systems.

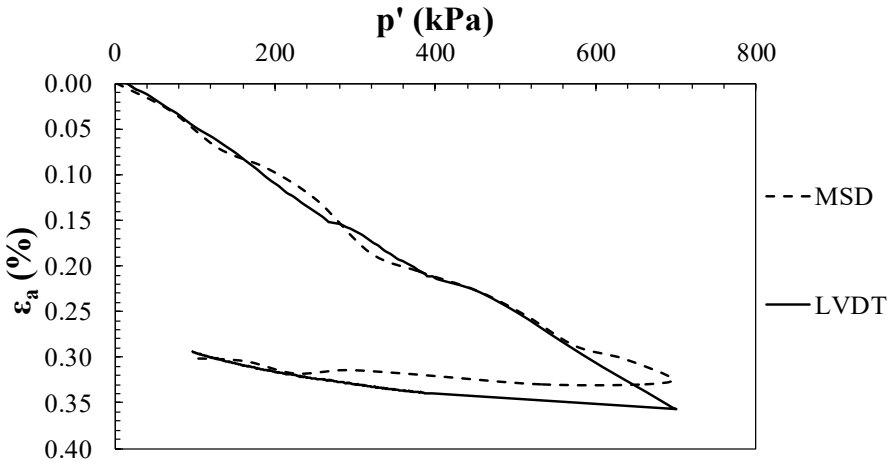

Figure 5.28 Comparison in terms of axial strains between internal and external system (Ventini et al., 2019a)

The radial displacements Δr of the specimen are traditionally computed based on the measurement of current volume (by the DPT transducer) and height of the specimen (LVDT data). Figure 5.29 compares this kind of measurements with those from the MSD.

It can be observed that there is a large difference between the two kind of measurements: the magnetic system gives a maximum radial displacement equal to approximately a fifth of that one measured by the external system.

The smaller radial strain observed with the Magnetic Shape Detector is probably related to the membrane penetration, that is not

evaluated by the external system, and is also related with the magnet's stroke limit in the radial direction. This second phenomenon was progressively increased as the mean effective stress increased. Therefore, the set up of the magnetic system requires further development operations to minimize the non-linearity errors generated by the complex magnetic field.

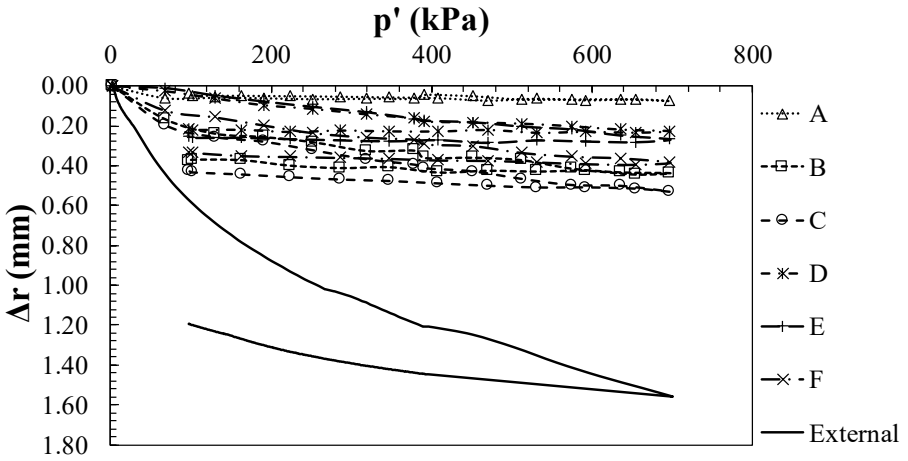

Figure 5.29 Radial displacement Δr versus mean effective stress for magnets (MSD) and external measurements (Ventini et al., 2019a)

Clearly, the same difference can be observed in terms of specimen radial strains (Figure 5.30).

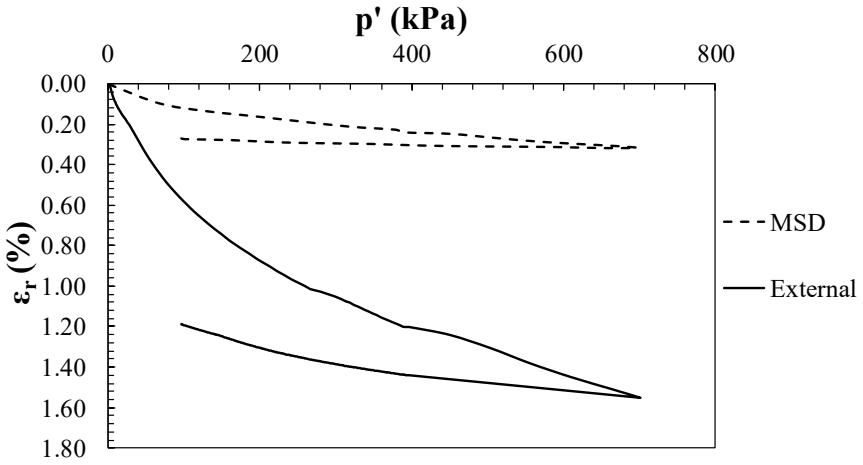

Figure 5.30 Comparison in terms of radial strains between internal and external system (Ventini et al., 2019a)

Data shown in Figure 5.28 and Figure 5.30 explain the trend of the curves in Figure 5.31. In particular, the External curve represents the DPT transducer measurement instead the MSD curve represents volumetric strains calculated using Equation 5.5 with ε_a and ε_r axial and radial strains measured by the magnetic system and reported in Figure 5.28 and Figure 5.30:

$$\varepsilon_v = \varepsilon_a + 2\varepsilon_r \quad (5.5)$$

Another aim of the research is to propose an alternative method for measuring the volumetric strains of the specimen under partial saturated conditions, as well as allowing a more accurate measurement of the same even in saturated conditions.

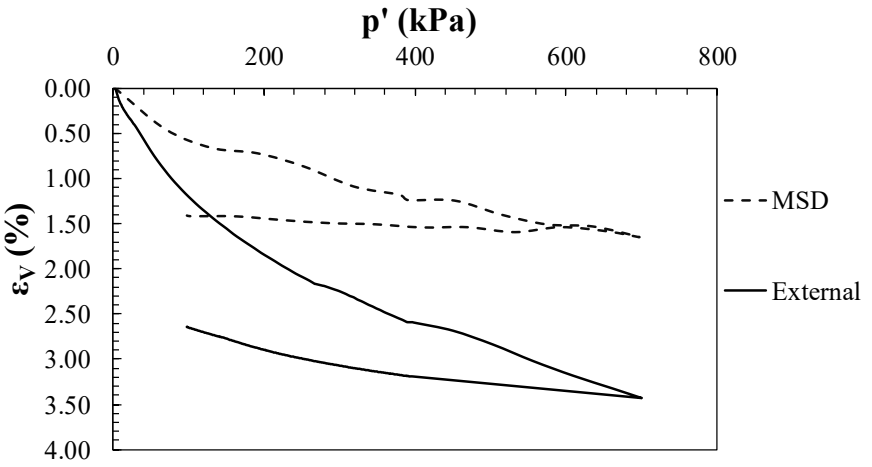

Figure 5.31 Volumetric strains ε_v computed via the processing of the MSD and External system data (Ventini et al., 2019a)

As final aspect, Figure 5.32 reports the average shape of the lateral surface of the specimen at fixed time, highlighting the inhomogeneities of the deformation field along the specimen height. The material used has a high stiffness therefore the displacements are very small. The specimen's height was equal to 405.9 mm and 404.6 mm at the beginning and at the end of the isotropic compression phase respectively. This does not allow a clear comparison between the profile reconstructed by the software and the images obtained when the equipment was disassembled. However, the high potential of this type of processing offered by the system is undeniable, contrary to traditional methods. It is clear that the volume change determination taking into account the non-uniformity of the specimen deformation would better represent the real observed behaviour.

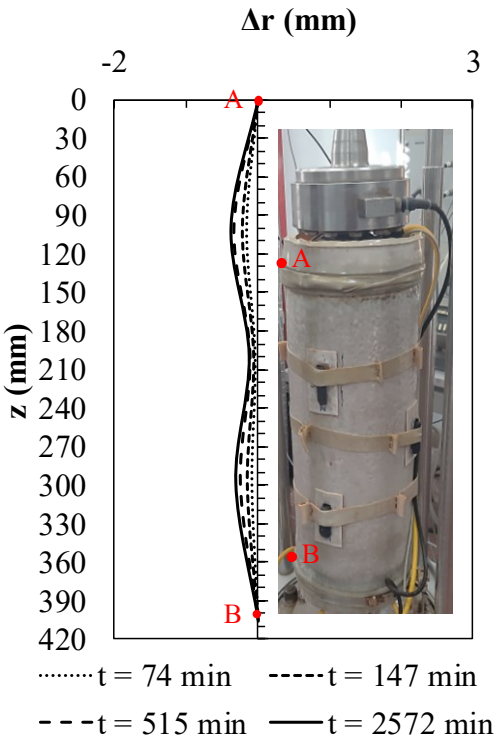

Figure 5.32 Progressive development of the lateral profile of the specimen during IC-FS

Considering different tests performed, a good agreement of the measurements referred to the vertical direction was observed. As said problems arisen in the radial direction, although there are possible links to local inhomogeneities.

The limestone used is extremely rigid and, consequently, displacements recorded are very small. Although the volumetric strains measured by the magnets are smaller than those provided by the external system, as expected, the actual difference between the two measurement systems seems not entirely justified. These aspects must be analysed with further setting up operations.

The limits and potential of this system lie in the large amount of data collected. This certainly allows a more accurate interpretation compared to traditional local measurement techniques, but also causes problems in the interpretation for a correct characterization of the mechanical behaviour of the specimens.

5.3 Oedometric tests

Evaluation of and comparison between the deformation behaviour of rockfill dams have been the subject of several studies (Sowers et al., 1965; Clements, 1984; Dascal, 1987; Pinto and Marques Filho, 1998; Won and Kim, 2008). These studies highlighted that several parameters influence the in situ rockfill short-term and long-term deformation behaviour. The most important factors include rock particle mineralogy and strength, degree of compaction, gradation and rock particle susceptibility to strength loss caused by wetting. In order to discuss the effect of these influencing parameters on rockfill compressibility, results of large and small oedometric tests will be presented and discussed in this section.

5.3.1 Large oedometric tests

The test programme included classic large oedometer tests on dry and saturated specimens and tests with specimen flooding at some particular vertical stress.

Figures from 5.33 to 5.36 show the results of large oedometric tests in terms of void index versus the applied vertical stress in semi-logarithmic scale for the Coreno and Redisole rockfill.

Specimens of **Coreno** rockfill have similar compressibility, regardless of the initial degree of saturation (Figure 5.33): the void ratio-vertical stress curves look to coincide for the stress levels considered, indicating a similar granular structure that causes a similar deformation response.

It can also be seen that a moderate collapse was recorded during flooding (LO-CCU-S10 test). It seems that limestone adapt to loading and form a stable and stiff assembly, also when they are wetted.

Probably there is no effect neither of the initial saturation degree nor of the wetting phase in the post-yield region.

On the contrary, the test results on **Redisole** rockfill (Figures 5.34-5.36) show the remarkable effect of the degree of saturation on the material behaviour as the dry specimen is less compressible than the saturated one. Furthermore, a sudden additional crushing upon wetting performed at three different vertical stresses is evident (Figures from 5.34 to 5.36). The amount of collapse strain was very close to the strain difference between the normal compression lines corresponding to the initial water content (dry state) and the saturated state. The subsequent loading after collapse leads to a curve that follows the normal compression line for the saturated material. Therefore, as the vertical stress at which wetting occurs increases, the amount of the volumetric collapse increases.

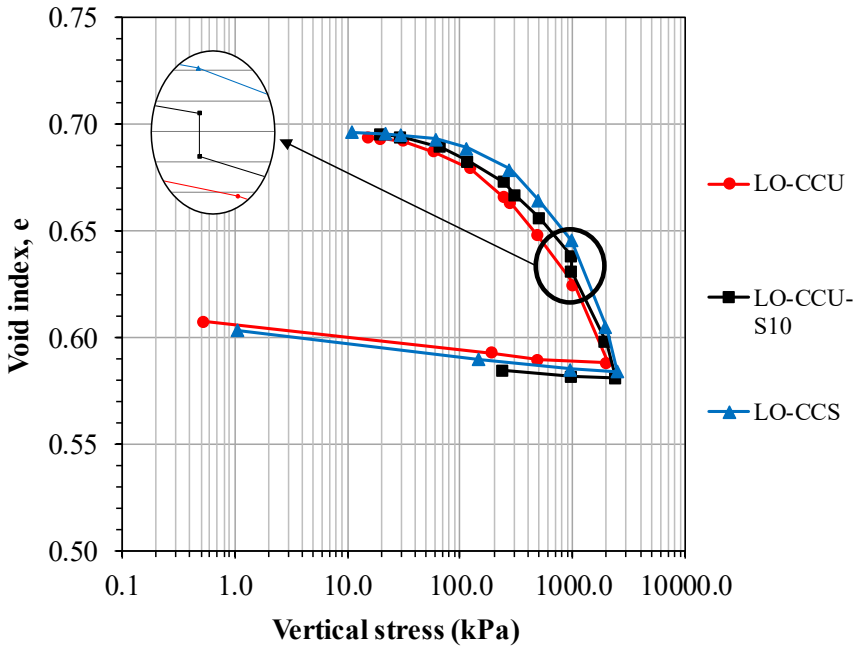

Figure 5.33 Results of large oedometric tests on Coreno rockfill with a zoom of the saturation phase performed at 1000 kPa

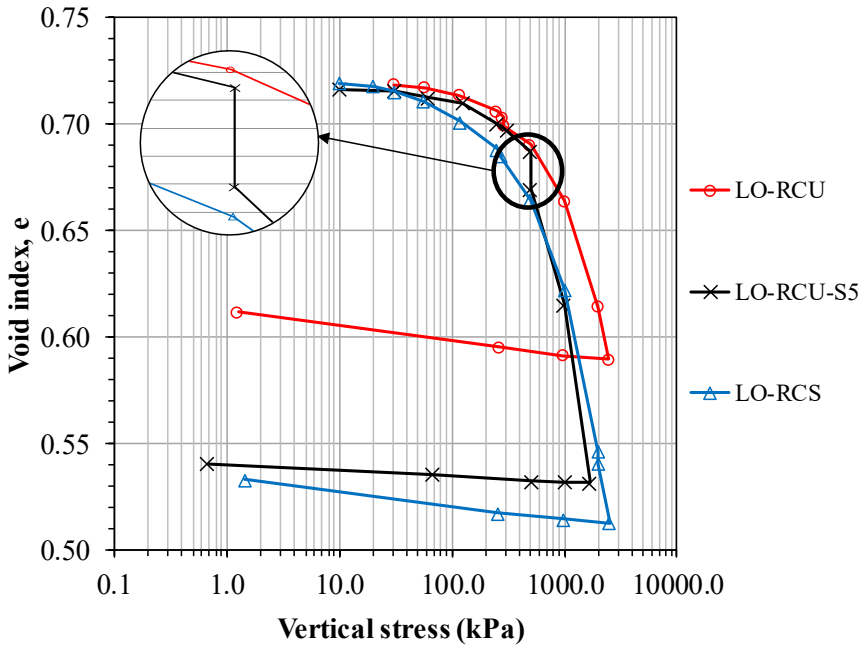

Figure 5.34 Results of large oedometric tests on Redisole rockfill with a zoom of the saturation phase performed at 500 kPa

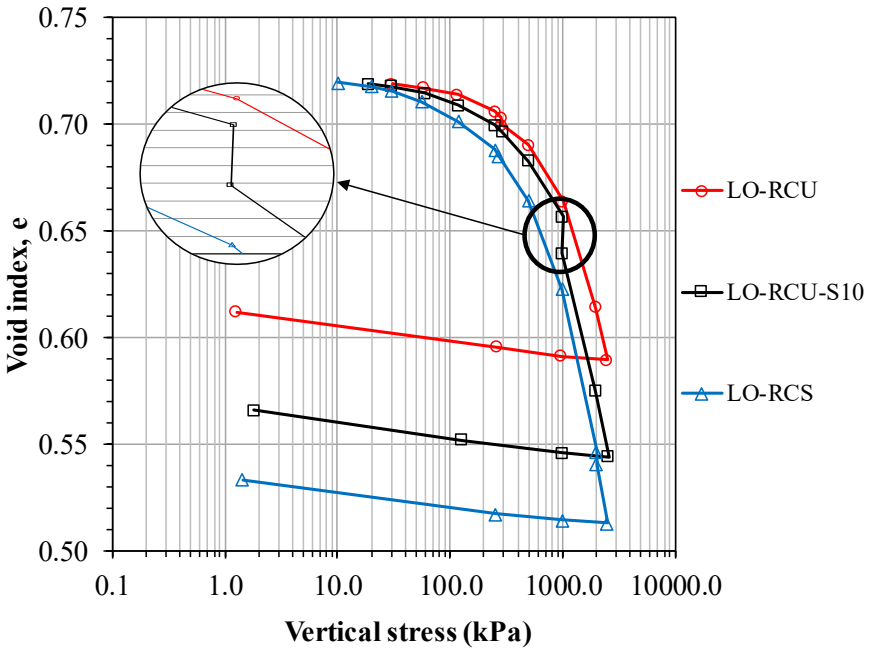

Figure 5.35 Results of large oedometric tests on Redisole rockfill with a zoom of the saturation phase performed at 1000 kPa

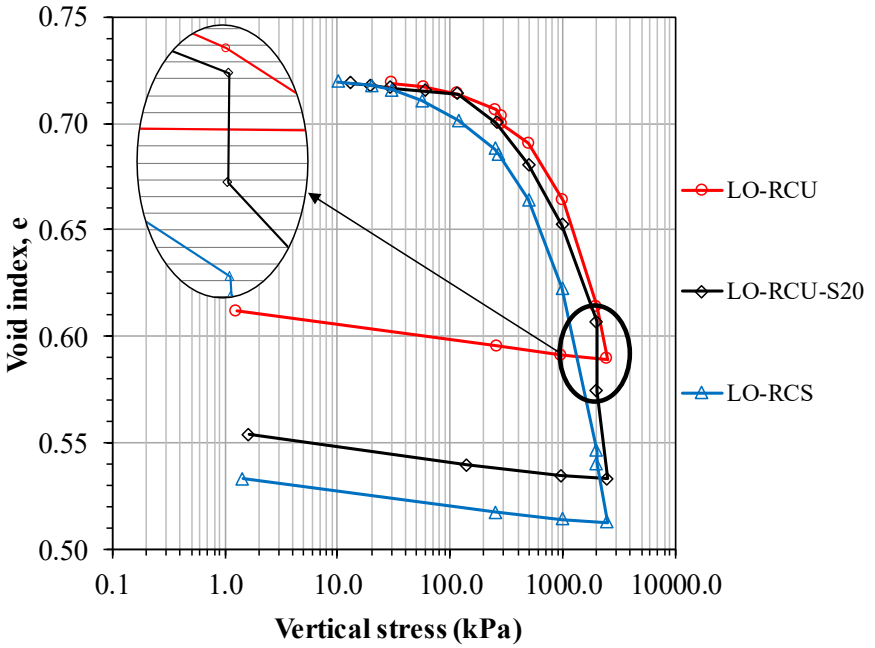

Figure 5.36 Results of large oedometric tests on Redisole rockfill with a zoom of the saturation phase performed at 2000 kPa

In a zoned earth dam the upstream shoulder are typically made of rockfill and becomes inundated when the water reservoir level is increased. The downstream shoulder is, however, typically subjected to rainfall infiltration (and evapotranspiration) from and towards the atmosphere. Similar hydraulic boundary conditions are expected in rockfill embankments used in highway or railway construction.

The very high permeability of a rockfill makes it extremely unlikely in practice a condition of saturated flow. The large open voids of the rockfill remain therefore essentially filled with air and water vapor during the lifetime of these structures. If the rock blocks are

not fully saturated water may also penetrate the particles through the connected porosity and also along cracks. A volumetric collapse due to wetting of the rockfill will tend to create voids and cracks, which could lead to a preferential path connecting the upstream and downstream slopes of the dam. This could cause irreversible damage.

It is interesting to note that the volume change behaviour of the two rockfill materials with the same grain size distribution are significantly different from each other. Redisole material is more compressible than Coreno rockfill and this is probably due to the greater particle strength of the Coreno grains (Table 4.5), less prone to crushing.

The test programme included also a test on a dry specimen prepared with an initial relative density of 0.50 (LO-RCU loose) as reported in Table 5.4. The comparison between the results of LO-RCU loose and the LO-RCU tests is shown in Figure 5.37.

From the e-log(σ_v) curves it is evident that the yield stress decreases with increase in initial void ratio as has been found by many other researchers, e.g. Hagerty et al. (1993), Pestana and Whittle (1995) and Nakata et al. (2001). A yield stress can be defined for soil subjected to one-dimensional compression at the point where the relation of the deformation to the stress increment changes rapidly on a semi-logarithmic plot.

Field (1963) suggested that the average number of contact points per particle, often defined as the co-ordination number C_a, increases as the void ratio decreases, following the equation:

$$C_a = \frac{12}{1+e} \tag{5.6}$$

An analysis by Jaeger (1967) suggested that the tensile stress for a particle in a matrix decreases with increasing co-ordination number, thus further explaining why the yield stress increases with decreasing void ratio.

It can also be seen that the lines merge after yielding, approaching a common e-log(σ_v) curve as reported by Nakata et al. (2001). It would seem that there was no influence due to initial void ratio (or relative density) in the post-yield region.

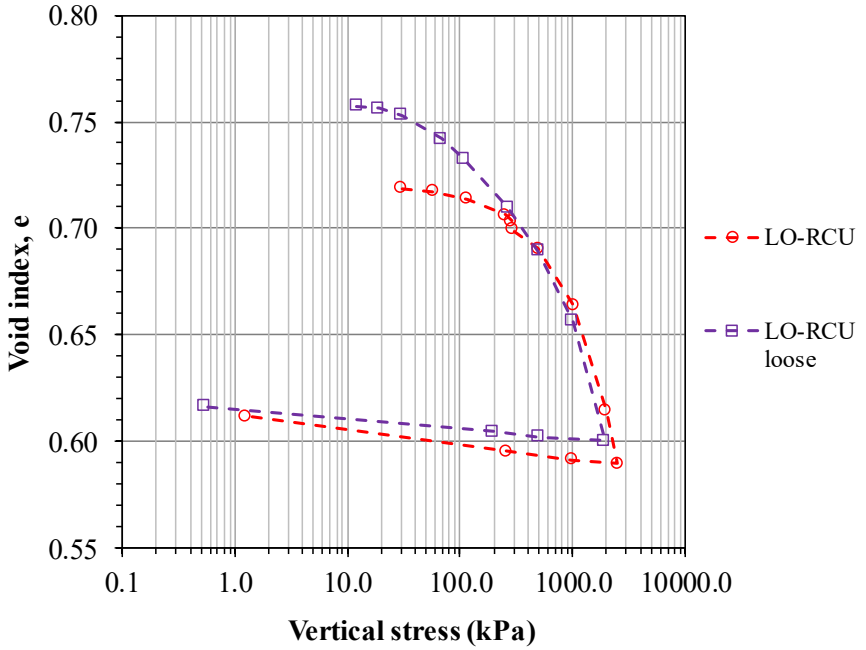

Figure 5.37 Results of large oedometric tests on dense and loose specimens of Redisole rockfill

The same results are shown in e/e_0-$\log(\sigma_v)$ plane in term of void index ratio vs vertical stress (Figure 5.38). It can be seen that the looser specimen is more compressible that the denser one. Larger voids among grains promote the development of plastic deformation as well as the grain breakage on loading. A higher compressibility associated with relatively high grain breakage is thus observed in the LO-RCU loose test (Figure 5.39). In fact, the value of B_g associated with this test is 11.23 against 8.13 for the LO-RCU test.

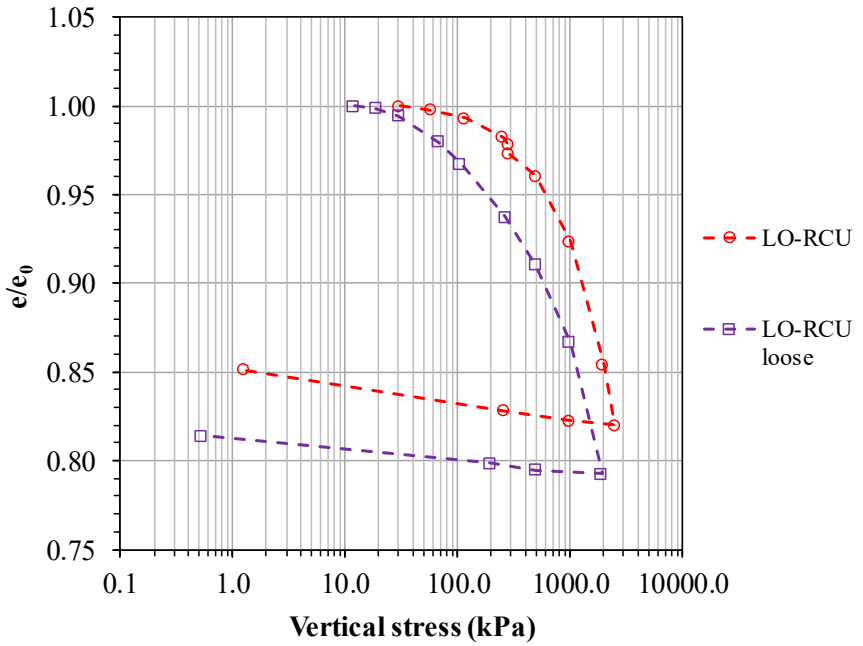

Figure 5.38 Comparison between large oedometric test results on dense and loose specimens in term of void index ratio vs vertical stress

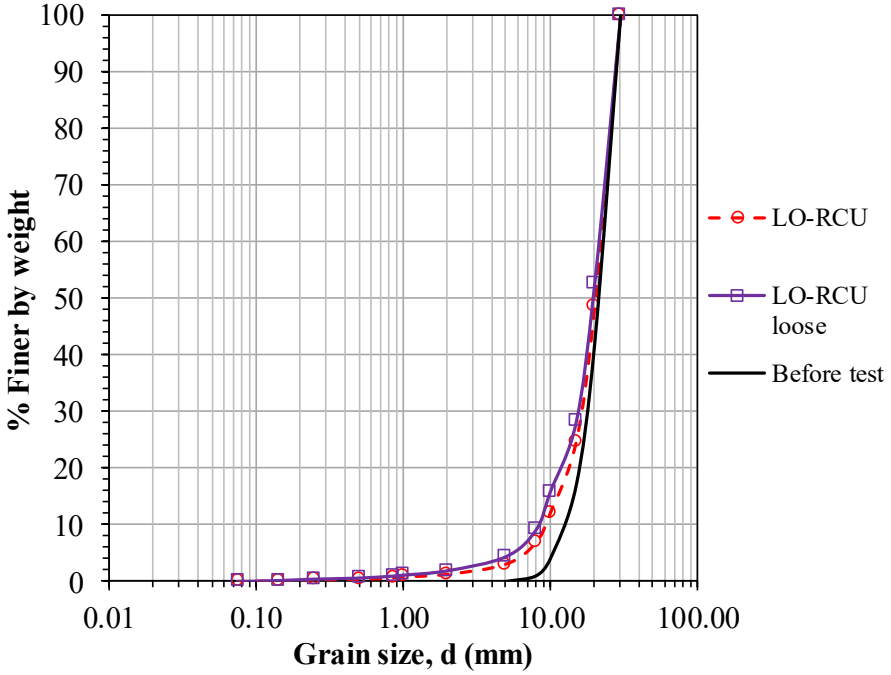

Figure 5.39 Grain size distributions after LO-RCU and LO-RCU loose tests

Furthermore, two large oedometric tests were carried out on dry specimens of Redisole rockfill prepared with two different grain size distributions in order to investigate the effect of particle size on compressibility. Results are reported in Figure 5.40.

In the LO-RCU test the grain size distribution used is the Coarse one, so the maximum grain size is equal to 30 mm. This is lower than the maximum grain size (d_{max} = 40 mm) used in the LO-RPU. These two specimens also have different initial relative density as reported in Table 5.4: D_r = 0.70 for LO-RCU test and D_r = 1.00 for LO-RPU test.

As shown in Figure 5.40, the total variation of the void index increases with median particle size. This is more evident in Figure 5.41, where the results are shown in the e/e_0-$\log(\sigma_v)$ plane.

It can also be seen that, following yield, the curves for both type of test are parallel as are the unloading lines.

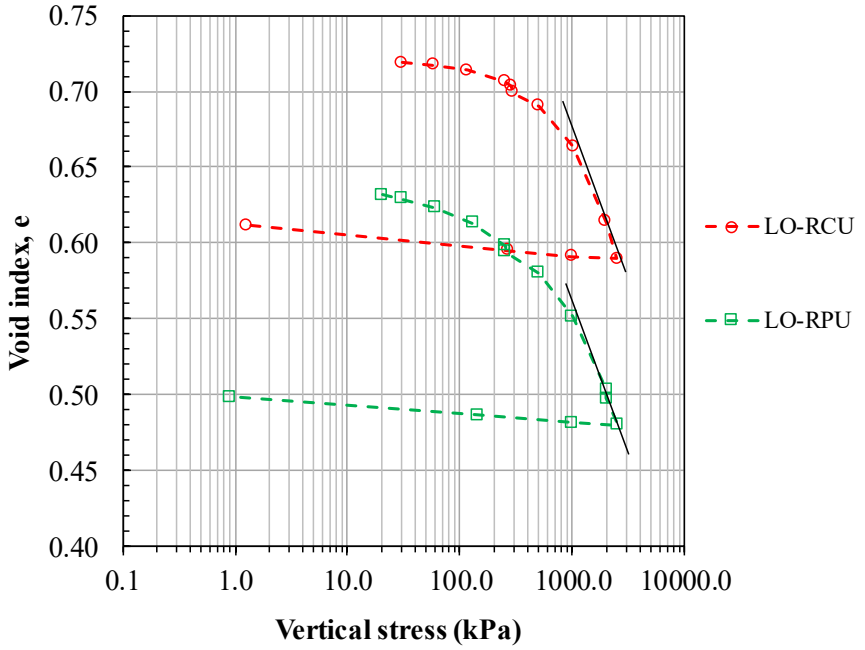

Figure 5.40 Comparison between large oedometric test results on specimens of Redisole rockfill prepared with different grain size distributions

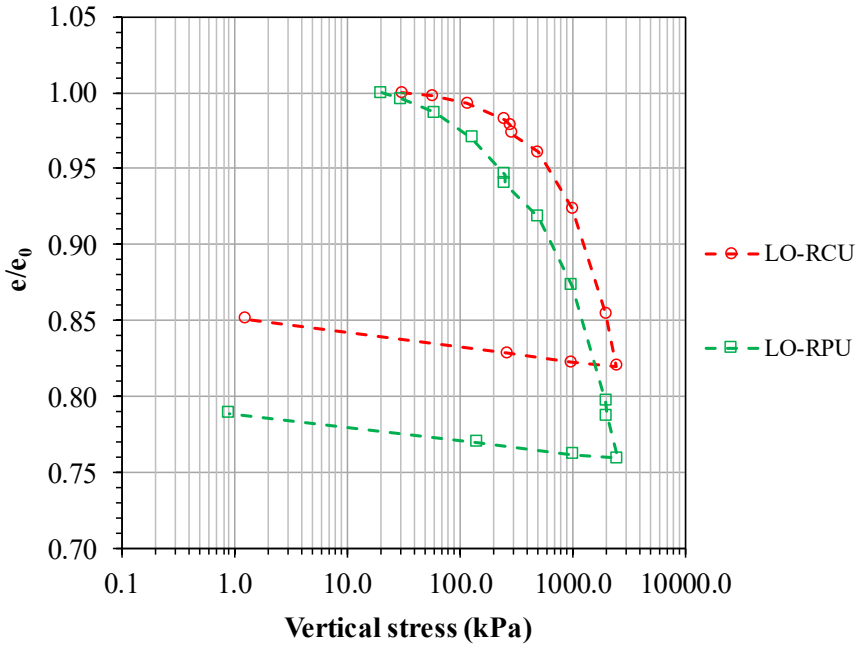

Figure 5.41 Comparison in term of void index ratio vs vertical stress between large oedometric test results on specimens of Redisole rockfill prepared with different grain size distributions

The compressibility curves shown in Figures 5.40 and 5.41 were obtained using specimens prepared with Coarse and Parallel grain size distributions, selected by means of the parallel gradation technique (see paragraph 4.3). The results indicate that the cumulative effect of initial grain size distributions and initial void index results in different e-log(σ_v) relation. However, seems to be a link in terms of slope of the loading and unloading lines.

5.3.2 Small oedometric tests

The experimental programme involved small oedometric tests on specimens of two different gravels having the same grading (Fine grain size distribution), reconstituted at the same initial relative density (D_r=0.70).

Figure 5.42 shows the comparison between the results obtained with the dry and the saturated specimens prepared with **Coreno** rockfill. As for the large oedometric tests (Figure 5.33), the curves seem to merge in a single line for the stress level considered.

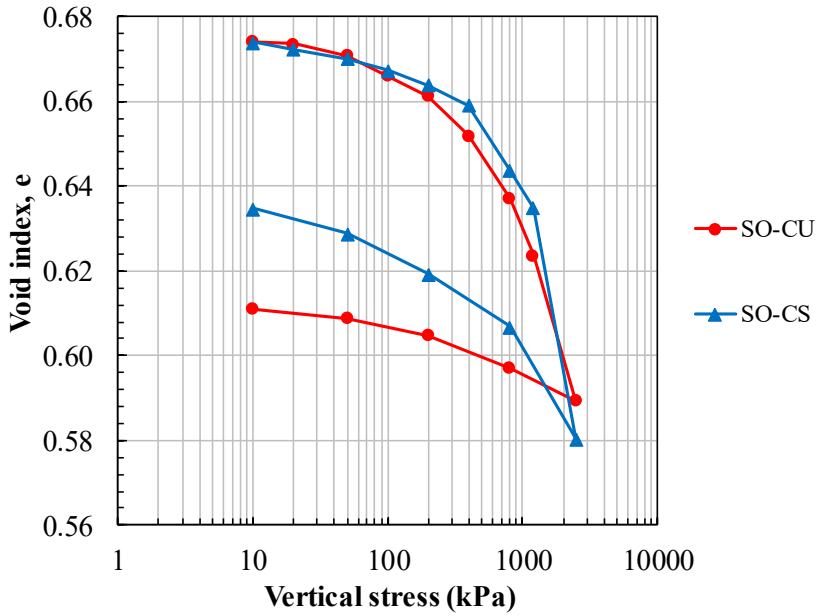

Figure 5.42 Results of small oedometric tests on dry and saturated specimens of Coreno rockfill

Tests including wetting phases (Figure 5.43) seem to show that no collapse occurred upon wetting in the post yield region. It is also confirmed that the degree of saturation has no effect on the compressibility of this calcareous material.

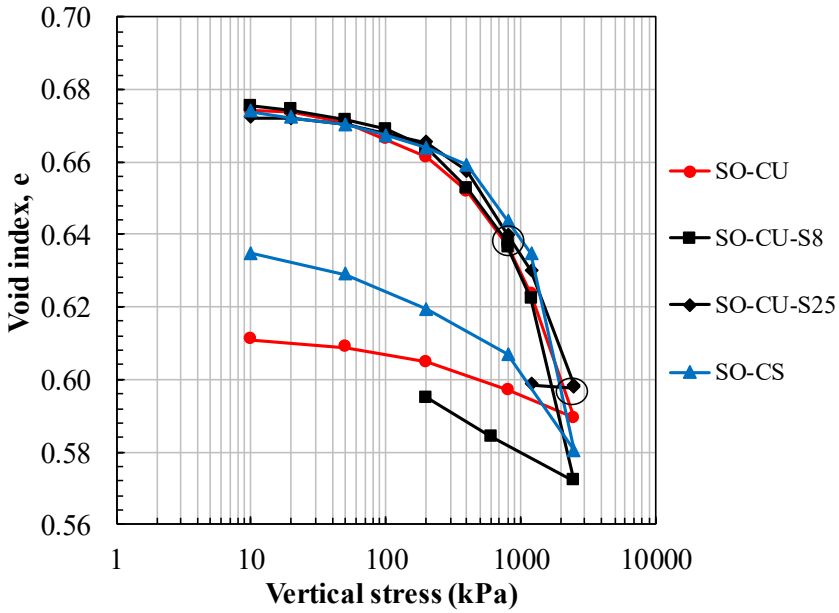

Figure 5.43 Results of small oedometric tests on specimens of Coreno rockfill. Open circles indicate specimen flooding

Furthermore, a test carried out with the relative humidity control system has been performed (Figure 3.6). Results shown in Figure 5.44 highlight that, for medium stress levels, the humified specimen is less deformable than the dry and saturated ones while, for high stress levels, the three curves merge in a single line. It can be thus concluded that the relative humidity as well as the degree of

saturation of the specimen during the test do not have a significant effect on the position of the normal compression line and on compressibility of this material.

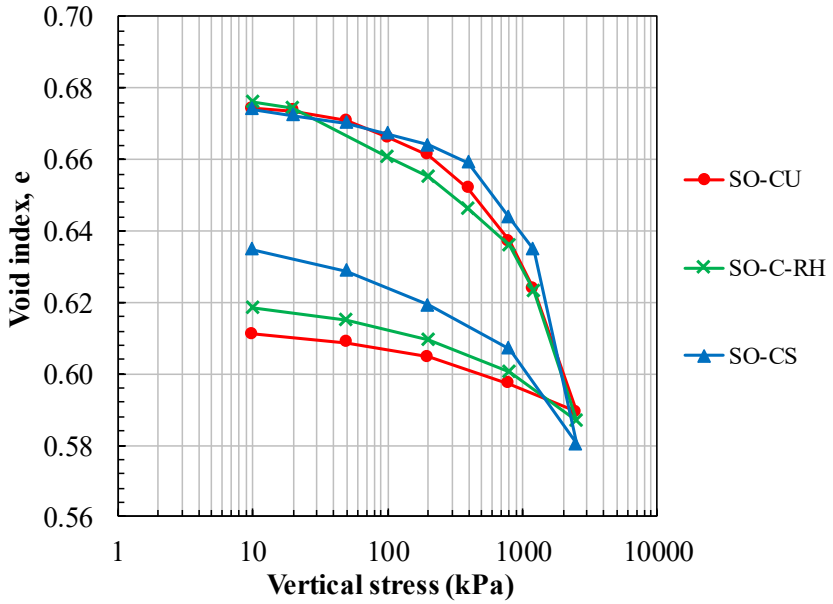

Figure 5.44 Results of small oedometric tests on specimens of Coreno rockfill including the relative humidity control test

The trend of relative humidity measured by means of two iButtons placed in two different section of the specimen, for each load step is shown in Figure 5.45. Except an abnormal peak in the early stages of the test, the average relative humidity reached is around 72%. It seems that there is no influence of the application of the load on the relative humidity, as expected.

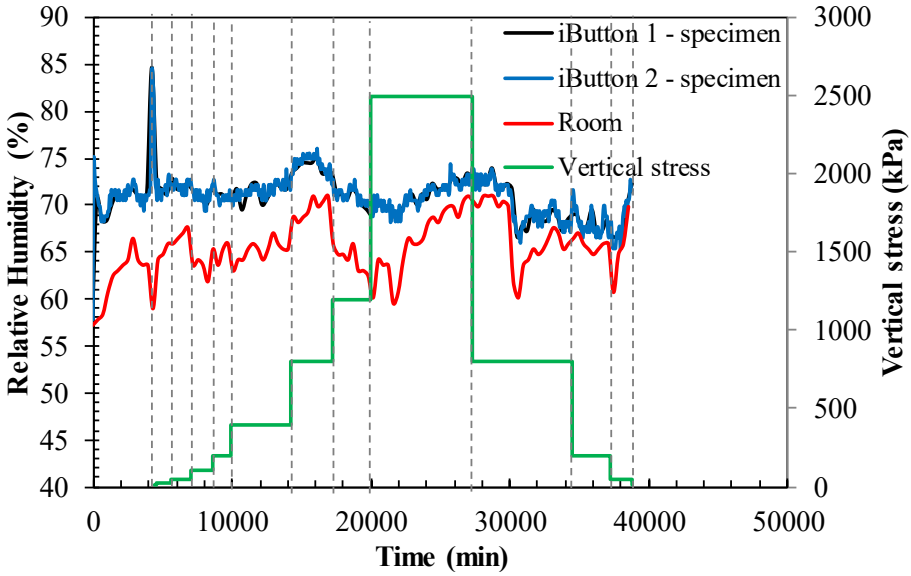

Figure 5.45 Measurements of the relative humidity (RH) and vertical stress over time during the SO-C-RH test

It is interesting to note that all the compression curves obtained by oedometric tests performed in a large oedometer (Coarse curve) and in a small oedometer (Fine curve) at the same initial relative density (D_r=0.70) merge in the same line at high stresses (Figure 5.46). This result refers to the two grain size distributions determined by the parallel scaling technique: the two soils thus have the same uniformity coefficient but a different initial void ratio. The result shows that for the tested limestone the compressibility curves at high stresses are independent of the initial void index. Furthermore, it demonstrates the validity of the parallel gradation technique as a grain size reduction technique necessary to make reliable laboratory experimentation.

Moreover, examination of Figure 5.46 shows that the yield stresses increase as the initial void ratio decrease so with reducing median particle size as reported by Nakata et al. (2001).

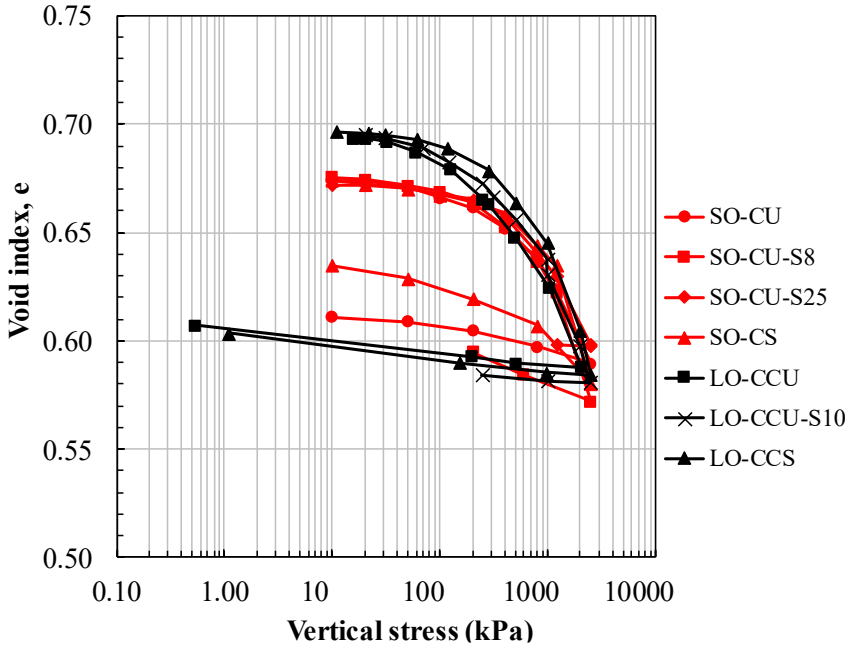

Figure 5.46 Comparison between small and large oedometric tests results on specimens of Coreno rockfill

Furthermore, specimens with greater d_{max} are more compressible than others (Figure 5.46). This is probably due to the fact that soils with different grain size distributions exhibit distinct grain breakage, which significantly influences the soil compressibility. As clearly shown by the B_g values in Table 5.8 the particle breakage has been more significant for the specimens prepared with the Coarse grading curve. These results are expected because the large

size grains are less resistant to breakage, as verified with the grain crushing tests on ambient humidity and saturated grains (Table 4.5).

Table 5.8 Breakage factors (Marsal 1967) of oedometric tests on Coreno specimens

Test	B_g (%)
SO-CU	3.34
SO-CU-S8	4.50
SO-CU-S25	3.31
SO-CS	3.88
LO-CCU	4.95
LO-CCU-S10	5.23
LO-CCS	5.90

As a part of the study on the effect of the degree of saturation on the stress-strain behaviour of rockfills, the **Redisole** rockfill was subjected to a series of oedometric tests in dry and wet conditions using the small size oedometer. Results shown in Figure 5.47 highlight that, within the stress range considered, the behaviour of crushable material is greatly affected by the water whereas, as see before, the non-crushable calcareous rockfill reacts the same whether it is subjected to dry or wet conditions.

As seen before from large oedometric results, wetting under load test performed on Redisole specimen indicated a high collapse potential. In the SO-RU-S8 test collapse deformations reached value of 2.50% for a vertical load of 800 kPa. However, the compressibility after wetting is not the same of the saturated specimen, as seen in the large oedometric tests reported in Figures

from 5.34 to 5.36. This is probably due to the different breakage mechanism that takes place. The water-dependent features of rockfill mechanical behaviour are supposed to occur due to fracture propagation phenomena.

Compression tests performed by several authors (Sowers et al, 1965; Marsal, 1973; Clements, 1981) on rock wedges compressed against surfaces of the same or different material suggest that the breakage of the wedge contact area is the main mechanism which explains the deformation of rockfill as well as the effect of water. The water-dependent features of rockfill mechanical behaviour are supposed to occur due to fracture propagation phenomena. Hence, such dependence would occur only when particle breakage takes place. Since no particle breakage occurs during the particle rearrangement stage, no water dependence should be expected.

The above conclusion is confirmed by the data reported in the Table 5.9, where the values of B_g indicate a greater break of the grains for the saturated specimen.

Table 5.9 Breakage factors (Marsal 1967) of small oedometric tests on Redisole specimens

Test ID	**B_g (%)**
SO-RU	11.88
SO-RU-S8	15.87
SO-RS	20.30

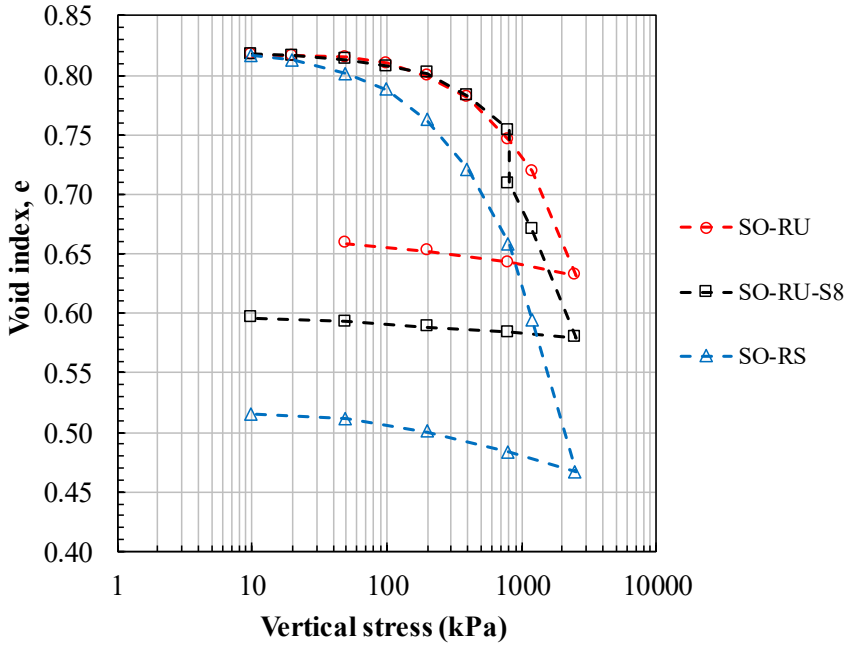

Figure 5.47 Results of small oedometric tests on specimens of Redisole rockfill

From the comparison between small and large oedometric tests on Redisole specimens reported in Figure 5.48, it is shown that the dry material attains a lower compressibility than the saturated specimen whether it is prepared with the Fine grading curve (SO-RU test) or with the Coarse grading curve (LO-RCU test).

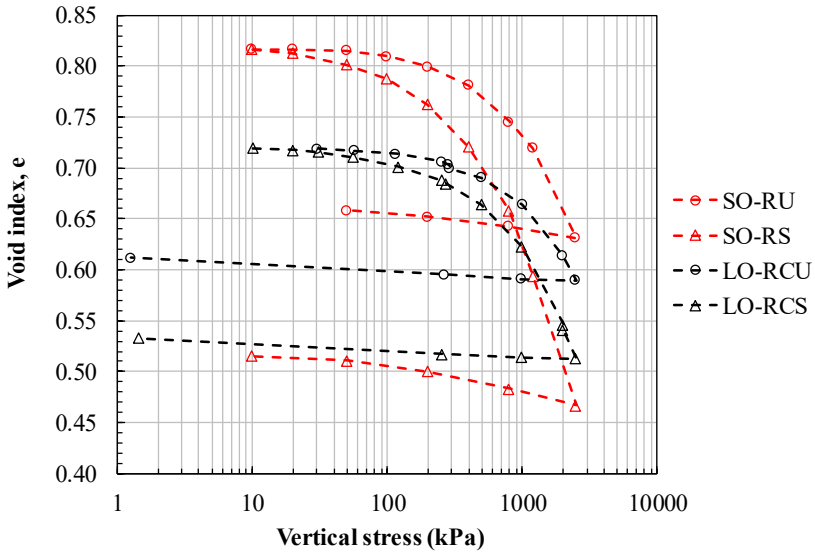

Figure 5.48 Comparison between small and large oedometric tests results on specimens of Redisole rockfill

Contrary to what observed in Figure 5.46 for Coreno rockfill, specimens with greater d_{max} are less compressible than others and the NCL is not unique. Also this can be interpreted in terms of particle breakage mechanisms, as done by several authors (Coop and Lee, 1995; Pestana and Whittle, 1995; McDowell and Bolton, 1998). It is widely accepted that during an initial stage, under low applied stresses, deformation occurs due only to particle rearrangement. Moreover, it is assumed that the onset of particle breakage leads to the bend in the NCL, causing the rapid increase of the material compressibility index.

In the large oedometric tests performed the yield stress is greater, therefore particle breakage is less significant for specimens with a greater d_{max}. These results are confirmed by the B_g values reported in Table 5.10 and from the comparison between grain size distributions after small and large oedometric tests on Redisole rockfill shown in Figure 5.49.

Table 5.10 Breakage factors (Marsal 1967) of small and large oedometric tests on Redisole specimens

Test ID	B_g (%)
SO-RU	11.88
SO-RS	20.30
LO-RCU	8.13
LO-RCS	13.24

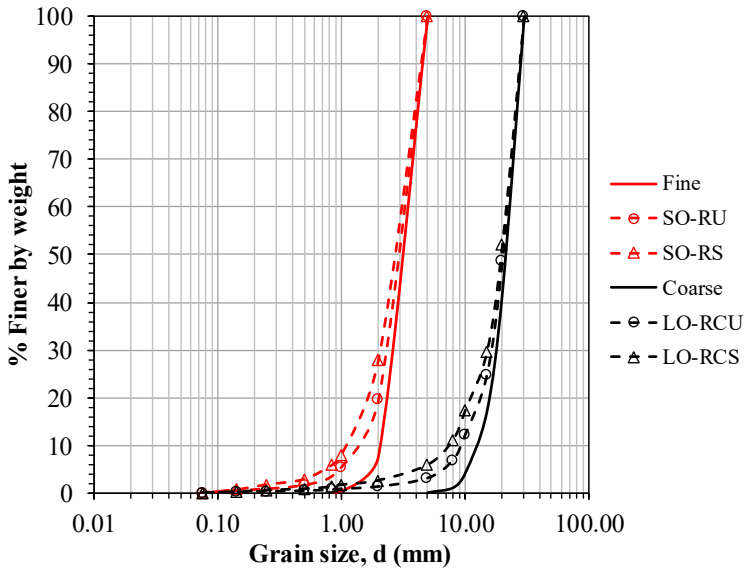

Figure 5.49 Comparison between grain size distributions after small and large oedometric tests on specimens of Redisole rockfill

Figure 5.50 compares the small oedometric test results on Coreno and Redisole rockfills. As expected, given the particle tensile strength values reported in Table 4.5, Coreno rockfill is less compressible than Redisole one since less influenced by grain breakage. It is even more evident that the degree of saturation has an important effect on Redisole material but not on the limestone since the compressibility curves seem to coincide. This is also related to the particle breakage.

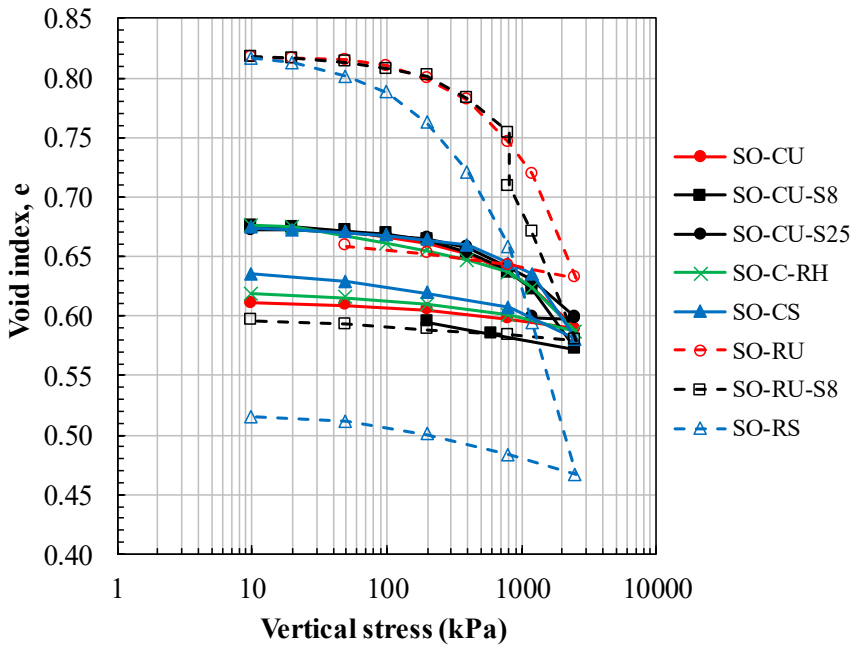

Figure 5.50 Comparison between small oedometric tests results on specimens of Coreno and Redisole rockfill

5.4 Final remarks

A set of large-scale triaxial and oedometric tests have been conducted to investigate the mechanical behaviour of two different rockfill materials.

The results of large triaxial tests show that the deformation behaviour of rockfill is significantly influenced by the loading path as well as the confining pressures. The strength envelope exhibits pronounced curvature at low confining pressures. However, the previous loading history appears to have only minor influence on the shear strength and volumetric strains of rockfill. The degree of saturation and the wetting are revealed to have considerable effect on the volumetric behaviour but small influence on the peak strength of rockfill, while the particle size has marked influence on both the deformation and the strength characteristics. Furthermore, isotropic compression tests have been presented to highlight the effect of the degree of saturation and so, relative humidity, on the rockfill compressibility. Wetting determines volumetric collapse that leads to the achievement of volumetric strains greater than the saturated test.

Then, a comparison between the internal magnetic system (MSD) and the external system for the measurement of axial and radial strains as well as volumetric strains has been reported. A good agreement in the axial direction and a significant difference in the measurements of internal and external systems in the radial

direction have emerged. Despite its high potential, the magnetic system requires further tuning operations.

From large and small oedometric tests emerged that the calcareous material, whose grains have greater tensile strength, is less compressible than Redisole rockfill and that its compressibility seem to be independent of the initial degree of saturation. Furthermore, the saturation-induced collapse deformation is negligible compared to that exhibited from the Redisole material. In this last case, the wetting of specimen at different vertical stress caused a volumetric collapse almost equivalent to the difference between the normal consolidation lines of the dry and saturated specimens.

For both Coreno and Redisole rockfills comparison among the e-log(σ_v) curves of specimens prepared with different initial relative density showed that the vertical yield stress increased with decreasing initial void ratio. After yielding the Coreno rockfill compressibility curves approach a common trend. On the contrary, the comparison between results of large oedometric tests on Redisole specimens prepared with Coarse and Parallel grading curves shows that the normal compression lines approached at high stresses are well distinct and parallel. In all the cases considered rockfill deformation increased with particle size.

Small oedometer tests confirm the results of large oedometer ones and the effectiveness of the parallel gradation technique to select the Fine grain size distribution from the Coarse one. Considering Coreno rockfill, all the curves obtained from large and small

oedometric tests merge in a single line for high stresses, suggesting the existence of a single compression line. This is probably to the fact that this material, under the load application, create a stable and rigid structure that won't easily deform. This is confirmed by the low values of B_g (Marsal, 1967).

Therefore, realistic prediction of the deformation of rockfill structures requires proper consideration of the effects of loading path, previous loading history and moisture content in laboratory testing and in numerical analysis.

5.5 References

Baldi G., Hight D. W., Thomas G. E. (1988). *A Reevaluation of Conventional Triaxial Test Methods*. Advanced Triaxial Testing of Soils and Rock, ASTM SPT 977, R. T. Donaghe, R. C. Chaney, and M. L. Silver, eds., ASTM International, West Conshohocken, PA, 219–263.

Bishop A.W., Wesley L. D. (1975). *A hydraulic triaxial apparatus for controlled stress path testing*. Géotechnique, 25(4), 657–670.

Chávez C. (2004). *Estudio del Comportamiento Triaxial de Materiales Granulares de Tamaño Medio con Énfasis en la Influenciade la Succión*. PhD Thesis, Universitat Politècnica de Catalunya, Spain.

Clements R. P. (1981). *The deformation of rockfill: inter-particle behaviour, bulk properties and behaviour in dams*. Ph.D. Thesis, Faculty of Engineering, King´s College, London University.

Clements R. P. (1984). *Post-construction deformation of rockfill dams*. Journal of Geotechnical Engineering, ASCE, 110(7), 821–840.

Coop M. R., Lee I. K. (1995). *The influence of pore water on the mechanics of granular soils*. Proc. 11th ECSMFE, Copenhagen, 1, 163-172.

Dascal, O. (1987). *Postconstruction deformations of rockfill dams*. Journal of Geotechnical Engineering, ASCE, 113(1), 46–59.

Dendani H., Flavigng E., Fry J. J. (1998). *Test for Embackment Dams: Interpratation and Validity*. Advanced Triaxial Testing of Soils and Rock, ASTM STP 977, R. T. Donaghe, R. C. Chaney, and M. L. Silver. Eds., American Society for Testing and Materials, Philadelphia, 486–500.

Field W. G. (1963). *Towards the statistical definition of a granular mass*. In: Proceedings 4th Australia and New Zealand conference on soil mechanics, 143-148.

Flora A., Lirer S., Viggiani C. (2007) *Studio sperimentale dei fattori influenti sulla compressibilità di un rockfill*. XXIII Convegno nazionale di Geotecnica, Padova.

Hagerty M. M., Hite D. R., Ulrich C. R., Hagerty D. J. (1993). *One-dimensional high pressure compression of granular media.*, Journal of Geotechnical Engineering, ASCE, 119(1), 1-18 (1993).

Indraratna B., Wijewardena L. S. S., Balasubramaniam A. S. (1993). *Large-scale triaxial testing of greywacke rockfill*. Géotechnique, 43(1), 37–51.

Jaeger J. C. (1967). *Failure of rocks under tensile* conditions. International Journal of Rock Mechanics and Mining Sciences & Geomechanics Abstracts, 4(2), 219-227.

Lade P. V., Duncan J. M. (1975). *Stress-path dependent behaviour of cohesionless soil*. Journal of the Geotechnical Engineering Division ASCE, 102(1), 51–68.

Lambe T. W., Whitman R. V. (1979). *Soil mechanics*, SI Version. Wiley, New York.

Marsal R. J. (1967). *Large scale testing of rockfill materials*. Journal of the Soil Mechanics and Foundation Division, ASCE, 93(2), 27-43.

Marsal R. J. (1973). *Mechanical properties of rockfill*. Embankment Dam Engineering, Casagrande Volume, Wiley, New York, 109–200.

McDowell G. R., Bolton M. D. (1998). *On the micromechanics of crushable aggregates*. Géotechnique, 48(5), 667-679.

Nakata Y., Kato Y., Hyodo M., Hyde A. F. L., Murata H. (2001). *One-dimensional compression behaviour of uniformly graded sand related to single particle crushing strength*. Soils and foundations, 41(2), 39-51.

Naylor D. J., Maranha Das Neves E., Mattar D., Veiga Pinto A. A. (1986). *Prediction of construction performance of Beliche dam*. Géotechnique, 36(3), 359-376.

Naylor D. J., Tong S., Shahkarami A. A. (1989). *Numerical Modeling of Saturation Shrinkage*. Numerical Methods in Geomechanics, NUMOG III, S. Pietruszczack and G. N. Pade, eds., Elsevier, Amsterdam, 636–648.

Nobari E. S., Duncan J. M. (1972). *Effect of Reservoir Filling on Stresses and Movements in Earth and Rockfill Dams*. Report No. TE-72–1, Department of Civil Engineering, Institute of Transportation and Traffic Engineering, University of California.

Oldecop L. A., Alonso E. E. (2001). *A model for rockfill compressibility*. Géotechnique, 51, 127-139.

Pestana J. M., Whittle A. J. (1995). *Compression model for cohesionless soils*. Géotechnique, 45(4), 611-631.

Pinto N. D. S., Marques Filho P. L. (1998). *Estimating the maximum face deflection in CFRDs.* Int. J. Hydropower Dams, 5, 28–32.

Pourjafar A., Mahin roosta R. (2011). *Evaluation of the collapse settlement behavior of sandy material using triaxial shear tests*. Proc., 6th National Congress of Civil Engineering, Semnan, Iran.

Soriano A., Sánchez F. J. (1996). *Deformaciones de Humectación en Escolleras. Simulación Numérica*. V. Jornadas Españolas de Presas, Valencia, España.

Sowers G. F., Williams R. C., Wallace T. S. (1965). *Compressibility of broken rock and the settlement of rockfills*. Proc., 6th ICSMFE, Vol. 2, University of Toronto Press, Montréal, 561–565.

Veiga Pinto A. (1983). *Previsão do Comportamento Estructural de Barragens de Enrocamento*. Ph.D. Thesis, Laboratorio Nacional de Engenharia Civil, Lisbon.

Ventini R., Flora A., Lirer S., Mancuso C. (2019a). *Magnetic measurement system of sandy gravel specimens shape during tests in a large triaxial apparatus*. E3S Web of Conferences, EDP Sciences, 92, 02004.

Ventini R., Flora A., Lirer S., Mancuso C. (2019b). *On the Effect of Grading and Degree of Saturation on Rockfill Volumetric Deformation.* National Conference of the Researchers of Geotechnical Engineering, 462-471.

Won M. S., Kim, Y. S. (2008). *A case study on the post-construction deformation of concrete face rockfill dams*. Canadian Geotechnical Journal, 45(6), 845–852.

Xu M., Song E., Chen J. (2012). *A large triaxial investigation of the stress-path-dependent behavior of compacted rockfill*. Acta Geotechnica, 7, 167-175.

CHAPTER 6

CONSIDERATIONS ON EXPERIMENTAL RESULTS

6.1 Introduction

As highlighted in the previous chapters, several factors influence the mechanical behaviour of a coarse-grained material.

In this chapter will be analyse the characteristics of the mechanical behaviour of rockfills, which emerged from the results of the oedometric and triaxial tests performed. The aim of this chapter is to present the findings from a laboratory study highlighting the influence of particle breakage and relative density D_r on compressibility, strength and dilatancy of the tested rockfills.

6.2 Effect of particle breakage on rockfill behaviour

During triaxial and oedometric compression tests particle breakage takes place. To analyse this peculiarity of grain rockfills behaviour after performing laboratory tests at different confining stress, suction and following different stress paths, the specimens were dried for sieve analysis.

Here, the particle breakage is expressed by the factor B_g (Marsal, 1967), i.e. the sum of decreases (or increases) in the percentage of particles retained in each sieve of the set of standard sieves from 40 to 0.075 mm in size. Considering various possible methods of particle breakage quantification, Marsal's (1967) breakage factor

has been chosen in this study because of its simplicity in computation and ability to measure the degree of particle degradation in a quantifiable manner.

In the triaxial test campaign, particle breakage was observed as a function of particle size, degree of saturation, confining pressure and stress path. As shown in paragraph 5.2.2 suction influences particle rearrangement and edges of individual soil particles breakage affecting the overall stress-strain behaviour of the limestone rockfill.

The particle splitting of the tested materials is also observed on shearing. The variation of the breakage factors with the confining stresses for the triaxial tests performed with a slope of the stress path $\alpha = \arctan(q/p') = 71.6°$ is shown in Figure 6.1 for the various grain size distributions used. The data indicated with Fine, Medium and Coarse refer to the Coreno rockfill while the Parallel data refer to the Redisole rockfill. Furthermore, the initial relative density of specimens prepared with the Parallel curve (D_r =100 %) is greater than that used in the other tests (D_r =70 %).

It can be noted that the breakage factor increases with the confining stress following a linear function for each grain size distribution of the Coreno rockfill. Instead, the confining stress-breakage factor relationship is a power law for the Redisole rockfill. It is also shown that the breakage is systematically more pronounced for the Redisole material than for Coreno rockfill. The highest values of the breakage factors in the Redisole material is due to the relatively low

strength of the particles, as confirmed by the grain crushing tests (Table 4.5).

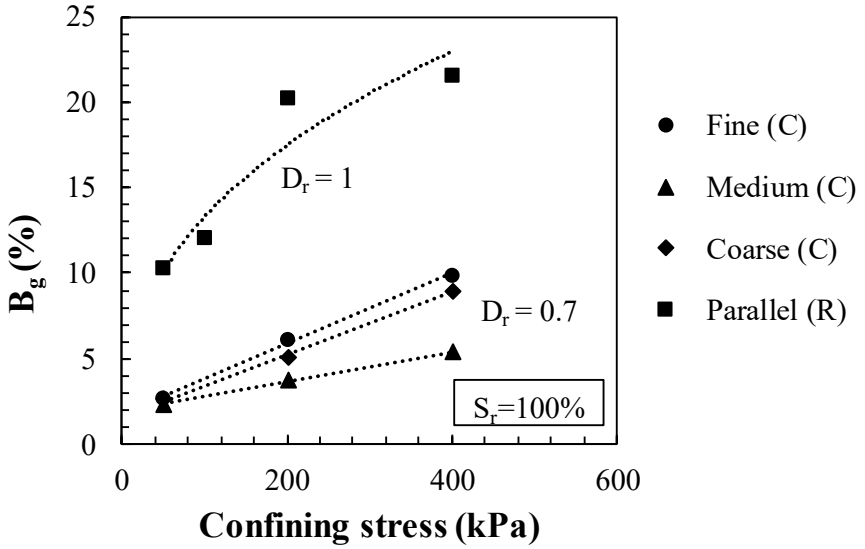

Figure 6.1 Variation of the breakage factor with confining stress in monotonic triaxial tests on saturated specimens

As shown in Figure 6.1, the breakage factors at a confining stress of 50 kPa are approximately identical for the three grain size distributions tested of Coreno rockfill. Therefore, it seems that the grading curve and therefore the grain size have a minimal effect on the breakage at such a low stress level. As the confining stress increases, the breakage factors of the various grain size distributions depart to each other. The breakage is quantitatively greater for the Fine grading curve than for the Coarse and Medium grading curves. However, the data obtained with the Fine and Coarse grading curves are very close confirming that the parallel technique is a

quite good way to scale the particle size for monotonic rockfill testing.

It is widely known that a uniformly graded granular material exhibits more crushing than a well-graded material with the same maximum particle size (Lee et al., 1967; Lade et al, 1996; Nakata et al., 2001). This effect is due to the increasing confinement of the particles (number of contacts) that decreases the average contact stress (Lade et al, 1996). However, several authors (Hardin, 1985; Hagerty, 1993; Lade et al., 1996) stated that breakage factor increases with the increase in maximum particle size because bigger particles have a higher probability to be affected by defects acting as "particle breakage triggers".

It is interesting to note that the Medium soil with greater d_{max} is less prone to breakage than the Fine soil having a lower uniformity coefficient. This result differs from what seen in the isotropic compression tests (see paragraph 5.2.2). Thus, under the conditions of the monotonic triaxial tests carried out, the effect of the soil uniformity on particle breakage is more significant than the particle size effect. This trend is confirmed by the micromechanical analysis performed as described in the paragraph 5.2.2. Once the average contact force $F_{i,v}$ has been calculated using Equation 5.4, the average contact stress on the single grain in the vertical direction $\sigma_{c,d}$ is expressed as:

$$\sigma_{c,d} = \frac{F_{i,v}^{1/3}}{\pi \cdot K^{\frac{2}{3}} \cdot (\frac{d_{50}}{2})^{2/3}} \tag{6.1}$$

With $K=3(1-\nu^2)/(4E)$, and ν and E respectively Poisson's ratio and Young's modulus of the rock.

The average values of $\sigma_{c,d}$ recorded during the tests are plotted against the breakage factors in Figure 6.2. As shown, the $\sigma_{c,d\ medium}$ acting on the Fine soil is greater than that on the Medium soil, resulting in a more significant particle breakage (Figure 6.1).

From the results of the micromechanical analysis it is evident that the $\sigma_{c,d\ medium}$ acting on the Redisole grains is greater than that acting on Coreno justifying its pronounced particle breakage (Figure 6.1).

As recognized in literature, a larger granular material possesses a lower crushing strength than a material with the same uniformity coefficient but lower d_{max}. On the contrary, Figure 6.1 shows that the breakage factors for the Coarse grained material systematically stands slightly below that of the Fine grading curve. This trend also differs from the results of the grain crushing tests described in paragraph 4.4.2, which showed a tensile strength of the grains having the diameter d_{50} of the Coarse grained material lower than that of the Fine grained ones.

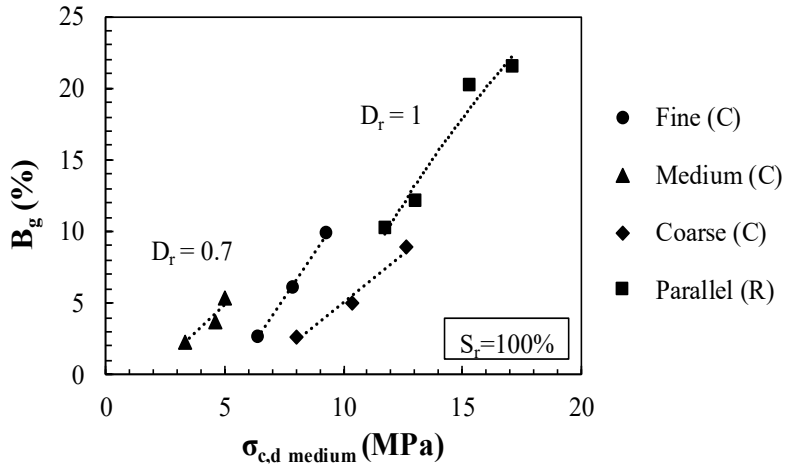

Figure 6.2 Variation of the breakage factor (Marsal, 1967) with the average contact stress on the single grain in the vertical direction in monotonic triaxial tests on saturated specimens

The evolution of the breakage factor with the confining stresses recorded during all the deviatoric tests are shown in Figures from 6.3 to 6.6. As well known in literature, particle breakage also depends on suction and the stress path.

Due to periodic filling and emptying of dam reservoir as well as cyclic changes of climate, rockfill materials are usually subjected to transitions from wet to dry states and vice versa. As discussed in paragraph 5.2.2 and 5.3, also in the monotonic tests the degree of saturation has a remarkable effect on the particle breakage (Figures 6.3, 6.5 and 6.6). Due to the reduction of tensile strength with suction (Table 4.5), at the same confining stress and initial relative density, saturated specimens (i.e. CF2 and CC2) are affected by greater particle breakage than unsaturated ones (i.e. CF2U, CC2U,

CC2U-S). Suction changes in granular materials soften the edges (acting as contact points between the aggregates) and make easier and faster the crack propagation (Oldecop and Alonso, 2001).

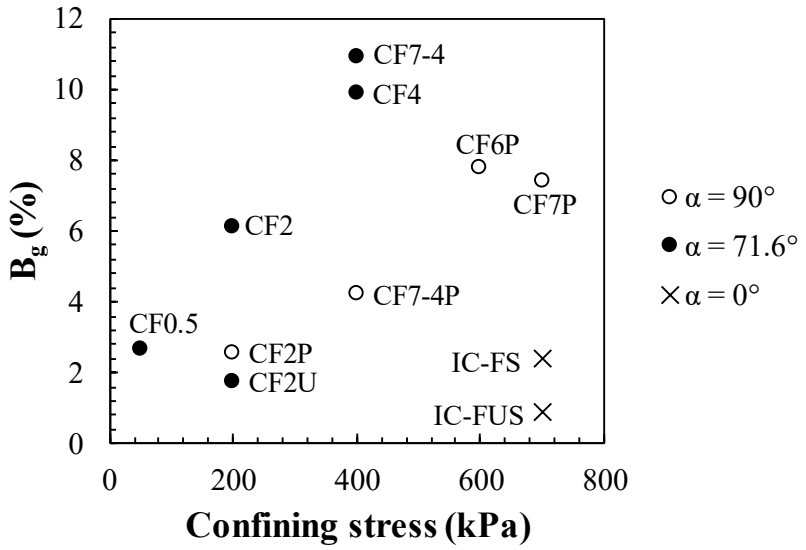

Figure 6.3 Breakage factor versus confining stress for the deviatoric tests on Coreno specimens (Fine grading curve)

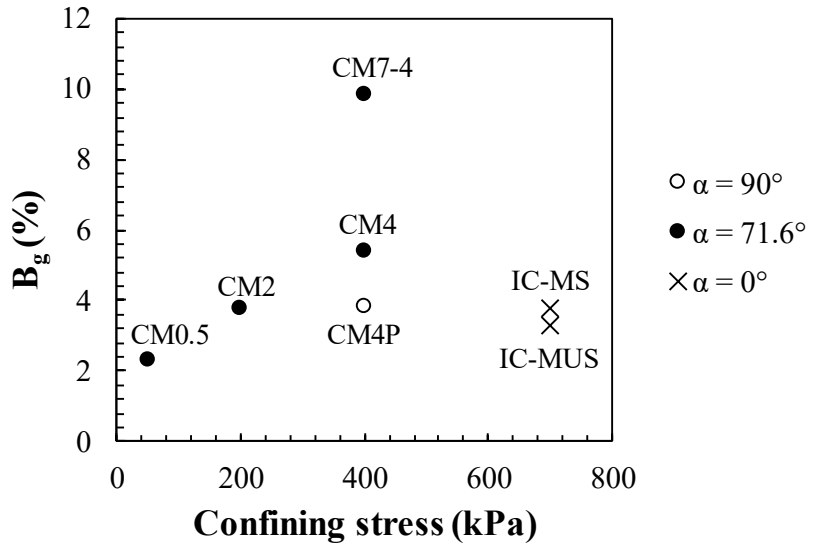

Figure 6.4 Breakage factor versus confining stress for the deviatoric tests on Coreno specimens (Medium grading curve)

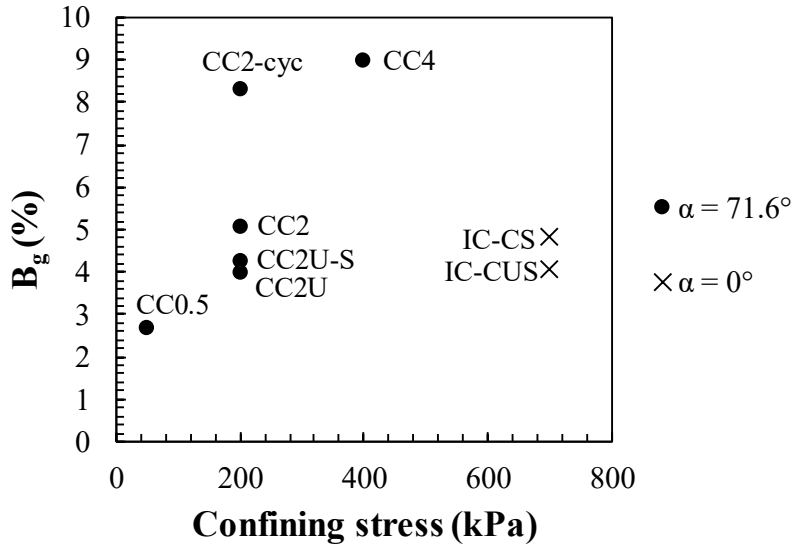

Figure 6.5 Breakage factor versus confining stress for the deviatoric tests on Coreno specimens (Coarse grading curve)

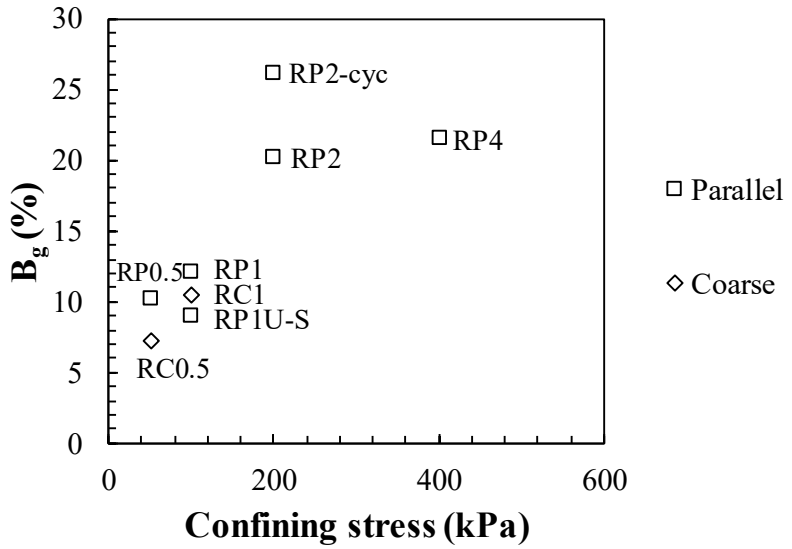

Figure 6.6 Breakage factor versus confining stress for the deviatoric tests on Redisole rockfill

The results of triaxial tests (monotonic and isotropic compression) at different α are presented in Figures from 6.3 to 6.5. As expected and discussed in paragraph 5.2.1, α has a major effect on the breakage of grains as well as on stress-strain behaviour. Along the stress path at α = 90° (empty points) particles are less prone to crushing justifying the dilatancy shown in the monotonic tests (paragraph 5.2.1). It is confirmed that smaller α would induce more particle breakage and suppress particle rotation, resulting in more contractive deformation behaviour. However, during isotropic compression tests (α = 0) the grain breakage is, for all the grain size distributions considered, always less then monotonic tests at the same confining stress. This highlights the fact that the deviatoric

stress has a greater influence on particle breakage than the mean effective stress.

Furthermore, also the previous loading history has an effect on the breakage factor. Stress paths different from the traditional ones as loading up to 700 kPa and unloading to 400 kPa and cyclic shear CRL tests can induce more splitting of the grains (Figures from 6.3 to 6.6). As shown in paragraph 5.2.1, the previous loading history does not seem to have a remarkable effect on the stress-strain behaviour but, as can be seen in Figures from 6.3 to 6.6, it can lead to an increase in the breakage of the grains, with consequent change of the soil fabric.

Comparing the results of the tests on Redisole specimens having two grain size distributions and the same uniformity coefficient (i.e. Coarse and Parallel), it emerges that the breakage factor also increases with the increase in size of the particles (Figure 6.6). This trend is found to be similar to that observed by Marsal (1967), Vesic and Clough (1968) and Marachi et al. (1969).

In Figures 6.7a and 6.7b the values of $B_g/(1 + e_c)$, with e_c the void index at the end of the consolidation phase, which represents the percentage of the volume of broken particles per unit of total volume are represented on the y-axis. On the x-axis there are the p'_{ult} (Figure 6.7a) and q_{ult} (Figure 6.7b) stresses recorded at the end of the test normalized to the tensile strength of the single grains shown in Table 4.5. The data shown refer only to tests on consolidated and sheared saturated specimens.

From the two figures, it is clear that the particle breakage increases as the applied stress increase and the tensile strength of the single grain decreases, as widely recognized. Furthermore, Coarse and Parallel specimens prepared with the Redisole material seem to follow a unique relationship in these two planes shown in Figure 6.7, contrary to what happens for the Coreno material, less prone to crushing.

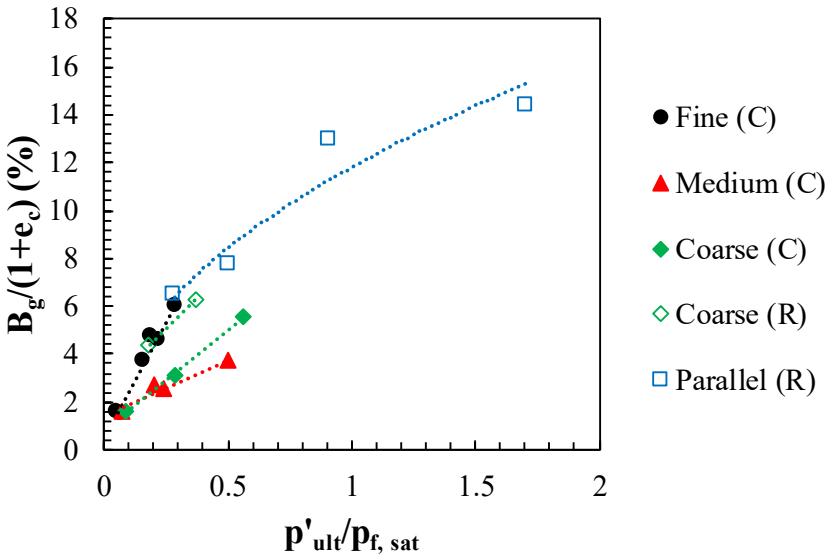

a)

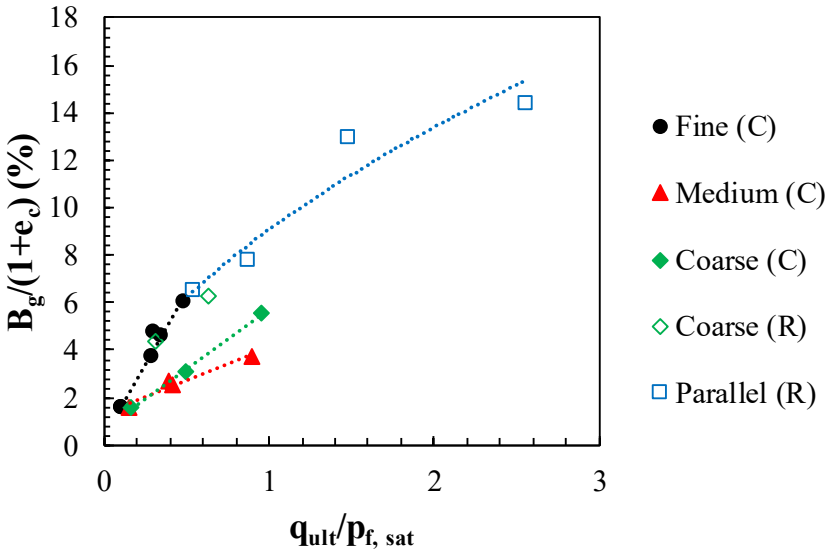

b)

Figure 6.7 Particle breakage at the end of triaxial tests on saturated specimens as a function of the ultimate values of p'(a) and q (b)

It is well known that particle size and gradation influence strength and volume change behaviour of coarse-grained material (Bishop, 1948; Leslie, 1963; Vallerga et al., 1957). Therefore, the changes in particle size and gradation due to particle breakage have an effect on the rockfill compressibility.

The relationship between the compressibility index C_c and the breakage factor B_g recorded after oedometric tests in large and small oedometer is reported in Figure 6.8. As well known, C_c increases with particle crushing and its variation with the breakage factor is a linear law for the Redisole rockfill. It is noteworthy observed that the tendency of data from two soils with proportional grain size tested in two different equipment follow the same linear

relation. These results once again confirm that parallel gradation technique is a very useful tool in predicting the behaviour of the rockfill material based on the tests carried out on modelled laboratory specimens.

As shown in Figure 6.8, the specimens prepared with the Fine grading curve (red points) are more compressible and more prone to crushing than Coarse (black points) specimens at the same test conditions, contrary to what is expected given the smaller grain size. However, the breakage factor is greater for the Parallel specimen (blue point) than the Fine one while C_c is lower.

It is interesting to note that the compressibility indexes are similar for LO-RCU, LO-RCU loose and LO-RPU tests, performed at the same degree of saturation. As seen in paragraph 5.3.1, two soils prepared with the same material and the same uniformity coefficient (i.e. LO-RCU and LO-RPU specimens) but different grain size have similar compressibility and C_c. Moreover, specimens LO-RCU loose and LO-RCU prepared with different initial relative density have different compressibility but the slope of the NCL is more or less the same. So, soils with different relative densities and grain size distributions but the same degree of saturation would exhibit different grain breakage, which does not significantly influence the compressibility index of the soil.

Figure 6.8 also shows the influence of the degree of saturation on Coreno and Redisole rockfills. The experimental data presented show that saturated and flooded crushable granular material samples are more compressible than dry samples, mainly due to the increase

of grain crushing in the presence of water. So, for specimens prepared with air dried grains, suction in capillary bonds of intergranular contacts is negligible, which is normally the case in rather coarse materials.

The variation of C_C with S_r is more pronounced than that of B_g for Coreno rockfill. The negligible difference in breakage for filled points is due to the high particle tensile strength of the limestone rockfill. Contrary to Redisole rockfill, Fine specimens of Coreno rockfill are less compressible and less prone to crushing than Coarse ones, as expected. However, it is interesting to note that, unless an experimental point, data referring to two different materials are collected in a narrow range in the C_C-B_g plane, being within the two limit curves shown in Figure 6.8.

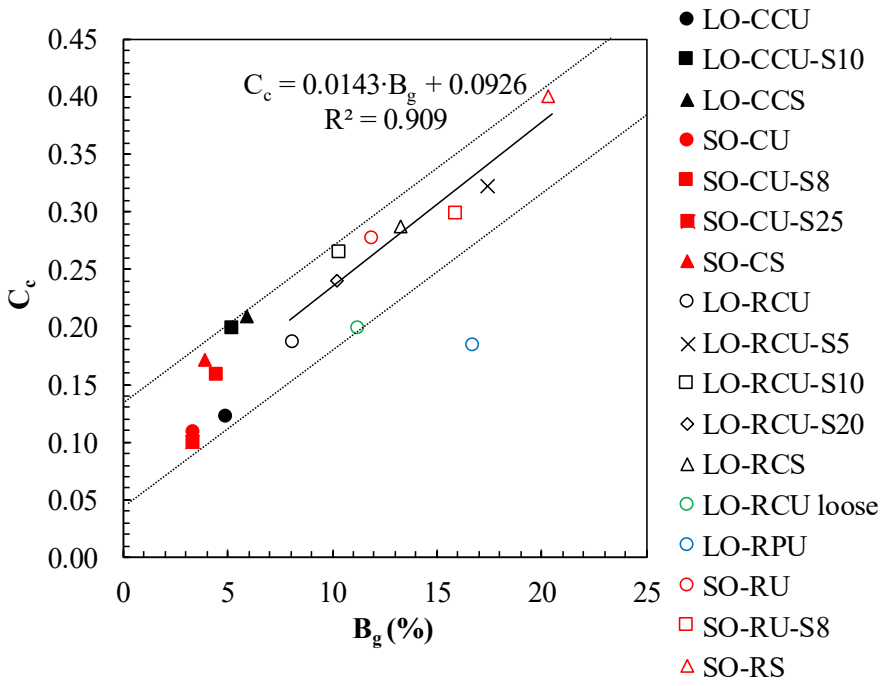

Figure 6.8 Variation of the compressibility index with breakage factor for Coreno and Redisole rockfill

It can be reasonably assumed that flooding triggers particle crushing. According to literature (i.e. Oldecop and Alonso, 2001) and also regarding results presented in this work, this phenomenon could be explained by a drop in capillary suction at the microcracks scale inside the particles, as well as corrosive attacks of water, reducing their crushing strength. It is noted in Figure 6.9 that the breakage factor increases for saturated specimens and it is always greater for Redisole rockfill (empty points). It is also significant to note that the effect of the degree of saturation is more pronounced for the Redisole material than the Coreno one, whose filled points

lie close together. Therefore, the uniqueness of the compressibility indexes of saturated and flooded limestone tests can be explained because they have reached the same grain size distribution, which was made possible due to similar grain crushing (and so B_g).

This highlight that the effect of water on compressibility and particle breakage cannot be overlooked. Nevertheless, the effect of saturation on particle crushing and, on the compressibility, could be more or less significant depending on the material properties and its sensitivity to the presence of water. Furthermore, B_g increased with increase in initial void ratio and grain size, as expected.

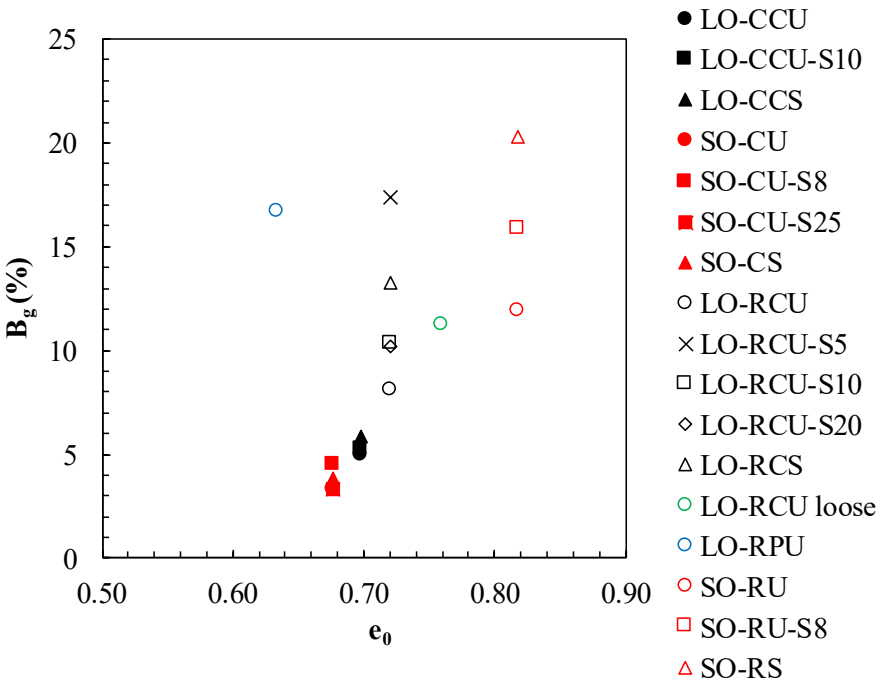

Figure 6.9 Particle breakage at the end of oedometric tests on Coreno and Redisole specimens

6.3 Strength: friction angle

The axial and volumetric strains at the peak deviator stresses q_{peak} recorded on testing are plotted against the peak deviator stresses normalized with the corresponding $\sigma'_{c.}$

In Figures 6.10 and 6.11 it can be seen that the axial strains at failure along α=90° (green points) are notably smaller than those at the same σ'_c derived from the conventional triaxial tests while the volumetric strains at failure are greater in absolute value and always negative (Table 6.1).

Table 6.1 Details of consolidated drained triaxial tests on Coreno rockfill

Test ID	σ'_c (kPa)	$\varepsilon_{a,\,peak}$ (%)	$\varepsilon_{v,\,peak}$ (%)	q_{peak} (kPa)
CF2	200	9.72	-0.51	1041.50
CF2P		4.85	-2.44	422.53
CF4	400	10.15	1.09	1716.16
CF7-4P		4.61	-2.12	776.34
CM4	400	11.44	0.81	1904.53
CM4P		4.73	-2.30	845.58

Furthermore, it is interesting to note that q_{peak}/σ'_c seems to be constant in α=90° tests as shown in Figure 6.10 and Figure 6.11. So, when the influence of varying confining pressure is removed, the peak deviator stress attained during shearing phase at constant p' is approximately constant for different axial and volumetric strains (Figure 6.12 and Figure 6.13). The data from α=71.6° tests on the

two materials considered lie within the two limit curves shown in Figure 6.10 and Figure 6.11.

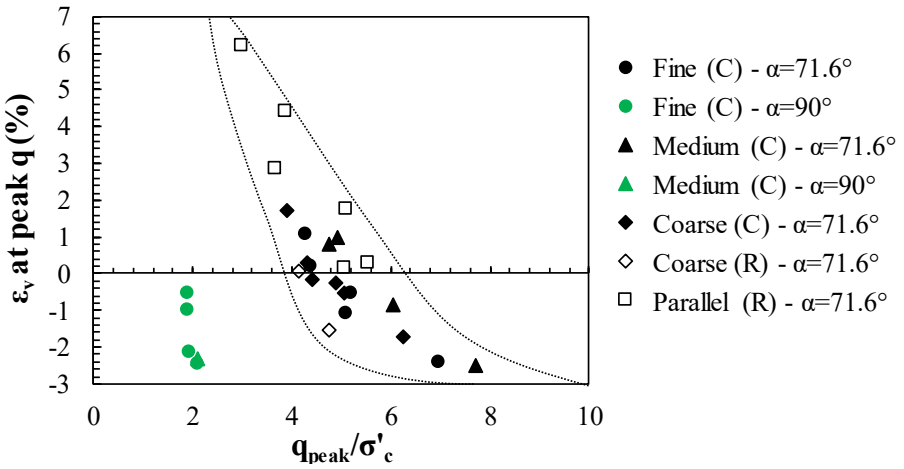

Figure 6.10 The volumetric strains at the peak deviatoric stresses of Coreno and Redisole specimens

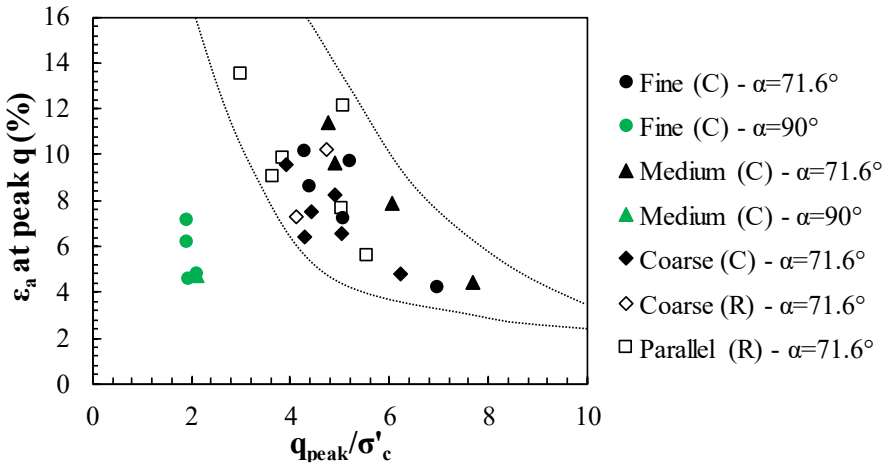

Figure 6.11 The axial strains at the peak deviatoric stresses of Coreno and Redisole specimens

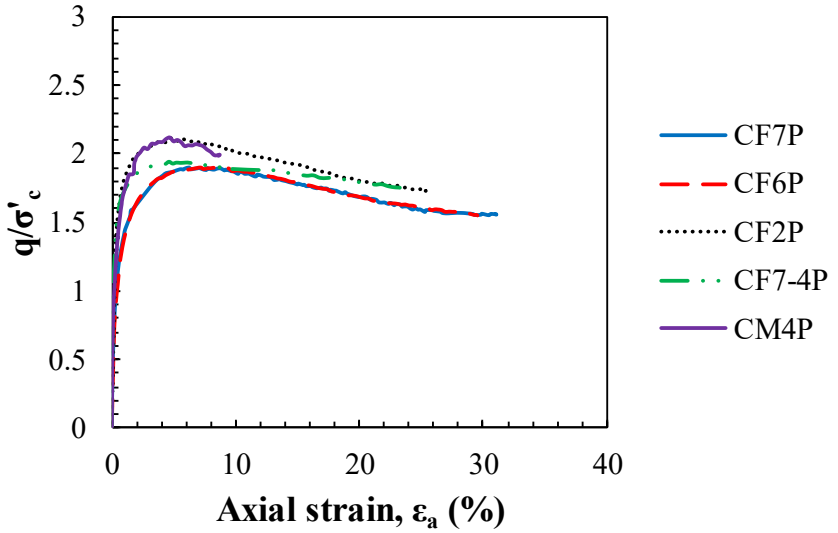

Figure 6.12 Axial strains versus stress ratio of Coreno specimens

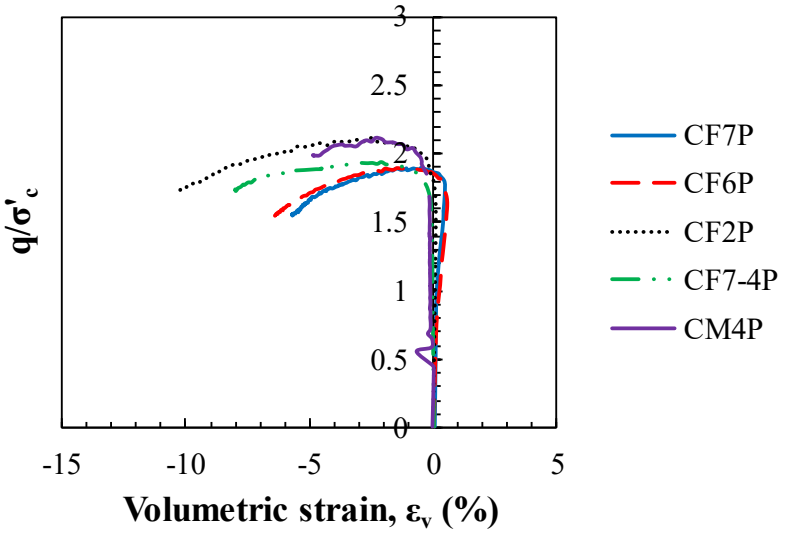

Figure 6.13 Volumetric strains versus stress ratio of Coreno specimens

The parameter used to express the limit condition of a coarse-grained material is generally the friction angle φ', defined by:

$$sen\varphi' = \frac{3\eta}{6+\eta} \tag{6.2}$$

with $\eta=q/p'$. If $\eta=\eta_{max}$, $sen\varphi'=sen\varphi'_{max}$ is the maximum shear strength of the material. It is known that compacted rockfills have excellent shear strength characteristics, expressed by values of the friction angle much higher than those commonly used for sands.

Most of the triaxial tests performed were stopped when the q/p' ratio had reached a constant value. Despite this, only in some cases stationary conditions have been reached, in which the specimen deforms at constant volume. For what has been said, the final parameters obtained during the trial will be defined as ultimate and not stationary. A summary of the results obtained is shown in Table 6.2.

It is interesting to note in Table 6.2 that CF4 and CF7-4, CM4 and CM7-4, CC2 and CC2-cyc, RP2 and RP2-cyc tests with different previous loading history but the same stress path in the shearing phase, have similar values of the peak friction angles. The maximum variation is 0.54°. These results obtained with both rockfills and all the grain size distributions tested, confirm that the previous loading history does not affect the peak friction angle. In terms of ultimate friction angle, the values vary between 0.5 and 3°.

Table 6.2 Experimental results from drained triaxial tests

Rockfill	Test ID	Grain size distribution	σ'_c kPa	p'_{ult} kPa	φ'_p °	φ'_{ult} °	B_g %
Coreno	CF0.5	Fine	50	165	50.81	50.29	2.67
	CF2		200	504	46.26	44.02	6.13
	CF4		400	907	43.01	40.95	9.87
	CF2P		200	201	51.13	42.00	2.54
	CF6P		600	599	46.13	38.07	7.80
	CF7P		700	700	46.20	38.12	7.42
	CF7-4P		400	399	47.04	42.41	4.20
	CF7-4		400	826	43.37	37.93	10.93
	CF2U		200	520	45.87	44.91	1.76
	CM0.5	Medium	50	149	52.69	48.60	2.31
	CM2		200	477	48.35	41.59	3.73
	CM4		400	988	44.78	43.49	5.36
	CM4P		400	400	51.05	45.72	3.81
	CM7-4		400	919	45.32	40.66	9.85
	CC0.5	Coarse	50	141	49.68	45.79	2.65
	CC2		200	467	43.57	41.80	5.05
	CC4		400	913	41.63	41.39	8.95
	CC2-cyc		200	446	43.22	40.52	8.28
	CC2U-S		200	448	45.76	41.45	4.25
	CC2U		200	468	45.82	41.98	3.95
Redisole	RC0.5		50	115	44.65	41.46	7.21
	RC1		100	231	42.42	41.46	10.50
	RP0.5	Parallel	50	132	47.82	46.19	10.25
	RP1		100	235	45.76	42.01	12.08
	RP2		200	426	40.66	39.73	20.22
	RP4		400	797	36.89	36.82	21.52
	RP2-cyc		200	443	41.19	40.21	26.10
	RP1U-S		100	243	45.97	43.22	9.00

The peak friction angle φ'_p and the friction angle at the end of the test φ'_{ult} are plotted against the confining stress for the two rockfill materials considered in Figure 6.14 and Figure 6.15, where each point represents the value of a single test at constant σ'_c on saturated specimen. As the confining stress is increased, the drained friction angle decreases for all the soils considered. The results can be interpolated with a power law of the type:

$$\varphi' = a(\sigma'_c)^b \tag{6.3}$$

with a and b material parameter, confirming what reported by Flora (1995).

The large reduction in the angle of shearing resistance at high confining stresses is associated with the significant increase in crushing of angular particles, as will be shown below. The marked influence of confining stress on shear resistance is well known phenomenon discussed by several authors (i.e. Bishop, 1966; Vesic and Clough, 1968; Indraratna et al., 1993). It is very important in the stability analysis of rockfill slopes and structures because the use of a constant mean internal friction angle may overestimate the safety factor.

The role of the grain size distribution on the angle of friction can be evaluated from the current test results. As shown in Figure 6.14, the well graded soil (i.e. Medium grading curve) has a higher peak friction angle than the other uniform soils. The differences between tested soils are not so marked in terms of φ'_{ult} (Figure 6.15) but the influence of the particle breakage is still remarkable. Being well-graded and containing large-diameter grains both are effective in

increasing the interlocking between particles. When soil is well-graded, there is more contact between particles and the load is more uniformly distributed between particles. The scalping technique, having led to an increase in the shear strength that emerged from the triaxial tests, seems to be the least precautionary technique for reducing the size of the grains necessary for reliable laboratory experimentation.

Considering the data obtained with the parallel gradation technique (Figure 6.14), in the case of the Coreno (C) rockfill the Fine soil has greater φ'_p than the Coarse one characterized by a larger grain size. If the rockfill Redisole (R) is considered, on the contrary, the Parallel soil which corresponds to a larger grain size, is more resistant than the Coarse one. Probably these different trends are linked to the particle tensile strength and the particle breakage, which are greater and lower respectively in the limestone. Therefore, since the Fine and Coarse soils break a little but by a similar amount, seems that the effect of the grain size has less impact on the overall mechanical behaviour compared to Redisole rockfill.

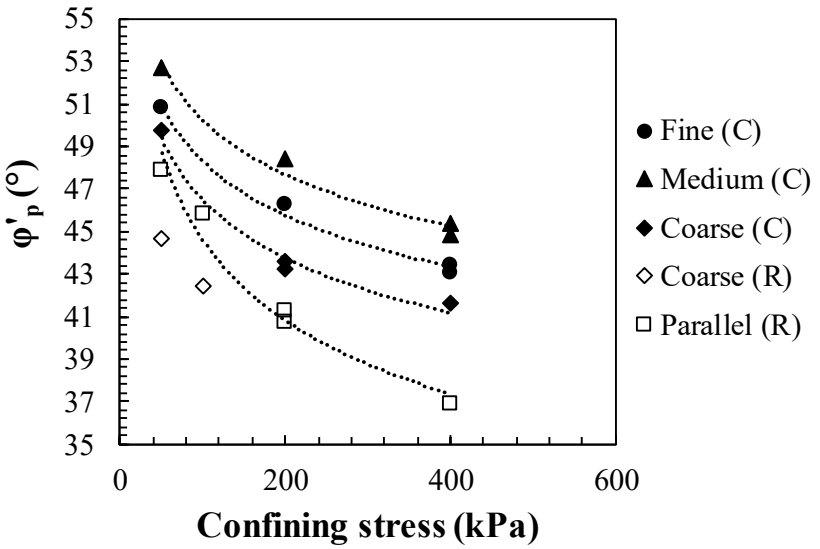

Figure 6.14 Variation of peak friction angle against confining stress for saturated specimens sheared at constant σ'c

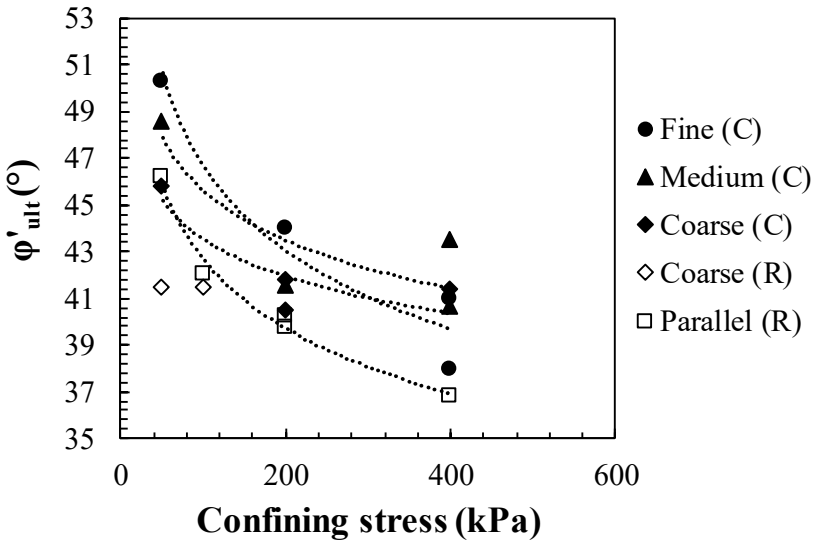

Figure 6.15 Variation of ultimate friction angle against confining stress for saturated specimens sheared at constant σ'c

It can be also observed in Figure 6.14 and Figure 6.15 that, given a value of σ'_c, the friction angles decrease with decreasing particle tensile strength p_f. This indicates a clear influence of the mechanical properties of the grains on the peak and on the ultimate strength of the material, which can be highlighted by expressing φ'_p and φ'_{ult} as a function of p'/p_f.

Figures 6.16 and 6.17 show the same data as in Figures 6.14 and 6.15 with respect to the dimensionless variable $p'/p_{f,sat}$. The particle tensile strength of saturated grains $p_{f,sat}$ is used since the results refer to saturated specimens. Contrary to what reported by Flora (1995) the regression is not unique for the soils considered neither in terms of φ'_p nor of φ'_{ult}. However, also in this case, the relationship φ'-$p'/p_{f,sat}$ follows a power law.

Anyway, the results presented are in contrast with the common practice of assuming a constant friction angle value under steady-state conditions (Figure 6.17).

According to test results presented in Figures 6.16 and 6.17, as the particle size becomes smaller, the shear strength tends to decrease for Redisole rockfill.

Furthermore, Coarse and Fine soils data follow the same regression so, for parallel grain size distributions of Coreno rockfill, the grain size seems to have no effect. This result is incompatible with the results of Redisole and of Baladi and Wu (1988) suggesting that an increase in the average grain size increases frictional resistance.

Moreover, by normalizing the stress by the particle tensile strength p_f (Figure 6.16), the Medium grading curve of the Coreno rockfill

shows the greater peak friction angles as seen in Figure 6.15. From the data shown in Figure 6.16 it can be also argued that the parallel gradation technique seems to be the more reliable for reducing the grain size of Coreno grains.

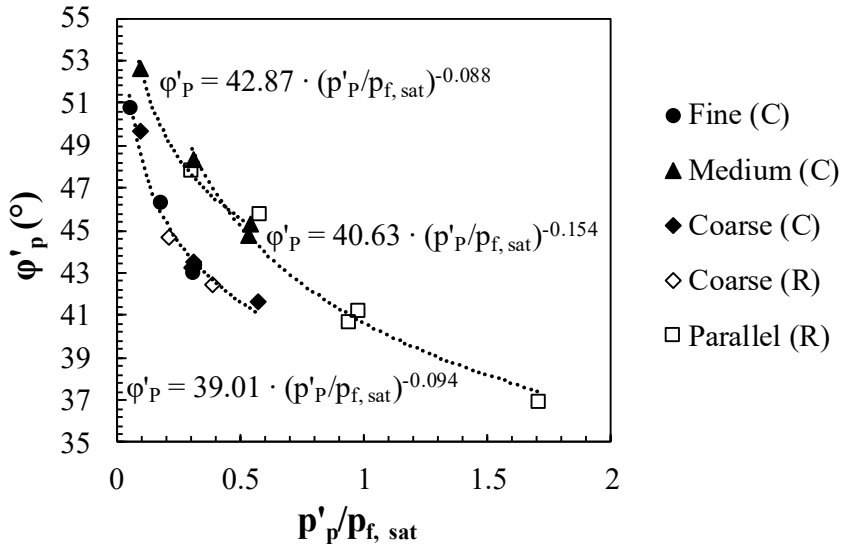

Figure 6.16 Variation of peak friction angle against stress ratio for saturated specimens sheared at constant σ'$_c$

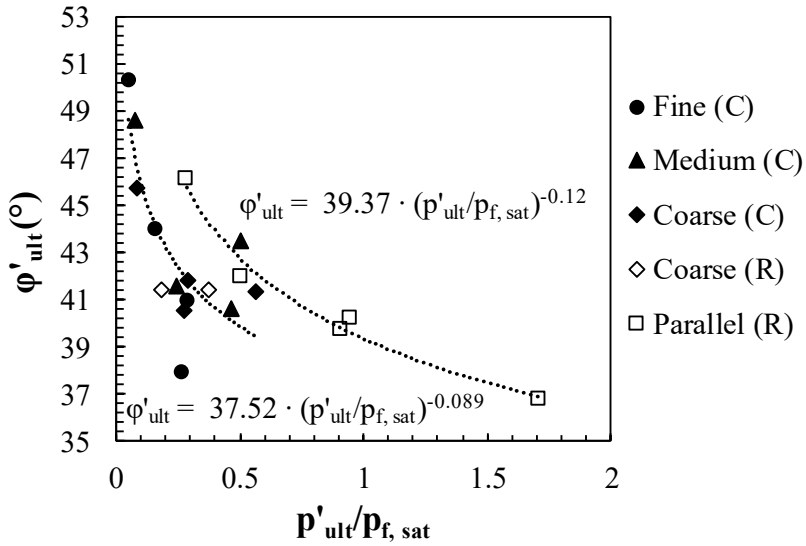

Figure 6.17 Variation of ultimate friction angle against stress ratio for saturated specimens sheared at constant σ'_c

In order to highlight the effect of the stress path followed in the deviatoric phase and therefore of α on the shear strength of the tested rockfill, the data of the tests on Fine soil are shown in Figure 6.18 and Figure 6.19. It is confirmed that the relationship φ'-p'/p_f follows a power law. As shown in Figure 6.18 the results of α = 90° tests give rise to slightly major φ'_p but the parameters a and b of the two regressions are very close together. On the contrary, the angles φ'_{ult} of α = 90° tests are lower and the coefficients b of the two regressions are very different (Figure 6.19). Surprisingly, it can be concluded that the soil ultimate strength is dependent on the stress path that, instead, has a negligible effect on the peak friction angle of the Coreno rockfill tested.

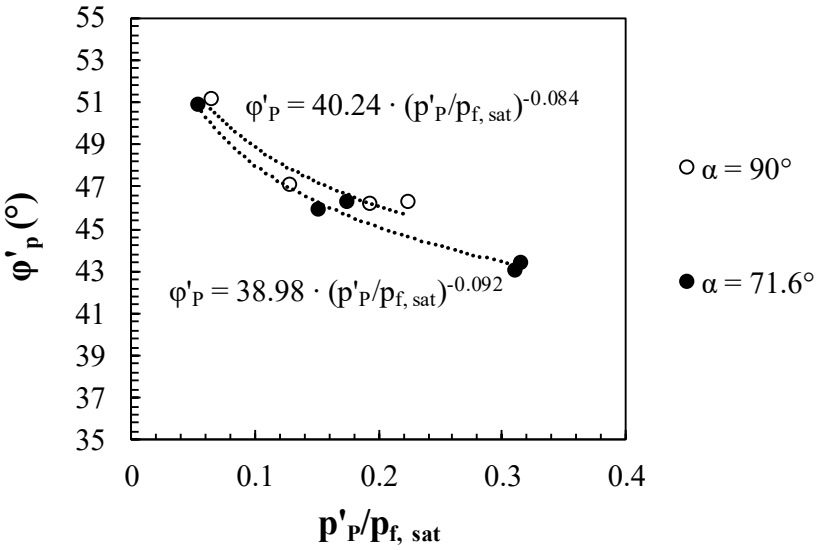

Figure 6.18 Variation of peak friction angle against stress ratio for saturated specimens prepared with the Fine grading curve: effect of α

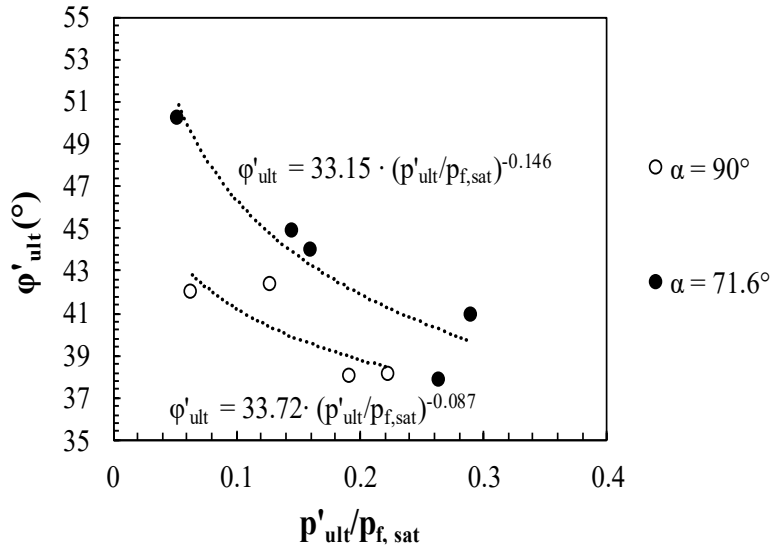

Figure 6.19 Variation of φ'ult against stress ratio for saturated specimens prepared with the Fine grading curve: effect of α

Several studies have been conducted investigating the relationship between the shear strength and the degree of saturation in granular soils (Bishop et al., 1960; Escario et al., 1986; Fredlund et al., 1995). Wetting tests performed during triaxial testing on large diameter specimens (Naylor et al., 1986; Terzaghi, 1960; Veiga Pinto, 1983) also identified the reduction of strength of flooded samples if compared with the "dry" ones.

The dependence of the strength on the degree of saturation was not directly attributed to the water content but rather to its influence on the fabric of the compacted soil. Lower degrees of saturation may justify the presence of aggregates of small soil particles causing the soil to behave as a coarser one (Alonso and Cardoso, 2010).

Figure 6.20 and Figure 6.21 show the peak and the ultimate friction angles versus the stress ratio $p'/p_{f,sat}$ for different grading curves of the Coreno rockfill. The degree of saturation has opposing effects on the peak friction angles of the two soils (Figure 6.20). Instead, it is clear in Figure 6.21 that with increasing S_r the ultimate friction angle decreases, as expected, due to the water action on particle breakage.

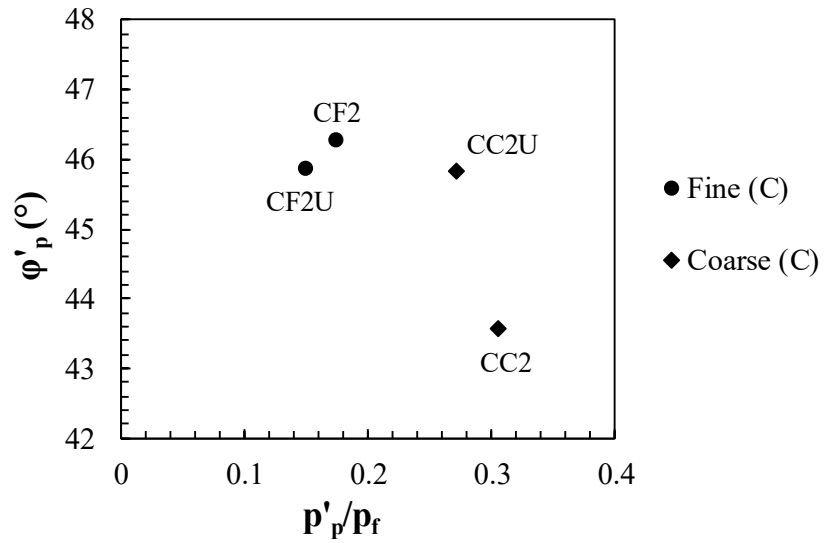

Figure 6.20 Variation of peak friction angle against stress ratio: effect of the degree of saturation

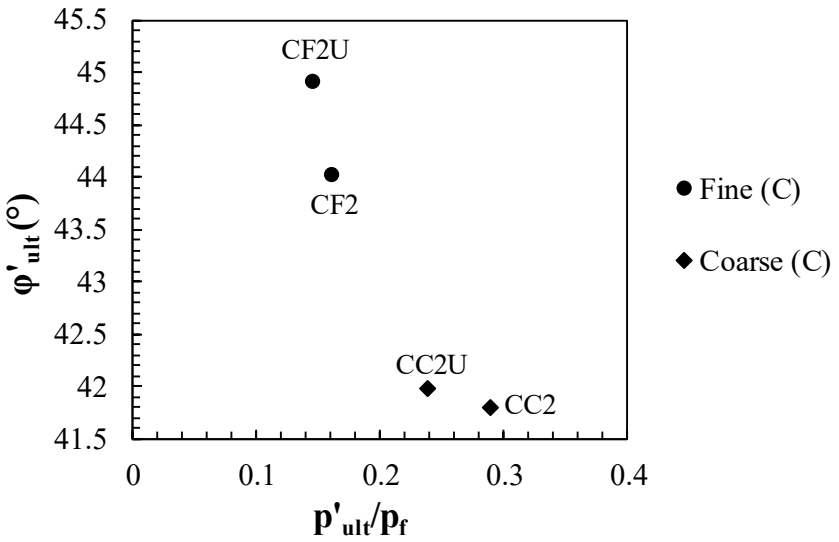

Figure 6.21 Variation of ultimate friction angle against stress ratio: effect of the degree of saturation

The effect of particle size on breakage was clearly evident in a series of triaxial tests carried out by Marsal (1967) and Marachi et al. (1969) on specimens of different sizes. For instance, Marachi et al. (1969) found that the reduction observed in the value of the internal friction angle can be closely related to the grain breakage intensity, particularly developed in large specimens. They showed that the amount of particle breakage increases and the maximum shear strength φ_p decreases when the particle size increases.

Similar relationship has been obtained for Redisole rockfill, both in term of maximum and ultimate friction angles, as shown in Figure 6.22 and Figure 6.23. Comparing the Redisole Parallel (open squares, D_r=100%) with the Redisole Coarse (open diamonds, Dr=70%), it can be argued that the increase in initial relative density increases soil shear strength.

Another interesting result of the investigation here presented is that all three the families of soils prepared with Coreno rockfill having different grain size distribution, show a single relation between the friction angle and the breakage factor when specimens having the same initial density are considered (Figure 6.22 and Figure 6.23). It is also interesting to note that data from tests on Coarse soil of Redisole material follows the same regression of Coreno rockfill. This confirm that within a given family of similar materials with the same initial density, the correspondence between the amount of grain breakage and internal friction (i.e. the maximum internal friction mobilised) is unique, regardless of their characteristic size (Marachi et al., 1969).

The φ'-B_g relationship is a power law for both the materials tested. Furthermore, particle breakage seems to play a fundamental role on both peak and ultimate conditions, as widely recognized in the literature.

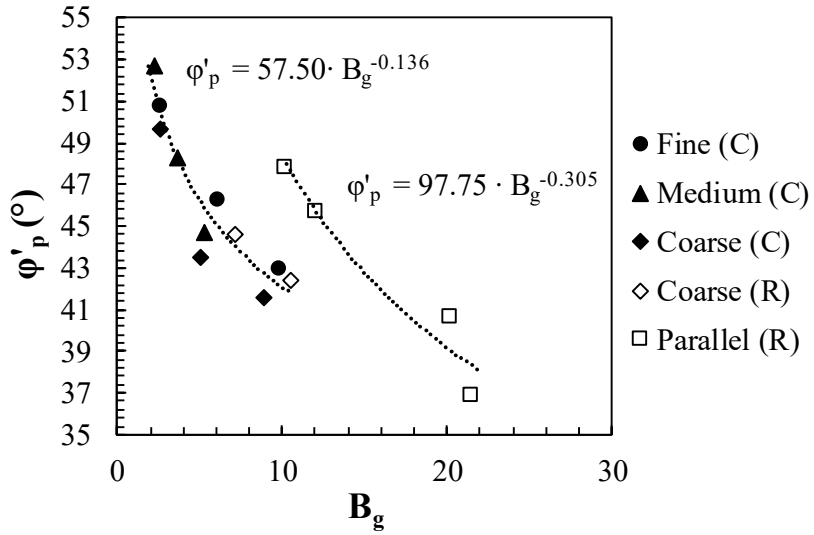

Figure 6.22 Variation of peak friction angle against breakage factor for saturated specimens sheared at constant σ'c

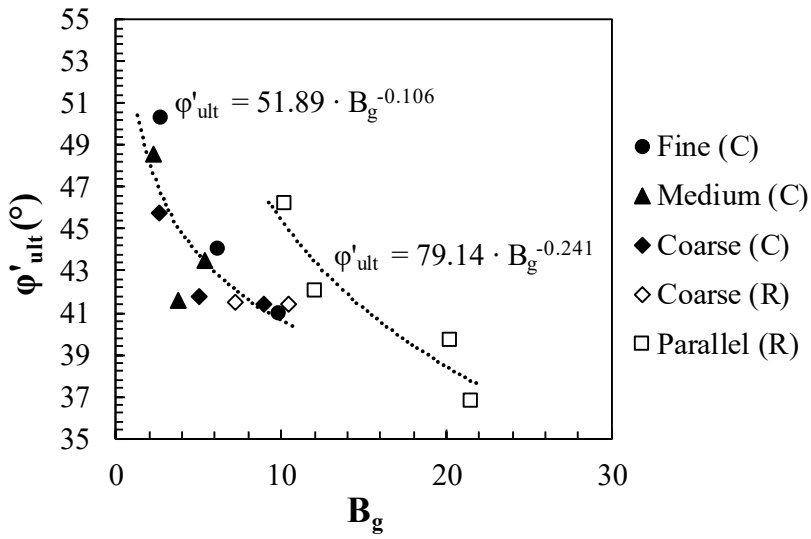

Figure 6.23 Variation ultimate friction angle against breakage factor for saturated specimens sheared at constant σ'c

6.4 The dilatancy of rockfill

Considerations of dilatancy in a triaxial test give a better feel for the way in which the soil is responding to a particular state of stress. The dilatancy of granular soils has received a great deal of attention, and some agreements about the topic have been reached (Rowe, 1962; Bolton, 1986).

The stress-dilatancy equation based on energy principles was presented by Rowe (1962), which is commonly used as a flow rule. Rowe's stress-dilatancy relation for triaxial compression is the following (Wood, 1991):

$$\frac{\delta\varepsilon_v}{\delta\varepsilon_s} = \frac{9(M-\eta)}{9+3M-2M\eta} \tag{6.4}$$

with the critical state parameter M determined as follows:

$$M = \frac{6 \cdot sen\varphi'_{cv}}{3 - sen\varphi'_{cv}} \quad (6.5)$$

with φ'_{cv} critical state friction angle.

In Equation 6.4 $\varepsilon_v = \varepsilon_1 + 2\varepsilon_3$ is the volumetric strain while $\varepsilon_s = 2/3 \cdot (\varepsilon_1 - \varepsilon_3)$ is the shear strain.

From the stress-dilatancy relation (Eq. 6.4) it is clear that at the critical state $\delta\varepsilon_v/\delta\varepsilon_s=0$ and therefore $q/p'=\eta=M$. Dense sands usually show a peak strength ($\eta>M$), represented by point B in Figure 6.24, before reaching the ultimate critical state ($\eta=M$), represented by point C. However, the stress ratio passes through the value $\eta=M$ in an early stage of the test (point A). Tatsuoka & Ishihara (1974) and Luong (1979) show that the stress ratio in point A (η_{mc}, where "mc" stands for maximum contraction), at which the sand deforms instantaneously at constant volume, plays an important role in governing the behaviour of the sand. Luong (1979) calls this stress ratio "characteristic stress ratio" while Tatsuoka and Ishihara (1974) call it "phase transformation stress ratio". Luong (1979) suggests determining the critical state friction angle in point A (φ'_{mc}) rather than in point C (φ'_{cv}) since the critical state condition may not be always reached in triaxial apparatus.

This is the case of most of the experimental tests here discussed. For these tests the critical state friction angle φ'_{cv} was calculated referring to point C of Figure 6.24, independently of the value of $\delta\varepsilon_v/\delta\varepsilon_s$. For example, with reference to CF4 and CF7P tests in which critical state conditions have not been and have been reached

respectively, the points A, B and C are highlighted both in the η:ε_a and in the ε_v:ε_a planes (Figure 6.25).

Furthermore, it is known from the literature that φ'_{cv} is unique for a given material regardless the void index and the stress path. However, as recognized from Flora et Modoni (1998), if grain breakage happens the final gradation is finer than the original one and so φ'_{cv} may be not the same for all the tests.

Figures from 6.26 to 6.29 show the values of characteristic (φ'_{mc}), peak (φ'_{p}, point B in Figure 6.24) and critical friction (φ'_{cv}) angles for some of the tests carried out on Coreno and Redisole materials. For each grading curve the data reported refer to specimens prepared with the same initial void index and shared at constant σ'_c. All the figures referring to Coreno show that φ'_{mc} slightly increases and φ'_{p} decreases with the confining stress σ'_c, according to Flora and Modoni (1998). On the contrary, both φ'_{mc} and φ'_{p} relative to the Parallel soil (Figure 6.29) decrease with σ'_c.

The critical state friction angle is a limit toward the φ'_{mc} and the φ'_{p} curves tend as σ'_c increases. The difference between the two curves represents the contribution of the dilatancy that vanish when critical state is reached.

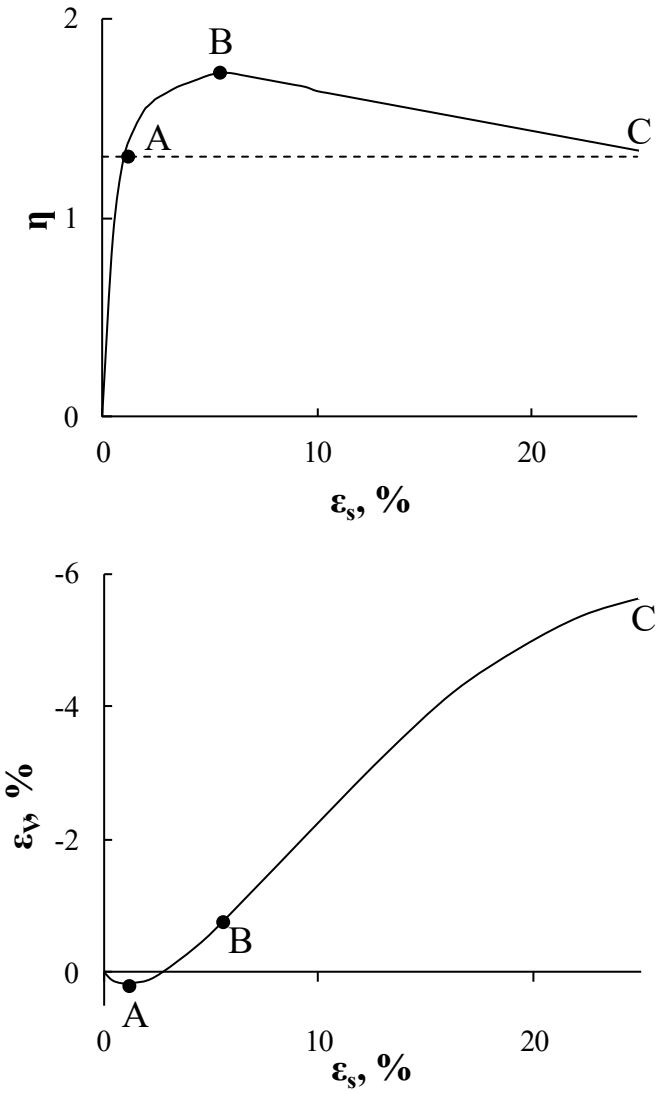

Figure 6.24 Conventional drained triaxial compression test on dense Fontainebleau sand: a) stress ratio η and triaxial shear strain ε_s; b) volumetric strain ε_v and triaxial shear strain ε_s (data from Luong, 1979)

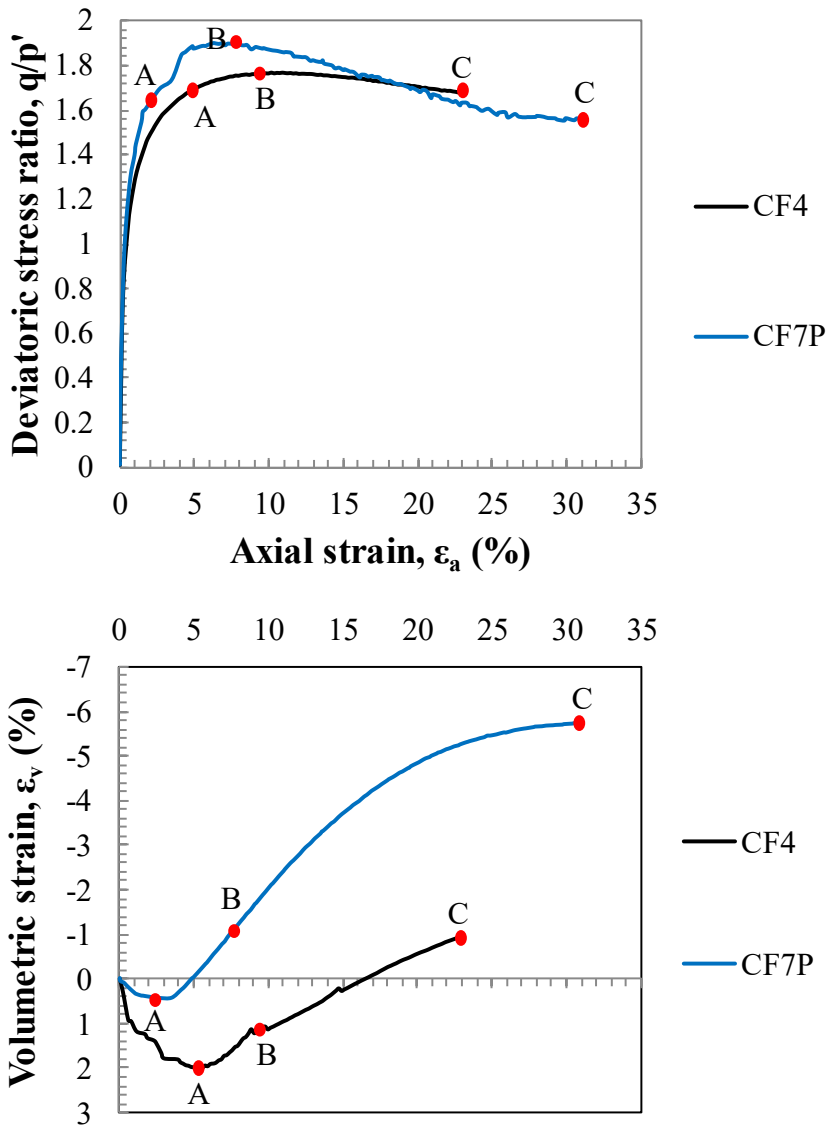

Figure 6.25 Conventional drained triaxial tests on Fine grading curve (Coreno)

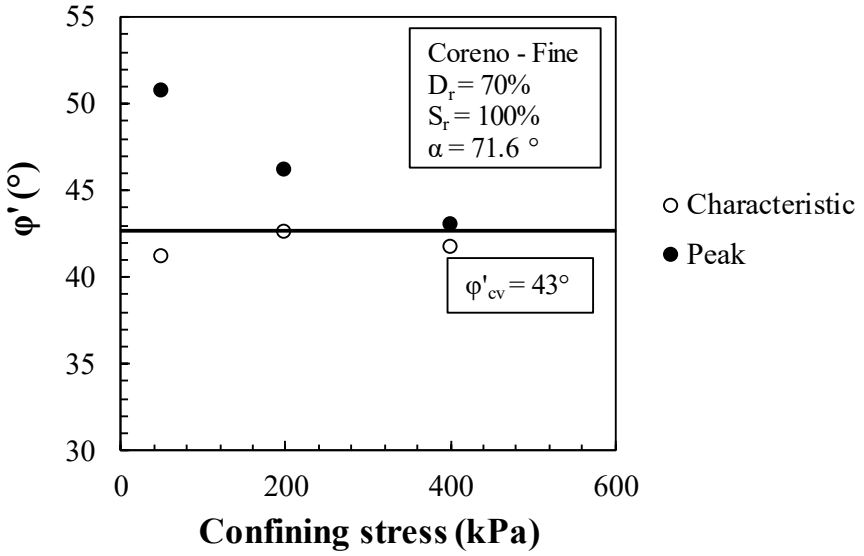

Figure 6.26 Characteristic, critical and peak friction angles for Fine soil (Coreno)

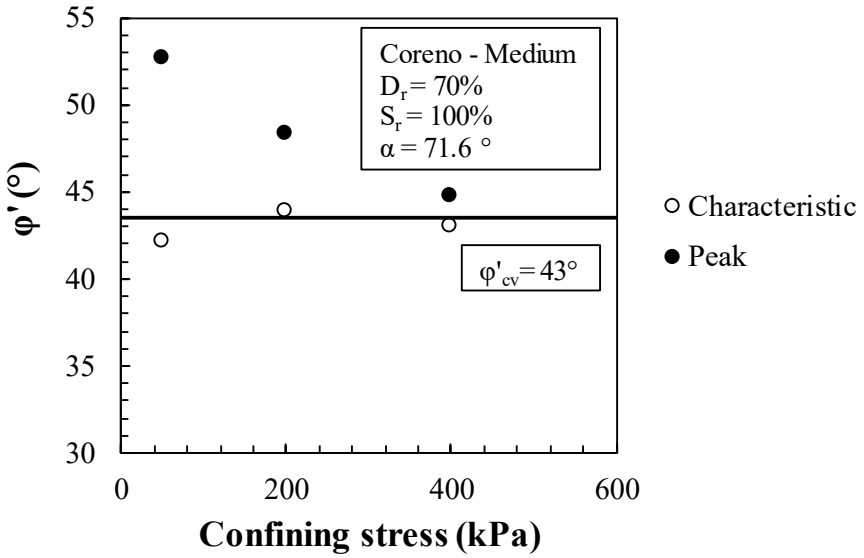

Figure 6.27 Characteristic, critical and peak friction angles for Medium soil (Coreno)

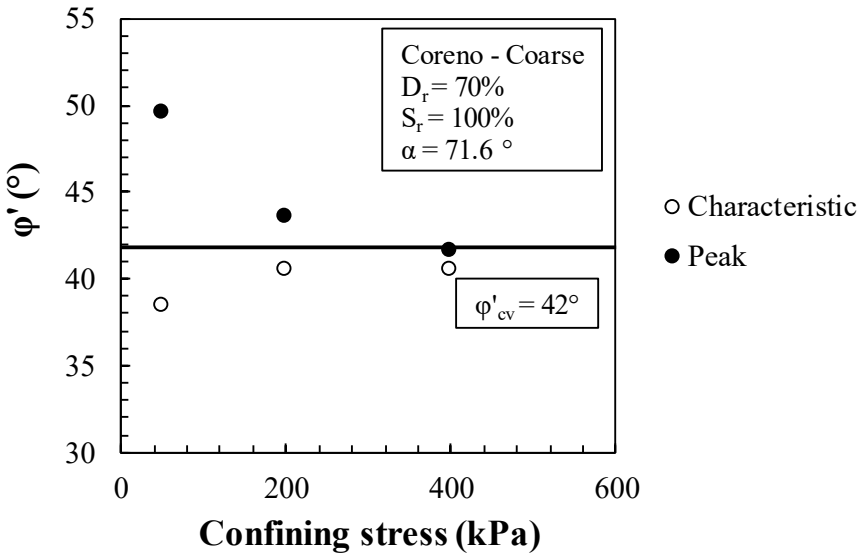

Figure 6.28 Characteristic, critical and peak friction angles for Coarse limestone soil (Coreno)

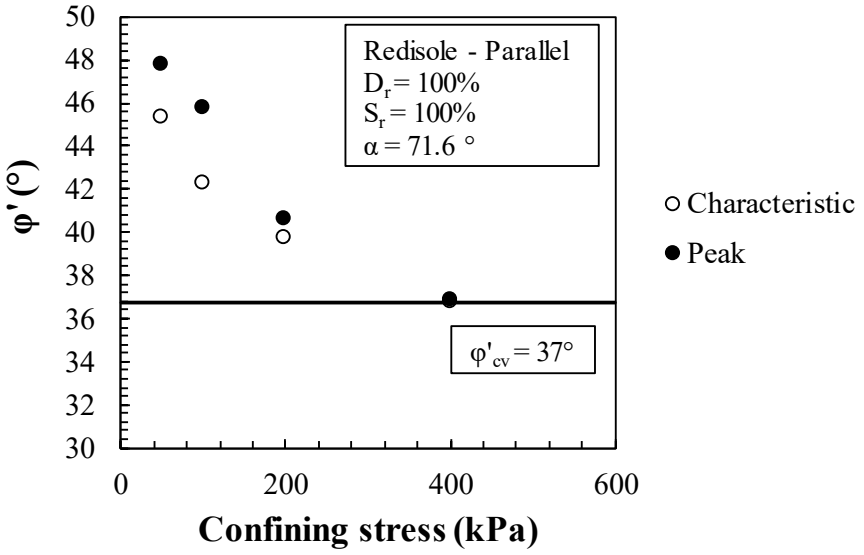

Figure 6.29 Characteristic, critical and peak friction angles for Parallel soil (Redisole)

Therefore, the angle at maximum contraction φ'_{mc} and constant volume friction angle φ'_{cv} cannot be considered coincident for the dense materials tested.

The dilation angle ψ can be calculated as the difference between φ'_{p} and φ'_{mc}. The results obtained with all the materials and grain size distributions tested are presented in Figure 6.30. It can be observed that ψ decreases as the confining stress increase tending to zero for medium-low stress levels. Lee and Seed (1967) demonstrated that, under high pressure, the shear strength of sand increased while the dilatancy decreased. They attributed this observation to particle crushing and rearrangement on shearing.

The curves are expected to show different trend for different materials. As a matter of fact, the analysis of the experimental data indicates a clear difference between the slopes of the logarithmic regressions relating to the Coreno and Redisole rockfills and a strong similarity between the Fine, Medium and Coarse curves relating to the limestone material.

It appears that specimens prepared with different grain size distributions, but the same material and the same initial relative density exhibit similar dilatancy. This can be linked to the high particle tensile strength and the consequent little grain breakage which reduces the effect of the grain size on the mechanical behaviour of the material. Despite an initial relative density of 100 %, Redisole rockfill has low values of the dilation angle.

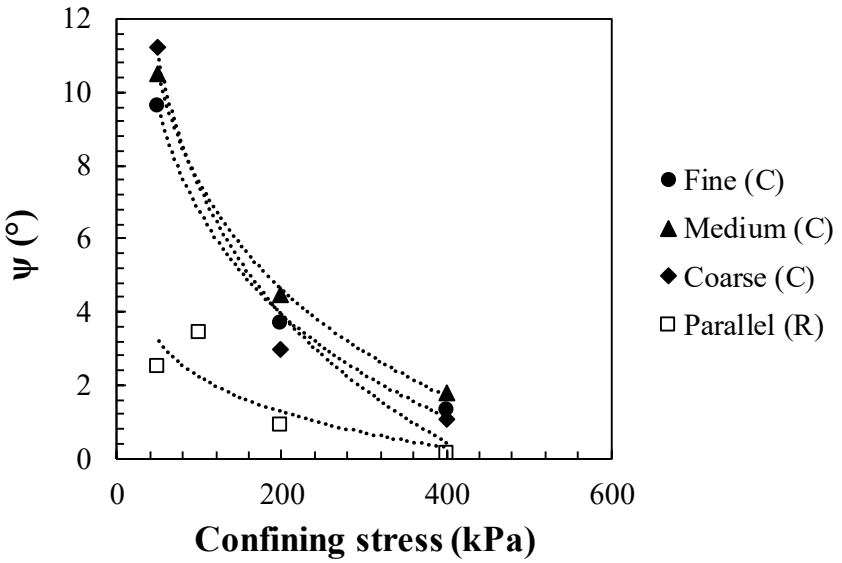

Figure 6.30 Relationships between dilation angle and confining stress for Coreno and Redisole rockfills

6.5 Final remarks

The edges and particle breakage on loading has always been a concern for researchers and engineers, and especially in the construction and maintenance of high rockfill dams, roads and rail tracks.

The study of particle breakage and its effects on the shear strength and compressibility of tested rockfills under monotonic triaxial loading improve the understanding of their mechanical behaviour.

The index used to quantify the breakage of particles is that of Marsal (1967), B_g.

The material of the Redisole dam, which has a low particle tensile strength, showed a greater breakage compared to the limestone

material. With reference to the latter, the Fine and Coarse curves showed very similar B_g indexes while the well-graded Medium soil exhibited less grain breakage than the other two. Thus, under the same test conditions, the soil uniformity seems to influence the grain breakage more than the grain size. This result was confirmed by the micromechanical analysis performed.

Laboratory investigations in large and small oedometer have been conducted to determine the relationship between B_g and the compressibility index C_c and its dependence on the degree of saturation and the grain size distributions. It emerged that the effect of the degree of saturation on B_g and C_c could be significant depending on the material properties and its sensitivity to the presence of water.

The effects of the degree of saturation, the grain size distribution, the stress path and the previous loading history on the particle breakage exhibited during shearing and on shear strength were presented and discussed. In addition, the role of the particle tensile strength on the peak and ultimate friction angles has been highlighted.

The triaxial test campaign showed that the parallel gradation technique is more reliable than the scalping technique for reducing the grain size. Indeed, parallel grain size distributions exhibited the same behaviour in terms of particle breakage and friction angles.

Finally, the contribution of dilatancy has been presented by means of the variation of the peak and maximum contraction angles with the confining stress. In terms of dilation angle, it emerged that

regardless of the grain size distribution, the limestone material has a unique dilation angle versus confining stress relationship.

6.6 References

Alonso E. E., Cardoso R. (2010). *Behavior of materials for earth and rockfill dams: Perspective from unsaturated soil mechanics*. Front. Archit. Civ. Eng. China, 4(1), 1-39.

Baladi G. Y., Wu T. T. H. (1988). *Interpretation of Triaxial Test Results of Cohesionless Soils: A New Model*. In Advanced Triaxial Testing of Soil and Rock. ASTM International, West Conshohocken, PA.

Bishop A. W. (1948). *A new sampling tool for use in cohesionless sands below groundwater level*. Géotechnique,1, 125-131.

Bishop A. W. (1966). *The strength of soils as engineering materials.* Géotechnique, 16(2), 91-128.

Bishop A. W., Alpan I., Blight G. E., Donald I. B. (1960). *Factors controlling the strength of partly saturated cohesive soils*. Conference on Strength of Cohesive Soils, Boulder, Colorado, USA. Arizona, ASCE, 503-532.

Bolton M. D. (1986). *The strength and dilatancy of sands*. Géotechnique, 36(1), 65-78.

Escario V., Saez J. (1986). *The shear strength of partially saturated soils*. Géotechnique, 36(3), 453-456.

Flora A. (1995). *Caratterizzazione geotecnica e modellazione dei materiali a grana grossa*. PhD Thesis. University of Napoli Federico II.

Flora A., Modoni G. (1998). *Complex testing and simple analysis of coarse grained materials*. Proc. of a Workshop in Napoli on

Prediction and Performance in Geotechnical Engineering, Hevelius edizioni, Benevento.

Fredlund D. G., Xing A., Fredlund M. D., Barbour S. L. (1995). *The relationship of the unsaturated soil shear strength to the soil water characteristic curve*. Canadian Geotechnical Journal, 33: 440-448.

Hagerty M. M., Hite D. R., Ullrich C. R., Hagerty D. J. (1993). *One dimensional high pressure compression of granular media*. Journal of Geotechnical Engineering, 119(1), 1-18.

Hardin B. O. (1985). *Crushing of soil particles*. Journal of Geotechnical Engineering, ASCE, 111(10), 1177-1192.

Indraratna B., Wijewardena L. S. S., Balasubramaniam A. S. (1993). *Large-scale triaxial testing of greywacke rockfill*. Géotechnique, 43(1), 37-51.

Lade P. V., Yamamuro J. A., Bopp P. A. (1996). *Significance of particle crushing in granular materials*. Journal of Geotechnical Engineering, ASCE, 122(4), 309-316.

Lee K. L., Farhoomand I. (1967). *Compressibility and crushing of granular soil in anisotropic triaxial compression*. Canadian Geotechnical Journal, 4(1), 68-86.

Lee K. L., Seed H. B. (1967). *Drained strength characteristics of sand*. Journal of the Soil Mechanics and Foundations Divisions, ASCE, 93, No. SM6, 117–141.

Lewis J. G. (1956). *Shear strength of rockfill*. Proceedings of 2nd Australia-New Zealand Conference on Soil Mechanics and Foundation Engineering, 50-52.

Luong M. P. (1979). *Les phénomènes cycliques dans les sables*. Journées de rhéologie: cycles dans les sols-rupture-instabilités, Publication 2. Vaulx-en-Velin: Ecole Nationale des Travaux Publics d'Etat.

Marachi N. D., Chan C. K., Seed H. B., Duncan J. M. (1969). *Strength and deformation characteristics of rockfill materials.* Department of Civil Engineering, Report No. TE-69-5. University of California.

Marsal R. J. (1967). *Large scale testing of rockfill materials*. Journal of the Soil Mechanics and Foundation Division, ASCE, 93(2), 27-43.

Nakata Y., Hyodo M., Hyde A. F. L., Kato Y., Murata H. (2001). *Microscopic particle crushing of sand subjected to high pressure one-dimensional compression*. Soils and Foundations, 41(1), 69-82.

Naylor D. J., Maranha das Neves E., Mattar D., Veiga Pinto A. A. (1986). *Prediction of construction performance of Beliche Dam*. Géotechnique, 36(3), 359-376.

Oldecop L. A., Alonso E. E. (2001). *A model for rockfill compressibility*. Géotechnique, 51, 127-139.

Rowe P. W. (1962). *The stress-dilatancy relation for static equilibrium of an assembly of particles in contact*. Proceedings of the Royal Society of London, 269, 500-527.

Terzaghi K. (1960). *Discussion on salt springs and lower bear riverdams*. Transactions of ASCE, 125(2), 139-148.

Vallerga B., Seed H., Monismith C., Cooper R. (1957). *Effect of Shape, Size, and Surface Roughness of Aggregate Particles on the Strength of Granular Materials.* Road and Paving Materials, West Conshohocken, PA: ASTM International, 63-76.

Veiga Pinto A. A. (1983). *Prediction of the structural behavior of rockfill dams*. Dissertation of the Doctoral Degree. Lisbon, Portugal, National Laboratory of Civil Engineering, Portugal.

Vesic A. S., Clough G. W. (1968). *Behavior of granular materials under high stresses*. Journal of the Soil Mechanics and Foundations Division, 94(3), 661-688.

Wood D. M. (1991). *Soil Behaviour and Critical State Soil Mechanics*. Cambridge University Press, ISBN: 9781139878272.

CHAPTER 7

UNIFIED FRAMEWORK

7.1 Introduction

As highlighted in the previous chapters, the particle breakage influences the overall mechanical behaviour of rockfill. If grains are broken into smaller particles due to the application of external forces or the water action, the physical and mechanical properties of coarse-grained material shows significant changes. Therefore, the original engineering properties used in the design of a structure is going to change during its engineering life, affecting the stability of the structure. Hence, an understanding of the way granular materials crush during compression, shearing and wetting is of considerable importance in engineering practice.

In literature and by the experimental data here reported it has been highlighted that grain crushing is influenced by both intrinsic (particle tensile strength, angularity) and state parameters (induced stress level, void index, moisture content), as shown by Lee and Farhoomand (1967), Hardin (1985), Hagerty et al. (1993), Lade et al. (1996), McDowell and Bolton (1998), Coop et al. (2004), Tarantino and Hyde (2005), Wood and Maeda (2008).

During a generic stress path if the grains break, fine material is produced and the grain size distribution curve becomes less steep. Furthermore, on crushing the soil becomes less permeable and more resistant to crushing. Some authors (Luzzani and Coop, 2002; Coop

et al., 2004) have experimentally verified that grain breakage stops due to very high deformation states, which are difficult to reach with traditional triaxial equipment.

The particle breakage has a remarkable effect on the critical state, i.e. a state of constant volume and constant shear stress at a constant mean effective stress (Roscoe et al, 1958). At high stress levels, however, particles undergo breakage that results in a continuous change of soil gradation. The breakage causes additional compressibility and volume change, resulting in uncertainty in defining the critical state condition.

Hence, it is expected that for the soil to reach the critical state, a stable gradation should be reached for a specific stress level (Luzzani and Coop, 2002). This implies that such gradation would be more stable than the original one and can sustain a higher level of stress without further breakage of soil grains.

Many constitutive models were proposed to capture the stress-strain behaviour of rockfill material but, usually, cannot take into account the influence of particle breakage on the stress-strain behaviours. However, Wood and Maeda (2008) thought that the constitutive model could incorporate the evolution of the particle size distribution as a model state parameter. This state parameter is similar to that proposed by Einav (2007). A series of critical state lines (CSLs) resulting from particle crushing compose a critical state surface (Wood and Maeda, 2008). Furthermore, the large-scale triaxial experimental results of rockfill material (Liu et al., 2005; Liu et al., 2011) indicate that due to particle breakage the slope of

CSL in p-q plane is nonlinear and dependent on the confining stress. Daouadji et al. (2001) suggested that the change in the grain size distribution caused by the breakage imposes a downward shift on the CSL. Wood and Maeda (2008) suggested that the effect of particle breakage on the CSL position in the e-log(p') space is essentially a parallel downward shift as a function of a grading state index.

Flora & Lirer (2009) - personal communication - proposed a simple model based on the concept that the CSL progressively shifts downward as breakage continuously affects the soil gradation with increasing stress. This model will be applied to the tested materials in the present chapter.

7.2 A particle breakage model for rockfill material

It is widely known that particle breakage occurred in specimens subjected to triaxial stress conditions is due to both the isotropic and the deviatoric rate of the load. While the spherical component of the load essentially involves the breaking of the edges, the deviatoric component involves the splitting of the grains.

The work proposed by Flora & Lirer (2009) is based on the fact that the particle breakage is mainly due to the deviatoric stress. In this hypothesis, the authors suggest that in the q-p' plane there are elliptic curves with equal value of the particle crushing, centred in the origin of the axes and with a major axis (a) larger than the minor one (b), as shown in Figure 7.1. The greater the major axis (a) to the

minor one (b) ratio is, the smaller the influence of p' on particle breakage. Flora & Lirer (2009) adopted two different values of a/b (i.e. 1.25 and 10) and verified that the results of applying the model seem to be independent of the ellipse eccentricity. The size of the axes of the ellipse grows as the particle breakage increases but their ratio was considered constant in the model.

Having compared the various alternative methods, the particle breakage index B_g, proposed by Marsal (1967) has been adopted in this study in order to quantify the degradation of rockfills. In particular, it was preferred to use the dimensionless parameter $B_{gn}=B_g/(1+e_c)$ with e_c the void index at the end of the consolidation phase, in order to take into account the relative density of the specimens.

Therefore, considering a generic specimen, it is possible to obtain the same breakage factor by following different stress paths (e.g., OA'D'- OA'D'' in Figure 7.1) that end on the same elliptical curve. During the stress path the specimen undergoes a continuous evolution of the grain size distribution.

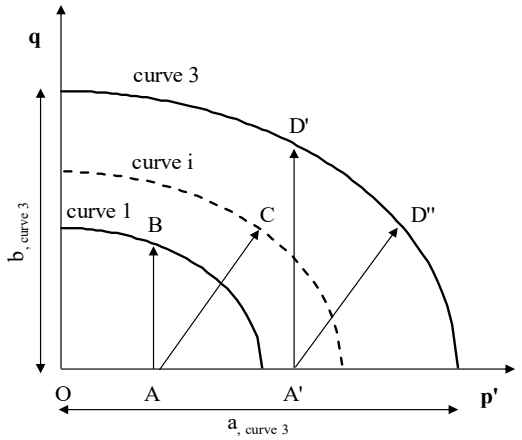

Figure 7.1 Place of points with the same level of grain crushing (Flora & Lirer – personal communication, 2009)

According to Russell e Khalili (2004) and Wood e Maeda (2008), Flora & Lirer (2009) hypothesized the existence of different critical state lines defined by intercept Γ and slope λ function of B_{gn}, as follows:

$$\nu = \Gamma(B_{gn}) - \lambda(B_{gn}) lnp' \tag{7.1}$$

with ν specific volume.

As suggested by Wood and Maeda (2008), the authors assumed that the particle breakage causes a downward shift of the critical state line (λ=cost) from the initial position, expressed by the following equation:

$$\nu = \Gamma_0 - \lambda\, lnp' \tag{7.2}$$

to the limit critical state line with the following equation:

$$\nu = \Gamma_{min} - \lambda\, lnp' \tag{7.3}$$

Therefore, the intercept Γ of the generic CSL varies as follows:

$$\Gamma_{min} < \Gamma(B_{gn}) < \Gamma_0 \quad (7.4)$$

The points belonging to the same ellipse in the q-p' plane will have the same end-point breakage factor and therefore have to belong to the same critical state line. In this context, the law of degradation of the initial critical state line (Eq. 7.2) as a function of B_{gn}, adopted by the authors, is of the type:

$$\Gamma(B_{gn}) = \Gamma_{min} + (\Gamma_0 - \Gamma_{min}) \cdot \frac{1}{1+B_{gn}{}^{\alpha}} \quad (7.5)$$

Γ_0 and λ are chosen starting from the isotropic compression curve of the loose specimen, taken as the limit curve in the e-p' plane. As for the other two parameters, Γ_{min} and α the authors suggest the use of a best fitting procedure.

7.3 Application of the model to the experimental data

The hypothesis of the model proposed by Flora & Lirer (2009) according to which the splitting of the grains is mainly due to the deviatoric stress has been confirmed by the results shown in the paragraph 6.2 and in Table 7.1. It can be observed that the values of B_{gn} are very close for the same values of q_{ult} and higher p'_{ult} differences. Therefore, different stress paths lead to the same position of the end points in terms of particle breakage.

Table 7.1 Experimental results from drained triaxial tests on Fine and Medium grading curves

Test ID	Grain size distribution	p'_{ult} MPa	q_{ult} MPa	B_g %	B_{gn} %
CF0.5	Fine	0.16	0.34	2.67	1.60
CF2P		0.20	0.35	2.54	1.53
CF6P		0.60	0.93	7.80	4.77
CF7P		0.70	1.09	7.42	4.59
CM2	Medium	0.48	0.81	3.73	2.55
CM4P		0.40	0.78	3.81	2.69

Knowing the triaxial tests results on the material tested, it was possible to find the B_{gn}-a relationship, function of the intrinsic and state properties of the material.

Two different values of a/b have been considered, i.e. 1.25 and 10. The regressions obtained for all the materials tested and the two ratios analysed are shown in Figures 7.2 and 7.3. All data refer to tests on specimens saturated from the beginning of the tests, consolidated and directly sheared.

Redisole data follow a logarithmic law while for Coreno rockfill data follow a power law. However, two different regressions can be considered for Coreno: one for the Medium grading curve and one for the Fine-Coarse grading curves. The full points lie close together for small B_{gn} values and then increase with different trends. The regressions found can be used to determine the B_{gn} values directly from the applied stresses. This is useful when it is not possible to do the sieve analysis.

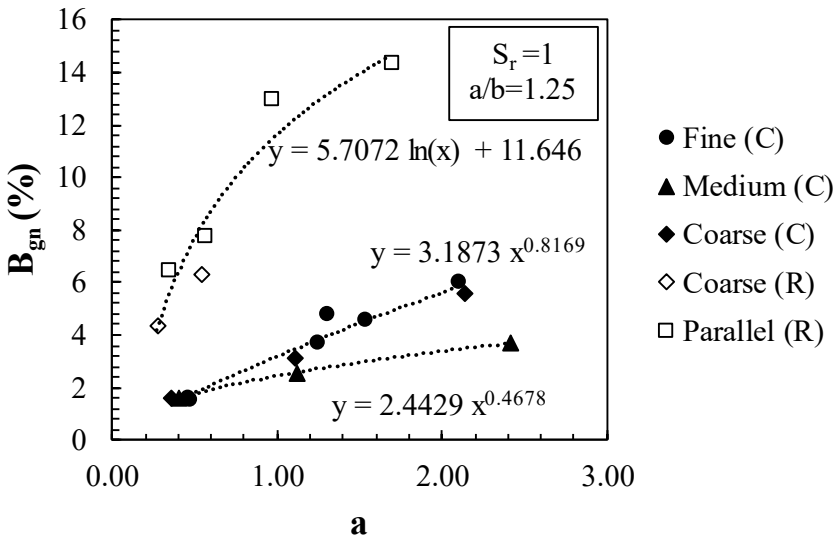

Figure 7.2 B_{gn} versus ellipse major axis a for a/b = 1.25

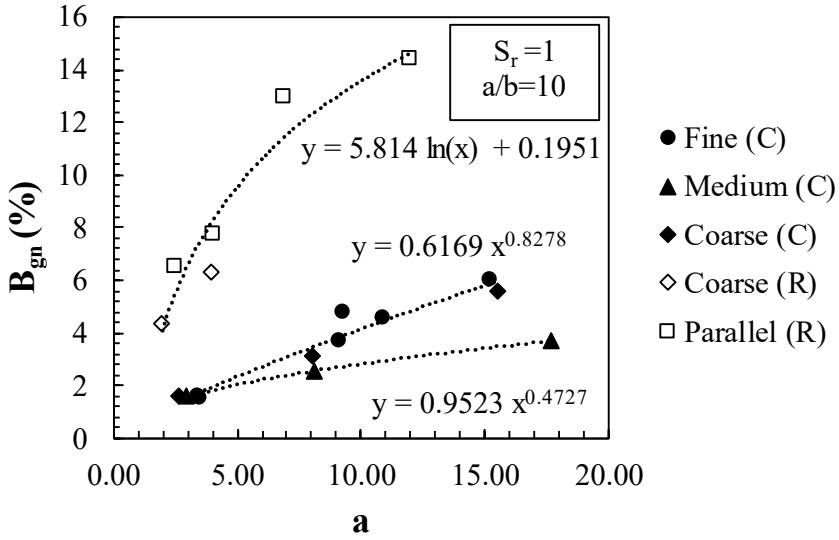

Figure 7.3 B_{gn} versus ellipse major axis a for a/b = 10

Once the axis dimensions a and b are known, the construction of the elliptic curves at equal B_{gn} is immediate: the ellipses related to the Fine grading curve are shown in Figures 7.4 and 7.5 as an example.

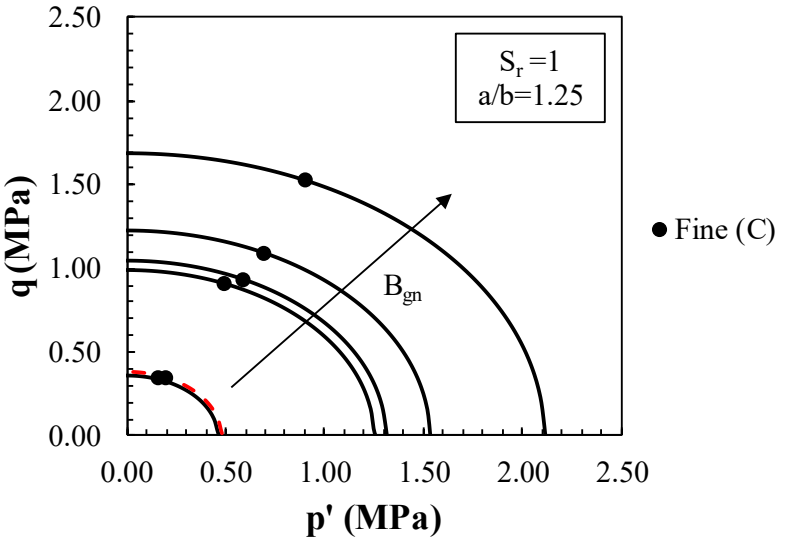

Figure 7.4 Ellipses with a/b= 1.25 for triaxial tests on the Fine soil

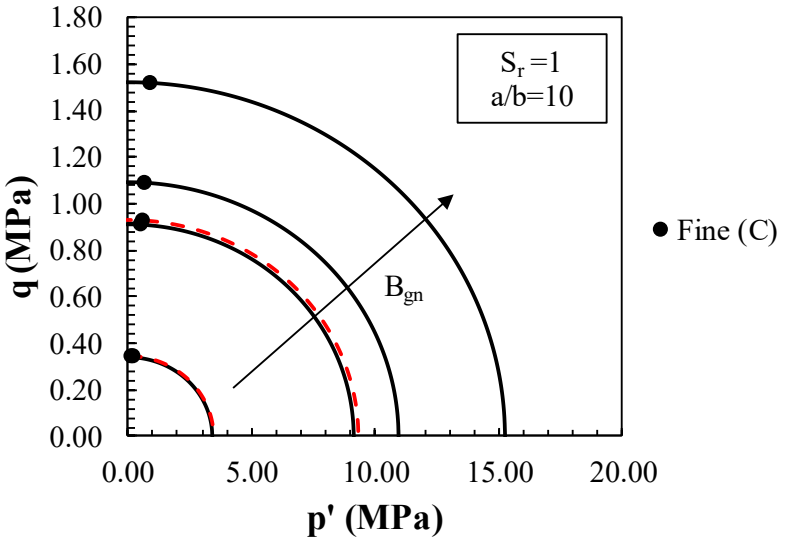

Figure 7.5 Ellipses with a/b= 10 for triaxial tests on the Fine soil

The parameters of the model can be determined from the Fine soil data. With reference to these, the slope of the critical state lines was not determined from the isotropic compression curve of the loose specimen as proposed by Flora & Lirer (2009).

As shown in Figure 5.4 and Table 7.1, during the CF6P and CF7P tests critical state conditions and the same level of grain crushing (i.e. B_{gn}) were reached. Consequently, it is appropriate to assume that the two relative points lie on the same CSL in the e-p' plane (Figure 7.6).

At this point it is possible to consider several CSLs, each passing through the point (lnp', e_{ult}) and all having the same slope $\lambda = 0.19$. In order to determine the intercept Γ of each CSL activated during all the tests, the Equation 7.5 has been used.

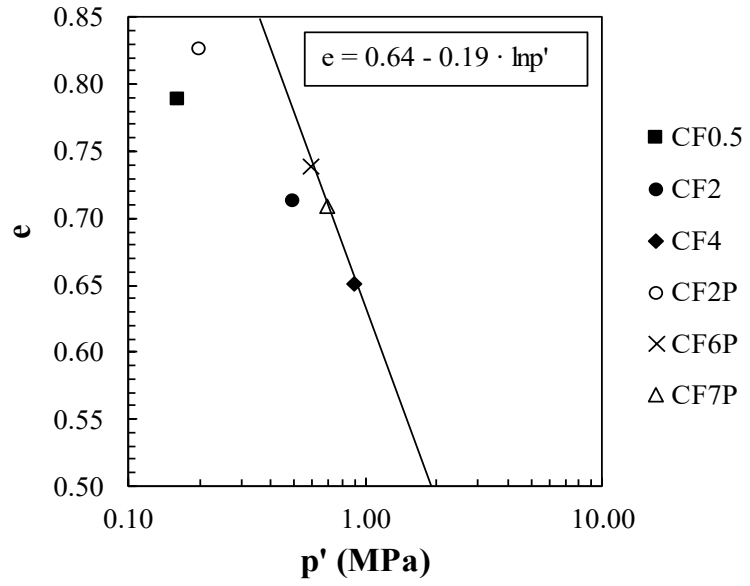

Figure 7.6 Critical state line for Fine soil

To obtain the parameters of the degradation law (Eq. 7.5), it is believed that it is not possible to determine Γ_0 by a best fitting procedure, as suggested by Flora & Lirer (2009). Instead, it was preferred to obtain Γ_0 as well as Γ_{min} by using the maximum and minimum void indexes respectively, reported in Table 4.2.

The value of α (Eq. 7.5) determined by means of a best fitting procedure is 1.15. Once α, B_{gn} and the limit void indexes are known, the intercept Γ of each CSL passing from triaxial test point is immediately determined by using Eq. 7.5. The trend of Γ as a function of B_{gn} is shown in Figure 7.7.

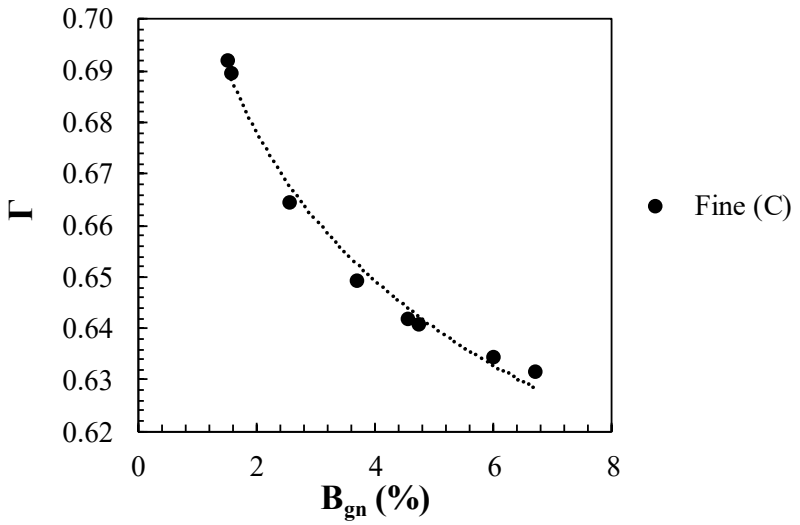

Figure 7.7 Intercept Γ versus B_{gn} for the saturated specimens of Coreno Fine rockfill

With the values of Γ reported in Figure 7.7 and the constant slope $\lambda = 0.19$, it is possible to determine the values of the void indexes in critical state conditions and the positions of the activated CSLs even

for tests that did not reach this condition. This is the power of the adopted model.

Furthermore, since the relationship B_{gn}-a is unique for Fine and Coarse soils (as shown in Figures 7.2 and 7.3), it is appropriate to hypothesize that the model parameters (λ and α) obtained for Fine soil are equally valid for Coarse grading curve of Coreno rockfill. Instead, Γ_0 and Γ_{min} have been obtained with the maximum and minimum void indexes respectively, reported in Table 4.2 for the Coarse grading curve. These values are very close to that of the Coreno Fine soil. The Γ-B_{gn} relationship obtained for the saturated specimens of Coreno Coarse rockfill is reported in Figure 7.8.

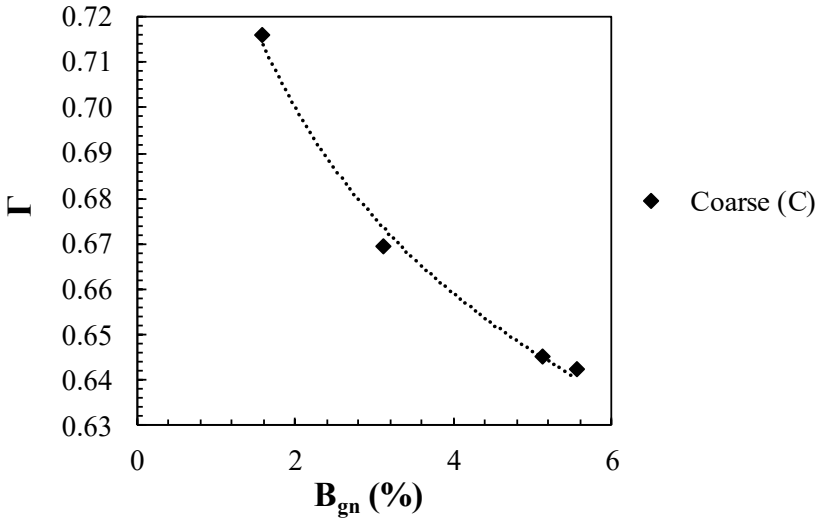

Figure 7.8 Intercept of the CSLs versus B_{gn} for the saturated specimens of Coreno Coarse rockfill

With reference to the Medium soil, using the same procedure described in this paragraph, the following parameters were obtained

which are useful for adopting the degradation law proposed by Flora & Lirer (2009): λ = 0.14 and α = 2.16. So, it can be argued that the limestone material has a unique slope of the CSLs regardless of the grain size distribution. The results in terms of Γ- B_{gn} relationship for the Medium grading curve are reported in Figure 7.9.

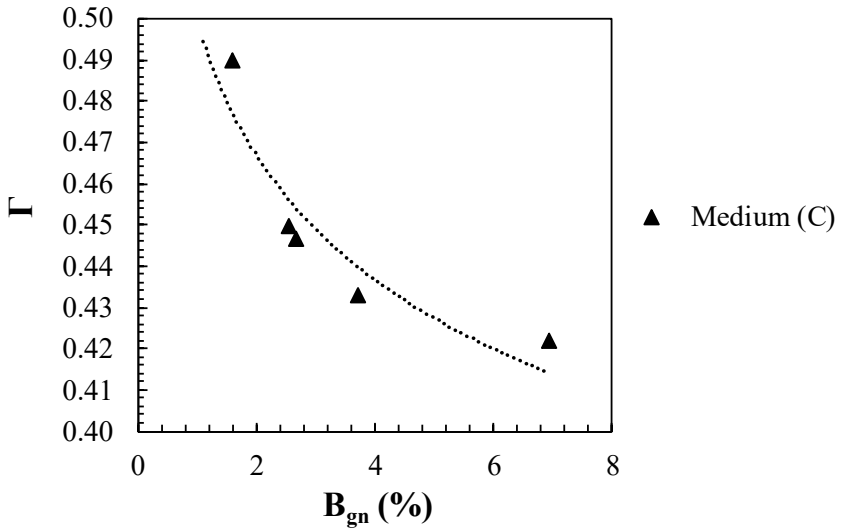

Figure 7.9 Intercept of the CSLs versus B_{gn} for the saturated specimens of Coreno Medium rockfill

The effect of the critical state line position on the mechanical properties of the soil can be expressed by using the parameter ψ (Been and Jefferies, 1985), defined as:

$$\psi = e_0 - e_{ss} \quad (7.6)$$

with e_{ss} the critical void ratio for the current CSL and at the current mean stress. The ultimate friction angle φ'_{ult} is expected to be decreasing as ψ increases.

From Figure 7.10 it is clear that the values of the ultimate friction angle φ'_{ult} decrease with increasing ψ, confirming the expected trend for all materials tested.

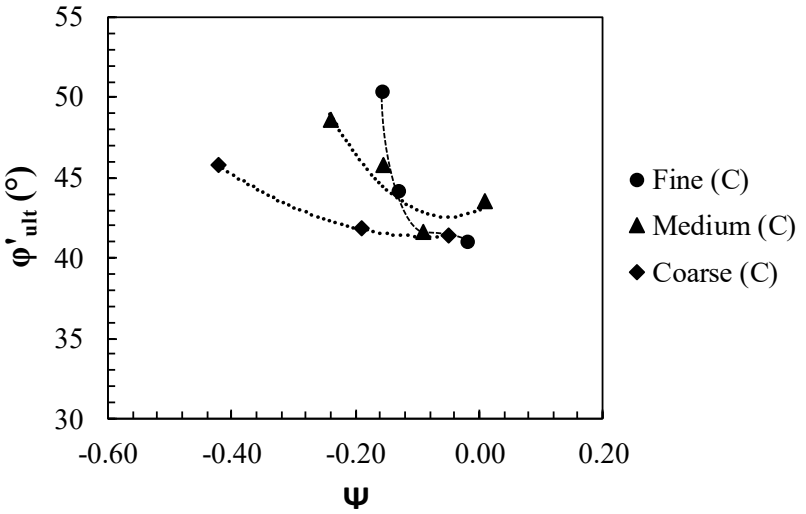

Figure 7.10 Ultimate friction angle versus the state parameter ψ for the saturated specimens of Coreno rockfill

The model parameters were determined using the results of tests on saturated specimens. However, the validity of the model is demonstrated by its application to tests on unsaturated specimens.
As widely recognized in literature, the unsaturated CSLs are found to be parallel to the saturated line for each matric suction in the e-p' space. Therefore, it can be reasonable to use the same slope λ.
As shown in Figure 7.11, from the application of the model to unsaturated tests it emerges that, when the degree of saturation increases, the intercept Γ decreases, as stated by many authors (Wang et al., 2002; Kayadelen et al., 2007). Thus, the critical state

lines can be considered depending on the water content and so on the matric suction, as widely accepted in literature.

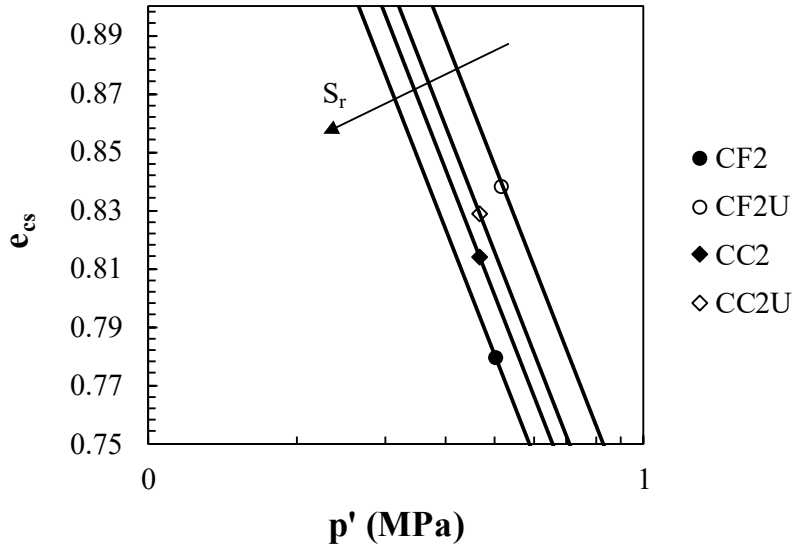

Figure 7.11 Critical state lines for the unsaturated specimens of Coreno rockfill

Unfortunately, it is not possible to apply the model to the rockfill Redisole since there is no data available for the calculation of the request parameters.

The advantage of this procedure remains the fact that the parameters of the simple model adopted will represent the effect of the critical state framework on the mechanical behaviour of rockfill and its link with the particle breakage and water content.

7.4 References

Been K., Jefferies M. G. (1985). *A state parameter for sands*. Géotechnique, 35(2), 99-112.

Coop M. R., Sorensen K. K., Bodas-Freitas T., Georgoutos G. (2004). *Particle Breakage during Shearing of a Carbonate Sand*. Géotechnique, 54(3), 157-163.

Daouadji A., Hicher P. Y., Rahma A. (2001). *An elastoplastic model for granular materials taking into account grain breakage*. European Journal of Mechanics – A/ Solids, Elsevier 20 (1), 113–137.

Einav I. (2007). *Breakage mechanics—part I: theory.* Journal of the Mechanics and Physics of Solids, 55(6), 1274-1297.

Hagerty M. M., Hite D. R., Ullrich C. R., Hagerty D. J. (1993). *One dimensional high pressure compression of granular media*. Journal of Geotechnical Engineering, 119(1), 1-18.

Hardin B. O. (1985). *Crushing of soil particles*. Journal of Geotechnical Engineering, ASCE, 111(10), 1177-1192.

Kayadelen C., Sivrikaya O., Taşkıran T., Güneyli H. (2007). *Critical-state parameters of an unsaturated residual clayey soil from Turkey*. Engineering Geology, 94, 1-9.

Lade P. V., Yamamuro J. A., Bopp P. A. (1996). *Significance of particle crushing in granular materials*. Journal of Geotechnical Engineering, ASCE, 122(4), 309-316.

Lee K. L., Farhoomand I. (1967). *Compressibility and crushing of granular soil in anisotropic triaxial compression*. Canadian Geotechnical Journal, 4(1), 68-86.

Liu E. L., Chen S. S., Li G. Y. (2011). *Critical state of rockfill materials and a constitutive model considering grain crushing*. Rock and Soil Mechanics, 32, 148-154.

Liu M. C., Gao Y. F., Huang X. M. (2005). *Study on elasto-plastic constitutive model of rockfills with nonlinear strength characteristics*. Chinese Journal of Geotechnical Engineering, 27, 294-298.

Luzzani L., Coop M. R. (2002). *On the relationship between particle breakage and the critical state of sands*. Soils and Foundations, 42(2), 71-82.

Marsal R. J. (1967). *Large scale testing of rockfill materials*. Journal of the Soil Mechanics and Foundation Division, ASCE, 93(2), 27-43.

McDowell G. R., Bolton M. D. (1998). *On the micromechanics of crushable aggregates*. Géotechnique, 48(5), 667-679.

Roscoe K. H., Schofield M. A., Wroth C. P. (1958). *On the yielding of soils*. Géotechnique, 8(1), 22-53.

Russell A. R., Khalili N. (2004). *A bounding surface plasticity model for sands exhibiting particle crushing*. Canadian Geotechnical Journal, 41(6), 1179-1192.

Tarantino A., Hyde A. F. L. (2005). *An experimental investigation of work dissipation in crushable materials*. Géotechnique, 55(8), 575-584.

Wang Q., Pufahl D.E., Fredlund D.G. (2002). *A study of critical state on an unsaturated silty soil*. Canadian Geotechnical Journal, 39, 213-218.

Wood D. M., Maeda K. (2008). *Changing grading of soil: effect on critical states.* Acta Geotechnica, 3(1), 3-14.

CONCLUSIONS

The research developed in this thesis allows deepening some important aspects of the mechanical behaviour of compacted rockfills.

The literature review has shown that the particles breakage has been identified quite a long time ago as a key feature in granular materials. Furthermore, some peculiar aspects relating to strength, dilatancy, compressibility and critical state condition have been highlighted. It is widely known in literature that the behaviour of granular materials depends on the geology, shape and size of the grains as well as the stress acting, the relative density, the stress path and the water action expressed through the degree of saturation or alternately total suction or relative humidity.

To study the effect of these factors on the mechanical response of coarse-grained soils, triaxial and oedometric tests were conducted on large and medium specimens of two different rockfills: a limestone material with high strength and low porosity and a rockfill with low particle tensile strength coming from a real dam (i.e. Redisole dam). Several grain crushing and compaction tests were conducted in order to characterize the tested materials.

First, this research was oriented toward the upgraded and set up of the existing equipment and innovative systems designed to make laboratory testing more reliable. However, in order to obtain consistent results in laboratory tests, literature and standards puts forward some restrictions on specimen dimensions with regard to

the maximum size of the particles. In other words, particles larger than the maximum size must be excluded when preparing the granular soil specimen for triaxial and oedometric tests. Further, for excluding particles exceeding the specific standard limit, different methods have been explored. The scalping and the parallel gradation techniques have been adopted in order to check which of these methods give rise to a material representative of the in-situ soil.

From the series of large triaxial and oedometric tests performed it may be concluded that particle breakage that has a remarkable effect on the overall rockfill behaviour, is accompanied by volumetric compression and occurs even for tests at modest confining stresses.

Moreover, the role of the degree of saturation, confining stress and particle tensile strength in determining the compressibility and strength of rockfill has been analysed. It emerged that water effects are associated with particle breakage because the velocity of crack propagation is significantly affected by water energy. The Redisole gravel is expected to be more sensitive to water effects, if compared with the limestone Coreno gravel.

Finally, on the basis of a simple model that idealising the critical state line as a series of parallel lines each associated with a certain level of particle breakage, the collected data will reproduce the effect of the grain size distributions in the critical state framework.

From the research work developed, there is an interest in deepening the study of some concepts that help to understand in a more

rational way the behaviour of granular materials in different stress-suction paths. Similarly, this theoretical study of the effect of particle breakage carried out can be analysed using the Discrete Element Method (DEM). Studies conducted with DEM show that in a granular structure, the stress is not transmitted uniformly on all particles. Stresses are transmitted by chains of heavily charged particles, while the rest of the particles remain almost unloaded. The breakage of a particle in these chains causes instability of the granular structure. Therefore, there is a reorganization towards a stable configuration of contacts and loads, showing an increase in macroscopic deformation.

APPENDIX

A.1 Membrane penetration: stress and deformation effects

Laboratory investigations aimed at studying the stress-strain behaviour of soils are often carried out using the triaxial apparatus, in which the specimen surface is wrapped in a flexible rubber membrane. In general, the rubber membrane used in the tests has a significant influence on both measured deviatoric stress and the volume change data.

The rubber membrane used in undrained triaxial deviatoric tests results in apparent increase in the measured strength as well as in drained triaxial tests, especially at low effective stresses.

Henkel and Gilbert (1952) suggested a method for estimating the rubber correction from a simple extension test on a typical rubber membrane. The authors hypothesized two limit schemes. The first assumes a perfect adherence between the specimen and the rubber membrane and provides that the correction must be made only to the axial stress. The second scheme, assuming a relative sliding between the membrane and the specimen, shows that the membrane modifies the radial stress acting on the specimen. This work was the basis for the subsequent formulations proposed for the calculation of the corrections to be made on the stresses (Duncan and Seed, 1967; Fukushima and Tatsuoka, 1984).

The increase in the deviatoric stress is largely due to the membrane stiffness (E_m) that depends on the material type, thickness and

dimension of the membrane itself (for example Henkel and Gilbert, 1952; Frydman et al., 1973; LaRochelle et al., 1988). ASTM D 4767-11 suggests to determine the average secant module E_m from extension test and also specifies to calculate the increase in deviatoric stress due to membrane, defined as membrane resistance, q_m, with the following equation:

$$q_m = \frac{4E_m t_m \varepsilon_a}{D_c} \quad \text{(A.1)}$$

where t_m is the thickness of the membrane, ε_a is the axial strain and D_c is the post-consolidation diameter of the sample. Equation A.1 is obtained when the rubber membrane is modelled as a hollow cylinder, and the E_m is assumed to be constant along its length.

The measured deviatoric stress is corrected at each ε_a value; however, the correction is neglected if the error in the deviatoric stress is <5% (ASTMD 4767-11). The correction calculated using the membrane stiffness (Eq. A.1) is more reliable method to calculate the precise deviatoric stress values from the measured data.

The accurate measurement of deformations under applied stresses is essential to formulate stress-strain models of soil behaviour. In the case of saturated specimens, the volume changes are usually measured as the quantity of water exchanged by the specimens as measured by the drainage line. Alternatively, for both saturated and unsaturated specimens, the volume change is often measured by the amount of water exchanged by the triaxial cell after suitable correction for expansion of the cell itself.

Under drained loading paths requiring changes in confining pressure, volume changes of coarse-grained soils occur not only in response to soil deformations but also because of the penetration or withdrawal of the membrane into or out of the interstices of the granular soil specimen. The measured volume changes must therefore be corrected for membrane penetration effects in order to compute the volumetric deformation of the soil skeleton. Clearly, the reliability of soil volumetric strain will depend on how accurately membrane corrections have been assessed.

Newland and Allely (1959) were the first to discuss the importance of the membrane effect. These authors recognized the occurrence of volume change caused by membrane penetration in triaxial tests on granular materials, wherein the effective confining pressure does not remain constant. Newland and Allely (1959) suggested a method to correct the volume change by the membrane penetration effect, assuming that the granular material behaved isotropically during hydrostatic loading. The soil volumetric strain of a saturated specimen of a coarse-grained soil subjected to an increment of hydrostatic stress under drained conditions was calculated as three times the axial strain obtained by measuring the axial deformation. The total volume change for the corresponding increment of stress was also measured. The volume change caused by membrane penetration was determined as the difference between the measured total and calculated soil volume changes.

Roscoe et al. (1963) suggested an alternative method for correction of membrane effects. Their program consisted of testing, under

ambient pressure conditions, triaxial specimen containing cylindrical brass rods throughout the height of the sample. They were coaxially placed within a saturated sand specimen of a fixed diameter and height. The height of the brass rods was equal to the specimen height, but the diameters ranged from about one sixth to one tenth of the diameter of the soil specimen. This resulted in a different volume of soil in each setup. Ambient pressures were increased from 35 to 690 kPa, and corresponding total volume change were measured for each setup. This total volume change had two components: the first one represented the volumetric compression of the soil skeleton under the applied ambient stress and was consequently a function of the volume of soil in the setup; the second component was due to the membrane penetration under the same ambient stress. This last component of total volume change, being a function of the surface area of the specimen, was constant for each setup. The membrane penetration was obtained for each value of ambient pressure by plotting volume change measured against rod diameter and extrapolating the resulting straight line. By extrapolation, a volume change corresponding to a rod diameter equal to that of the soil specimen and hence zero soil volume was obtained. Since brass is relatively incompressible, this extrapolated volume change was attributed to membrane penetration.

The membrane penetration effect can be significant for coarse-grained soils. It is widely known that the particle size is one of the main factors influencing the membrane penetration for any applied

cell pressure. The particle shape, their size distribution, and the density of the sample have minor effects.

Steinbach (1967) tested 18 sand samples of different mean particle size and gradation and, like Roscoe et al. (1963), assumed the specimens to be isotropic and obtained the membrane penetration from measurements of volumetric and axial strain. According to Steinbach (1967) the membrane effect for graded materials is similar to that of a uniform material with particles equal to the 50 percent size of the graded material. In view of this observation, it appeared that it should be possible to find a relationship between particle size and membrane penetration effect.

Raju and Sadasivan (1974) suggested modifications for further improvement to the method proposed by Roscoe et al. (1963). They argue that, because the stiffness of the dummy brass rod is much greater than that of the soil, when the top loading platen rests on the brass rod, the vertical stress on the soil will be less than the applied hydrostatic stress, resulting in a nonhydrostatic compression of the soil skeleton. These authors recommended to replace the conventional rigid top platen with an annular flexible and lubricated top platen, so that the brass rod passed through it and the application of a uniform hydrostatic stress to the soil was insured. Raju and Sadasivan (1974) suggested a new linear relationship between total volume change and soil volume in order to obtain membrane correction by extrapolation to zero soil volume.

Frydman et al. (1973) conducted tests on three samples of monosized glass microspheres. Isotropic compression tests were

carried out on full triaxial specimens and on hollow cylinder specimens with a rubber latex membranes of 0.03 cm thickness. Also in this research the total measured volume change was separated into two parts: the first was due to membrane penetration as a function of surface area, whereas the second portion was due to glass microspheres skeleton deformation and consequently a function of its volume. Unlike the Roscoe et al. (1963) technique, where the specimen surface area was kept constant, both specimen surface area and volume were varied by varying the inside diameter of the hollow specimens. Thus, specimens at identical densities but having different surface area to volume ratios were subjected to the same magnitude of hydrostatic stress increment. Corresponding changes in total volume were plotted against specimen surface area to volume ratio. The membrane penetration per unit surface area and the soil volumetric strain for the associated increment in hydrostatic stress was graphically determined. These results agree with previous investigations finding the major factor influencing the membrane effect is the particle size. Frydman et al. (1973) developed a unique relation between the membrane effect and particle size for membranes of usual thickness and suggested that this relation may be used to estimate the membrane effect for any granular soil.

Vaid and Negussey (1984), supported by experimental evidence, proposed alternative methods for estimating membrane penetration. The authors questioned the use of methods based on assumptions that are seriously violated in practice because sand specimens and

perhaps natural deposits, have an inherent anisotropy and can not be considered isotropic in hydrostatic loading. Baldi and Nova (1984) by means of drained and undrained tests, performed a qualitative analysis to find which factors influence the membrane penetration and, at least approximately, to what extent. It is shown that apparent volumetric strain due to membrane penetration decreases linearly with increasing sample diameter. They proposed a correction factor depending on the volumetric stiffness of the sample which is not a constant but depends markedly on the state of stress. Baldi and Nova (1984) derived an expression assuming the grains to be in spherical shape with an equivalent diameter, d_g, which is in contact with the membrane layer. The expression proposed was as follows:

$$\varepsilon_{vm} = \frac{1}{8} d_g \left(\frac{\sigma_c' d_g}{E_m t_m}\right) \qquad \text{(A.2)}$$

where ε_{vm} is the volumetric strain due to membrane penetration; d_g is the equivalent diameter when converted to spherical shape; σ'_c is the effective confining pressure; E_m is the stiffness of the rubber membrane and t_m is the thickness of the membrane. Literatures on the correction procedure to estimate the membrane penetration effect showed the importance of membrane stiffness E_m, which, as mentioned before, in turn depends on the material type, membrane thickness t_m, and the membrane diameter, d_m. The value of E_m used in the present work is that obtained from Flora (1995) and so E_m=1800 kPa.

Numerous authors have used a single grain size to study the membrane effect. However, the adoption of a single representative

diameter of the grain size distribution represents an approximation as worse as the soil is well graded. Despite this experimental evidence, in the present work the stresses and volumetric strains were corrected using the (A.1) and (A.2) respectively.